UNIVERSITY OF SOUTHAMPTON

FACULTY OF NATURAL AND ENVIRONMENTAL SCIENCES

School of Chemistry

Towards the Development of a Continuous-Flow Semi-Biotic Device: Transcription from DNA-loaded Liquid Crystalline Phases

by

Richard James Wilson

Thesis for the degree of Doctor of Philosophy

September 2014

UNIVERSITY OF SOUTHAMPTON

ABSTRACT

FACULTY OF NATURAL AND ENVIRONMENTAL SCIENCES

Chemistry

Doctor of Philosophy

TOWARDS THE DEVELOPMENT OF A CONTINUOUS-FLOW SEMI-BIOTIC DEVICE: TRANSCRIPTION FROM DNA-LOADED LIQUID CRYSTALLINE PHASES

by Richard James Wilson

Research published by Corsi *et al.* (2008) has reported how linearized *ds*DNA encoding for the firefly luciferase gene can be contained within the inverse hexagonal phase of the phospholipid 1,2-dioleoyl-*sn*-glycero-3-phosphoethanolamine (DOPE), whilst remaining transcriptionally active. The work presented herein builds upon the novel discovery reported by Corsi *et al.*, by fully characterizing and then modifying the reported system to allow for batch, and then continuous-flow, production of mRNA from *ds*DNA-containing liquid crystalline phases, in the context of establishing proof of concept for a continuous-flow transcription-translation capable 'semi-biotic' device.

To give a better understanding of the lipid-based method of template *ds*DNA containment for transcription, experiments were performed to assess the transcriptional activity and characterize the partitioning of nucleic acids (*ds*DNA and *m*RNA) in DOPE-based transcription assays; these experiments included varying the ionic, reagent concentration and incubation conditions. A number of experiments were also carried out investigating the effect of doping the liquid crystalline phase with the positively charged lipid species 1,2-dioleoyl-3-trimethylammonium-propane (DOTAP), and replacing DOPE with the unsaturated monoglyceride monoolein (MO). Investigations have shown that DOPE (95%):DOTAP (5%) liquid crystalline phases were able to achieve similar levels of *ds*DNA partitioning as pure DOPE lipid buttons; however, these DOTAP-containing phases were transcriptionally inactive. Substitution of DOPE for monoolein did not yield comparable levels of *ds*DNA partitioning.

A batch transcription protocol was developed as a logical progression from one-off transcription towards continuous-flow transcription from *ds*DNA-containing liquid crystalline phases. Individual liquid crystalline phases, preloaded with *ds*DNA, were subjected to multiple transcriptions in an effort to establish the maximum lifespan of the phase and the optimal batch transcription parameters. Polarizing light microscopy, small-angle x-ray scattering (SAXS) and mass spectrometry were used assess the effect upon the liquid crystalline phase of multiple cycles of batch transcription, whilst quantitative DNA gel electrophoresis was performed to assess the level of *ds*DNA partitioning over successive batch transcription assays from individual lipid phases. Investigations into batch transcription from *ds*DNA-containing DOPE liquid crystalline phases have shown that the partitioned *ds*DNA leaches out from within the phase during the course of successive transcription reactions.

In order to assess the viability of a transcription-translation capable semi-biotic device that utilizes lyotropic liquid crystalline phases, investigations were made into the suitability of the optimal batch transcription system when incorporated into a thermostatically controlled polydimethylsiloxane (PDMS) continuous-flow transcription device. Finally, a critical comparison was made between the initially proposed mechanism of *ds*DNA containment using lipid-based liquid crystalline phases and some of the recently reported alternative methods of *ds*DNA immobilization.

Contents

List of figures

DECLARATION OF AUTHORSHIP

I, Richard James Wilson,

declare that the thesis entitled

Towards the Development of a Continuous-Flow Semi-Biotic Device:
Transcription from DNA-loaded Liquid Crystalline Phases

and the work presented in the thesis are both my own, and have been generated by me as the result of my own original research. I confirm that:

- this work was done wholly or mainly while in candidature for a research degree at this University;
- where any part of this thesis has previously been submitted for a degree or any other qualification at this University or any other institution, this has been clearly stated;
- where I have consulted the published work of others, this is always clearly attributed;
- where I have quoted from the work of others, the source is always given. With the exception of such quotations, this thesis is entirely my own work;
- I have acknowledged all main sources of help;
- where the thesis is based on work done by myself jointly with others, I have made clear exactly what was done by others and what I have contributed myself;
- parts of this work have been published as:
  1. Black, C. F.; Wilson, R. J.; Nylander, T.; Dymond, M. K.; Attard, G. S. Linear dsDNA partitions spontaneously into the inverse hexagonal lyotropic liquid crystalline phases of phospholipids. *J. Am. Chem. Soc.* **2010**, 132 (28), 9728-32.
  2. Wilson, R. J.; Tyas, S. R.; Black, C. F.; Dymond, M. K.; Attard, G. S. Partitioning of ssRNA molecules between preformed monolithic H(II) liquid crystalline phases of lipids and supernatant isotropic phases. *Biomacromolecules* **2010**, *11*, 3022-27.

Signed: ……

Date:……

Acknowledgements

First and foremost, I would like to express my thanks to Professor George Attard for his continued support, guidance and encouragement throughout the duration of this work. I am truly grateful for his supervision and patience; he inspired me as a researcher and ensured that there was never a dull moment as a PhD research student in the Attard research group! George was responsible for the provision of personal protective equipment and assessment of health and safety during research group outings, most notably during our visits to Malta and the MAX IV laboratory, SE.

Secondly, I would like to thank Dr Marcus Dymond for his practical and theoretical expertise, not least when together we worked through the night processing SAXS samples using the I911-4 station at the MAX IV laboratory. Marcus' honesty and sincerity added perspective to many a discussion, whilst his sense of humour reminded me of the importance of being able to laugh at both yourself and life. Marcus currently holds the record for fastest lap-time on a scooter round the MAX IV laboratory out of the Attard research group members, past and present.

My gratitude is extended to Professor Tommy Nylander, of Lund University, SE, and the MAX IV laboratory staff, Ana Labrador and Tomás Plivelic, for their kind support and entertainment during the beam-time the Attard research group had utilizing the yellow mini-hutch for SAXS experiments on the I911 beamline. I will always very fondly look back upon the times we spent working long, coffee-fueled hours processing SAXS samples whilst consuming copious amounts of Swedish confectionary.

I would also like to thank Professor Hywel Morgan and Dr Barbara Cortese, of the School of Electronic and Computer Science, and Dr Maria-Nefeli Tsaloglou, of the National Environment Research Council, Southampton, for their time, help and input with the design and development of prototype continuous-flow devices, along with the use of their laboratory space and resources.

I am grateful to my PhD advisor, Dr Ali Tavassoli, for offering sound, timely advice and feedback on my research, and for the kind use of his laboratory space and facilities as required.

I am indebted to the members of the Attard research group, past and present, whom I had the pleasure to work and made the work environment so enjoyable. In particular, Stephanie Tweed and Richard Gillams, deserve special mention; their continued friendship, liberal support and thoughtful input (on all aspects of life, both when it was

needed and when it wasn't) helped to make my PhD studentship the memorable experience it was. Specific thanks go to Stephanie Tweed, for assistance with mass spectrometry, and to Richard Gillams, for assistance with Xmgrace software and interesting discussions concerning (but not limited to) the course-grained simulation of biological membranes.

Special thanks goes to my family and friends for their unrelenting support and the encouragement provided. The understanding shown by my children, James and Sam, on the occasions I had to work long hours and got home past their bedtime or worked over the weekend, and by my fiancée, Kimberley, whilst I spent many hours in solitude completing my thesis, will never be forgotten or underappreciated. To my grandparents, parents, fiancée, children and friends: your continued support has been invaluable. Having family and friends that always took an active interest in the research I've undertaken helped to maintain my enthusiasm, even in times of frustration.

Finally, I acknowledge the generous funding I have received from both the EC FP6 Neonuclei project, for the initial stages of my research, and from the University of Southampton Life Sciences Interfaces forum, for funding my PhD studentship.

Definitions and abbreviations

Abbreviation	Meaning
d^2r	Detection, decision and response
DNA	Deoxyribonucleic acid
dNTP	Deoxyribonucleoside triphosphate
DOPE	1,2-dioleoyl-*sn*-glycero-3-phosphoethanolamine
DOTAP	1,2-dioleoyl-3-trimethylammonium-propane
*ds*DNA	Double-stranded DNA
DTT	Dithiothreitol
ESI-MS	Electrospray ionization mass spectrometry
Full buffer	Full transcription reaction buffer, containing, amongst other components, spermidine and triton X-100
GFP	Green fluorescent protein
H_{II}	Inverse hexagonal (phase)
LC	Liquid crystal(-line)
*lin*pRSET-EmGFP	Linearised double-stranded DNA incorporating T7 promoter, ampicillin-resistance and emerald-green fluorescent protein genes
*lin*T7GFP	Linearised double-stranded DNA incorporating T7 promoter, ampicillin-resistance and green fluorescent protein genes
*lin*T7luc	Linearised double-stranded DNA incorporating T7 promoter, ampicillin-resistance and luciferase genes
MO	Monoolein
*m*RNA	Messenger ribonucleic acid
NL	Neutral loss
PCR	Polymerase-chain reaction
PDMS	Polydimethylsiloxane
PE	*See DOPE*
pRSET-EmGFP	Circular plasmid double-stranded DNA incorporating T7 promoter, ampicillin-resistance and emerald-green fluorescent protein genes
pT7GFP	Circular plasmid double-stranded DNA incorporating T7 promoter, ampicillin resistance and green fluorescent protein genes

Abbreviation	Meaning
pT7luc	Circular plasmid double-stranded DNA incorporating T7 promoter, ampicillin resistance and luciferase genes
RNA	Ribonucleic acid
[RNA]	Ribonucleic acid concentration
rNTP	Ribonucleoside triphosphate
RT	Room temperature
SAXS	Small-angle X-ray scattering
SD	Standard deviation
SN	Supernatant
SPS	Solution phase system
*ss*RNA	Single-stranded RNA
TAP	*See DOTAP*
X-DNA	X-shaped DNA

Chapter 1:

Introduction

1. Introduction

1.1 Semi-biotic device concept

1.1.1 Semi-biotic systems

Semi-biotic systems are systems that incorporate biologically derived components and integrates them with synthetic components to produce a hybrid 'semi-biotic' device.[1] For example, a semi-biotic system could combine a biological process, such as transcription of DNA, combined with a synthetic chassis device, such as a microfluidic system. These hybrid devices offer several potential advantages over traditional applications of biological systems and solid-state devices. Solid-state devices have inherent limits to their ability to adapt to different conditions, and so by producing a hybrid device, it is possible that semi-biotic systems could be designed to exhibit higher degrees of adaptability and autonomy. An advantage of semi-biotic systems over their 'standard' biological counterparts is their ability to be custom-designed to fulfil a desired function or purpose. Through careful design and integration of biological systems with suitable synthetic components, a specific and tailor-made hybrid device can be produced, which could offer potential benefits over the traditional applications of biological processes. For example, such a device could be engineered to incorporate 'clean' functionality, utilizing cell-free technologies to enable protein synthesis in a less complex mixture than found in some traditional biotechnology applications, allowing for simplified, cleaner and more efficient protein purification.

Possible applications for semi-biotic systems include synthetic RNA or peptide foundries, which could then be integrated with a detection, decision and response (d^2r) system, to create a fully autonomous semi-biotic device.

1.1.2 Coupled transcription/translation

Coupled transcription-translation systems are readily available from commercial life sciences suppliers, such as Promega,[2] New England Biolabs,[3] and Invitrogen.[4] Coupled systems are able to express the protein of a gene of interest, often from a multitude of template sources, including circular plasmid DNA, linearized plasmid DNA and PCR product, through transcription and then translation of the supplied template. Of particular benefit to life science researchers are the numerous kits offering eukaryotic cell-free protein expression – increasing the speed at which high quality and high yield protein can be expressed. Cell-based protein expression requires a far more time-consuming preparation and intensive protocol, when compared to the cell-free expression systems currently available. However, whilst cell-free expression kits reduce the amount of time required to express protein, from several days using a cell-

based system to a couple of hours,[5] protein expression is still confined by the requirement for expression to be performed in a batch-wise manner, theoretically increasing the amount of user input required to produce a reduced amount of protein than would be available if a system utilizing a continuous protein expression method could be developed.

The initial cell-free protein synthesis systems date back almost five decades, with much technical advancement since the basic system devised by Nirrenberg and Matthaei.[6] Whilst the simplest cell-free translation systems relied upon an exogenously added mRNA template for translation (uncoupled translation systems),[7] it was advantageous to have systems that were able to express protein directly from a DNA template containing the gene of interest, with transcription and translation occuring in a single reaction vessel (coupled transcription-translation systems). Beneficially, coupled systems were able to offer higher protein yields and faster operation times, although required the inclusion of a highly processive RNA polymerase, such as that encoded by the T7 bacteriophage, limiting the available templates for exogenous addition to the system.[8] For the purpose of this research, a coupled system using the highly processive T7 RNA polymerase was ideal, due to the preceding research by Corsi *et al.* using T7 DNA vectors.[9]

Protein expression systems were initially constrained to batch processing due to the limited amount of resources (such as lysate, polymerase, amino acids, ATP) available to the system. With a limit upon the resources available, the key reaction components required for protein expression, especially high-energy phosphates, will become in short supply over a relatively short timescale, causing batch processing systems to have a short lifetime (1 hour or less) and thus a lower yield of protein than would be desirable.[10] The short lifetime and limited yield of the early batch-formatted reactions was overcome by Spirin *et al* in 1988, through the development of a continuous-flow cell-free (CFCF) protein expression system.[11] The CFCF translation system was able to ensure a constant supply of the resources required to sustain protein expression over a much-extended lifetime (20-40 hours). The continuous-flow method relies upon the forced flow of feeding buffer, containing amino acids, adenosine triphosphate (ATP) and guanosine triphosphate (GTP), through the reaction mixture, with the polypeptide product actively removed via pump and ultrafiltration membrane for the duration of the reaction.

The continuous-flow cell-free method developed by Spirin *et al.* set the precedent for cell-free translation systems that offered higher yields and extended lifetimes over the initial batch-formatted systems. An evolution of the CFCF method was reported by Kim

and Choi in 1996.[12] Utilizing a semi-continuous continuous-exchange cell-free (CECF) method, continuous supply of feeding buffer was supplied using passive exchange *via* dialysis membrane from a feeding buffer pool to the reaction pool. By-products were also removed from the reaction pool by the same process. Whilst the CECF method simplifies the protein expression process using a cell-free system, it is at a disadvantage when compared to CFCF because it is not easily miniaturised and automated, limiting it's applications for high throughput or microfluidic devices.

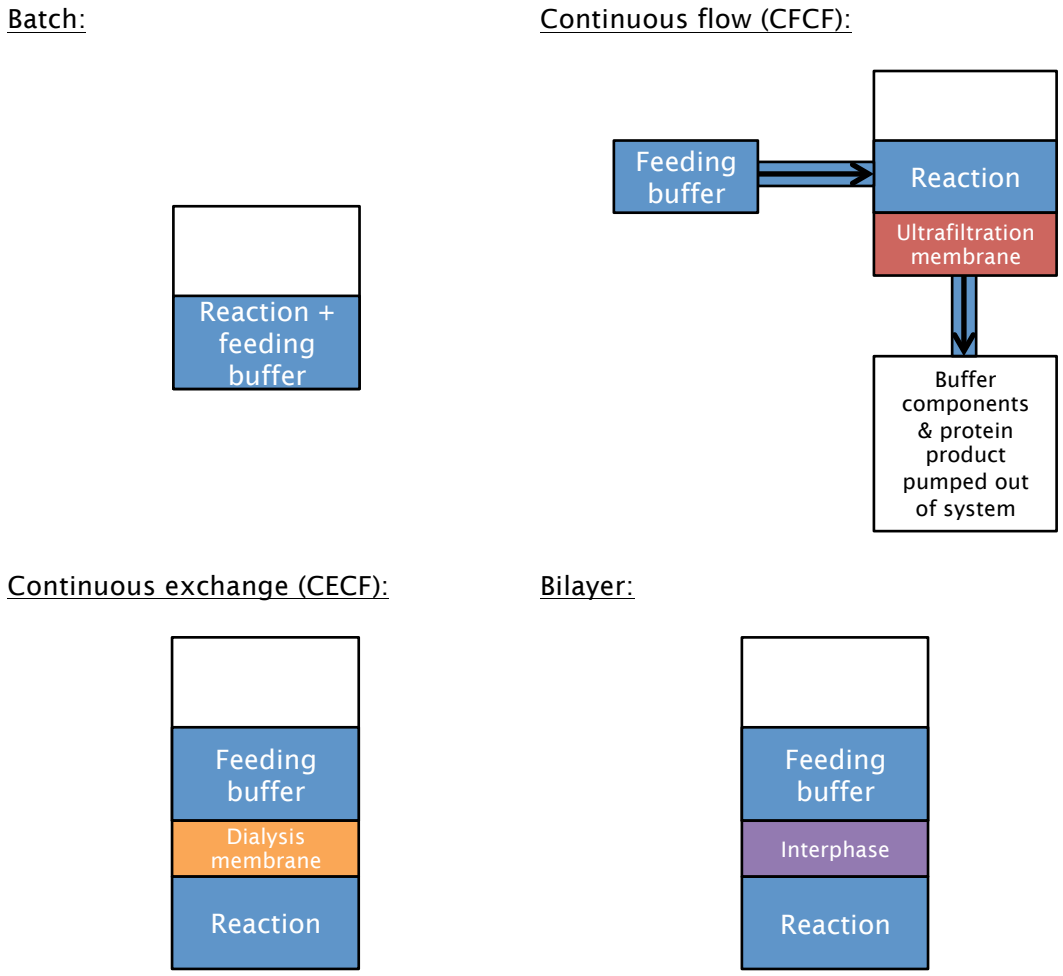

Figure 1.1 Comparison of cell-free translation system apparatus set-ups. Continuous exchange (CECF) set-ups allow the buffer components to flow through the dialysis membrane in both directions, whilst bilayer set-ups allow both buffer components and protein product to flow through the dialysis membrane in both directions.

Bilayer cell-free translation systems are a further advance upon the CECF method. Through removing the dialysis membrane present in CECF systems, bilayer systems are able to passively transport feeding buffer into the reaction pool, whilst also transporting protein product away from the reaction pool.[8,13] Endo *et al.* also report a bilayer translation system that is compatible using high-throughput formats, for example combining the bilayer translation system with robotic automation, offering an

advantage over the CFCF systems reported by Kim and Choi.[14] Sawasaki reports that using a bilayer diffusion method of protein expression, yields of more than 10 times those expected of batch-format expression systems can be achieved.[15]

Ultimately, the goal for translation systems has been to maximise the yield of the expressed protein, whether using coupled or uncoupled systems, and this has been done through either utilization of high-throughput methods in conjunction with cell-free translation systems, or through establishing the most efficient method of batch-formatted systems. Whilst CFCF, CECF and bilayer translation systems have allowed for increased reaction lifetimes, thus increasing the yield of protein obtained, methods such as ATP and GTP regeneration, concentration of the cell extract lysate, and mutation of the genes involved in amino acid catabolism have allowed batch-format translation to yield higher quantities of expressed protein without the need for the more complex apparatus set-up required by continuous and semi-continuous protein expression formats.[16–18]

1.1.3 Continuous-flow devices for coupled transcription-translation

While there have been numerous reports in the literature of cell-free transcription-translation systems, an ideal system would combine high yield, portability, simplicity and high efficiency in a practical form factor, features that many of the systems reported fail to combine. It therefore seemed logical to look towards ever-expanding field of research that is microfluidics to fulfill these requirements.

Microfluidic research over the last decade has developed the field of microfluidics so significantly that microfluidic technologies are now viewed as an enabling tool in experimental science, particularly within synthetic biology, analytical and synthetic chemistry.[19] Microfluidic devices are those that deal with small volumes of fluids using channels with dimensions in the region of micrometres; the small volumes they process at any one time, under laminar flow conditions with their channels, allow them to finely control concentrations of molecules, enabling reduced reagent consumption, reduced reaction timescales, and increased reaction efficiency.[20] Devices can be fabricated from a number of materials, namely glass, silicon, steel, and the polymer polydimethylsiloxane (PDMS), dependent upon the exact properties required and the intended usage of the device. Glass, silicon, and steel devices can be ideal for devices incorporating microelectronics, whilst those fabricated from PDMS benefit from the polymers' gas permeability, allowing fabrication of biological devices capable of supporting living cells.[21] The use of PDMS to produce such systems also allows rapid prototyping, with systems able to go from design to complete fabrication in under 24

hours.[22] Such rapid prototyping processes typically involves the use of computer-aided design software to produce the design of the device microfluidic channels, conversion of the design into a high-resolution transparency, photolithography to create a master positive-relief photoresist, and then casting of PDMS against the photoresist to produce the upper and lower PDMS layers of the device, which can then be chemically bonded together.

Microfluidic devices have already been utilized for a number of synthetic biology processes, in both continuous flow and batch-wise systems; processes to have benefitted from microfluidic device technology include *ds*DNA amplification, immunoassays, cell culturing, and cell-free protein expression.[23–25] Such devices have been known to offer increased mixing and separation efficiencies, improved reaction selectivity and reduced reaction times for their selected biological process.[26]

Continuous-flow cell-free transcription-translation microfluidic devices have been reported in the literature; some notable examples are those reported by Dittrich (2005), Courtois (2008) and Khnouf (2009).[27–29] The device fabricated by Dittrich *et al.* relied upon the formation of a water-in-oil emulsion, wherein templates from a gene library are continually mixed with the transcription-translation component solution, with protein expression occurring in the device's microfluidic channel upon incubation at 37 °C. Courtois' device utilized the components of a commercially available protein expression system, with the *E. coli* lysate and amino acids supplied *via* one input flow and the remaining protein expression components supplied *via* a second input flow. Protein expression then occurred *in vitro* with incubation at room temperature for 6.5 hours. Khnouf's device relied on passive pumping of an all-in-one solution of transcription-translation components across an array of 192 microchannels connected by pairs of wells. All three devices share commonality, however, in their reliance upon both template *ds*DNA and protein expression components to be pumped into the device, whether through an all-in-one input or segregated input solutions.

The use of a DOPE liquid crystalline phase for template *ds*DNA containment within a continuous-flow microfluidic device for coupled transcription-translation is a novel but exciting application. It has the potential to offer increased transcription-translation throughput batch systems, reduced reagent consumption and wastage, and improved simplicity by requiring only one input of protein expression components into a small form factor device; its major advantage over the aforementioned transcription-translation microfluidic devices being the containment of reusable template *ds*DNA within the 'fabric' of the device.

1.2 Interactions of nucleic acids with DOPE H_{II} phases

1.2.1 Phospholipids in biological systems

'Naked nuclei', that is, cell nuclei stripped of their nuclear membranes, have lipid content in the region of 4-10% of the total cell content.[30] Due to the low water content of cells, it is speculated that the lipids present within cell nuclei may be arranged into a structure that bears relation to lyotropic liquid crystalline phases, brought on by self-organization of the lipids in a low water content environment.

When the concentration of amphiphile, compared to the bulk solvent, is very low, molecules will be dispersed randomly within the system with no long-range ordering. Increasing the amphiphile concentration with respect to the bulk solvent, to above the 'critical micellar concentration', will lead to spontaneous self-assembly of the amphiphiles to form aggregates, protecting the hydrophobic tails of the amphiphiles from the polar solvent.[31] The structure of the amphiphile aggregate formed is dependent upon both the concentration and chemical structure of the amphiphile, and the temperature of the system. Initially, amphiphiles aggregate to form micelles, the simplest type of aggregate, at concentrations slightly above the critical micellar concentration (some amphiphile structures may lead to the formation of vesicles or hexosomes, rather than micelles at concentrations slightly above the critical micellar concentration). True lyotropic liquid crystalline phases are formed as the concentration of amphiphile in polar solvent is increased beyond the point where micellar aggregates are forced to distribute regularly within space.[32-34]

As the amphiphile concentration increases, the number of amphiphile aggregates present in the closed system increases; this leads to self-assembly of increasingly ordered structures to accommodate the aggregates. The initially randomly ordered micelles (L_1) will become more ordered as amphiphile concentration increases, causing the micelles to self-assemble in a cubic structure (I_1), before eventually forcing the cubic structured micelles to fuse, producing a hexagonal structure (H_1). The hexagonal structure consists of amphiphile rods, arranged with outer rods surrounding a central rod in a hexagonal array. Increasing the amphiphile concentration further causes the hexagonal structure to change structure, becoming a bicontinuous cubic phase (Ia3d, V_1) for some lyotropic liquid crystal systems. Further increasing the amphiphile concentration, a lamellar structure (L_α) forms, consisting of amphiphile sheets separated by thin layers of polar solvent. Past the lamellar phase, if amphiphile concentration is increased above 80%, some lyotropic liquid crystalline systems can

form inverse topology lyotropic phases, such as the inverse cubic, inverse hexagonal (H_{II}), and inverse micellar cubic phases.[35]

Whilst it is known that phospholipids are required in the composition of biological membranes within cells, allowing intracellular compartmentalization,[36] there are many reports that phospholipids have additional physiological roles; for example, phospholipids are integral to signal transduction and cytoskeletal support.[37-39] It is also proposed that endonuclear phospholipids have a primary role in cellular processes such as transcription, *ds*DNA replication, and the cell cycle.[40-42] It is this involvement in the process of *in vivo* transcription that makes the use of liquid crystalline phases composed of phospholipids an ideal choice for containment of template *ds*DNA whilst maintaining transcriptional activity.

The zwitterionic phospholipid 1,2-dioleoyl-*sn*-glycero-3-phosphoethanolamine (DOPE) was used by Corsi *et al.* (2008) to produce the lyotropic liquid crystalline phases that they reported supported transcriptional activity from linearized template *ds*DNA contained within them.[9] As a zwitterionic species, DOPE possesses both formal negative and positive charges, which counteract to give an overall net neutral charge (Figure 1.2). The overall structure of DOPE consists of a polar headgroup region, consisting of a phosphate and an alcohol, and a hydrophobic tail region consisting of fatty acids. The phospholipid aggregates with other phospholipids in the presence of water to minimise the interactions between the hydrophilic tails and water.

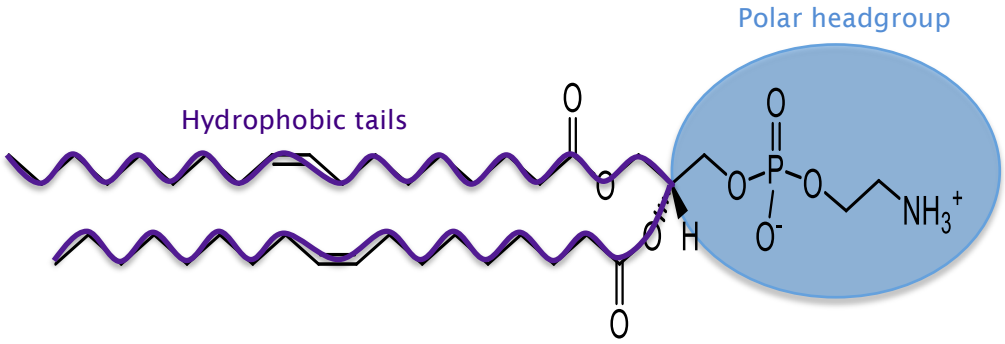

Figure 1.2 Chemical structure of 1,2-dioleoyl-*sn*-glycerol-3-phosphoethanolamine (DOPE), highlighting the hydrophobic tail region (purple) and polar head group region (blue).

In the aforementioned publication, DOPE concentrations are such that the amphiphile concentration is sufficient enough to lead to the formation of the inverse hexagonal phase (H_{II}), the most common non-bilayer phase in biological systems.[43] Inverse topology phases have water encapsulated by aggregated amphiphiles, with the

hydrophobic tails pointing outwards; columns of polar solvent are encapsulated by amphiphiles, as shown in Figure 1.3.

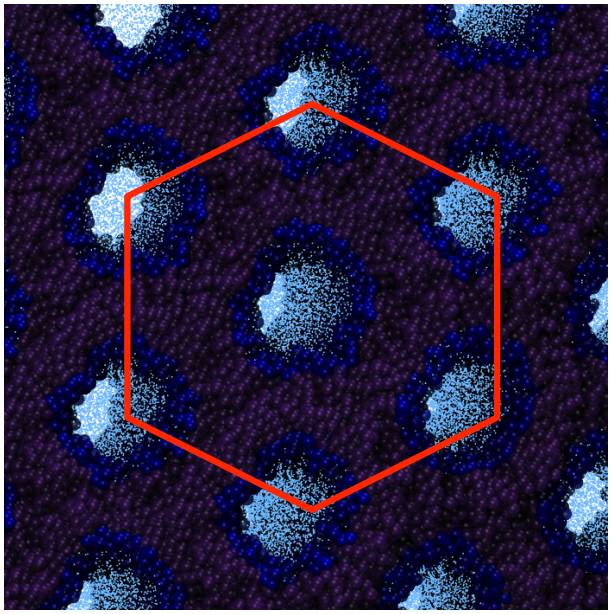

Figure 1.3 Coarse-grained simulation showing the inverse hexagonal (H_{II}) phase of DOPE. Water molecules (light blue) fill the columnar voids enclosed by the polar head groups of the phospholipid molecules (dark blue). Red hexagon highlights the H_{II} phase structure. Simulation constructed and image rendered by R Gillams (used with permission).

1.2.2 *ds*DNA partitioning

The most common conformation of *ds*DNA, out of three known conformations, is B-DNA; its overall width is approximately 2 nm, whilst the length of one turn of the helix (ten base pairs) is 3.4 nm, making the average length per base pair 3.4 Å.[44,45] B-DNA is characterised by the prominence of a large major groove, alongside a smaller minor groove, on a right-handed, open double helix, where there is rotation of 36 ° between successive base pairs. This conformation presents the negatively charged phosphate backbone of the *ds*DNA towards any potentially interacting surface - for example, the positively charged head groups of DOPE molecules within a liquid crystalline phase.

Previous research published by Koltover *et al.* has shown that linearized *ds*DNA is able to partition within liquid crystalline phases, occupying the aqueous channels found in inverse hexagonal phases, such as that of DOPE.[46] This location of DNA within the pores of the H_{II} phase is made possible by the channels being marginally larger in diameter than the dsDNA (~ 2 nm). It is proposed that this is the mechanism of the *ds*DNA containment within the inverse hexagonal phase of DOPE reported by Corsi *et al.* (2008), rather than the linearized *ds*DNA remaining in the aqueous supernatant solution above the phase or associating with the DOPE phase surface. Kolt *et al.*

suggest it is possible that, under low ionic concentrations, electrostatic interactions between the negatively charged DNA backbone and positively charged DOPE head groups further stabilise the location of dsDNA within the H_{II} channels (see Figure 1.4).

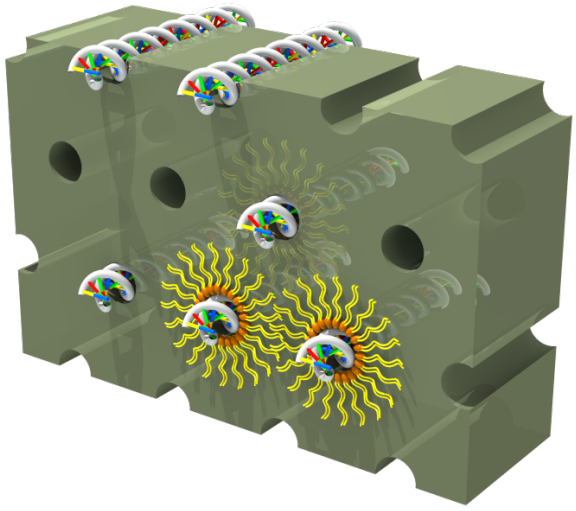

Figure 1.4 Schematic of H_{II} phase DOPE identifying the proposed location of linearized *ds*DNA within the aqueous channels.

For the success of a potential continuous-flow transcription-translation device, it is imperative that the linearized template *ds*DNA remains associated with the containing liquid crystalline phase for a maximal time period. In a continuous-flow situation, any template *ds*DNA that was removed from within the phase during the process of transcription by RNA polymerase would likely be washed away from the phase by the continual flow of fresh reagents; over time, this would lead to a reduction in the amount of template *ds*DNA available within the phase, until the phase was rendered barren and requiring regeneration or replacement.

1.2.3 *m*RNA partitioning

*m*RNA is synthesised by RNA polymerase, during the transcription of template DNA; throughout the research presented herein, mRNA is synthesized through transcription of T7 promoted linearized *ds*DNA, containing the gene for emerald-green fluorescent protein, by T7RNA polymerase (New England Biolabs). For successful transcription of template DNA to occur, there are several critical components required: template DNA (ideally dsDNA), activated ribonucleoside triphosphates (rNTPs), the presence of divalent metal cations (e.g. Mg^{2+}) and RNA polymerase. RNA polymerase catalyzes the initiation and elongation of RNA chains, following the sequence defined by the *ds*DNA

template, transcribing between the promoter and terminator sites of the template; the mRNA produced by transcription is single stranded, synthesized in the 5' to 3' direction.[47] Due to the single stranded nature of mRNA, it is by far more flexible than *ds*DNA, possessing a coherence length of 0.8 nm, which is shorter than the coherence length of *ds*DNA, at ~ 15 nm.[48] The coherence length is defined as the distance over which the cosine of the angle from the origin becomes 1; *m*RNA is therefore able to adopt a much more coiled structure than *ds*DNA.

Under the conditions reported by Corsi *et al.*, transcript *m*RNA could assume a highly coiled secondary structure within the transcription solution, due to its low coherence length. Alternatively, the transcript *m*RNA could undergo a substantial change in its conformation, allowing it to reside within the aqueous pores of the inverse hexagonal phase, alongside the template *ds*DNA contained within them. It is considered far more likely, due to entropic favourability, that the transcript *m*RNA would not undergo this conformational change, competing with the linearized *ds*DNA present within the system. This preference of *m*RNA to reside in aqueous solution, rather than associating with the liquid crystalline phase, is integral to the design of a continuous-flow transcription-translation device; aggregation of *m*RNA molecules upon or within the DOPE H_{II} phase would likely impede product yields through inaccessibility of the template *ds*DNA contained within the phase and reduction in the amount of aqueous phase *m*RNA able to outflow from the device.

1.3 Outline of thesis

The work presented within this thesis is concerned with the development of a transcription system, first published by Corsi *et al.* (2008)[9] utilizing the inverse hexagonal phase of the phospholipid DOPE for template *ds*DNA containment, for the intended purpose of fabricating a transcription-translation capable continuous-flow semi-biotic device using lyotropic liquid crystalline phases for *ds*DNA containment.

Chapter 2 presents the results from the experiments designed to characterize solution-based *in vitro* transcription based upon a commercially available transcription kit protocol. An optimal solution-based transcription assay protocol was developed, including specifications for the transcription assay buffer.

With the optimal solution-based transcription protocol developed, Chapter 3 characterizes the one-off transcription of linearized template *ds*DNA contained within the zwitterionic phospholipid DOPE. As part of the investigations, the partitioning of both linear *ds*DNA and *m*RNA within the system is analysed, alongside the development of an alternative method of nucleic acid partition coefficient analysis utilizing quantitative agarose gel electrophoresis.

The development of the one-off transcription protocol to allow batch transcription from linear *ds*DNA-containing liquid crystalline phases is presented in Chapter 4. Modifications were made to the protocol developed in Chapter 3 to allow optimal and prolonged batch transcription from individual *ds*DNA-containing DOPE lipid phases, with a view to developing an optimal protocol for continuous-flow transcription. The effects of sustained transcription upon the lipid phase were explored, and investigations into the effect of lipid composition and assay solution composition upon nucleic acid partitioning are reported.

Chapter 5 details the work carried out to assess the feasibility of producing a prototype continuous-flow semi-biotic device utilizing *ds*DNA-containing liquid crystalline phases. A crude continuous-flow device was fabricated using the rapid-prototyping material polydimethylsiloxane (PDMS) and some rudimentary testing to assess transcription-translation compatibility performed. A review of alternative methods of template *ds*DNA-containment is also presented in this chapter.

Conclusions based on the observations reported in this thesis are presented in Chapter 6, whilst supplementary experimental details are presented in the Annexes.

1.4 References

1. Attard, G. S. Semibiotics.org. (2008). at <http://www.semibiotics.org/cms/>

2. Promega. Eukaryotic Cell-Free Protein Expression. (2014). at <http://www.promega.co.uk/products/protein-expression-and-mass-spectrometry/eukaryotic-cell-free-protein-expression/>

3. New England Biolabs. PURExpress In Vitro Protein Synthesis Kit. (2014). at <https://www.neb.com/products/e6800-purexpress-invitro-protein-synthesis-kit>

4. Invitrogen. Overview of the Expressway Cell-Free Expression Systems. (2014). at <http://tools.lifetechnologies.com/content/sfs/brochures/B-062313-Xprsswy_Bro_fin.pdf>

5. Promega. Cell-Free Expression. (2009). at <http://www.promega.com/literature/Brochures/Proteomics/Cell-Free Expression.pdf>

6. Nirenberg, M. W. & Matthaei, J. H. The dependence of cell-free protein synthesis in E. coli upon naturally occurring or synthetic polyribonucleotides. *Proc. Natl. Acad. Sci. U. S. A.* **47,** 1588–1602 (1961).

7. Jermutus, L., Ryabova, L. A. & Plückthun, A. Recent advances in producing and selecting functional proteins by using cell-free translation. *Curr. Opin. Biotechnol.* **9,** 534–548 (1998).

8. Katzen, F., Chang, G. & Kudlicki, W. The past, present and future of cell-free protein synthesis. *Trends Biotechnol.* **23,** 150–156 (2005).

9. Corsi, J. *et al.* DNA that is dispersed in the liquid crystalline phases of phospholipids is actively transcribed. *Chem. Commun.* 2307–2309 (2008). doi:10.1039/b801199k

10. Kim, D. M. & Swartz, J. R. Prolonging cell-free protein synthesis with a novel ATP regeneration system. *Biotechnol. Bioeng.* **66,** 180–188 (1999).

11. Spirin, A. S., Baranov, V. I., Ryabova, L. A., Ovodov, S. Y. & Alakhov, Y. B. A continuous cell-free translation system capable of producing polypeptides in high yield. *Science (80-.).* **242,** 1162–1164 (1988).

12. Kim, D. M., Kigawa, T., Choi, C. Y. & Yokoyama, S. A highly efficient cell-free protein synthesis system from Escherichia coli. *Eur. J. Biochem.* **239,** 881–886 (1996).

13. Spirin, A. S. High-throughput cell-free systems for synthesis of functionally active proteins. *Trends Biotechnol.* **22,** 538–545 (2004).

14. Endo, Y. & Sawasaki, T. High-throughput, genome-scale protein production method based on the wheat germ cell-free expression system. *J. Struct. Funct. Genomics* **5,** 45–57 (2004).

15. Sawasaki, T. *et al.* A bilayer cell-free protein synthesis system for high-throughput screening of gene products. *FEBS Lett.* **514,** 102–105 (2002).

16. Kim, D. M. & Choi, C. Y. A semicontinuous prokaryotic coupled transcription/translation system using a dialysis membrane. *Biotechnol. Prog.* **12,** 645–649 (1996).

17. Kim, D. M. & Swartz, J. R. Prolonging cell-free protein synthesis by selective reagent additions. *Biotechnol. Prog.* **16,** 385–390 (2000).

18. Michel-Reydellet, N., Calhoun, K. & Swartz, J. Amino acid stabilization for cell-free protein synthesis by modification of the Escherichia coli genome. *Metab. Eng.* **6,** 197–203 (2004).

19. deMello, A. & Morgan, H. 10th Anniversary Issue: UK. *Lab Chip* **11,** 1191–1192 (2011).

20. Whitesides, G. M. The origins and the future of microfluidics. *Nature* **442,** 368–373 (2006).

21. Regehr, K. J. *et al.* Biological implications of polydimethylsiloxane-based microfluidic cell culture. *Lab Chip* **9,** 2132–2139 (2009).

22. Duffy, D. C., McDonald, J. C., Schueller, O. J. A. & Whitesides, G. M. Rapid prototyping of microfluidic systems in poly(dimethylsiloxane). *Anal. Chem.* **70,** 4974–4984 (1998).

23. Khandurina, J. & Guttman, A. Bioanalysis in microfluidic devices. *J. Chromatogr. A* **943,** 159–183 (2002).

24. Andersson, H. & Van den Berg, A. Microfluidic devices for cellomics: A review. *Sensors Actuators, B Chem.* **92,** 315–325 (2003).

25. Zhang, C., Xu, J., Ma, W. & Zheng, W. PCR microfluidic devices for DNA amplification. *Biotechnol. Adv.* **24,** 243–284 (2006).

26. Gulati, S. *et al.* Opportunities for microfluidic technologies in synthetic biology. *J. R. Soc. Interface* **6 Suppl 4,** S493–506 (2009).

27. Dittrich, P. S., Jahnz, M. & Schwille, P. A new embedded process for compartmentalized cell-free protein expression and on-line detection in microfluidic devices. *Chembiochem* **6,** 811–814 (2005).

28. Courtois, F. *et al.* An integrated device for monitoring time-dependent in vitro expression from single genes in picolitre droplets. *Chembiochem* **9,** 439–446 (2008).

29. Khnouf, R., Beebe, D. & Fan, Z. Cell-free protein expression in a microchannel array with passive pumping. *Lab Chip* **9,** 56–61 (2009).

30. Hunt, A. N., Clark, G. T., Attard, G. S. & Postle, A. D. Highly saturated endonuclear phosphatidylcholine is synthesized in situ and colocated with CDP-choline pathway enzymes. *J. Biol. Chem.* **276,** 8492–8499 (2001).

31. Luzzati, V. & Tardieu, A. Lipid phases: structure and structural transitions. *Annu. Rev. Phys. Chem.* **25,** 79–94 (1974).

32. Tate, M. W., Eikenberry, E. F., Turner, D. C., Shyamsunder, E. & Gruner, S. M. Nonbilayer phases of membrane lipids. *Chem. Phys. Lipids* **57,** 147–164 (1991).

33. Gruner, S., Cullis, P. & Hope…, M. Lipid polymorphism: the molecular basis of nonbilayer phases. *Annu. Rev. …* **14,** 211–238 (1985).

34. Tardieu, A., Luzzati, V. & Reman, F. Structure and polymorphism of the hydrocarbon chains of lipids: a study of lecithin-water phases. *J. Mol. Biol.* **75,** 711–733 (1973).

35. Marsh, D. *Handbook of Lipid Bilayers*. (CRC Press, 1990).

36. Alberts, B. *et al. Molecular Biology of The Cell*. (Garland Publishing, 1994).

37. Alessenko, A. V & Burlakova, E. B. Functional role of phospholipids in the nuclear events. *Bioelectrochemistry* **58,** 13–21 (2002).

38. Martelli, A. M. *et al.* Metabolism and signaling activities of nuclear lipids. *Cell. Mol. Life Sci.* **61,** 1143–1156 (2004).

39. McKiernan, A., MacDonald, R. & MacDonald…, R. Cytoskeletal protein binding kinetics at planar phospholipid membranes. *Biophys. J.* **73,** 1987–1998 (1997).

40. Albi, E. & Viola Magni, M. P. The role of intranuclear lipids. *Biol. Cell* **96,** 657–667 (2004).

41. Odom, A. R., Stahlberg, A., Wente, S. R. & York, J. D. A role for nuclear inositol 1,4,5-trisphosphate kinase in transcriptional control. *Science (80-.).* **287,** 2026–2029 (2000).

42. Irvine, R. F. Nuclear lipid signalling. *Nat. Rev. Mol. cell Biol.* **4,** 349–360 (2003).

43. Seddon, J. M. Structure of the inverted hexagonal (HII) phase, and non-lamellar phase-transitions of lipids. *Biochim. Biophys. Acta* **1031,** 1–69 (1990).

44. Ghosh, A. & Bansal, M. A glossary of DNA structures from A to Z. *Acta Crystallogr. Sect. D, Biol. Crystallogr.* **59,** 620–626 (2003).

45. Rich, A. DNA comes in many forms. *Gene* **135,** 99–109 (1993).

46. Koltover, I., Salditt, T., Rädler, J. O. & Safinya, C. R. An inverted hexagonal phase of cationic liposome-DNA complexes related to DNA release and delivery. *Science (80-.).* **281,** 78–81 (1998).

47. Steitz, T. A. Visualizing polynucleotide polymerase machines at work. *EMBO J.* **25,** 3458–3468 (2006).

48. Wynveen, A., Lee, D. J., Kornyshev, A. A. & Leikin, S. Helical coherence of DNA in crystals and solution. *Nucleic Acids Res.* **36,** 5540–5551 (2008).

Chapter 2:

Optimization of the Transcription Assay

2. Optimization of the Transcription Assay

2.1 Rationale

It is known that 'naked nuclei', have lipid content in the region of 5-14% of the total cell content;[1] it is reasonable, therefore, to postulate that the lipid content within cell nuclei is arranged into such a structure that it bears relation to lyotropic liquid crystalline phases, brought on by the self-organization of the lipids in an environment with low water content. Lyotropic liquid crystalline phases form as the concentration of lipid increases past the ordered structures of micelles and lamellar phases; it is therefore feasible, and indeed likely, that lyotropic liquid crystalline phases could be formed within cell nuclei, due to the low concentration of water and presence of substantive quantities of lipid. With this in mind, Corsi *et al.* postulated that 'if the cell nucleus has a liquid crystalline mesostructure that is the result of lipid self-assembly, then the normal nuclear functions (and in particular transcription) should be able to occur within the orientationally and spatially ordered environment that is characteristic of lyotropic liquid crystalline phases'.[2] In the same publication, Corsi reports results detailing how linearized T7*luc ds*DNA can be transcribed from within the inverse hexagonal (H_{II}) liquid crystalline phase of DOPE, supporting the theory that lyotropic liquid crystalline phases should be capable of supporting transcription.

Whilst it has already been reported that linearized *ds*DNA remains transcriptionally active when contained within H_{II} phase DOPE, details of the effect of transcription components upon the transcriptional activity, or indeed the optimal transcription assay parameters, have yet to be published. It was therefore deemed prudent that, prior to detailed investigation into the transcription assay parameters in the presence of liquid crystalline phases, investigation into the solution-based optimal transcription assay parameters should be undertaken. This would allow for identification of the optimum transcription parameters for linearized *ds*DNA in solution, which would then assist with determination of the optimal parameters for transcription from linearized *ds*DNA contained within lyotropic liquid crystalline phases.

2.2 Methodology

2.2.1 Introduction to transcription

In the research presented within this thesis, transcription of *ds*DNA was performed using T7 RNA polymerase (figure 2.1); a 98 kDA single subunit enzyme that catalyses the synthesis of mRNA in the 5' to 3' direction when in the presence of a *ds*DNA template containing a T7 phage promoter. The publication from Corsi *et al.* (2008) concerning the transcription of linearized *ds*DNA contained within the H_{II} phase of DOPE made use of this highly selective polymerase for their *in vitro* transcription studies, transcribing a linearized T7 plasmid encoding for firefly luciferase. T7 RNA polymerase is able to produce good quality biologically active mRNA, thus making the mRNA suitable for *in vitro* translation, which would be required as part of a coupled transcription/translation cassette within a semi-biotic device capable of protein synthesis.

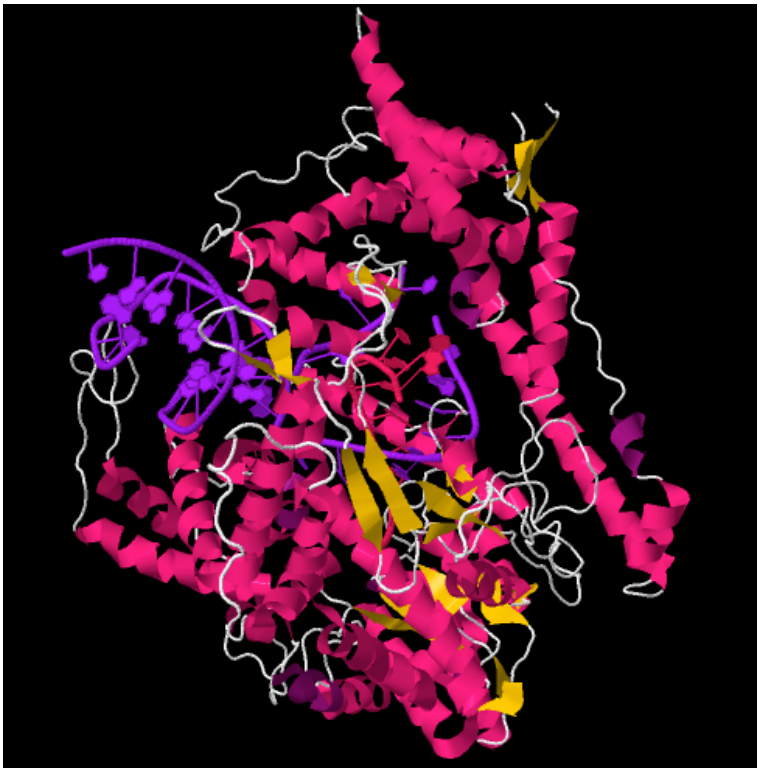

Figure 2.1 Structural basis for the transition from initiation to elongation during transcription in T7 RNA polymerase (RCSB protein databank file 1MSW), determined by Yin *et al.*[3] Structure identification: alpha helices (pink); beta strands (gold); loops (white); template DNA (purple). Image produced using Jmol: an open-source Java viewer for chemical structures in 3D. http://www.jmol.org/

T7 RNA polymerase and its transcription cycle has been well documented, which is ideal for *in vitro* investigation into a system involving the addition of lyotropic liquid

crystalline phases. The T7 RNA polymerase transcription process starts the recognition of a specific promoter sequence (TAATACGACTCACTATAGGGAGA, 5' → 3') by the T7 RNA polymerase. With the promoter sequence recognized, the template *ds*DNA becomes bound by the β-hairpin specificity loop and melting of the *ds*DNA occurs, alongside the transition of the DNA from the binding to the initiation region. An unstable initiation complex is formed, which synthesizes and then releases abortive transcripts of length 2-8 nt (the abortive phase). During the abortive phase, the polymerase unit maintains contact with the binding region of the T7 promoter whilst the initiation complex moves downstream, causing template *ds*DNA to accumulate in the active site.[4] Isomerisation of the complex post-abortive phase results in the formation of a stable elongation complex, along with the release of upstream promoter contact.[5,6] The specific mechanism of transformation between the initiation and elongation complex are still debated; however, there are two main proposed mechanisms, namely the 'scrunching model', where the RNA-DNA hybrid remains at a roughly fixed length of 3 nucleotides, or the 'inchworm model', where the RNA-DNA hybrid grows in length with the polymerase rearranging to accommodate accordingly.[7,8] The transcription cycle finishes with the process of termination; transcript mRNA and the template *ds*DNA is released from the T7 RNA polymerase complex. Prior to another cycle of transcription being able to take place, the polymerase must revert to the initiation complex structure from the conformation of the elongation complex.[9] For transcription experiments utilizing *lin*T7luc *ds*DNA, the termination of transcription occurs when the T7 RNA polymerase reaches the end of the linearized template *ds*DNA, due to the lack of a T7 terminator in the plasmid (thus preventing regulation of termination *via* transcription termination signals).

Although there is an abundance of commercially available transcription kits available, each coming with their own complimentary reaction buffer, the key components required for such buffers are well documented which allows for the easy modification and in-house production of a bespoke transcription buffer.[10,11] This is particularly advantageous for analytical transcription experiments, where the transcriptional yield needs to be quantified and then contrasted with other experiments under analogous incubation conditions – something that would become problematic if using a commercially-available transcription buffer solution that later became obsolete or had its composition revised. Table 2.1 details the composition of a typical transcription buffer solution, based upon the buffer compositions reported by Alunni-Fabbroni *et al.,*[10] Milligan *et al.,*[11] and analysis of the composition of several commercially available transcription buffer solutions.

Table 2.1 Typical composition of a transcription reaction buffer solution.

Component	Final concentration
Tris buffer	40 mM
$MgCl_2$	25 mM
Dithiothreitol (DTT)	10 mM
Spermidine	2.5 mM
Triton X-100	0.01% v/v

The presence, or indeed absence, of each of the transcription buffer components detailed previously can have a profound effect upon the transcriptional activity observed from an assay. For example, the ionic concentration of transcription reagent species, such as spermidine and magnesium chloride, need to be optimized to ensure optimal transcription yield. Spermidine and magnesium chloride both play vital roles in the transcription of template *ds*DNA by T7 RNA polymerase; spermidine, for its role in stimulating transcription by T7 RNA polymerase,[12] and $MgCl_2$, for its structural role in the two metal ion ligation required in the catalytic mechanism of T7 RNA polymerase (Figure 2.2).[13,14] However, presence of ionic species at too higher concentration could lead to reduction in transcriptional yield or indeed inhibition of transcription completely. For example, it is already known that non-promoter binding of T7 RNA polymerase to template *ds*DNA is inhibited at concentrations of 40 mM sodium chloride.[15]

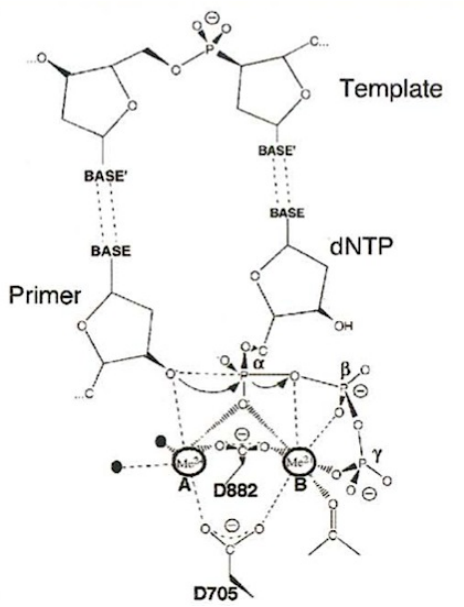

Figure 2.2 The two metal ion mechanism of polynucleotide polymerases, shown here with two divalent metal cations (Me^{2+}), as proposed by Doublié *et al.*[14] The active site features two metal ions that stabilize the resulting pentacoordinated transition state. Metal ion A activates the primer's 3'-OH for attack on the α-

phosphate of the dNTP. Metal ion B plays the dual role of stabilizing the negative charge that builds up on the leaving oxygen, and chelating the β- and γ-phosphates. Reproduced, with permission from Elsevier, from Brautigam *et al.* in *Curr. Opin. Struct. Biol.* **8,** 54-63 (1998).[16]

2.2.2 Transcription from *lin*T7luc *ds*DNA

The plasmid used for the transcription studies previously reported by Corsi *et al.* (2008) was pT7luc (Figure 2.1),[2] a vector encoding for the firefly luciferase luminescent protein with a T7 promoter region.

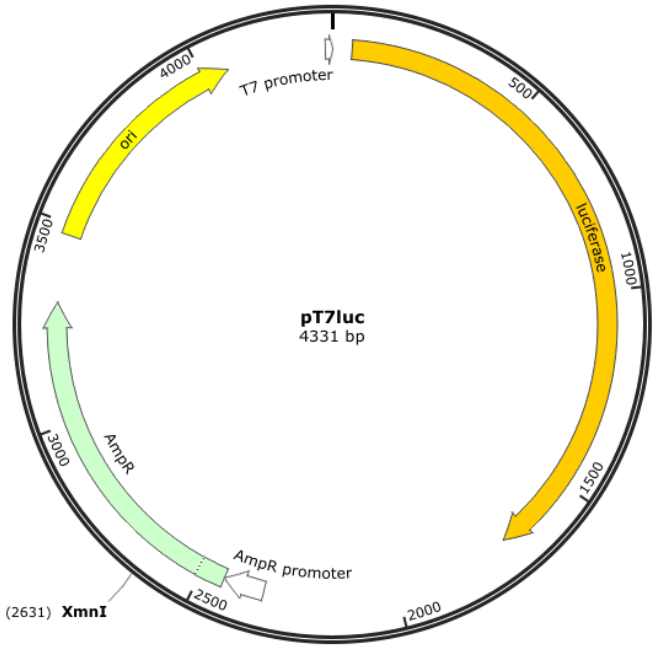

Figure 2.3 Plasmid map of pT7luc *ds*DNA (4331 bp); luciferase, ampicillin resistance (AmpR) and origin of replication (ori) sequences highlighted. pT7luc *ds*DNA is restricted using *XmnI* restriction enzyme, cutting at the 2631 bp position (highlighted, within the AmpR region), to produce *lin*T7*luc ds*DNA.

Due to the narrow pore diameter (4 nm) of the channels within inverse hexagonal phase DOPE, the circular plasmid was linearized using XmnI at the 2631 bp position. This linearization of pT7luc (producing *lin*T7luc *ds*DNA) ensured that the strands of *ds*DNA were not only structurally able to reside within the H_{II} phase pores of DOPE, but that they would give rise to an mRNA product of uniform length (2631 bp) when transcribed by T7 RNA polymerase, which would be easily identifiable by post-transcription gel electrophoresis of the transcription product. Note that linearization of the pT7luc vector using the restriction endonuclease XmnI means that the T7 promoter sequence would be located 1700 bp from the cleaved 5' end of the linear strand of *ds*DNA, towards the centre of the *ds*DNA strand.

2.2.3 Transcription from *lin*T7GFP and *lin*pRSET-EmGFP *ds*DNA

The overall vision for the semi-biotic device concept was for it to eventually have the potential to produce not only transcript mRNA, as a standalone synthetic RNA foundry, but to also utilize it as a synthetic peptide foundry, with the ability to produce a chosen protein structure. Incorporating the device with an integrated detection, decision and response (d^2r) system would thus allow the device to be able to detect the concentration of a specific target molecule, make a decision based upon the detection reading and then respond appropriately to it.

With the proposed end use of the semi-biotic device in mind, it was therefore important that in future stages of development that the biological products produced by the device, whether mRNA or protein, should be easily quantifiable. The decision was therefore made to move away from using pT7luc to produce the linearized *ds*DNA required for compartmentalization within liquid crystalline phases, and instead utilize a plasmid encoding for a protein that could be easily quantified using fluorescence, for example green fluorescent protein (GFP).

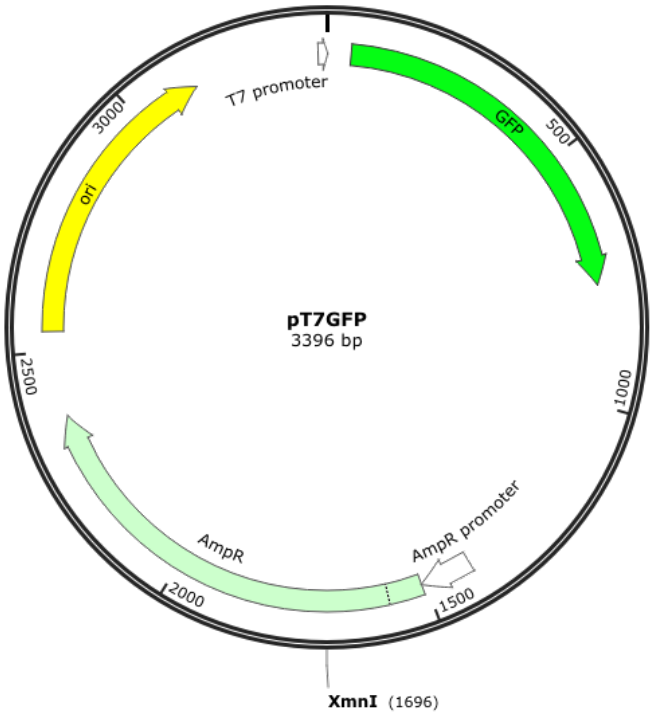

Figure 2.4 Plasmid map of pT7GFP *ds*DNA (3396 bp); green fluorescent protein (GFP), ampicillin resistance (AmpR) and origin of replication (ori) sequences highlighted. pT7GFP *ds*DNA is restricted using *XmnI* restriction enzyme, cutting at the 1696 bp position (highlighted, within the AmpR region), to produce *lin*T7*GFP ds*DNA.

Research by Black *et al.* (2010) has previously been published reporting the use of pT7GFP *ds*DNA (see Figure 2.2) in experiments where the linearized *ds*DNA has been successfully partitioned within DOPE-based liquid crystalline phases, indicating, as one would expect, that the use of an alternative linearized plasmid has no detrimental effect upon *ds*DNA partitioning.[17] Whilst the pT7GFP plasmid would have been suitable for use within the research presented herein, there are numerous commercially available plasmids within the life sciences market, encoding for fluorescent proteins, which have been enhanced for improved transcription, translation and protein purification. Figure 2.3 shows the plasmid map of Invitrogen™ pRSET-EmGFP *ds*DNA, which encodes for emerald green fluorescent protein, whilst also containing the ampicillin resistance gene and T7 promoter sequence (as per pT7luc and pT7GFP). Unlike pT7luc and pT7GFP, however, pRSET-EmGFP contains the 6xHis tag, allowing for simplified protein purification *via* commercially available metal binding resins.

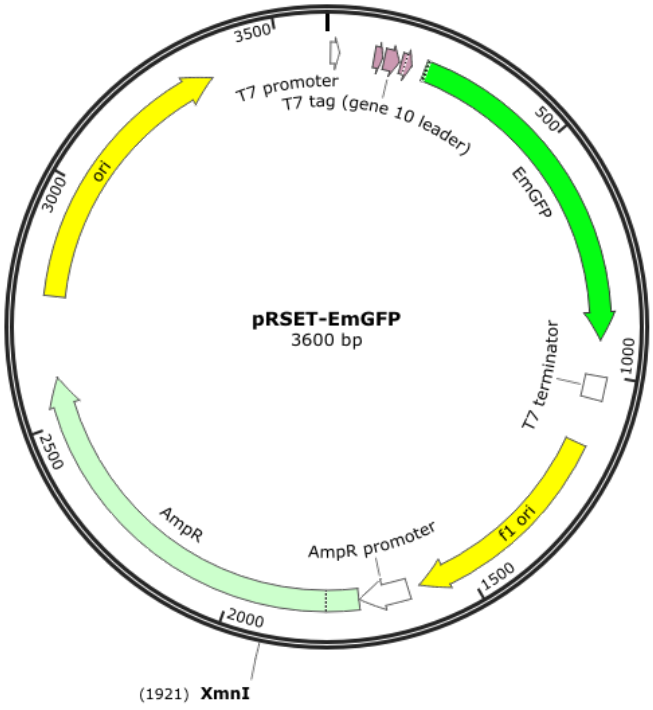

Figure 2.5 Plasmid map of Invitrogen™ pRSET-EmGFP *ds*DNA (3600 bp); emerald-green fluorescent protein (EmGFP), ampicillin resistance (AmpR) and origin of replication (ori and f1 ori) sequences highlighted. pRSET-EmGFP *ds*DNA is restricted using *XmnI* restriction enzyme, cutting at the 1921 bp position (highlighted, within the AmpR region), to produce *lin*pRSET-EmGFP *ds*DNA.

The Invitrogen™ vector pRSET-EmGFP (Figure 2.3) was chosen for use throughout the work reported in this research, due to its similarity to the vectors used in previously reported work on the partitioning of linear *ds*DNA within DOPE-based liquid crystalline phases and its suitability for easy UV quantification and purification of the emerald green fluorescent protein it encodes for. pRSET-EmGFP is 3600 bp in length, contains:

a bacteriophage T7 promoter and terminator; an N-terminal fusion peptide encoding 6xHis tag; emerald green fluorescent protein (EmGFP) gene; ampicillin resistance gene; pUC origin for high-copy replication in E. coli. EmGFP has an excitation wavelength of 487 nm, with emission at 509 nm. Note that linearization of the pRSET-EmGFP vector using the restriction endonuclease XmnI means that the T7 promoter sequence would be located 1600 bp from the cleaved 5' end of the linear strand of *ds*DNA, towards the centre of the *ds*DNA strand (as per *lin*T7luc *ds*DNA).

2.2.4 Transcription assay parameters

The characterisation of the solution-based transcription assay was important to investigate prior to commencing research into transcriptional behaviour in the presence of lyotropic liquid crystalline phases. Although transcription using bacteriophage DNA polymerases is well studied, the study of transcription from *ds*DNA contained within lyotropic liquid crystalline phases is a new and novel area of research, being first reported by Corsi *et al.* in 2008.[2] As stated in section 2.2.1, there are a number of components required for transcription of template *ds*DNA by T7 RNA polymerase to successfully occur. Through characterizing the behaviour of the solution-based transcription system, it offered a complete set of transcription data in the absence of liquid crystalline phases to which the results from the subsequent transcription in the presence of liquid crystalline phase experiments could be compared and contrasted.

The key parameters that were varied when investigating the impact upon transcriptional yield from solution-based transcription assays were:

- linear template *ds*DNA concentration;
- T7 RNA polymerase concentration;
- assay incubation time;
- assay incubation temperature;
- magnesium chloride concentration;
- total assay reaction volume (maintaining constant component concentration).

The standard solution-based transcription assay composition is detailed in table 2.2, with a standard assay volume of 20 µL and standard incubation period of 2 hours at 37 °C in a thermostatically-controlled water bath.

Table 2.2 Standard solution-based transcription assay composition.

Component	Final concentration
*lin*pRSET-EmGFP template *ds*DNA	0.05 μg μL^{-1}
rNTPs	20 mM
T7 RNA polymerase	2.5 U μL^{-1} (~21 nM)
Tris buffer	40 mM
$MgCl_2$	25 mM
Dithiothreitol (DTT)	10 mM
Spermidine	2.5 mM
Triton X-100	0.01% v/v
RNAsin	10 mM

2.2.5 Methods of analysis

2.2.5.1 Transcriptional yield

UV-visible spectrophotometry was performed using a NanoDrop ND-1000 instrument to quantify the concentration of all mRNA samples purified. For analytical purposes, measurements using the ND-1000 were recorded in triplicate by loading a fresh aliquot of each sample a total of three times, cleaning the ND-1000 arm between replicates. Post-measurement, the mean concentration and standard deviation was calculated. Using the NanoDrop nucleic acid software, measurements were processed using type ratio RNA-40 for purified mRNA samples. Concentration values were recorded in units of ng μL^{-1}, along with associated 260/280 and 260/230 sample absorbance ratios as a measure of sample purity and integrity.

A 260/280 ratio of ~2.0 is generally accepted as pure for RNA, whilst a 260/230 ratio appreciably lower than 1.8 may indicate the presence of co-purified contaminants.

2.2.5.2 Agarose gel electrophoresis

DNA and RNA samples were routinely tested for purity and integrity using agarose gel electrophoresis throughout the work presented in this chapter. Protocols for both DNA and RNA gel electrophoresis can be found in the appendices of this thesis.

2.3 Optimizing the parameters of the transcription assay

2.3.1 Effect of DNA template concentration upon RNA yield

Investigation into the effect of linear template *ds*DNA contribution upon solution-based transcription yield was carried out, allowing for a calibration plot comparing template *ds*DNA concentration to mRNA yield to be produced (Figure 2.6). This calibration plot could then be used for a number of investigative purposes, for example: when considering the amount of linear *ds*DNA to preload lyotropic liquid crystalline phases with during later stages of research; estimating the amount of accessible template *ds*DNA to produce an observed mRNA yield from transcription using DNA-containing liquid crystalline phases; determining if template *ds*DNA concentration was a limiting factor in the transcription reaction under standard conditions.

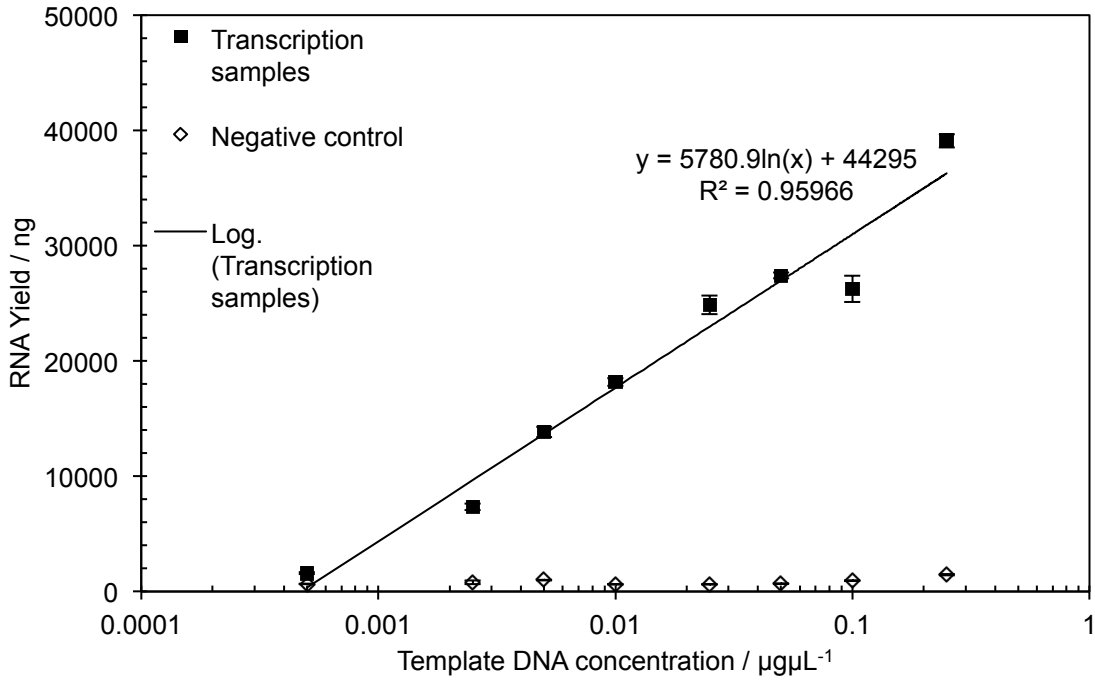

Figure 2.6 mRNA yield from solution-based transcription assay, varying the concentration of pRSET-EmGFP template *ds*DNA available for transcription. The transcription assay was incubated for 2 hours (37 ˚C). Results are shown for solution-based transcription samples (black squares) and negative control samples (no T7 RNA polymerase, hollow diamonds). RW/6295/22

Data from the incubation of the transcription assays for 2 hours (37 ˚C) when varying the concentration of linear template *ds*DNA present in the reaction (Figure 2.6) indicates that, under the standard conditions detailed in section 2.2.4, template *ds*DNA concentration is limiting the yield of mRNA. The standard conditions suggest a

template *ds*DNA concentration of 0.05 μgμL^{-1}, yet for an incubation period of 2 hours (37 ˚C), increasing the template concentration produces a linear increase in the amount of mRNA produced in a reaction of equal volume and transcription component composition. Even at the maximum template concentration trialled, 0.25 μgμL^{-1}, no apparent plateau in the mRNA yield from the 2 hour transcription reactions was observed. These results suggested that, if required, mRNA yields could be easily increased through provision of additional linear template *ds*DNA within the transcription reaction composition.

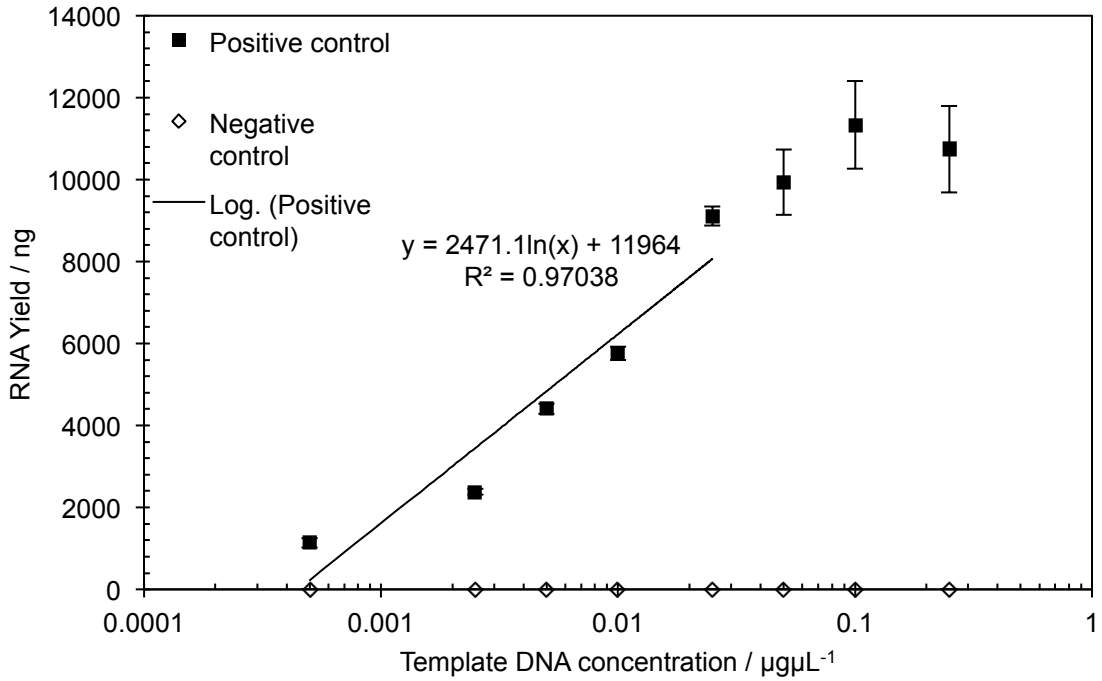

Figure 2.7 mRNA yield from solution-based transcription assay, varying the amount of linear pRSET-EmGFP template *ds*DNA available for transcription. The transcription assay was incubated for 40 minutes (37 ˚C). Results are shown for solution-based transcription samples (black squares) and negative control samples (no T7 RNA polymerase, hollow diamonds). RW/6456/09

Decreasing the incubation period from 2 hours to 40 minutes (37 ˚C), as shown in Figure 2.7, a similarly linear trend between the template *ds*DNA concentration and mRNA yield is observed. However, towards the higher template *ds*DNA concentrations trialled (>0.05 μgμL^{-1}), an apparent threshold in the maximum mRNA yield is achieved, suggesting that for this shorter incubation time, the template *ds*DNA concentration is no longer the factor limiting mRNA yield.

2.3.2 Effect of T7 RNA polymerase concentration upon RNA yield

The concentration of T7 RNA polymerase was varied to ensure that batch transcription experiments utilized the optimum concentration of polymerase, ensuring a good balance between mRNA yield and overall cost per transcription reaction microlitre.

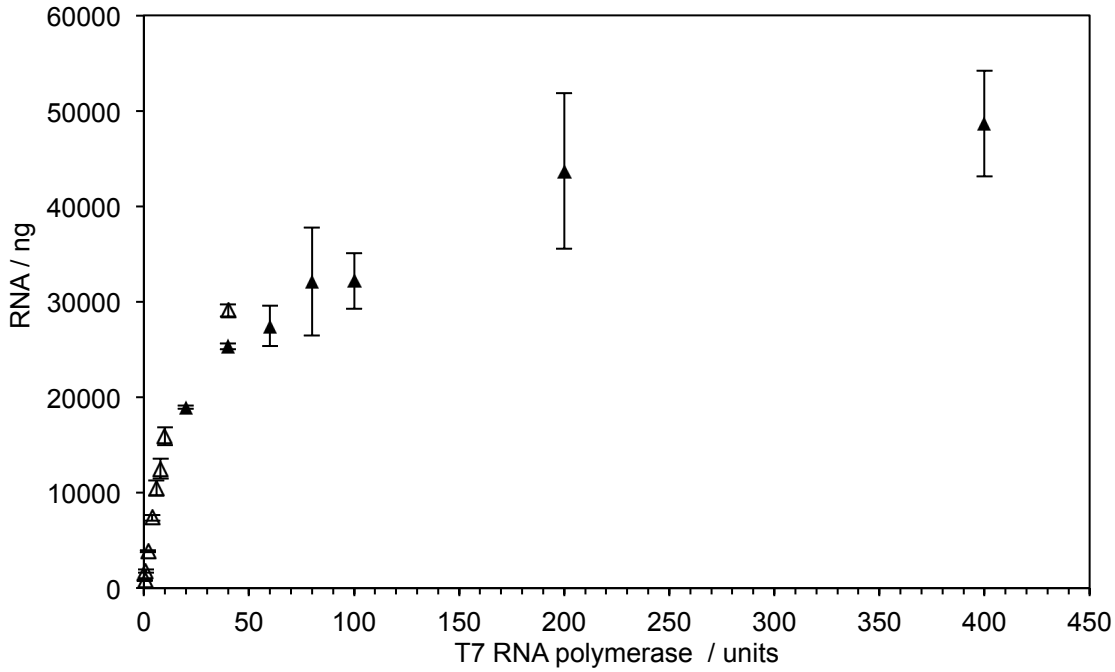

Figure 2.8 mRNA yield from solution-based transcription assay, varying the concentration of T7 RNA polymerase added to the transcription samples. The transcription assay was incubated for 2 hours (37 °C). Results are shown for low concentration polymerase samples (hollow triangles) and high concentration polymerase samples (black triangles). RW/6456/12

The manufacturer's recommended concentration for T7 RNA polymerase (New England Biolabs, Inc., USA) is 2.5 units per transcription reaction microlitre, equating to 50 units of polymerase per 20 microlitre transcription reaction. Within experimental error, doubling this concentration of T7 RNA polymerase to 5 units per microlitre produces an increase in mRNA yield of ~27%; further increases in the polymerase concentration do produce additional increases in mRNA yield, however, increasing the polymerase concentration from the recommended amount by four-fold or even eight-fold could potentially lead to less repeatability in results, due to significantly increased steric crowding within the transcription solution, and would make a continuous-flow transcription system using such high polymerase concentrations prohibitively expensive.

2.3.3 Effect of incubation time upon RNA yield

A time-course experiment to assess the kinetic effect of T7 RNA polymerase concentration upon mRNA yield was performed, giving insight into the rate at which transcription occurs during incubation (37 ˚C) under standard transcription conditions (20 µL total reaction volume, 25 mM $MgCl_2$, 1 µg linear template *ds*DNA, 50 units T7 RNA polymerase).

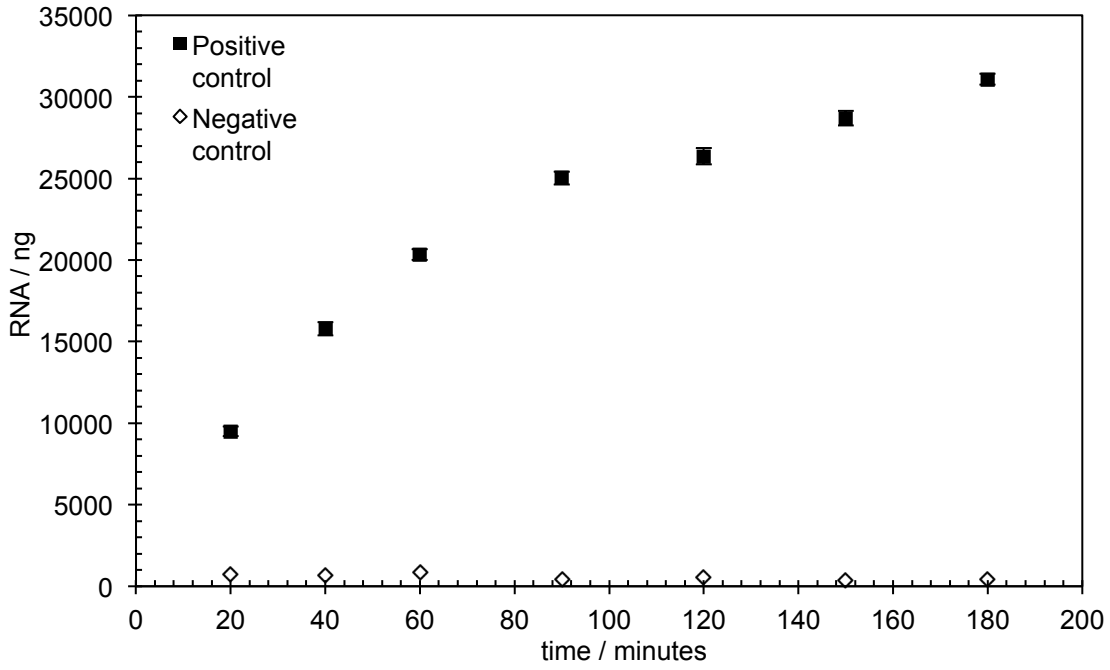

Figure 2.9 mRNA yield from solution-based transcription assay, varying the incubation period of the transcription samples. The transcription assay was incubated, for the period shown above, at 37 ˚C. Results are shown for positive control samples (black squares) and negative control samples (no T7 RNA polymerase, hollow diamonds). RW/6147/17

The standard incubation period for solution-based transcription, based upon previous research carried out by Corsi *et al.*, is 2 hours. As can be seen from Figure 2.9, this offers a significant yield of mRNA from a 20 µL transcription reaction containing 25 mM $MgCl_2$, 50 units of T7 RNA polymerase and 1 µg of linear template *ds*DNA. The fastest rate of transcription occurs during the incubation period up to 60 minutes; the rate of mRNA production slows beyond this time, suggesting an eventual plateau in the amount of mRNA yielded from the reaction. 30 minute additional increments in incubation period, from 90 minutes onwards, do not produce significant increases in mRNA yield, when compared to the initial linear rate of mRNA production, with incremental increases in mRNA yield between 5-9% observed.

2.3.4 Effect of incubation temperature upon RNA yield

Incubation temperature, and its effect upon the mRNA yield from transcription, was investigated during the precursory research into solution-based transcription, as part of the assessment into the suitability for a DOPE-based transcription system within a continuous-flow device. Any potential semi-biotic device would require a mechanism for incubation of transcription and translation assay components within the channel of the device; whilst a PDMS microfluidic device would likely offer good thermal management within the channels of the device, the assay components have to be pumped in *via* tubing connected to an external reagent supply source, likely fed into the device by electronically-controlled syringe pump.[18] Outside of the device channels, incubation temperatures will be much harder to control, and thus it was important to understand the effect upon the mRNA yield when the transcription assay is subjected to a variety of incubation temperatures.

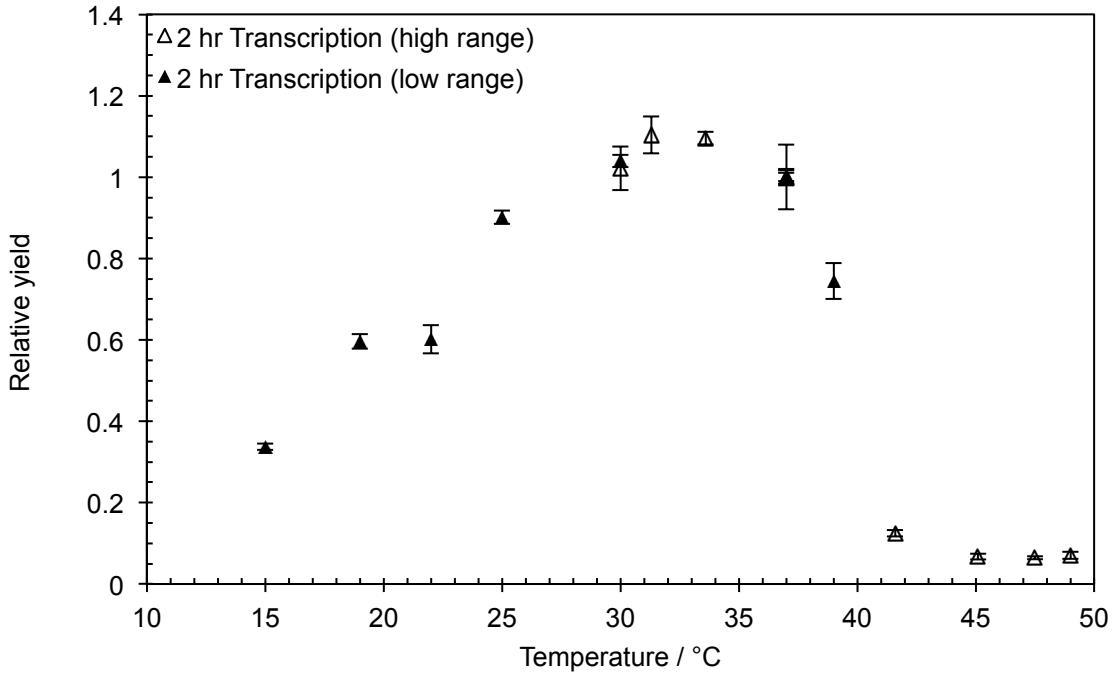

Figure 2.10 mRNA yield from solution-based transcription assay, varying the incubation temperature of the transcription samples. The transcription assay was incubated, at the temperature shown above, for 2 hours. Results are shown for high temperature samples (hollow triangles) and low temperature samples (black triangles). RW/6456/13

As would be expected, Figure 2.10 shows that increasing the assay incubation temperature above physiological temperature results in a sharp decrease in transcriptional yield, before complete loss of transcriptional activity above ~ 42 ˚C, likely due to denaturation of the T7 RNA polymerase under extreme temperature conditions. This should not present a significant issue for application of the

transcription system within a continuous-flow device, as thermostatic controls can be utilized to ensure that heating to the device is cut off at an appropriate maximum temperature threshold (38 °C). Below physiological temperature, a drop of ~ 7 °C can be tolerated with no significant effect upon the transcriptional yield, which is encouraging when considering application of the system to within a semi-biotic device. These results indicate that any marginal reductions in incubation temperature should have an unappreciable effect upon mRNA yield, allowing a reduced warm-up and thermal equilibration period for the device.

2.3.5 Effect of assay concentration of $MgCl_2$ upon RNA yield

The presence of magnesium ions within the transcription reaction is of the utmost importance; divalent metal cations, in this case Mg^{2+} ions, are required to act as ligands in the two metal ion transcription mechanism of T7 RNA polymerase.[13,14] A reduction in the number of Mg^{2+} cations available in the transcription solution would be expected to act as a limiting factor in the transcription of the linear template *ds*DNA by T7 RNA polymerase, as two divalent metal cations are required for each polymerase molecule during transcription; thus any transcription assay composition where the number of polymerase molecules present in the reaction is greater than half the number of Mg^{2+} cations would mean that it was impossible for all polymerase molecules to be transcriptionally active at any one point in time. Conversely, a small excess of available Mg^{2+} cations would be expected to be beneficial to the transcriptional reaction, with increased transcriptional yields observed, as each polymerase molecule should have two divalent magnesium cations readily available for interaction as ligands at all times during the incubation period.

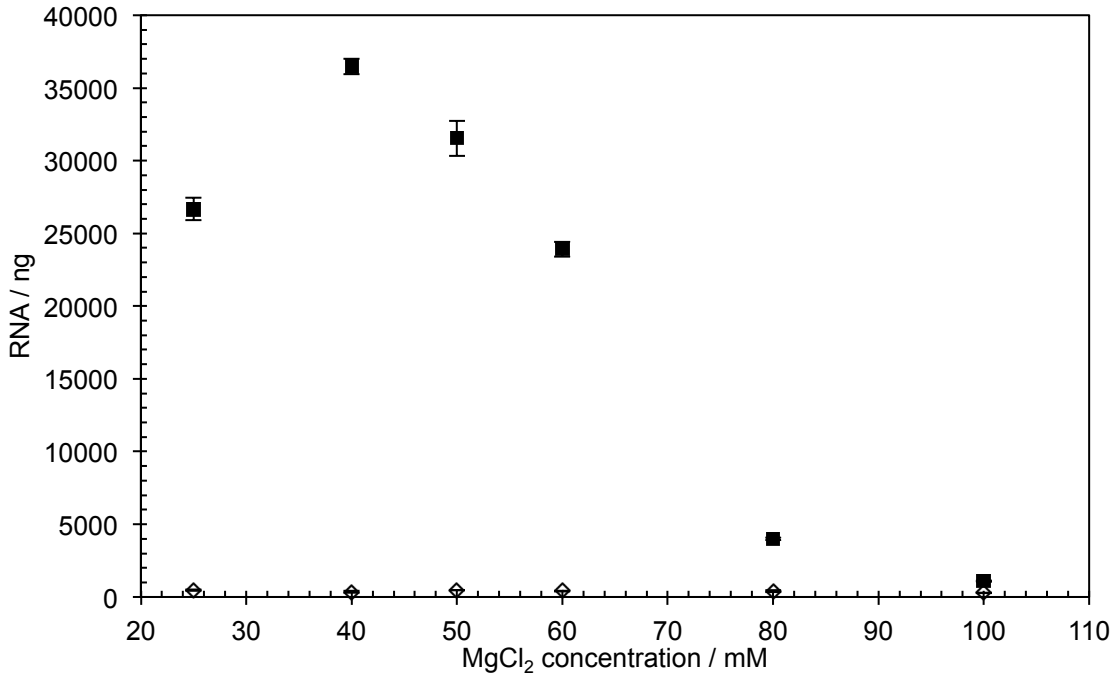

Figure 2.11 mRNA yield from solution-based transcription assay, varying the total concentration of $MgCl_2$ present in the transcription samples. The transcription assay was incubated for 2 hours (37 °C). Results are shown for transcription samples (black squares) and negative control samples (no T7 RNA polymerase, hollow diamonds). RW/6295/19

Recommendation for the standard reaction conditions, as described in section 2.2.4, is that the total concentration of $MgCl_2$ within the reaction should be 25 mM. As can be seen in Figure 2.11, increasing the concentration of $MgCl_2$ in the transcription reaction to ~40 mM significantly increases the amount of mRNA produced when maintaining otherwise standard reaction conditions (2 h, 37 °C, 1 µg linear template *ds*DNA), yielding 36.8% more mRNA when compared to using an $MgCl_2$ concentration of 25 mM. Incremental increases in the $MgCl_2$ concentration beyond 40 mM lead to a linear decrease in the amount of mRNA yielded, for $MgCl_2$ concentrations from ~50 mM to ~80 mM, beyond which negligible yields of mRNA are achieved. At an increased $MgCl_2$ concentration of ~55 mM, mRNA yields observed are comparable with those seen when only 25 mM $MgCl_2$ is present in the reaction mixture. One potential explanation for the decrease in mRNA yield observed above $MgCl_2$ concentrations beyond 40 mM is that the presence of such a high quantity of Mg^{2+} cations is significantly reducing the ability of the polymerase to bind effectively to the linear template *ds*DNA, as it has already been reported that high ionic concentrations inhibit the non-promoter interior site binding of the polymerase to the template *ds*DNA.[15]

Any inhibitory effect upon polymerase-*ds*DNA binding efficiency is likely to be further exacerbated due to increased stability of the template *ds*DNA duplex in transcription buffer solutions with elevated concentrations of divalent metal cations, such as Mg^{2+}.

*ds*DNA duplexes are known to be stabilized by mono- and di-valent cations in solution; for solutions where the concentration ratio of $[Mg^{2+}]^{0.5}/[Mon^{+}]$, where $[Mon^{+}]$ is the overall solution concentration of monovalent cations, is higher than 0.22 $M^{+1/2}$, the stabilizing effect of Mg^{2+} is dominant and determines the overall stability of the *ds*DNA duplex.[19] Higher concentrations of Mg^{2+} will increase base-stacking interactions within the *ds*DNA duplex, as the abundance of Mg^{2+} cations are able to further mask the destabilizing charge repulsion between the negatively charged phosphate backbones of the nucleic acid.[20] Increased stability of the template *ds*DNA duplex will hinder the unwinding of the DNA double helix by T7 RNA polymerase, significantly reducing the level of transcriptional activity observed. For transcription buffer solutions containing greater than 80 mM $MgCl_2$ it is likely that the template *ds*DNA duplex has been sufficiently stabilized by Mg^{2+} cations such that it is almost impossible for T7 RNA polymerase to unwind any of the template *ds*DNA and proceed with transcription, leading to the loss in transcriptional activity observed in Figure 2.11.

2.3.6 Effect of transcription assay volume upon RNA yield

Varying the volume of the transcription reaction was of notable interest, not only in preparation for the experiments investigating transcription of linear *ds*DNA contained within lyotropic liquid crystalline phases, but for the eventual development of a semi-biotic device, where transcription would likely occur in particularly small volumes of solution within the channels of the device. It was therefore interesting to investigate any potential effect upon the mRNA yield per reaction µL if the transcription reaction volume was scaled up or down, when compared to the standard transcription assay volume, as described in section 2.2.4. When the total volume of the transcription assay reaction was increased or decreased, the proportional composition of all reaction components remained constant. However, it is worth considering that the smaller the reaction volume, the greater the proportional effect of the associated pipetting error when preparing the transcription reaction from stock solutions of the required transcription components.

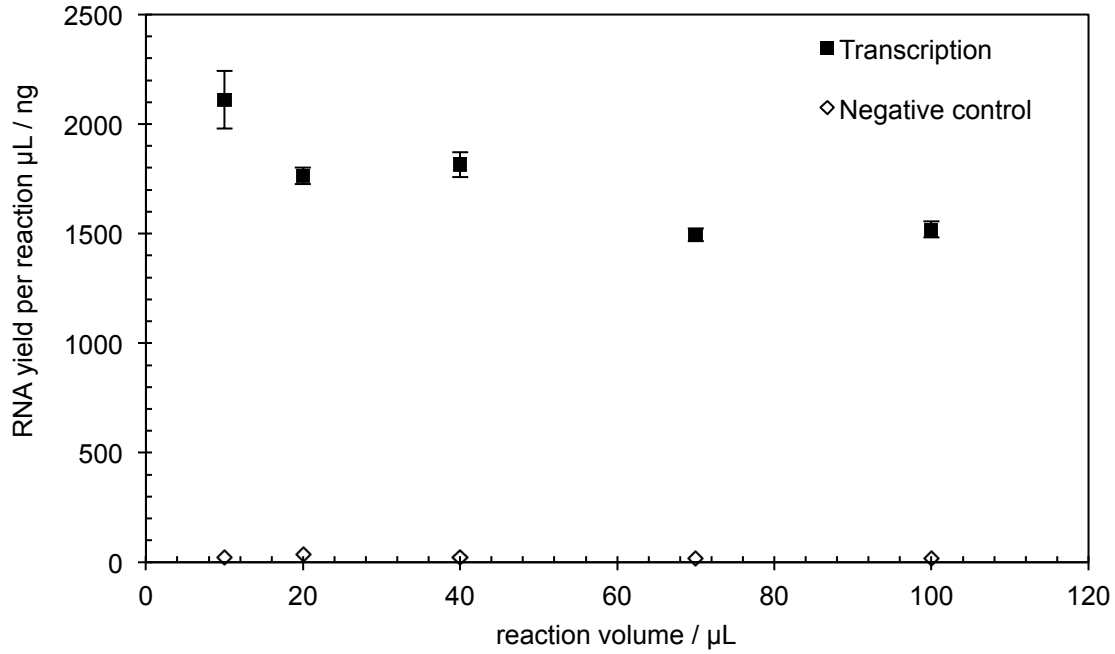

Figure 2.12 mRNA yield per µL of transcription reaction, from solution-based transcription assay, varying the total initial reaction volume. The transcription assay was incubated for 2 hours (37 °C). Results are shown for transcription samples (black squares) and negative control samples (no T7 RNA polymerase, hollow diamonds). RW/6511/10

The increase in the total transcription reaction volume to twice that recommended in the standard protocol of the T7 RNA polymerase used (from 20 µL to 40 µL) showed no appreciable difference in the mRNA yield per reaction microlitre, within experimental error (Figure 2.11). Further increases to the reaction volume (to 70 µL and then 100 µL) did appreciably reduce the yield of mRNA produced by the reaction, to approximately 85% of the mRNA yield achieved when transcription was performed under standard conditions (20 µL). The level of experimental error associated with the transcriptional yields from these larger reaction volumes remained largely consistent, despite the increase in total reaction volume. However, decreasing the total transcription reaction volume to half that recommended in the standard protocol (from 20 µL to 10 µL), not only was the level of experimental error associated with the transcription yield increased, as expected due to the increased effect of pipetting errors when measuring smaller volumes of transcription component solutions, but the amount of mRNA yielded per reaction microlitre also increased, on average by 19.7% of the yield achieved under standard conditions (20 µL).

2.4 Establishment of a reliable transcription assay

2.4.1 Optimized transcription assay parameters

A series of experiments was carried out to establish the optimal transcription assay parameters for solution phase transcription. Table 2.3 compares the initial transcription assay parameters, used by Corsi *et al.*, and the empirical optimal parameters as established by the experiments presented within this chapter.

Table 2.3 Comparison of the initial and experimentally-determined optimal parameters for solution-based transcription.

Assay parameter	Initial parameter value (Corsi *et al.*)	Optimized parameter value (empirical)
Template *ds*DNA concentration	0.05 μg μL^{-1}	0.05 μg μL^{-1}
T7 RNA polymerase concentration	2.5 U μL^{-1} (~21 nM)	2.5 U μL^{-1} (~21 nM)
Incubation time	120 min.	90-180 min.
Incubation temperature	37 ˚C	30-37 ˚C
$MgCl_2$ concentration	25 mM	40 mM
Reaction volume	20 μL	20 μL

Direct comparison of the initial parameters for solution-based transcription to the optimal parameters determined experimentally (table 2.3) highlights that modifications could be made to the incubation time, incubation temperature and concentration of $MgCl_2$ present in the transcription reaction buffer. Additional flexibility in the production of mRNA can be yielded through the ability to perform transcription within broader time and temperature constraints, without significant detriment to the transcriptional yield. A simple and cost-effective increase to the $MgCl_2$ content of the transcription reaction buffer, from 25 to 40 mM, yields an increase in solution-based transcriptional yield of 36.8% (Figure 2.11).

Modifications to the template *ds*DNA concentration, T7 RNA polymerase concentration, and reaction volume, are not necessary, as variation of these parameters yielded no significant increase in the amount of mRNA obtained from solution-based transcription.

2.5 Discussion

The experiments presented within this chapter have determined that there is some flexibility in the transcription reaction parameters, for example incubation time, incubation temperature, and concentration of divalent magnesium cations in solution, when compared to the parameters used in previously published work. By increasing the concentration of divalent magnesium cations within the transcription solution to 40 mM, transcriptional yields can be increased by almost 40%; however, considering the intended application of transcription from systems containing lyotropic liquid crystalline phases, the presence of additional salts may adversely affect the liquid crystalline phase structure, within which the template *ds*DNA for transcription is contained. Indeed, it has been reported that the presence of biological buffer solution molecules, such as $MgCl_2$, can lead to a membrane softening effect in model lipid membranes, due to interactions with the lipid headgroup regions.[21]

The broad range of temperatures over which transcription successfully occurs, whilst still producing high transcriptional yields, offers increased flexibility for the incubation of transcription reactions; it is clearly not imperative that the temperature of the system is maintained at a precise 37 °C, providing it is maintained within the temperature band encompassed between 30-37 °C. This flexibility with regard to incubation temperature would be particularly advantageous for the envisaged application of transcription within a continuous-flow semi-biotic device, where maintenance of a constant, precise temperature within the device could be problematic, depending upon the fabrication materials utilized. It would also allow for the option of a more simplistic method of heating to be utilized for the device, for example external heating *via* hot plate, rather than requiring the fabrication and integration of a heater within the device. Irrespective of heating method, with transcriptional yields acceptable from temperatures as low as 30 °C, the initialization time required for the device to reach an appropriate operating temperature would be minimized.

With the optimal parameters for solution-based transcription determined (table 2.3), experimental studies into the transcription of template *ds*DNA contained within liquid crystalline phases could commence. Chapter 3 presents the research conducted into one-off transcription in the presence of DNA-containing H_{II} phases.

2.6 Annex

2.6.1 pT7EmGFP preparation

2.6.1.1 Culture and purification of circular plasmid

Plasmid extraction and purification was performed using the Promega PureYield Maxiprep system (Promega, A2393), following a modified version of the vacuum manifold protocol. *E. coli* DH5α cells containing the pRSET-EmGFP plasmid were cultured and harvested as detailed below.

LB medium (Sigma, L3022) was prepared in an Erlenmeyer flask (600 mL LB broth) and autoclaved (121 ˚C, 15 minutes). Two starter cultures were prepared using culture tubes (5 mL LB broth) and inoculated with ampicillin to a final concentration of 100 µg/mL, before introducing a small scrape of T7GFP DH5α cell stock glycerol freeze. The starter cultures are then incubated with gentle rotation (100 rpm, 6-8 hours, 37 ˚C). Conical flasks (two, 500 mL) were then sterilised by autoclaving (121 ˚C, 15 minutes), with LB broth (250 mL each) added and inoculated with ampicillin (100 µg/mL). Aliquots of starter culture (1 mL) were then introduced and the broth incubated overnight (100 rpm, 12-16 hours, 37 ˚C).

Post-incubation, each flask of cells was split into falcon tubes (three 50 mL tubes per conical flask) and centrifuged (5,000 *g*, 10 minutes, 4 ˚C), with the supernatant discarded until all of the flask contents had been harvested. Each falcon tube contained a small pellet of cells post-centrifugation, which were re-suspended (4 mL re-suspension buffer each, vortexed) and then combined into a single tube, leaving one tube for each of the original flask cultures containing the re-suspended cells. The combined cells were then lysed (12 mL cell lysis buffer, three gentle inversions) and incubated (3 minutes, RT) before neutralising the solution (12 mL neutralisation solution, 10-15 gentle inversions).

Once neutralised, the lysate was centrifuged (7,000 *g*, 30 minutes, RT) and immediately split between clearing columns (two columns per falcon tube). Application of the vacuum pulled the lysate through the clearing columns, leaving the DNA bound to the binding columns. The clearing columns were then removed, with the binding columns washed with endotoxin removal wash (5 mL per column) and column wash (two 20 mL washes per column). Upon completion of the washing, the columns were dried under vacuum to remove residual ethanol (10 minutes), and any remaining ethanol wiped from the column tips. Using the Promega Eluator, DNA was eluted under

vacuum by addition of two aliquots of nuclease-free water (500 µL per column). This eluted the DNA in approximately 0.6 mL of water, due to water retention within the DNA binding columns.

2.6.1.2 Linearization using XmnI restriction endonuclease

pT7GFP DNA purified using the Promega PureYield Maxiprep system was linearized at the 1921 bp position, using the XmnI restriction enzyme (NEB, R0194), which has a restriction site sequence as shown in Figure 2.13.

5' . . . G A A N N ▼ N N T T C . . . 3'
3' . . . C T T N N ▲ N N A A G . . . 5'

Figure 2.13 Restriction site sequence for the XmnI restriction enzyme.

For each circular DNA plasmid sample, restriction would be performed using a 1.2x excess of XmnI enzyme, incubated for 16-17 hours (37 °C), with reaction component quantities based upon an 11-hour incubation period. Detailed below is the procedure for calculating the amount of XmnI, BSA and NEBuffer 4 required for a set volume of plasmid DNA at a known concentration.

- *One unit of XmnI will digest 1 µg DNA in 1 hour, based upon a 50 uL total reaction volume.*
- *Assuming XmnI concentration is 20 U µL^{-1}, 0.05 µL of XmnI will therefore digest 1 µg DNA in 1 hour, based upon a 50 µL total reaction volume.*
- *0.5 µL of XmnI will therefore digest 1 µg DNA in 1 hour, based upon a 500 µL total reaction volume.*
- *Extending the incubation period to 11 hours will therefore lessen the amount of XmnI required to digest 1 µg DNA to 0.0455 µL, based upon a 500 µL total reaction volume.*
- *Increasing the amount of XmnI used to a level of 1.2x excess increases the volume of XmnI required to digest 1 µg DNA, over 11 hours, in a total reaction volume of 500 µL, to 0.0546 µL. To ensure complete digestion, the incubation period is extended to 16-17 hours.*

$$Z = 500\mu L(DNA) + Y\mu L(XmnI) + \left[\tfrac{Z}{10}\right](buffer) + \left[\tfrac{Z}{100}\right](BSA) \qquad (2.1)$$

where Z is the final volume of the reaction and Y is 0.0546 µL of XmnI multiplied by the number of µg of DNA to digest.

This leads to Equation 2.2:

$$Z = \left[\frac{500 + Y}{0.89}\right]\mu L \qquad (2.2)$$

2.6.1.3 Purification of linearized plasmid

Once restricted with XmnI, linearized pRSET-EmGFP *ds*DNA was purified using DNA binding (white) columns from the Promega PureYield Maxiprep system and an adaptation of the system protocol, devised for the purification of linear rather than circular *ds*DNA. Linearized *ds*DNA was purified post-inactivation of the XmnI restriction endonuclease (20 minutes, 65 ˚C) as detailed below.

A completed restriction digest reaction was added to an equal volume of membrane binding solution (Promega, A9301) and vortexed thoroughly, before pouring the mixture onto a PureYield DNA binding column, applying a vacuum until all solution had passed through the binding column membrane. The binding column was then washed with column wash solution (20 mL) and the wash pulled through the membrane under vacuum. A vacuum was applied to the columns for a further 10 minutes, when there was no further detectable ethanol odour. Any residual ethanol on the tip of the binding column was removed by blotting with tissue. Linear *ds*DNA was then eluted using a Promega Eluator, typically eluting with warmed nuclease-free water (two 500 µL aliquots) under vacuum. Note that the elution volume could be decreased or increased if a more concentrated or dilute product was required; however, minimum elution volume did not fall below 400 µL, nor did the total elution volume exceed 1 mL.

2.7 References

1. Hunt, A. N., Clark, G. T., Attard, G. S. & Postle, A. D. Highly saturated endonuclear phosphatidylcholine is synthesized in situ and colocated with CDP-choline pathway enzymes. *J. Biol. Chem.* **276,** 8492–8499 (2001).

2. Corsi, J. *et al.* DNA that is dispersed in the liquid crystalline phases of phospholipids is actively transcribed. *Chem. Commun.* 2307–2309 (2008). doi:10.1039/b801199k

3. Yin, Y. W. & Steitz, T. A. Structural basis for the transition from initiation to elongation transcription in T7 RNA polymerase. *Science (80-.).* **298,** 1387–1395 (2002).

4. Cheetham, G. M. & Steitz, T. A. Structure of a transcribing T7 RNA polymerase initiation complex. *Science (80-.).* **286,** 2305–2309 (1999).

5. Steitz, T. A. Visualizing polynucleotide polymerase machines at work. *EMBO J.* **25,** 3458–3468 (2006).

6. Martin, C. T., Muller, D. K. & Coleman, J. E. Processivity in early stages of transcription by T7-RNA polymerase. *Biochemistry* **27,** 3966–3974 (1988).

7. Guo, Q., Nayak, D., Brieba, L. G. & Sousa, R. Major conformational changes during T7RNAP transcription initiation coincide with, and are required for, promoter release. *J. Mol. Biol.* **353,** 256–270 (2005).

8. Theis, K., Gong, P. & Martin, C. T. Topological and conformational analysis of the initiation and elongation complex of t7 RNA polymerase suggests a new twist. *Biochemistry* **43,** 12709–12715 (2004).

9. Ma, K., Temiakov, D., Anikin, M. & McAllister, W. T. Probing conformational changes in T7 RNA polymerase during initiation and termination by using engineered disulfide linkages. *Proc. Natl. Acad. Sci. U. S. A.* **102,** 17612–17617 (2005).

10. Alunni-Fabbroni, M., Manfioletti, G., Manzini, G. & Xodo, L. E. Inhibition of T7 RNA polymerase transcription by phosphate and phosphorothioate triplex-forming oligonucleotides targeted to a R.Y site downstream from the promoter. *Eur. J. Biochem.* **226,** 831–839 (1994).

11. Milligan, J. F., Groebe, D. R., Witherell, G. W. & Uhlenbeck, O. C. Oligoribonucleotide synthesis using T7 RNA polymerase and synthetic DNA templates. *Nucleic Acids Res.* **15,** 8783–8798 (1987).

12. Watanabe, Y., Igarashi, K., Mitsui, K. & Hirose, S. Differential stimulation by polyamines of phage DNA-directed in vitro synthesis of proteins. *Biochim. Biophys. Acta* **740,** 362–368 (1983).

13. Steitz, T. A. A mechanism for all polymerases. *Nature* **391,** 231–232 (1998).

14. Doublié, S., Tabor, S., Long, A. M., Richardson, C. C. & Ellenberger, T. Crystal structure of a bacteriophage T7 DNA replication complex at 2.2 A resolution. *Nature* **391,** 251–258 (1998).

15. Smeekens, S. P. & Romano, L. J. Promoter and nonspecific DNA binding by the T7 RNA polymerase. *Nucleic Acids Res.* **14,** 2811–2827 (1986).

16. Brautigam, C. A. & Steitz, T. A. Structural and functional insights provided by crystal structures of DNA polymerases and their substrate complexes. *Curr. Opin. Struct. Biol.* **8,** 54–63 (1998).

17. Black, C. F., Wilson, R. J., Nylander, T., Dymond, M. K. & Attard, G. S. Linear dsDNA partitions spontaneously into the inverse hexagonal lyotropic liquid crystalline phases of phospholipids. *J. Am. Chem. Soc.* **132,** 9728–9732 (2010).

18. Gulati, S. *et al.* Opportunities for microfluidic technologies in synthetic biology. *J. R. Soc. Interface* **6 Suppl 4,** S493–506 (2009).

19. Owczarzy, R., Moreira, B. G., You, Y., Behlke, M. A. & Walder, J. A. Predicting stability of DNA duplexes in solutions containing magnesium and monovalent cations. *Biochemistry* **47,** 5336–5353 (2008).

20. Misra, V. K. & Draper, D. E. On the role of magnesium ions in RNA stability. *Biopolymers* **48,** 113–135 (1998).

21. Peiró-Salvador, T., Ces, O., Templer, R. H. & Seddon, A. M. Buffers may adversely affect model lipid membranes: a cautionary tale. *Biochemistry* **48,** 11149–11151 (2009).

Chapter 3:

One-off Transcription in the Presence of DNA-containing H_{II} Phases

3. One-off Transcription in the Presence of DNA-containing H_{II} Phases

3.1 Rationale

Gene therapy is a promising therapeutic technique for the treatment of diseases, whereby a modified or improved gene can be transfected into a patient to supplement or alter the existing genetic material within the patient's cells. Since its conceptualization in the 1970s, gene therapy has been used in treatments for a number of diseases, for example leukaemia,[1] metachromatic leukodystrophy,[2] and Parkinson's disease.[3] The process of gene therapy involves the delivery of a gene packaged within a vector, such as an adenovirus, which is able to bind to cell membranes *in vivo*. The vector becomes packaged within a vesicle, which later breaks down to release the vector, so that the new gene can be inserted into the cell nucleus, utilizing the cell's own biological machinery to produce the therapeutic protein encoded by the transfected gene.[4] However, contrasting to their intended therapeutic application, the viral vectors first utilized for gene therapy could often cause undesirable and sometimes lethal immune responses; a predicament which bore the necessity to develop synthetic non-viral gene vectors.[5]

The use of DNA-lipid complexes (DNA lipoplexes) for gene delivery as an alternative to transfection *via* traditional viral gene delivery vectors is well documented in the literature.[5-9] The considerable research interest in DNA lipoplexes for use as non-viral gene delivery vectors is due to the ability to easily mass-produce DNA lipoplexes, with the inherent reduced immunogenicity they possess, when compared to the viral vectors historically used for gene therapy.[6] However, unlike viral vectors, which yield relatively high transfection efficiency, the most well studied of the DNA lipoplex gene vectors - those comprised of cationic lipids – have suffered from low transfection efficiency.[10] Although significant progress with respect to the transfection efficiency of cationic DNA lipoplexes has been made since Felgner *et al.* first reported the successful *in vitro* transfection of cationic lipid in 1987,[11] doubts remain as to whether a 'magic' lipid, with both highly efficient cellular entry and gene dissociation, can be found. This has not significantly impeded upon research utilizing cationic lipid/DNA lipoplexes, however, with such complexes having been used in a number of clinical trials for gene therapy treatment of cancer and cystic fibrosis, producing some encouraging results.[11,12]

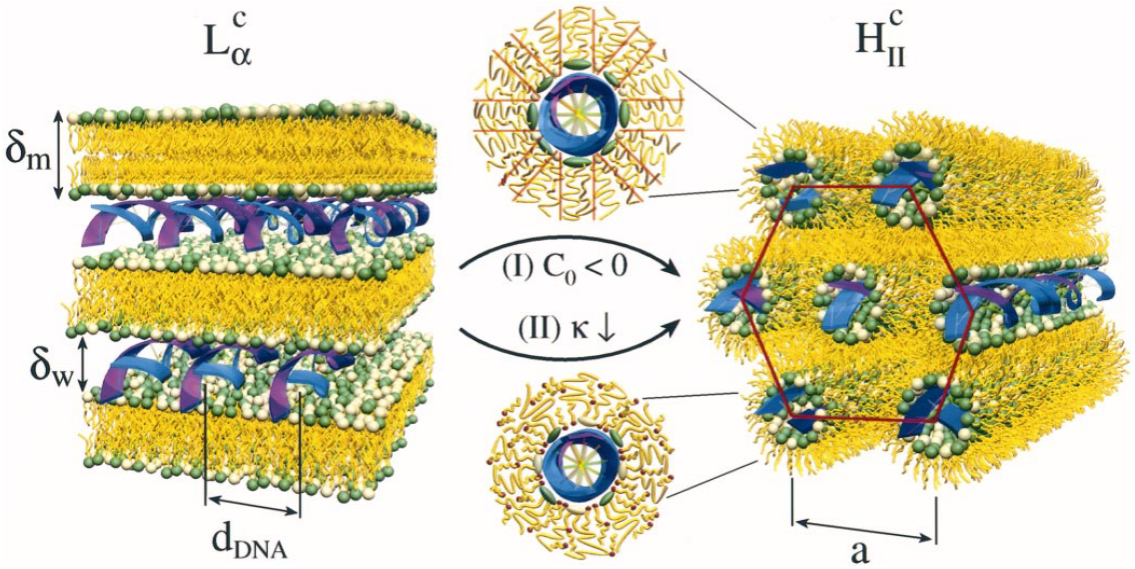

Figure 3.1 Schematic of lamellar (L_α^c) and inverse hexagonal phase (H_{II}^c) cationic liposome-DNA complexes. **Pathway I:** The lamellar complex (L_α^c) is driven towards the inverse hexagonal complex (H_{II}^c) through the addition of the helper-lipid DOPE, which drives the natural curvature (C_o) negative. **Pathway II:** The transition from L_α^c to H_{II}^c is achieved with the addition of helper-lipids consisting of mixtures of DOPC and the membrane-soluble cosurfactant hexanol, which significantly reduces the membrane bending rigidity (κ). From Koltover *et al. Science* **281**, 78 (1998).[7] Reprinted with permission from AAAS.

Through the addition of helper-lipids to DNA lipoplexes, the structure of the complex can be significantly altered (Figure 3.1). For example, the addition of the type II lipid DOPE to a lamellar DOTAP-DNA lipoplex can drive the structure to form an inverse hexagonal phase, with DNA contained within the columnar pores. Changes to the lipoplexes naturally give rise to changes in the biological properties of the phase; inverse hexagonal complexes are more efficient at cellular entry,[13] whilst lamellar complexes containing type 0 helper lipids, such as DOPC, have been observed to dissociate more efficiently with the DNA they initially contained.[14]

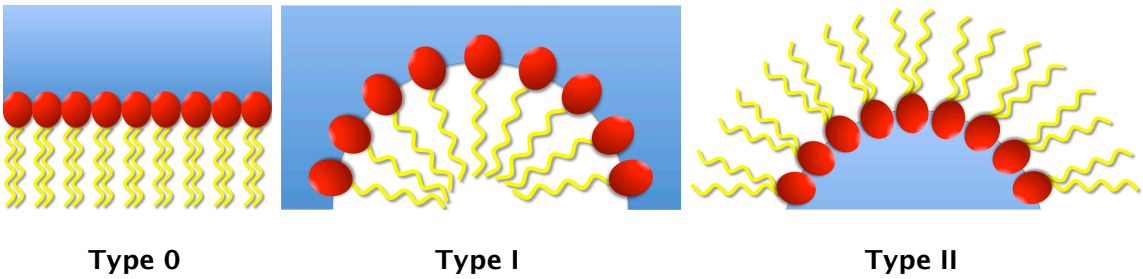

Figure 3.2 Comparison of type 0, I and II lipid classes.

Cationic lipoplexes successfully associate with DNA molecules they are mixed with due to the overall positive charge of the lipoplex, which is able to associate with the negatively charged phosphate backbone of DNA. However, as discussed above, highly

cationic lipoplexes suffer from reduced efficiency when DNA is required to dissociate from the lipoplex. Results have recently been published detailing how linearized double-stranded T7luc DNA can be contained using the zwitterionic phospholipid DOPE (1,2-dioleoyl-*sn*-glycero-3-phosphoethanolamine), to form an inverse hexagonal phase which the DNA has associated to, yet remains transcriptionally active.[15] It has been reported that DOPE-DNA lipoplexes exist in systems that contain divalent metal cations, and suggested that electrostatic interactions between these cations and the negatively charged phosphate backbone of DNA, combined with the release of further counterions, provides a driving force for the DNA to associate with the inverse hexagonal phase of DOPE.[16,17]

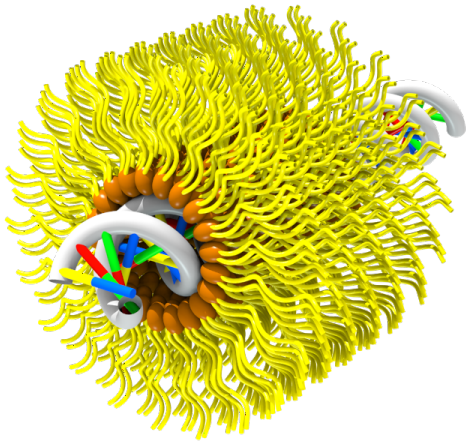

Figure 3.3 Linear *ds*DNA located within the columnar pores of inverse hexagonal phase DOPE, as proposed by Corsi *et al.*[15]

With numerous publications outlining the successful developments with the use of DNA lipoplexes for gene therapy, and the more recent reports of transcriptionally-active DNA-containing DOPE H_{II} phases, research was carried out into the viability of these phases for one-off transcription reactions, where the template *ds*DNA is contained with the DOPE phase, with a view to develop an *in vivo* continuous-flow transcription device utilizing a DOPE-DNA lipoplex. Many of the properties vital for efficient transfection in gene therapy using lipoplex gene vectors were parallel to the novel application intended for the research described in this thesis, such as low cytotoxicity, and the efficient association and dissociation of DNA.

The research presented in this chapter focuses on the suitability of DOPE H_{II} phases for sustaining single transcription reactions when linear *ds*DNA is associated with the phase. This encompasses the partitioning of dsDNA within the system, the partitioning of mRNA within the system, the effect of the system incubation conditions upon transcriptional activity, and the empirical transcription assay and DOPE-DNA phase parameters for optimized one-off transcription.

3.2 Methodology

3.2.1 Phase preparation

1,2-dioleoyl-*sn*-glycero-3-phosphoethanolamine (DOPE) was used to produce the lipid buttons described in this chapter. DOPE is a zwitterionic phospholipid that has been shown to have linearized *ds*DNA associate with it within the structure of an inverse hexagonal (H_{II}) liquid crystalline phase, providing divalent metal cations are present in solution. Linearized T7 *ds*DNA partitioned within the H_{II} phase of DOPE has been reported to remain transcriptionally active.[15]

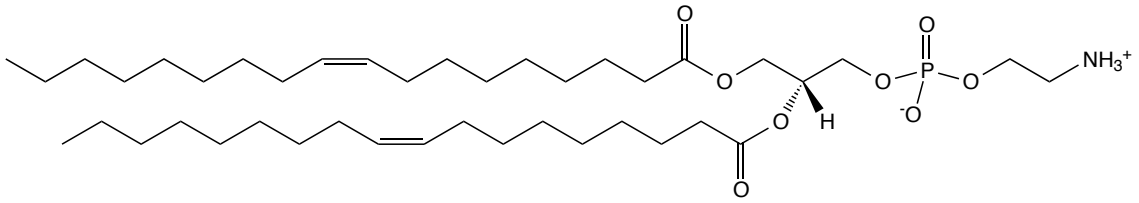

Figure 3.4 Structure of the zwitterionic phospholipid 1,2-dioleoyl-*sn*-glycero-3-phosphoethanolamine (DOPE).

It has already been postulated that linear *ds*DNA is able to reside within the aqueous pore channels of DOPE H_{II} phases due to the interaction between the divalent cations and the negatively charged DNA phosphate backbone, and the entropic gain caused by the release of counterions associated with the DNA molecule upon insertion into the pore channel. Therefore, *ds*DNA-containing DOPE H_{II} phases were typically prepared using a rehydration solution of isotonic saline, providing the counterions required to ensure an entropic gain upon release from association with the linear *ds*DNA molecules, and transcription buffer solution, containing, amongst other components, 25 mM $MgCl_2$, providing the divalent metal cations required to screen the charges of DOPE to give an overall positive charge upon the surface of the aqueous pore channel.

Lipid buttons were prepared by dispensing aliquots of DOPE dissolved in chloroform solution (6 µL, 0.5 mg µL-1) into 0.2 mL polypropylene PCR tubes via Eppendorf pipette with suitable filtered tip, minimizing smearing of the solution when dispensing. Solutions were then allowed to stand (15 minutes, RT) in capped tubes, before centrifugation (17,000 g, 30 seconds, RT) to ensure all lipid/chloroform solution was located at the bottom of the PCR tubes. The PCR tubes were then uncapped and warmed (2 hours, 50 °C) to aid the removal of chloroform, before drying the samples overnight using freeze-drying apparatus. Note that the vacuum was applied slowly, to minimize the bubbling of chloroform solution. Upon complete chloroform removal, the

DOPE liquid crystalline phases appeared as a white to translucent semi-spherical 'button' at the bottom of the PCR tubes (Figure 3.5).

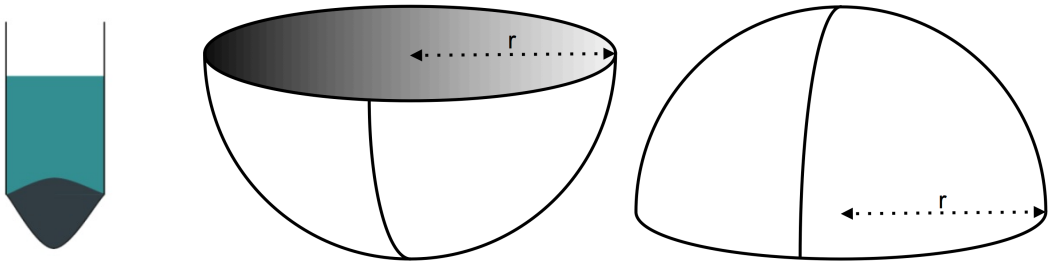

Figure 3.5 Left: Schematic of a DOPE liquid crystalline phase (grey) in a PCR tube, overlaid with aqueous solution containing linear *ds*DNA and transcription buffer. **Centre:** Planar surface area presented by lipid button (shaded). **Righ:t** Convex surface area presented by lipid button.

A 2 mg DOPE lipid button can be approximated to occupy a volume of 2.22×10^{9} m^3 and have an exposed upper surface area of 3.27×10^{-6} m^2, assuming that the density of the lipid button is 0.9 g cm^{-3}. Full calculations of the lipid button dimensions can be found in section 3.9, Annex 1.

Post-rehydration with isotonic saline solution (2 µL), lipid buttons were loaded linear *ds*DNA by lyophilization or incubation at 37 ˚C with an aqueous supernatant solution containing linear *ds*DNA and transcription buffer.

3.2.2 One-off transcription from DNA-containing H_{II} phases

One-off transcription assays were performed on lipid buttons, preloaded with linear *ds*DNA, prepared as described in section 3.2.1. Lipid buttons were loaded with 1 µg of linear *ds*DNA (unless stated otherwise) to achieve a total *ds*DNA concentration of 0.05 µg/µL per 20 µL transcription assay, analogous to positive control transcription assays in solution. Transcription assay solution (20 uL) was layered upon each *ds*DNA containing lipid button, forming an aqueous supernatant phase above each button. The specification of the transcription assay solution for one-off transcription assays (unless stated otherwise) is presented in table 3.1.

Table 3.1 Composition of transcription assay in the presence of *ds*DNA-containing lipid buttons

Component	**Volume of stock component per assay (20 µL)**	**Component concentration per assay (20 µL)**
Nuclease-free water	14.95 µL	-
rNTPs (80 mM each)	1.25 µL	20 mM (5 mM each)
10x transcription buffer	2 µL	1x
$MgCl_2$ (0.5 M)	1 µL	25 mM
T7 RNA polymerase	0.8 µL	40 u (17 nM)

For each one-off transcription assay, a lipid buttons was overlaid with transcription assay solution and incubated for 2 h (37 °C), prior to supernatant removal by Eppendorf pipette and purification of the mRNA product.

3.2.3 System parameters

To enable the characterization of the DNA-DOPE lipid button transcription system, a number of analyses were performed. The foci of this work, and some of the parameters investigated as part of the experimental work presented herein, are detailed below.

- Analysis of previously published data on *ds*DNA partitioning (section 3.3):
    - Potential and probable locations of linearized *ds*DNA within the system.

- Analysis of previously published data on mRNA partitioning (section 3.4):
    - Potential and probable locations of mRNA within the system when the DOPE H_{II} phase contains either 0, 1, or 10 µg of linearized *ds*DNA.

- Further investigation into the partitioning of *ds*DNA within DOPE liquid crystalline phases (section 3.5):
    - Development of a quantitative DNA gel electrophoresis method of *ds*DNA partition coefficient (K_p) calculation.
    - Comparison of the quantitative DNA gel electrophoresis and PCR methods of *ds*DNA K_p calculation.
    - The effect of the following parameters upon *ds*DNA partitioning:
        - DOPE lipid button mass;
        - *ds*DNA incubation solution composition;

  - *ds*DNA incubation period;
  - *ds*DNA incubation solution $MgCl_2$ concentration;
  - *ds*DNA incubation with individual transcription buffer components.

- Transcriptional activity of *ds*DNA-containing DOPE liquid crystalline phases (section 3.6):
  - Transcription from *ds*DNA-containing DOPE H_{II} phases prepared *via* either lyophilization or 100 h incubation.
  - Time course investigation.

The optimal parameters for the DNA-DOPE lipid button transcription system are presented in section 3.7.

3.2.4 Methods of analysis

3.2.4.1 Partitioning of DNA

The partition coefficient (K_p) values presented within this research indicate the proportion of *ds*DNA that has not partitioned within the liquid crystalline phases studied (see equation 3.1).

$$K_p = \frac{[DNA]_{SN}}{[DNA]_{TOT}} \qquad 3.1$$

where K_p is the partition coefficient, $[DNA]_{SN}$ is the concentration of DNA in the supernatant (as determined by quantitative DNA gel electrophoresis), and $[DNA]_{TOT}$ is the total DNA concentration used in the experiment.

A K_p value of 1, for example, would indicate that 100% of the *ds*DNA introduced into the liquid crystalline system remains outside of the liquid crystalline structure, residing in any aqueous solution layered above the phase surface. Conversely, an example K_p value of 0.005 would indicate that 0.5% of the *ds*DNA introduced into the system remains outside of the liquid crystalline structure, thus 99.5% of *ds*DNA is partitioned within the liquid crystalline structure.

Equation 3.2 demonstrates the composition of the total DNA concentration within the system:

$$[DNA]_{TOT} = [DNA]_{SN} + [DNA]_{LC} \quad 3.2$$

where $[DNA]_{LC}$ is the concentration of DNA associated with the liquid crystalline phase.

Partition coefficient (K_p) values presented within this chapter were calculated *via* PCR quantification, prior to development of an improved method utilizing quantitative DNA gel electrophoresis, which improved experimental throughput whilst yielding comparable K_p calculation (for full experimental details see Section 3.9, Annex 2).

3.2.4.2 Partitioning of mRNA

The partition coefficient (K_p) of mRNA in the presence of DOPE H_{II} phases was calculated in a broadly similar way to the method utilized for *ds*DNA partitioning (equations 3.3 and 3.4).

$$K_p = \frac{[mRNA]_{SN}}{[mRNA]_{TOT}} \quad 3.3$$

where K_p is the partition coefficient, $[mRNA]_{SN}$ is the concentration of mRNA in the supernatant, and $[mRNA]_{TOT}$ is the sum of the mRNA found in the supernatant and liquid crystalline phases post-purification.

The composition of the total mRNA concentration within the system is given by:

$$[mRNA]_{TOT} = [mRNA]_{SN} + [mRNA]_{LC} \quad 3.4$$

where $[mRNA]_{LC}$ is the concentration of mRNA associated with the liquid crystalline phase.

3.2.4.3 Transcriptional yield

UV-visible spectrophotometry was performed using a NanoDrop ND-1000 instrument to quantify the concentration of all mRNA samples purified. For analytical purposes, measurements using the ND-1000 were recorded in triplicate by loading a fresh aliquot of each sample a total of three times, cleaning the ND-1000 arm between replicates.

Post-measurement, the mean concentration and standard deviation was calculated. Using the NanoDrop nucleic acid software, measurements were processed using type ratio RNA-40 for purified mRNA samples. Concentration values were recorded in units of ng μL^{-1}, along with associated 260/280 and 260/230 sample absorbance ratios as a measure of sample purity and integrity.

A 260/280 ratio of ~2.0 is generally accepted as pure for RNA, whilst a 260/230 ratio appreciably lower than 1.8 may indicate the presence of co-purified contaminants.

3.2.4.4 Agarose gel electrophoresis

DNA and RNA samples were routinely tested for purity and integrity using agarose gel electrophoresis throughout the work presented in this chapter. Protocols for both DNA and RNA gel electrophoresis can be found in Appendix A.

3.3 *ds*DNA partitioning

3.3.1 *ds*DNA partitioning in the presence of DOPE H_{II} phases

We have previously reported that linear *ds*DNA partitions into the aqueous pore channels of H_{II} phase DOPE, displacing water molecules initially located within the channels.[18] During this research, two preparation methods were utilized to produce the *ds*DNA-containing DOPE H_{II} phases; preparation by lyophilization, and preparation by incubation at 37 ˚C of an aqueous *ds*DNA-containing solution above rehydrated DOPE H_{II} phases (see section 3.2 for phase preparation method).

The partition coefficients presented in Figure 3.6, as a function of incubation time at 37 ˚C for linear T7GFP *ds*DNA, were obtained using PCR to amplify the *ds*DNA present within monolithic DOPE H_{II} phases prepared *via* either lyophilization or incubation with complete transcription buffer solution.

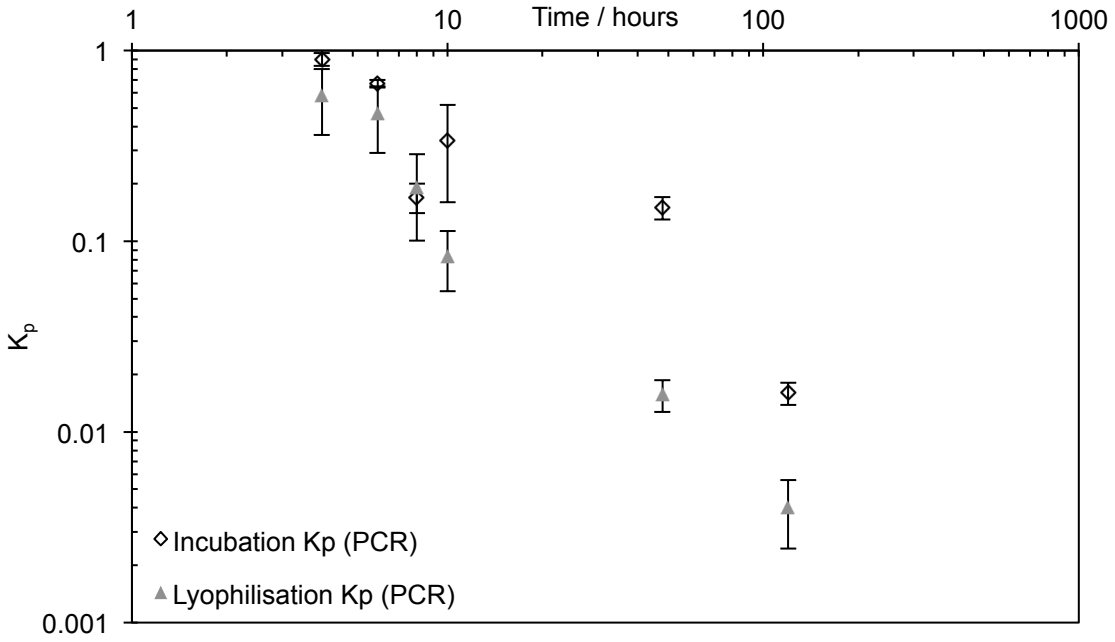

Figure 3.6 Relationship between the partition coefficient (K_p) for *lin*pT7GFP *ds*DNA and the time of incubation at 37 ˚C, quantified by PCR experiment. Grey triangles show the partition coefficients obtained from experiments in which the linear *ds*DNA was mixed with the lipid *via* lyophilization. Hollow diamonds show the partition coefficients from experiments in which the linear *ds*DNA was initially added to the supernatant liquid above the H_{II} phase (i.e., K_p = 1). Data published by Black, Wilson *et al.* in J. Am. Chem. Soc. **2010**, *132*, 9726-9732.[18]

Figure 3.6 clearly shows that *lin*T7GFP *ds*DNA exhibits a strong preference to partitioning within the H_{II} phase of DOPE, with the amount of linear *ds*DNA associating

with the liquid crystalline phase increasing proportionally with the period of incubation at 37 ˚C, for *ds*DNA/DOPE H_{II} phase systems prepared *via* either lyophilization or incubation of *ds*DNA-containing aqueous solution above DOPE H_{II} phases. Utilizing the aqueous supernatant method of incubation, all of the *ds*DNA within the system initially resides within the supernatant solution (t = 0, K_p = 1), and as such, partitioning of the linear *ds*DNA within the DOPE H_{II} phase is slower than that observed for DOPE samples prepared *via* the lyophilization method. By 100 hours of incubation at 37 ˚C, the data shows a partition coefficient of $\leq 8 \times 10^{-3}$ for *ds*DNA-containing DOPE phases prepared *via* the lyophilization method, or $K_p \leq 1.7 \times 10^{-2}$ for *ds*DNA-containing DOPE phases prepared *via* the aqueous supernatant incubation method.

The partition coefficient data presented in Figure 3.6 indicate that linear *ds*DNA preferentially associates with the DOPE H_{II} phase, most likely within the pores of the inverse hexagonal structure, rather than merely associating with the H_{II} phase surface, to form an accretion layer of linear *ds*DNA. The pores within H_{II} phase DOPE have a diameter of 4 nm,[19] which is sufficient to accommodate a *ds*DNA helix in the B form (diameter ~2 nm). The partitioning of linear *ds*DNA within DOPE H_{II} phases, as observed in Figure 3.6, is consistent with the literature previously published reporting that DNA preferentially associates within the liquid crystalline phases of lipids.[5,7,8,15,20]

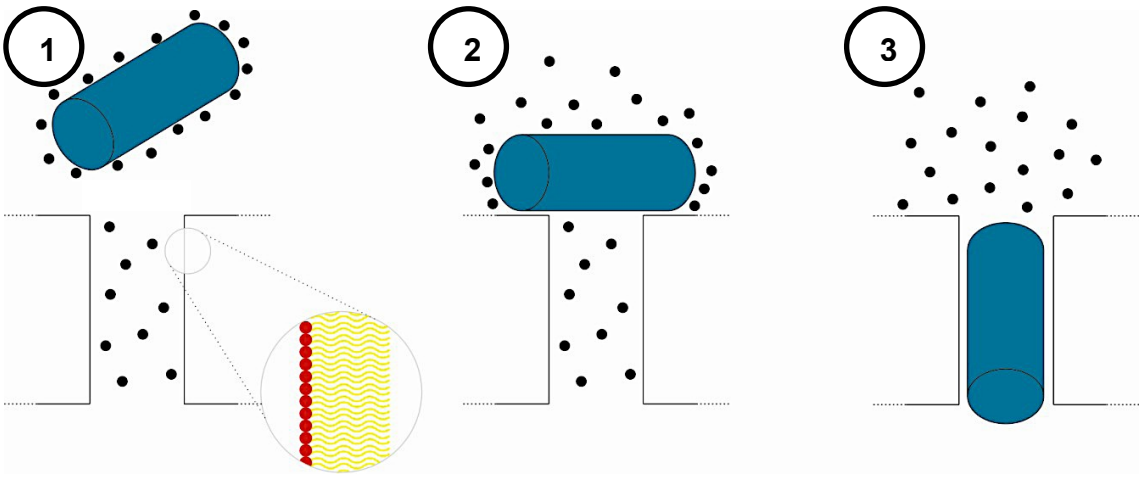

Figure 3.7 Illustration of the possible linear *ds*DNA locations within systems comprising an aqueous supernatant layer and H_{II} phase DOPE. Blue cylinders represent linear *ds*DNA, black spheres represent water molecules. Note that the phase pores have a diameter of 4 mm. **(1)** *ds*DNA in bulk water outside of the DOPE H_{II} phase pores. Magnification highlights the phospholipid-lined channel; red spheres show the hydrophilic heads, yellow lines show the hydrophobic tails. **(2)** *ds*DNA associated with the surface of the DOPE H_{II} phase. **(3)** *ds*DNA located within a channel in the DOPE H_{II} phase; water molecules have been displaced into the supernatant phase above.

Linear T7GFP *ds*DNA (3395 bp) has an estimated fully extended length of 1.2×10^{-6} m; assuming it is in the B DNA form, it can be represented as a cylinder with a radius of 10×10^{-10} m. With a pore diameter of 4×10^{-9} m within the DOPE H_{II} phase, it is clear that linear *ds*DNA molecules are able to reside within the structural constraints of the phase pores (Figure 3.7). If the linear *ds*DNA were to associate with the surface of the liquid crystalline phase, based upon an approximation for the surface area of a ~2 mg DOPE H_{II} phase lipid button (~7.1×10^{-6} m^2) and the longitudinal cross section of a *lin*T7GFP *ds*DNA cylinder (2.4×10^{-16} m^2 per molecule), 1 µg of linear *ds*DNA would form between 90-180 monolayers upon the external lipid surface, a level of *ds*DNA aggregation which would be explicable only through the occurrence of insolubility or colloidal coagulation. In contrast, there are estimated to be in the range of 1.5×10^{11} – 3.0×10^{11} pores in contact with the aqueous supernatant phase, based upon the unit cell dimension of H_{II} phase DOPE in water at 37 °C ($d = 7.0 \pm 0.4 \times 10^{-9}$ m), obtained by small angle X-ray diffraction. Within 1 µg of of *lin*T7GFP, there are ~2.7×10^{11} molecules of DNA, and so with in the region of 10^{11} DOPE H_{II} phase pores in contact with the aqueous supernatant layer, it is possible for all molecules of *ds*DNA to be located within the pores of the H_{II} phase. Under transcription conditions, the presence of 25 mM $MgCl_2$ provides a supply of divalent metal cations, which will likely contribute towards the partitioning of *ds*DNA into liquid crystalline phase DOPE, due to the entropic gain during release of Mg^{2+} counterions from the molecules of *ds*DNA as it inserts into the H_{II} phase pores. The entropic gain from the release of these counterions is much higher than the entropy loss that occurs when *ds*DNA molecules partition within the phase pores; *ds*DNA in solution adopts a random coil formation, leading to an entropic loss upon insertion into the phase, however this entropic loss is relatively small due to the relatively long coherence length of *ds*DNA, at ~1.5×10^{-8} m.[21] In the absence of divalent metal cations, this entropic loss, which would drive against *ds*DNA partitioning, would not be counteracted, and thus limited partitioning of *ds*DNA into the liquid crystalline phase would be observed.

With *lin*T7GFP preferentially partitioning to within the pores of liquid crystalline phase DOPE, and an equilibrium $K_p \leq 1.7 \times 10^{-2}$ at 100 hours, it was clear that the use of DOPE H_{II} phases as a method of storing the template *ds*DNA required for transcription was a viable option. However, further investigation into the process of mRNA partitioning in the presence of H_{II} phases was required. Whilst DOPE H_{II} phases offered a proven mechanism of template *ds*DNA storage for transcription,[15] if the mRNA produced during transcription were also preferentially associating with the DOPE H_{II} phase, rather than with the aqueous supernatant phase above, it would have a detrimental impact upon the transcriptional-activity of a *ds*DNA-containing DOPE H_{II} phase over time.

3.4 mRNA partitioning

3.4.1 mRNA partitioning in the presence of DOPE H_{II} phases

For the potential success of utilizing *ds*DNA-containing H_{II} phase DOPE as a vessel for template DNA supply for transcription, it is essential that the transcription product mRNA has a low preference to partition into the liquid crystalline phase (i.e. the partition coefficient for mRNA tends towards 1). If mRNA was observed to behave in a similar way to linear *ds*DNA, it would have a strong preference to partition to the liquid crystalline phase, as discussed in section 3.3, and thus RNA would only be released from the phase upon sufficient RNA production from the transcription reaction to saturate the liquid crystalline phase. Ideally, for an efficient transcription reaction, mRNA would partition minimally to the liquid crystalline phase, and preferentially partition to the aqueous supernatant, ensuring that there was minimal delay in RNA being isolated from the system.

Whilst vesicles produced from zwitterionic lipids, such as DOPE, will adsorb *ss*RNA molecules in the presence of divalent cations[22,23], and zwitterionic lipid bilayers exhibit binding to *ss*RNA molecules[24–26] in the presence of divalent cations, far less is known about the interaction between RNA and the lyotropic liquid crystalline phases used within this research. A set of new experiments were performed, investigating the effect upon RNA isolation from both the supernatant and liquid crystalline phases, when varying the amount of mRNA incubated in contact with the phase, for lipid buttons containing 0, 1, and 10 μg of partitioned linear *ds*DNA. The experiments used to investigate the partitioning of mRNA in the presence of DOPE liquid crystalline phases were performed under the same conditions as the DNA partitioning experiments, to allow for direct comparison between the experimental results observed for mRNA and *ds*DNA.

For DOPE H_{II} lipids with 0 μg of *ds*DNA in the phase (Figure 3.8), the amount of mRNA isolated from the aqueous supernatant phase increases linearly with increasing concentration of initial mRNA incubated in the presence of the lipid. The amount of mRNA isolated associated with the liquid crystalline phase can be observed to increase, albeit at a far slower rate than is observed for the supernatant phase, with the rate of increase declining as the initial incubating mRNA amount is increased beyond 20,000 ng.

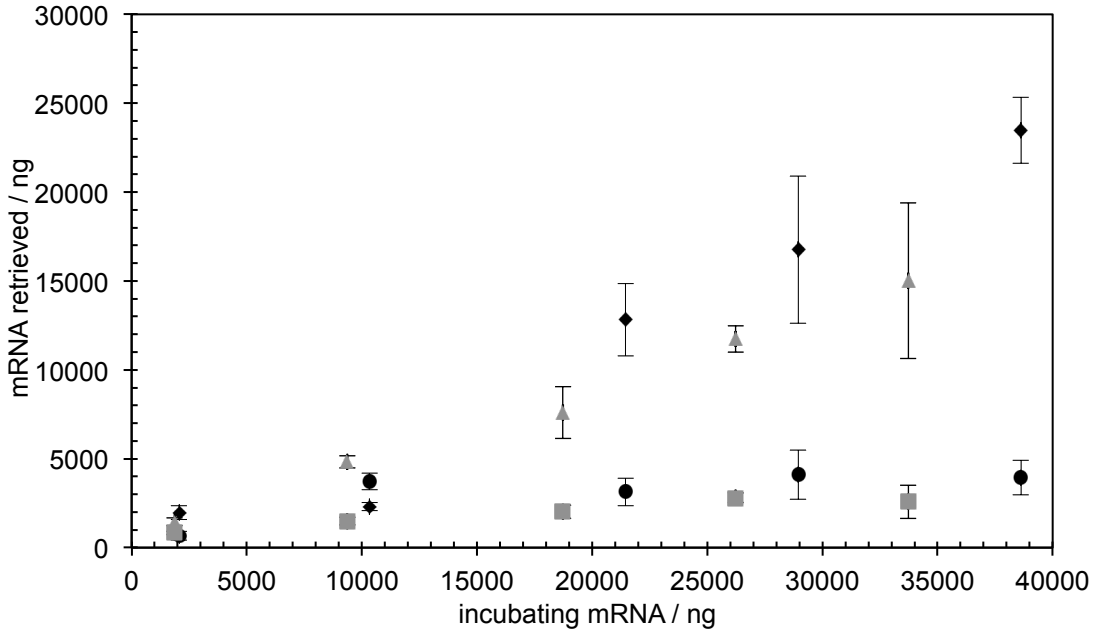

Figure 3.8 Amount of mRNA retrieved from the liquid crystal and aqueous supernatant phases of DOPE H_{II} lipids. luc-mRNA (supernatant, black diamonds; liquid crystal, black circles) and GFP-mRNA (supernatant, grey triangles; liquid crystal, grey squares) are shown. Data published by Wilson *et al.* in Biomacromolecules **2010**, *11*, 3022-3027.[27]

The addition of 1 μg linear *ds*DNA to the DOPE H_{II} phase has minimal effect upon the partitioning of mRNA within the system, when compared to the partitioning behaviour observed when mRNA is in the presence of DOPE H_{II} phases containing no *ds*DNA (Figure 3.9). This observation is consistent with expectations, as approximately 1 in 500 aqueous pores in the DOPE H_{II} phase would be occupied by linear *ds*DNA. This leaves the vast majority of the pores within the phase unoccupied, so the containment of 1 μg linear *ds*DNA would be unlikely to affect the behaviour of mRNA in the presence of the liquid crystalline phase. This observation is particularly encouraging, as it indicates that the majority of mRNA produced from a 20 μL transcription reaction could be easily isolated and purified if the transcription reaction were carried out in the presence of a DOPE H_{II} phase containing the standard amount of template *ds*DNA required (1 μg), for that volume of reaction, due to the bulk of the mRNA preferentially residing in the aqueous supernatant phase layered atop a DOPE H_{II} phase surface.

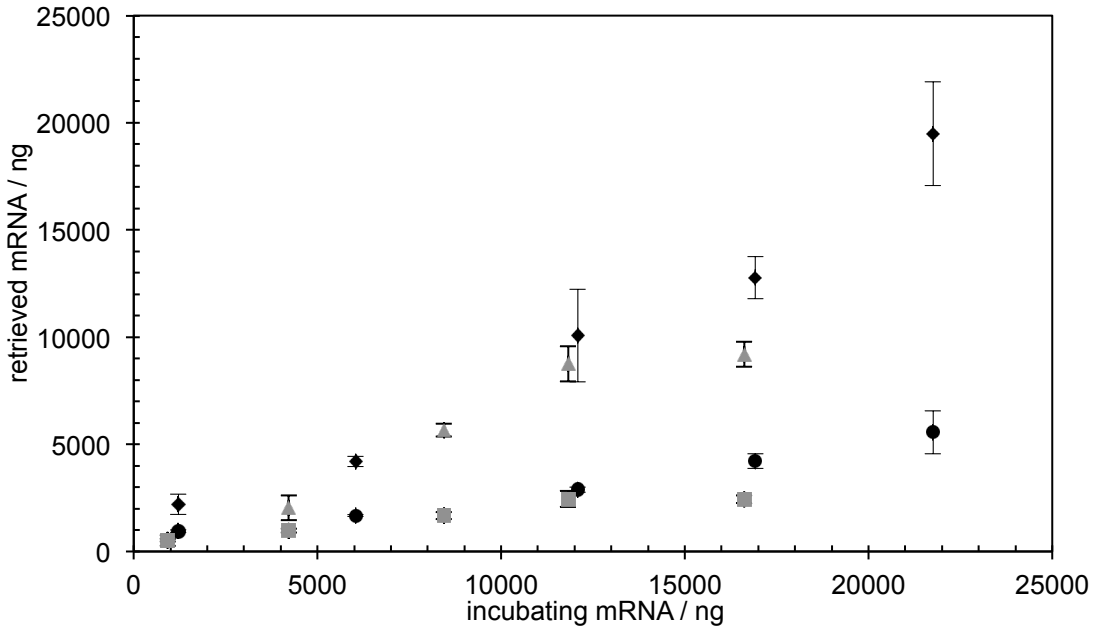

Figure 3.9 Amount of mRNA retrieved from the liquid crystal and aqueous supernatant phases of DOPE H_{II} lipids with 1 µg linear *ds*DNA in the phase. luc-mRNA (supernatant, black diamonds; liquid crystal, black circles) and GFP-mRNA (supernatant, grey triangles; liquid crystal, grey squares) are shown. Data published by Wilson *et al*. in Biomacromolecules **2010**, *11*, 3022-3027.[27]

If the amount of linear *ds*DNA within the DOPE H_{II} phases is increased ten-fold, to 10 µg, the linear *ds*DNA occupies approximately 1 in 50 pores within the H_{II} phase. In a situation where a *ds*DNA-containing DOPE H_{II} phase could be successfully reused for multiple transcription reactions, the ability to load the phase with an increased amount of template *ds*DNA would be desirable, as it would lead to an increase in the amount of transcription product yielded from a single phase, without requiring the user to devote additional laboratory time and finance towards the production of additional template *ds*DNA. Utilizing the current commercially available transcription kits, any template *ds*DNA input into a transcription reaction is lost during purification, so the user has to ensure they have a plentiful supply of template *ds*DNA to achieve high yields of transcription product mRNA across multiple transcription reactions.

By increasing the number of DOPE H_{II} phase pores filled with *ds*DNA to an equivalent of 1 pore in every 50 (10 µg *ds*DNA), it was still expected to be unlikely that the partitioning of mRNA between the liquid crystalline and aqueous supernatant phases would be significantly altered, when compared to DOPE H_{II} phases containing 0 or 1 µg linear *ds*DNA, due to the remaining availability of unoccupied phase pores (approximately 98% of the total phase pores).

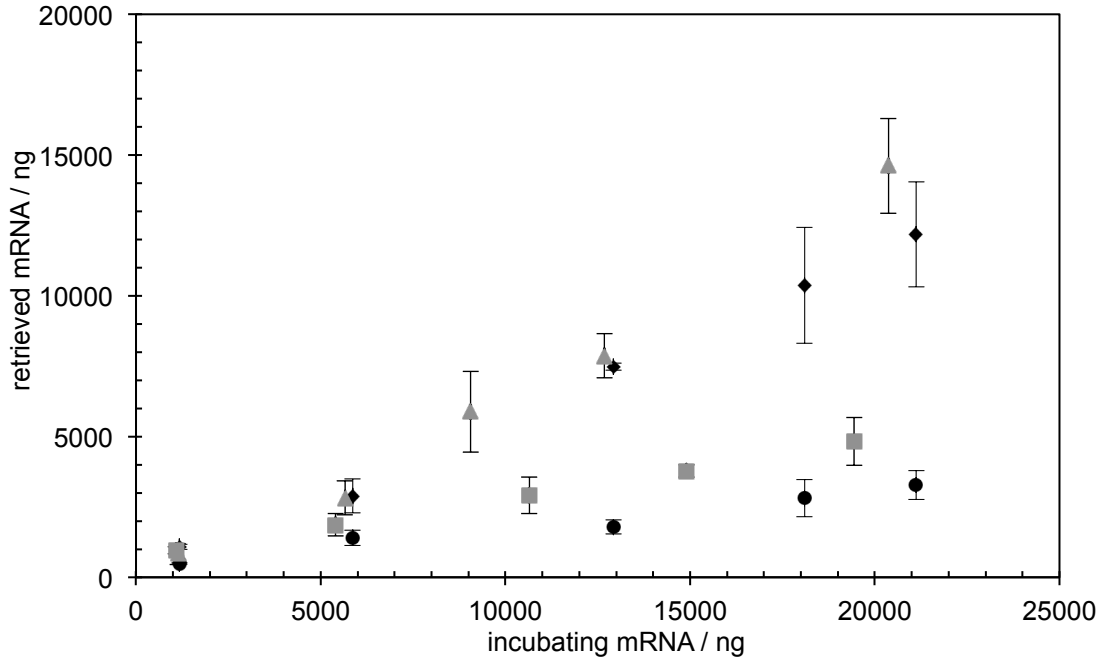

Figure 3.10 Amount of mRNA retrieved from the liquid crystal and aqueous supernatant phases of DOPE H_{II} lipids with 10 µg linear *ds*DNA in the phase. luc-mRNA (supernatant, black diamonds; liquid crystal, black circles) and GFP-mRNA (supernatant, grey triangles; liquid crystal, grey squares) are shown. Data published by Wilson *et al*. in Biomacromolecules **2010**, *11*, 3022-3027.[27]

Comparable to the mRNA partitioning behaviour observed in the presence of 0 and 1 µg *ds*DNA-containing DOPE H_{II} phases, Figure 3.10 shows that phases loaded with 10 µg *ds*DNA do not significantly affect the preference of mRNA to reside within the aqueous supernatant layered atop the liquid crystalline phase, with similar levels of mRNA partitioning to the H_{II} phase. Figure 3.11 illustrates the potential locations for mRNA within a system comprising a DOPE H_{II} phase and an aqueous supernatant layer.

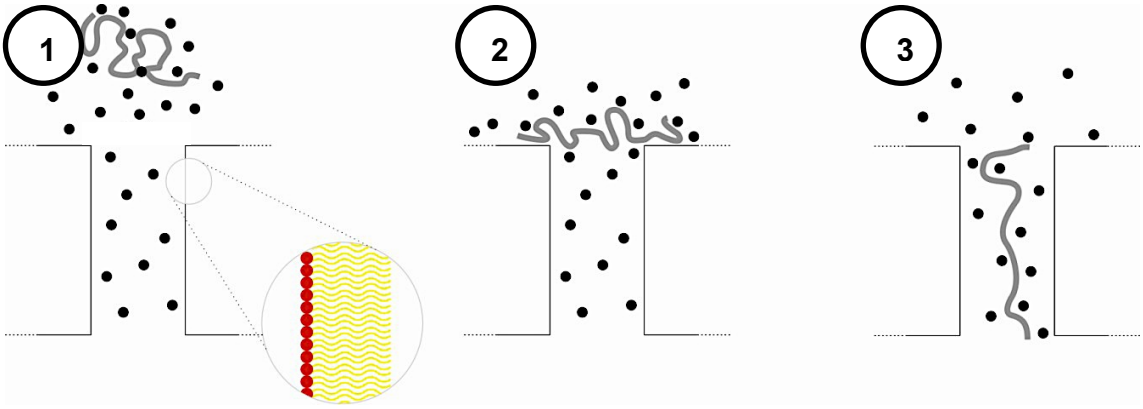

Figure 3.11 Illustration of the possible mRNA locations within the inverse hexagonal phase of DOPE; grey lines represent mRNA, black spheres represent water molecules. **(1)** mRNA in bulk water outside of the DOPE H_{II} phase pores. Magnification highlights the phospholipid-lined channel; red spheres represent hydrophilic heads, yellow lines represent hydrophilic tails. **(2)** mRNA associated with the surface of the DOPE H_{II} phase. **(3)** mRNA located within channels in the DOPE H_{II} phase; water molecules are present within the channels.

Under transcription conditions, DOPE lipid buttons preloaded with 1 µg linear *ds*DNA would have an aqueous solution comprising the transcription buffer and components overlaid upon it. mRNA, within the bulk water of the aqueous transcription solution overlaying the DOPE H_{II} phase, would assume a highly coiled secondary structure, due to its estimated low coherence length of ~0.8 nm.[28] For mRNA to associate with either the surface of the inverse hexagonal phase, or for it to locate within the channels, a substantial change in conformation would be required. Within a solution, the low coherence length of mRNA allows molecules to form highly coiled structures. For mRNA to associate with the surface of the phase, less of a conformational change is required than for mRNA to locate within the H_{II} phase channels, meaning that there is little, or no, negative entropic change, caused by the possible formation of a slightly more ordered structure compared to the secondary structure. For mRNA to locate within the pores, any positive entropic change produced from the small displacement of water molecules from the channel is outweighed by the small, negative entropic change that arises from confining mRNA molecules within the pores, breaking bonds and minimizing coiling from the secondary structure, allowing mRNA to locate within the H_{II} channel. Breaking bonds formed in the secondary structure that allow the mRNA to locate in the channels also produces a positive enthalpic contribution, causing a positive change in Gibbs free energy. This suggests that locating mRNA within the channels of a H_{II} phase would be far more unfavourable than if mRNA were to associate with the surface of the DOPE H_{II} phase.

Analysis of the combined amounts of mRNA retrieved from DOPE H_{II} phase systems containing 0, 1, and 10 µg *ds*DNA (Figures 3.8-3.10) allowed for calculation of the mRNA partition coefficients (where $K_p = 1$ indicates that all mRNA within the system is residing in the aqueous supernatant layer), which are presented as a function of incubating mRNA amount in Figure 3.12. The partition coefficient data presented in Figure 3.12 is consistent with the observation that transcript mRNA has a strong preference to reside in the isotropic supernatant solution above the liquid crystalline phase, for both pure DOPE H_{II} phases and phases containing linear *ds*DNA within the phase, with partition coefficients (K_p) in the range 0.6-0.8. It is interesting to note that the effect of preloading the liquid crystalline phase with linear *ds*DNA appears to have no appreciable effect upon the partitioning of mRNA within the system investigated, under our standard transcription conditions. This suggests that the small amount of mRNA that is associating with the liquid crystalline phase, rather than the isotropic supernatant solution, is doing so *via* a different mechanism of association than the mechanism occurring when *ds*DNA partitions within DOPE H_{II} phases.

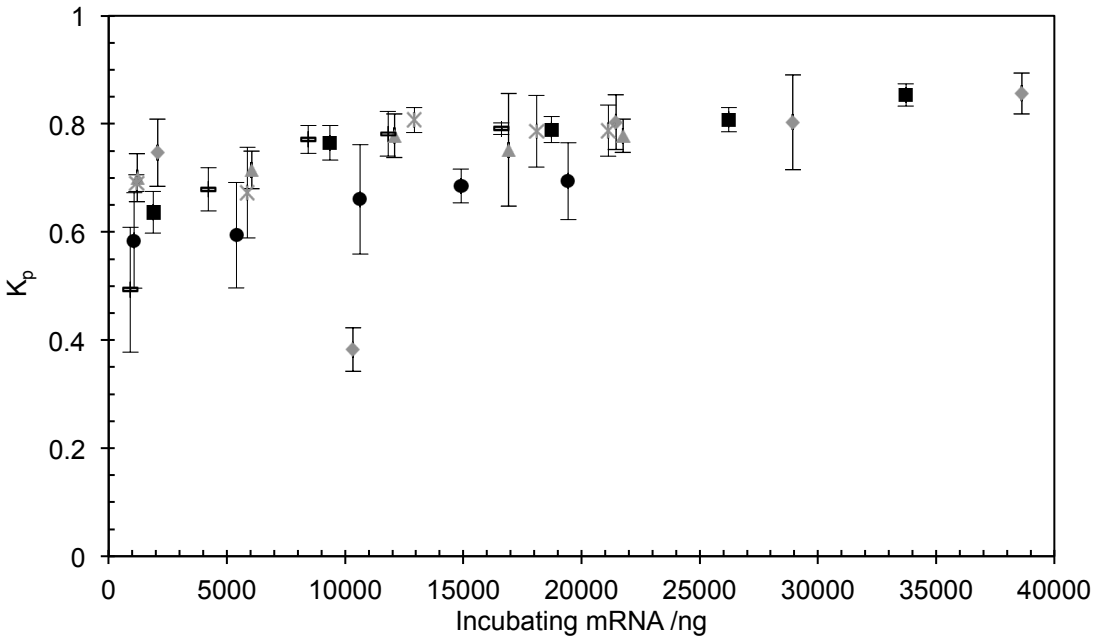

Figure 3.12 Partition coefficients (K_p) of GFP-mRNA and luc-mRNA for inverse hexagonal (H_{II}) liquid crystal phases of DOPE preloaded with linear *ds*DNA coding for the incubated mRNA. Grey diamonds, triangles and crosses correspond respectively to 0, 1, and 10 μg *lin*pT7luc *ds*DNA and luc-mRNA. Black squares, dashes, and circles correspond, respectively, to 0, 1, and 10 μg *lin*pT7GFP *ds*DNA and GFP-mRNA. Data published by Wilson *et al.* in Biomacromolecules **2010**, *11*, 3022-3027.[27]

With mRNA associating to the liquid crystalline phase, in small quantities, by a different method to the association of linear *ds*DNA to a liquid crystalline phase (partitioning into the pores), it is likely that the small amount of mRNA is associating with the surface of the liquid crystalline phase. However, the surface of the phase is covered with pore openings, accounting for 7.41×10^{-7} m^2 of the 3.27×10^{-6} m^2 total planar surface area of a 2.0 mg lipid button, so mRNA is unable to form a linear accretion layer upon the entire H_{II} phase planar surface area (see Annex 1 for supporting calculations, Section 3.9.1). Literature reports that RNA bound to giant lipid vesicles has a tendency to concentrate at bends and membrane junctions,[26] and so we propose that the first layer of *m*RNA associating with the surface of the H_{II} phase does so in the area between the pore openings (see Figure 3.13). Further deposition of mRNA then occurs at the sites of initial association, between the pore openings, leaving the *ds*DNA located within the pores of the DNA-containing liquid crystalline phases accessible for transcription. The presence of divalent ions within our standard reaction conditions at high concentration (25 mM $MgCl_2$, from full transcription buffer), are likely to assist the adsorption of mRNA onto the external surface of the DOPE H_{II} phase,[29] alongside the significant entropic losses that would occur through the partitioning of mRNA into the liquid crystalline phase.

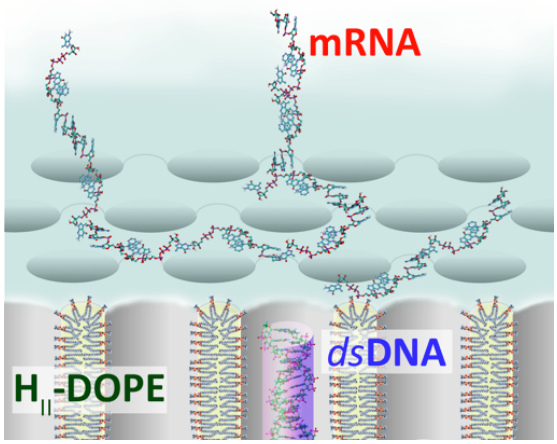

Figure 3.13 A single length of *ds*DNA (purple cylinder) can be seen localised within a pore of the H_{II} phase, with a small amount of mRNA forming an accretion layer on the external surface of the phase and the remainder residing in the isotropic solution overlaid upon the liquid crystalline phase. Reprinted with permission from Wilson *et al.* in Biomacromolecules **2010**, *11*, 3022-3027.[27] Copyright 2010 American Chemical Society.

Whilst it has been reported by Vlassov (2004) that RNA molecules in solution oligomerize, induced by high concentrations of divalent ions within solution, investigation into the oligomerisation of RNA under our standard reaction conditions (25 mM $MgCl_2$) did not support the formation of oligomers, using the method reported by Vlassov.[29] The formation of RNA oligomers would result in colloidal particles that would be attracted towards the flat surface of the DOPE H_{II} phase, supporting the limited association of RNA observed towards the liquid crystalline phase.

The mRNA partitioning behaviour observed in the presence of both pure DOPE and *ds*DNA-containing DOPE H_{II} phases strongly support the use of DOPE as a vessel for the provision of template *ds*DNA for *in situ* production of mRNA *via* supplementation of the system with transcription assay components. This is in no small part due to the observation that the bulk of any mRNA made by transcription of *ds*DNA contained within the liquid crystalline phase would preferentially reside within the aqueous supernatant layer above, allowing for simple and efficient extraction of the crude mRNA product prior to purification.

3.5 *ds*DNA partition coefficient (K_p) analysis

3.5.1 Developing a gel-based technique for K_p analysis

Notwithstanding the fact that the PCR method of *ds*DNA partition coefficient determination (section 3.9, Annex 2) offered a reliable method of doing so, it was, however, particularly time consuming and was restrictive in terms of the flexibility it offered to study more complex systems; for example when additional reagents were added to the *ds*DNA incubation solution, especially when the presence of these reagents would cause a significant increase in the ionic concentration of the PCR reaction mixture. Deviation away from the ideal PCR reaction conditions would have a detrimental effect upon the ability of the DNA polymerase to successfully amplify the *ds*DNA extracted from the DOPE H_{II} phase/supernatant aqueous phase systems, preventing reliable calculation of the *ds*DNA partition coefficient.

A method of *ds*DNA partition coefficient quantification was trialled, whereby linear *ds*DNA was incubated in the presence of rehydrated DOPE H_{II} phases, supplemented with transcription buffer, prior to the aqueous supernatant phase being loaded onto a DNA electrophoresis agarose gel. Through running the post-incubation samples against a range of *ds*DNA samples of known concentration on the same gel, a plot of gel band intensities against *ds*DNA quantity was generated, effectively acting as a calibration plot against which the post-incubation supernatant samples could be compared with. Whilst this technique presented some new challenges, such as careful control of the reference *ds*DNA loading amounts and ethidium bromide staining to minimize the likelihood of gel overexposure, the gel based technique did offer considerable time-savings and the potential to offer increased flexibility in analyzing systems were the incubation solution was supplemented with components that would hamper the PCR method of K_p quantification. Full experimental details concerning the DNA gel electrophoresis method of K_p quantification can be found in section 3.9, Annex 2.

In order to validate the DNA gel electrophoresis method of *ds*DNA partition coefficient quantification, an experiment was set up under conditions homogeneous to those used to generate the data presented in Figure 3.6. This allowed for direct comparison between the PCR and DNA gel electrophoresis methods of K_p quantification, the results of which are presented in Figure 3.14.

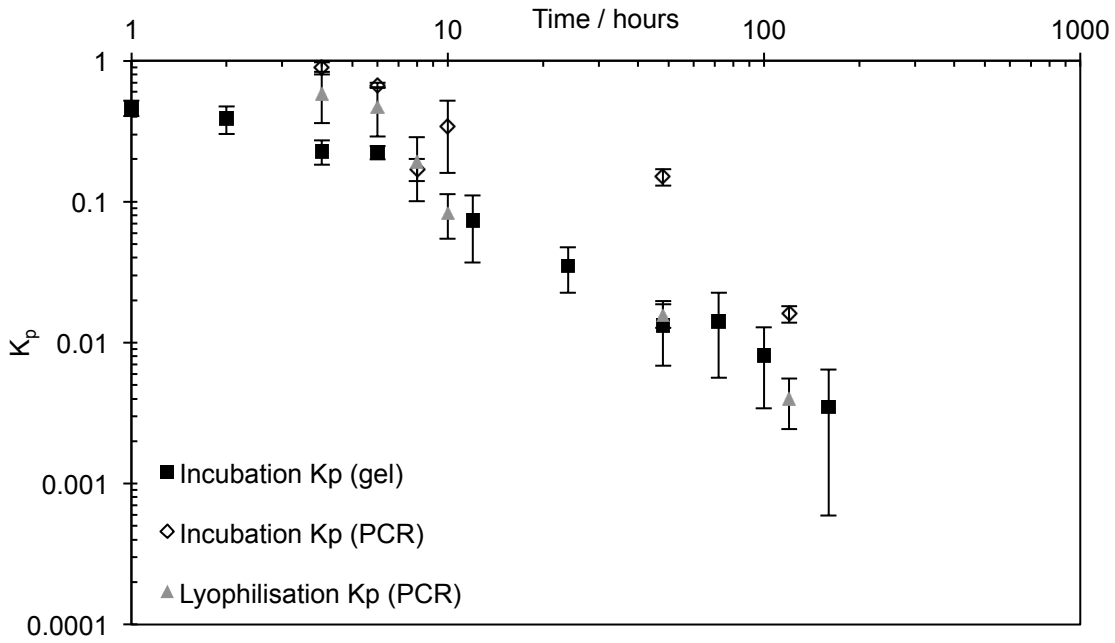

Figure 3.14 Relationship between the partition coefficient (K_p) for *lin*pT7GFP *ds*DNA and the time of incubation at 37 ˚C, quantified by PCR experiment, and the partition coefficient for *lin*pRSET-EmGFP *ds*DNA, quantified by DNA gel electrophoresis. Grey triangles show the partition coefficients obtained from experiments in which the linear *ds*DNA was mixed with the lipid *via* lyophilization, quantified by PCR experiment. Hollow diamonds show the partition coefficients from experiments in which the linear *ds*DNA was initially added to the supernatant liquid above the H_{II} phase (i.e., $K_p = 1$), quantified by PCR experiment. Black squares show the partition coefficients from experiments in which the linear *ds*DNA was initially added to the supernatant liquid above the H_{II} phase (i.e., $K_p = 1$), quantified by DNA gel electrophoresis. RW/6511/04

As can be seen in Figure 3.14, the DNA gel electrophoresis method of K_p quantification offered a broadly comparable method for accurately quantifying the *ds*DNA partition coefficient, although the method was less reliable for values where K_p was higher than ~0.2 (incubation periods below 8 hours under the experimental conditions described in Figure 3.14). This was due to the difficulty in reliably measuring the intensity of gel bands where there was more than 200 ng of linear *ds*DNA (equivalent to $K_p = 0.2$) present in the aqueous supernatant post-incubation, due to overexposure when gel analysis was performed. For partition coefficients lower than 0.2, the DNA gel electrophoresis method of K_p analysis produces a wholly consistent value for the partition coefficient when compared to the previously used PCR method; as such, partition coefficient quantification was performed using the DNA gel electrophoresis method for the results presented from this point onwards.

3.5.2 Effect of phase preparation upon K_p

With a reliable and swift method of K_p quantification by DNA gel electrophoresis established, throughput could be increased which allowed for a greater breadth of experiments into the factors affecting the partitioning of linear *ds*DNA into DOPE liquid crystalline phases to be performed. Of immediate interest was the effect of the DOPE H_{II} phase preparation upon the preferential association of linear *ds*DNA into the phase pores. Whilst the DOPE lipid 'buttons' were prepared in a controlled manner to minimize variation as far as possible, the dispensing of lipid in chloroform solution *via* Eppendorf pipette or SGE syringe (both of which frequently decrease in volume and require regeneration due to solidifying lipid), and the removal of chloroform under vacuum (causing minor bubbling which affected the available surface area of the buttons), meant that all lipid buttons in a batch had inherent variations, both in mass and available surface area.

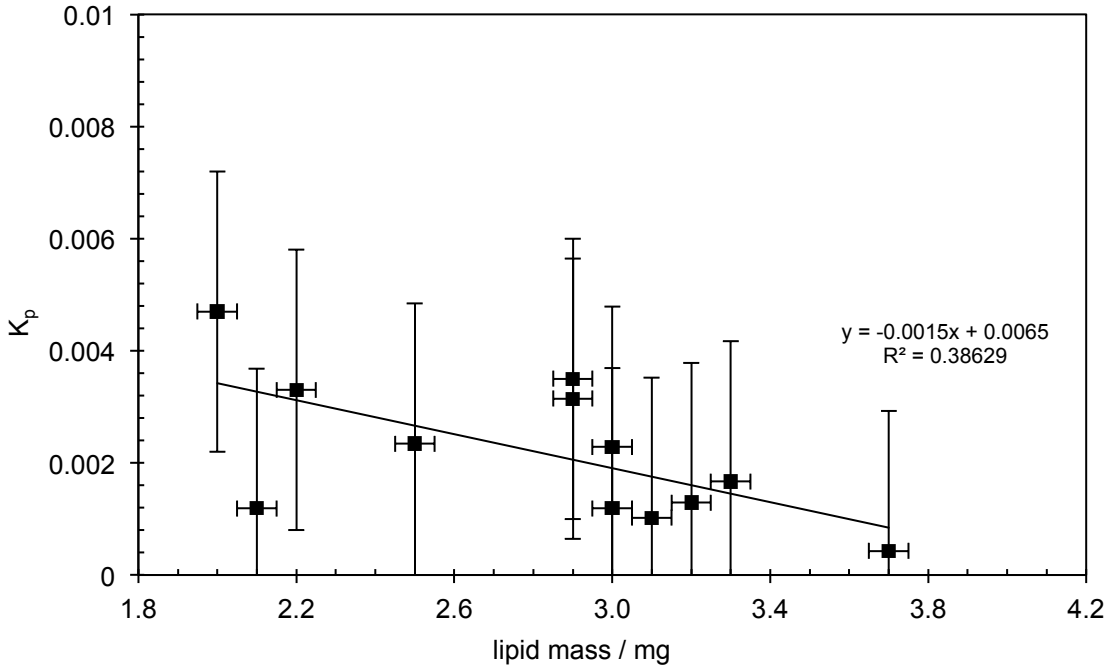

Figure 3.15 Relationship between the partition coefficient (K_p) for *lin*pRSET-EmGFP *ds*DNA and mass of DOPE H_{II} phase lipid button, quantified by DNA gel electrophoresis. Linear *ds*DNA (1 µg), supplemented with 1x transcription buffer, was incubated above the DOPE H_{II} phase for 100 hours at 37 °C (i.e. K_p = 1 when t = 0). RW/6511/06

Although an increase in the mass of the lipid buttons used for linear *ds*DNA partitioning broadly caused an increase in the amount of *ds*DNA partitioning within the lipid button (Figure 3.15), the trend observed did not have a high level of correlation, with an R^2 value of only 0.386. It could be assumed, therefore, that despite best efforts in producing lipid buttons of broadly equal mass, with frequent regeneration of the

syringes used to dispense the DOPE in chloroform solution, that there would always be some variation in the level of *ds*DNA partitioning observed across a batch of DOPE lipid buttons. However, as observed in Figure 3.15, the level of *ds*DNA partitioning remained within a range of ~0.0045 for DOPE buttons of mass 2.0-3.7 mg, which is equivalent to a maximum difference of only ± 4.5 ng DNA partitioned into the H_{II} phase of the lipid buttons (0.45% of the total linear *ds*DNA incubated above the lipid button for ~100 h). With such small variation in the level of *ds*DNA partitioning evident across a ~1 mg increase in lipid button mass, it is postulated that it is the available surface area, rather than outright mass, of the lipid button which contributes most significantly to the level of *ds*DNA partitioning observed. As a matter of good practice, the lipid buttons used for a given investigation should be confined to those produced in one batch, using the same component, equipment and technique, to minimize any variation in the surface area and mass of the lipid buttons.

3.5.3 Effect of *ds*DNA incubation conditions upon K_p

As outlined earlier in this chapter, it has already been postulated that linearized *ds*DNA is able to reside within the aqueous pore channels of H_{II} phase DOPE lipid buttons due to the interactions that occur within the system when cations, such as Na^+, associate with the negatively charged phosphate backbone of the *ds*DNA molecules, and when there are divalent metal cations (Mg^{2+}) screening the charges of the lipid to give an overall positive charge at the lipid interface with the aqueous pore channel.[15,18]

The introduction of isotonic saline solution (154 mM) to DOPE lipid buttons, during the process of lipid rehydration to ensure the formation of an inverse hexagonal phase, provides a source of monovalent cations which are thought to associate with the negatively charged phosphate backbone of the *ds*DNA molecules added during the ~100 h incubation required for partitioning into the phase pores. The entropic gain that occurs when the Na^+ ions are released from the *ds*DNA molecule is thought to provide some of the driving force required for partitioning of the DNA within the pores of the H_{II} phase. The remainder of the driving force is likely to arise from the overall positive charge upon the lipid interface, arising from the divalent magnesium cations present in the transcription buffer solution added during the ~100 h *ds*DNA incubation period.

To investigate the effect upon the partitioning of linear *ds*DNA within the DOPE lipid buttons, both rehydrated and non-rehydrated with isotonic saline, a number of distinct *ds*DNA incubation solutions were prepared, each containing 1 µg linear *ds*DNA. These

solutions, as described in Figure 3.16, were then incubated above a series of DOPE lipid buttons for 100 h at 37 ˚C.

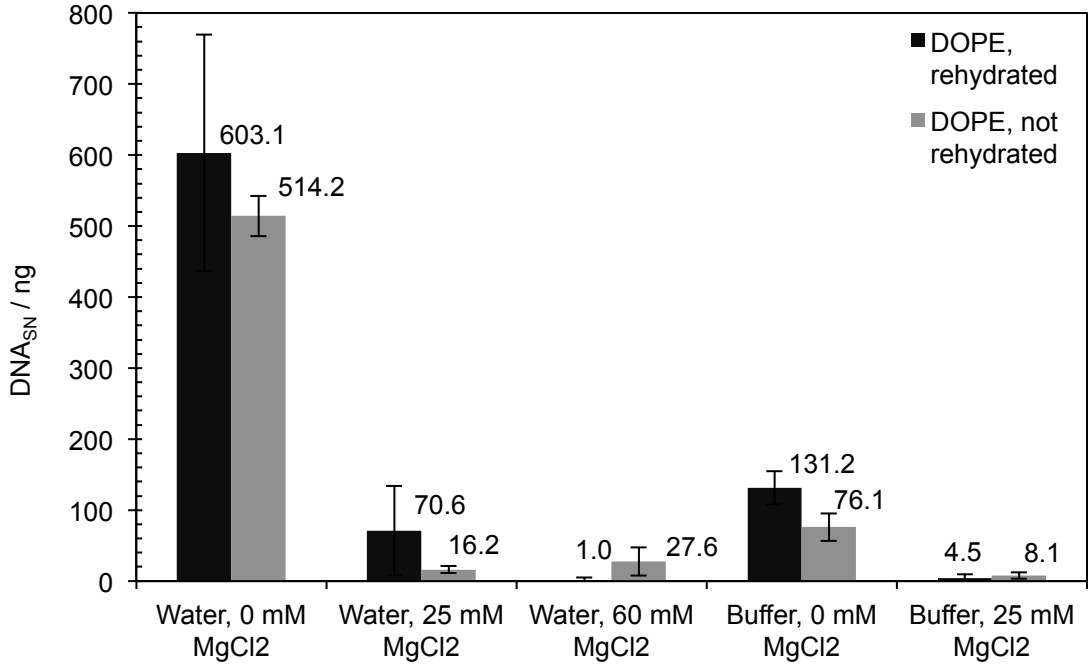

Figure 3.16 Amount of *lin*pRSET-EmGFP *ds*DNA remaining in solution under varying ionic conditions post-incubation (100 h, 37 ˚C) above rehydrated and non-rehydrated DOPE lipid buttons, quantified by DNA gel electrophoresis. Linear *ds*DNA was initially added to the supernatant liquid above the DOPE H_{II} phases (i.e. at t = 0, DNA_{SN} = 1000 ng) in solutions as described above. RW/6511/04

Excluding 60 mM $MgCl_2$ in water assay, higher levels of *ds*DNA partitioning into the liquid crystalline phase were observed for phases that had not been rehydrated with isotonic saline; this implies that, over a 100 h incubation period, the release of Na^+ ions from the *ds*DNA molecules in solution do not provide the significant driving force required for partitioning of *ds*DNA within the liquid crystal phase structure. Indeed, some partitioning into the phase is still observed, although to a far lower extent (~486 ng) for non-rehydrated buttons, when the linear *ds*DNA is incubated in the presence of water alone. This compares to rehydrated lipid buttons, incubated with the same water-only *ds*DNA solution, which achieved a similar level of partitioning into the phase (~397 ng), indicating that the the significance of these results is limited due to the difference between rehydrated and non-rehydrated lipid buttons residing within experimental error.

Incubation of 1 µg linear *ds*DNA with DOPE lipid buttons in the presence of $MgCl_2$ caused a significant increase in the partitioning of *ds*DNA within the liquid crystalline phase. For example, supplementation of the incubation solution with 25 mM $MgCl_2$ for non-rehydrated lipid buttons improved *ds*DNA partitioning within the phase to

~993 ng, compared to the previous amount of ~486 ng. With such a significant increase in the level of *ds*DNA partitioning observed, it was clear that the majority of the driving force for *ds*DNA partitioning within the liquid crystalline phase arose from the interactions of Mg^{2+} with the linear *ds*DNA and lipid interface. Increasing the level of $MgCl_2$ supplementation, for non-rehydrated lipid buttons, from 25 to 60 mM led to no change in the level of *ds*DNA partitioning observed, within experimental error.

A less substantial increase in *ds*DNA partitioning is observed when the *ds*DNA incubation solution is supplemented with transcription buffer, omitting the addition of $MgCl_2$, with ~924 ng linear *ds*DNA partitioning to within the liquid crystalline phase of non-rehydrated DOPE lipid buttons. As would be expected, supplementation of this buffer solution with 25 mM $MgCl_2$ leads to a further increase in *ds*DNA partitioning, with 99% of the initial supernatant linear *ds*DNA partitioning within the liquid crystalline phase of both rehydrated and non-rehydrated DOPE lipid buttons after 100 h incubation at 37 ˚C. Optimal incubation conditions, therefore, for the partitioning of linear *ds*DNA into the liquid crystalline phase of DOPE lipid buttons require complete transcription buffer solution, supplemented with 25 mM $MgCl_2$, incubated for 100 h at 37 ˚C above preformed DOPE lipid buttons.

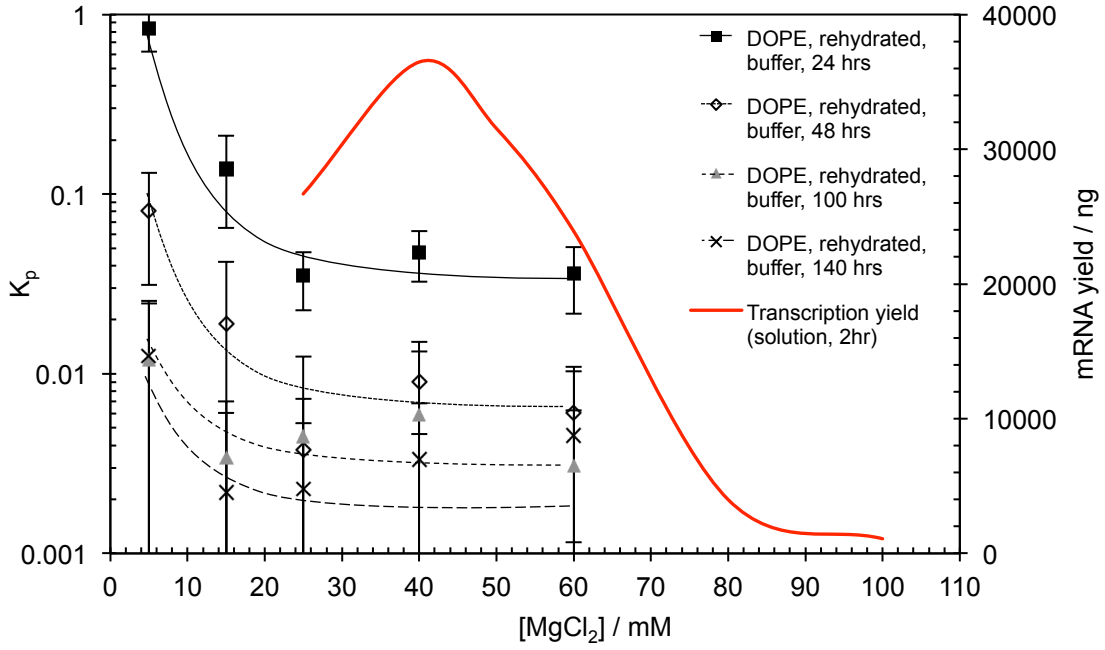

Figure 3.17 Relationship between the partition coefficients (K_p) for *lin*pRSET-EmGFP *ds*DNA above rehydrated DOPE lipid buttons, post-incubation (37 ˚C) across a concentration gradient of $MgCl_2$, quantified by DNA gel electrophoresis. Black squares show partition coefficients after 24 h; hollow diamonds show partition coefficients after 48 h; grey triangles show partition coefficients after 100 h; black crosses show partition coefficients after 140 h incubation. For each incubation period: at t = 0, K_p = 1. Red line shows the solution-based positive control transcription yield across a concentration gradient of $MgCl_2$. Note that the curves shown for each data set are drawn as guides to the eye, and are not directly fitted to the data. RW/6511/04

With the optimal conditions for linear *ds*DNA partitioning identified, the effect of incubation period of the supernatant solution above the DOPE lipid buttons was investigated. These investigations were performed utilizing DOPE lipid buttons that had been rehydrated with isotonic saline solution, with supernatant solutions containing 1 µg linear *ds*DNA, transcription buffer solution and a concentration gradient of $MgCl_2$, from 5-60 mM. The results of these investigations are compared to the solution-based transcription yield from a standard 20 µL transcription reaction containing an equal amount of template *ds*DNA, incubated for 2 h at 37˚C, across a concentration gradient of reaction buffer $MgCl_2$ content from 25-100 mM (Figure 3.17).

It is clear that the partitioning of linear *ds*DNA within the liquid crystalline phase of H_{II} phase DOPE lipid buttons is a slow process, with Figure 3.17 highlighting the reduction in the partition coefficient, K_p, over time. Within experimental error, K_p values for lipid buttons incubated for 100 or 140 h are similar for all concentrations of supplementary $MgCl_2$, with both data sets highlighting an optimal level of *ds*DNA partitioning in systems containing 15-25 mM $MgCl_2$. Utilizing an incubation solution containing $MgCl_2$ at this range of concentrations would be ideal, as it would ensure that subsequent transcription reactions from the *ds*DNA-containing lipid button would not be adversely affected by any remaining Mg^{2+}ions, post removal of the supernatant layer; the peak in solution-based transcriptional yield is observed for an $MgCl_2$ concentration of 40 mM (Figure 3.17).

3.5.4 Effect of individual transcription components upon K_p

With the data sets presented in Figure 3.16 identifying that transcription buffer solution has a contributory effect towards the partitioning of linear *ds*DNA within DOPE lipid buttons, an investigation was performed to identify the individual effect of each transcription buffer component upon *ds*DNA partitioning. The standard transcription buffer solution utilized for solution-based transcription, specifications for which can be found in table 2.2, contains $MgCl_2$ (25 mM), trizma (40 mM), spermidine (2.5 mM), triton X-100 (0.01% v/v), dithiothreitol (DTT, 10 mM) and RNAsin (10 mM); to assess each component's effect upon the partition coefficient, individual supernatant solutions containing 1 µg linear *ds*DNA and one of the transcription buffer components, at the component's recommended concentration, were incubated for 100 h at 37 ˚C above triplicate sets of DOPE lipid buttons. As per the experimental data presented in Figure 3.17, the investigation was performed using DOPE lipid buttons that had been rehydrated with isotonic saline solution prior to the 100 h incubation period.

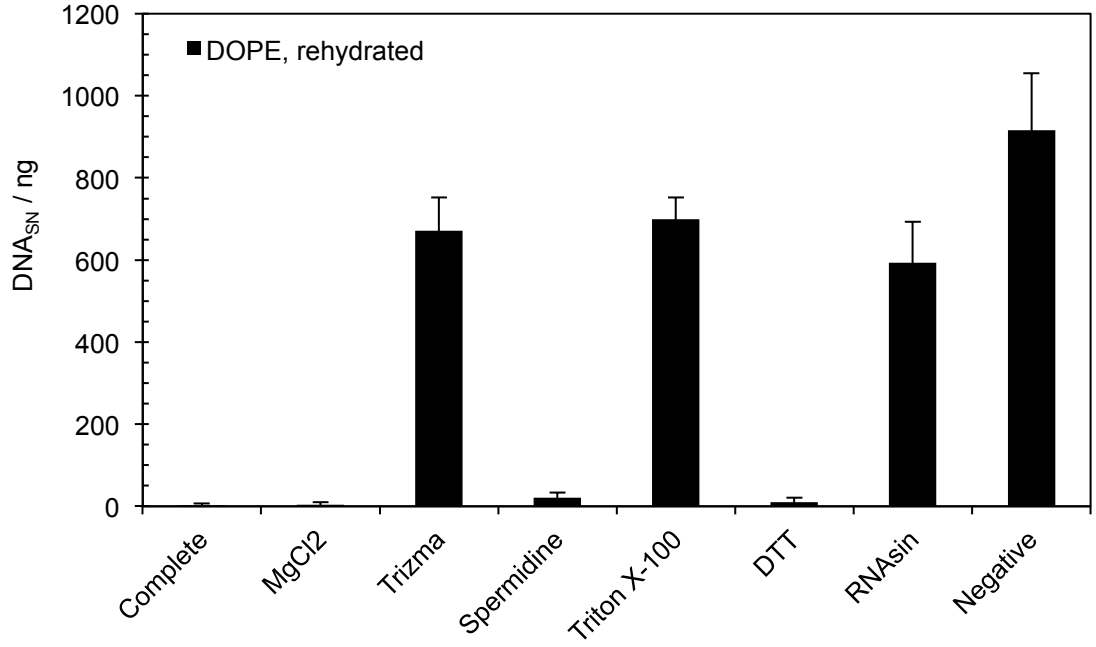

Figure 3.18 Amount of *lin*pRSET-EmGFP *ds*DNA remaining in solution post-incubation (100 h, 37 ˚C) with individual transcription buffer components above rehydrated DOPE lipid buttons, quantified by DNA gel electrophoresis. Linear *ds*DNA was initially added to the supernatant liquid above the DOPE H_{II} phases (i.e. at t = 0, DNA_{SN} = 1000 ng) in transcription buffer component solutions as described above. RW/6511/09

As demonstrated previously (Figure 3.16), complete transcription buffer, containing 25 mM $MgCl_2$, resulted in >99% of the linear supernatant *ds*DNA partitioning to within the liquid crystalline phase of the rehydrated DOPE lipid buttons (Figure 3.18). Within the complete transcription buffer, it is clear that three components contribute significantly towards the partitioning of linear *ds*DNA within the phase: $MgCl_2$ (25 mM), spermidine (2.5 mM), and DTT (10 mM). $MgCl_2$ and DTT resulted in >99% of the linear *ds*DNA being partitioned within the phase, whilst spermidine only resulted in 98% of the supernatant *ds*DNA partitioning. Compared to the negative control, where 1 µg of linear *ds*DNA was incubated above the lipid phase in water, trizma, triton X-100 and RNAsin can be observed to contribute minimally towards the partitioning of the supernatant *ds*DNA within the phase, each giving rise to a similar level of partitioning (~300-400 ng partitioned within the liquid crystalline phase, post 100 h incubation at 37 ˚C), within experimental error.

To further examine the individual effect upon *ds*DNA partitioning caused by $MgCl_2$, spermidine, and DTT, the partition coefficients were calculated and contrasted with that obtained when incubation of 1 µg linear *ds*DNA above DOPE lipid buttons had been performed for 100 h using complete transcription buffer solution (Figure 3.19).

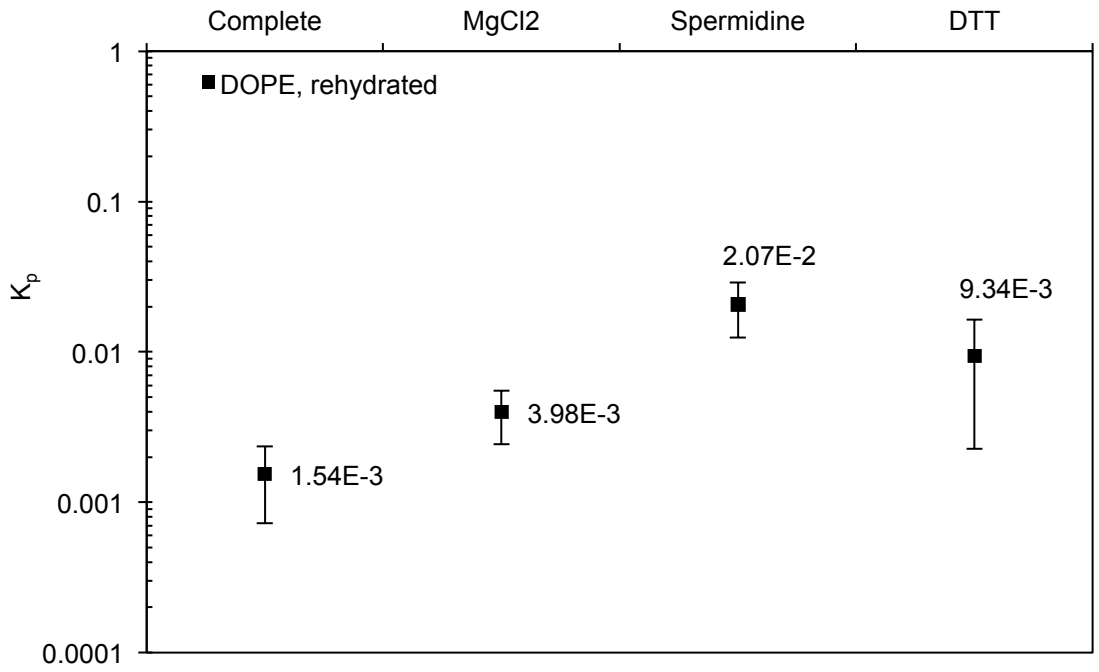

Figure 3.19 Relationship between the partition coefficient (K_p) for *lin*pRSET-EmGFP *ds*DNA and incubation solution composition, post-incubation (100 h, 37 ˚C), quantified by DNA gel electrophoresis. Linear *ds*DNA (1 µg), supplemented with transcription reaction components (as detailed above), was incubated above the DOPE H_{II} phase for 100 hours at 37 ˚C (i.e. K_p = 1 when t = 0). RW/6511/09

Figure 3.19 shows the partition coefficient data for lipid buttons prepared *via* 100 h incubation with 1 µg linear *ds*DNA and either complete transcription buffer solution, $MgCl_2$ (25 mM), spermidine (2.5 mM), or DTT (10 mM). Complete transcription buffer solution leads to the highest amount of linear *ds*DNA partitioning (K_p = 0.0015 ± 0.0008), with the majority of the driving force for partitioning effected by the $MgCl_2$ (25 mM) contained within the incubation supernatant solution; $MgCl_2$ had the most significant contribution towards *ds*DNA partitioning out of the tested transcription buffer components (K_p = 0.004 ± 0.002), however its partition coefficient did lie within experimental error of the higher mean partition coefficient observed for DTT (K_p = 0.009 ± 0.007). Whilst the partition coefficient achieved through incubating with $MgCl_2$ alone is only marginally higher than is achieved through the use of complete transcription buffer, which requires a greater number of resources and thus a higher end cost per lipid button, the use of complete transcription buffer for partitioning of linear *ds*DNA within the liquid crystalline phase of DOPE lipid buttons is to be recommended to ensure that the maximal amount of template *ds*DNA is contained within the phase prior to any transcriptional activity utilizing the lipid button.

3.6 Transcribing *ds*DNA contained within H_{II} phases

3.6.1 Transcription activity

Previous research published by Corsi *et al.* (2008) had shown that linear *ds*DNA-containing H_{II} phase DOPE lipid buttons prepared *via* lyophilization are transcriptionally active. Experimental data presented earlier within this chapter has shown, however, that such *ds*DNA-containing DOPE phases can be prepared *via* either lyophilization or incubation over approximately 100 h with a transcription buffer incubation solution. To test the transcriptional activity of *ds*DNA-containing DOPE phases prepared *via* the incubation method, some oversized lipid buttons (~6.5 mg) were loaded with 4 µg template *ds*DNA in the presence of complete transcription buffer over 100 hours (37 °C), before being washed with aliquots of nuclease-free water to remove excess incubation solution, and then subjected to transcription (scaled up to a total reaction volume of 80 µL) by layering complete transcription buffer solution and T7 RNA polymerase above the *ds*DNA-containing lipid buttons, incubating the reactions for a period of 2 hours in a waterbath (37 °C). mRNA produced from the lipid button transcription reactions was purified using a QIAGEN RNeasy mini spin kit prior to quantitation of the yield by NanoDrop UV-visible spectrophotometry.

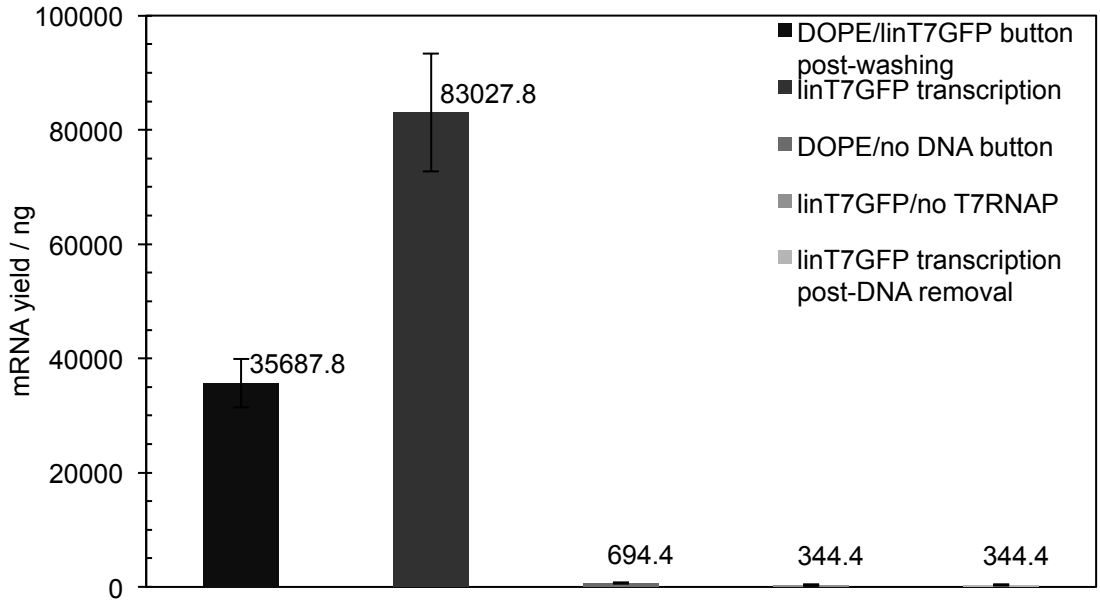

Figure 3.20 Amount of mRNA produced by transcription reactions from larger ~6.5 mg DOPE-DNA H_{II} phases preloaded with 4 µg template *ds*DNA (100 h incubation, 37 °C) compared to an equal amount of template *ds*DNA in solution phase transciption. The following negative controls were performed: DOPE H_{II} phase that had not been preloaded with *ds*DNA; solution-based assay (no T7RNAP); transcription upon the solution removed from above the DOPE H_{II} phase post-100 h incubation. Transcription reactions were incubated for 2 h at 37 °C. RW/5778/28

As shown in Figure 3.20, transcription in the absence of DOPE liquid crystalline phases offers mRNA yields greater than double that achieved for transcription from the template *ds*DNA contained within DOPE liquid crystalline phases, which often have isolation amounts in the region of one third to one half of that of a positive control assay incubated under identical conditions; this observation is coherent with previous transcription data from DOPE liquid crystalline phases published by Corsi *et al*.[15] The quadrupling of assay size has increased the amount of mRNA isolated, from both the positive control and liquid crystalline assays, to approximately four times that isolated from standard assay volume (20 µL) solution phase transcriptions, within experimental error. It can be concluded, therefore, that the amount of mRNA isolated is proportional to the total assay volume; however, due to the nature of the *ds*DNA partitioning within the H_{II} phase DOPE buttons, increases in yield may not be linearly proportional to increases in template *ds*DNA amount, as there is no guarantee that every molecule of *ds*DNA is equally accessible for transcription. Importantly, Figure 3.20 shows that *ds*DNA-containing DOPE phases prepared *via* 100-hour incubation are transcriptionally active, as per had been demonstrated by Corsi *et al*. with the lyophilization method of preparation.[15]

3.6.2 Effect of incubation time upon RNA yield

With experimental data identifying both *ds*DNA-containing DOPE lipid buttons prepared *via* either the lyophilization or incubation methods are transcriptionally active, a series of experiments were carried out to assess the effect of incubation period upon the mRNA yield produced. A comparison was made of H_{II} phase DOPE lipid buttons (~2 mg), loaded with 1 µg linear *ds*DNA, prepared *via* lyophilization, 100 hour incubation without saline rehydration or 100 hour incubation with saline rehydration. As per the experiment described in section 3.6.1, transcription was performed above the *ds*DNA-containing lipid buttons by layering complete transcription buffer solution and T7 RNA polymerase above the liquid crystalline phase (but to a total reaction volume of 20 µL), and incubating the reactions for a period of 2 hours in a waterbath (37 ˚C). Purification and quantitation of the mRNA produced from each reaction was performed in the same manner as before. The results from each lipid phase transcription time course investigation are presented in Figures 3.21-3.23.

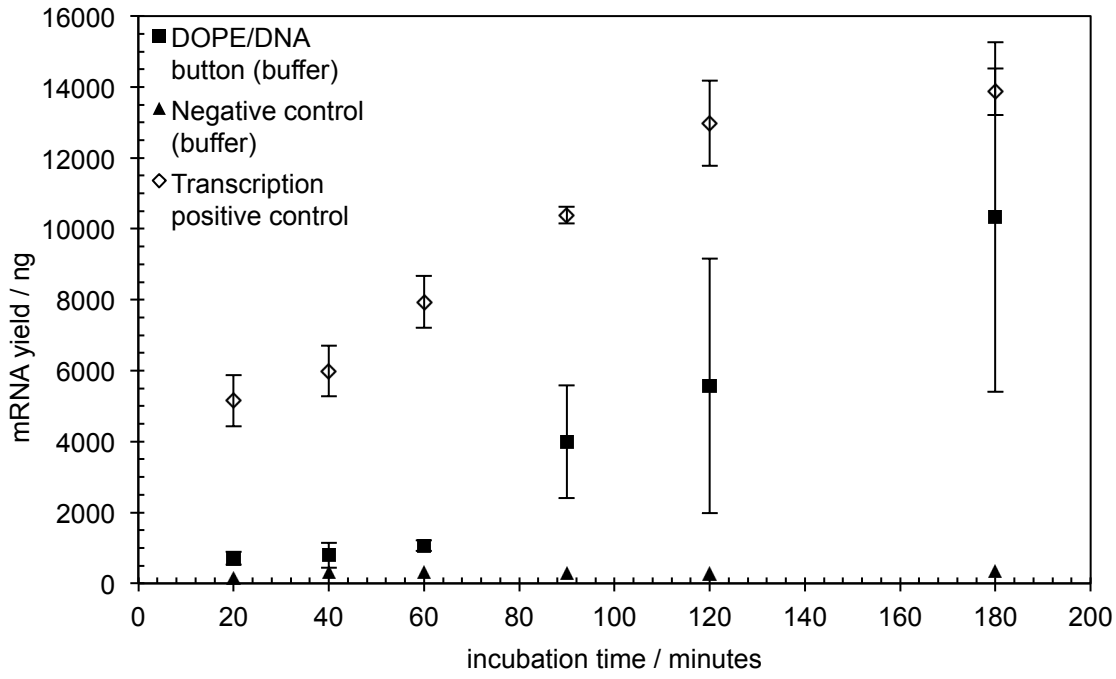

Figure 3.21 Time-course investigation: Amount of mRNA produced by transcription reactions from ~2 mg DOPE-DNA H_{II} phases, prepared *via* the lyophilization method, compared to an equal amount of template *ds*DNA in solution. Black squares show DOPE-DNA H_{II} phases that were prepared *via* the lyophilization method of *ds*DNA partitioning; black triangles show negative controls (no T7RNAP); hollow diamonds show solution-based positive control. Transcription reactions were incubated for time periods as shown above at 37 °C. RW/6147/05

Figure 3.21 shows the production of DOPE-DNA H_{II} phases prepared *via* the lyophilization method, as reported by Corsi *et al*. (2008).[15] As expected, the yields of mRNA produced by transcription from the *ds*DNA-containing lipid button after 2 hours of incubation remain within a third to one half of the positive control, solution phase transcription yield (within experimental error). As the incubation time of the reactions progress, the difference in mRNA yield obtained from the lipid button assay and the positive control assay closes; whilst the positive control assay yield appears to be reaching a plateau, the lipid button assay yields suggest that they would continue to rise to a similar plateau after a further period of incubation. These results suggest that the partitioning of linear *ds*DNA within DOPE lipid buttons prepared *via* lyophilization slows the rate at which the transcription reaction proceeds; this is likely due to the restricted accessibility of the linear *ds*DNA molecules sited within the aqueous channels of the H_{II} phase when compared to the uninhibited accessibility of template *ds*DNA within solution phase positive control transcription assays.

As discussed in section 3.5.3, the rehydration of DOPE lipid buttons with isotonic saline prior to the incubation of linear *ds*DNA above the phases to partition the *ds*DNA within had no significant effect upon the partition coefficient, within experimental

error. Despite this, transcription upon *ds*DNA-containing DOPE buttons prepared both with and without isotonic saline rehydration were carried out to assess if the rehydration process had any residual effect upon the transcriptional activity of the buttons, especially as lipid buttons prepared *via* the lyophilization method of *ds*DNA partitioning require rehydration with isotonic saline before use.

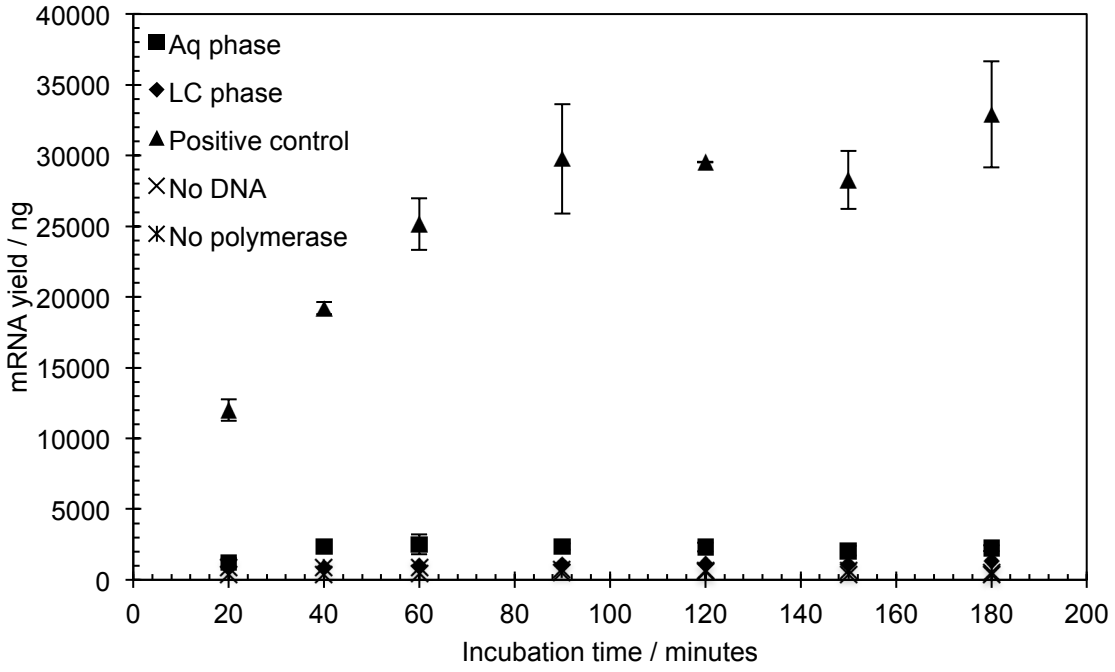

Figure 3.22 Time-course investigation: Amount of mRNA produced by transcription reactions from non-rehydrated ~2 mg DOPE-DNA H_{II} phases (130 h incubation, 37 °C) compared to an equal amount of template *ds*DNA in solution. Black squares show aqueous supernatant mRNA from DOPE-DNA H_{II} phases that **had not** been rehydrated with isotonic saline prior to *ds*DNA incubation; black diamonds show liquid crystalline phase mRNA from DOPE-DNA H_{II} phases that **had not** been rehydrated with isotonic saline prior to *ds*DNA incubation; black triangles show negative controls (no T7RNAP); hollow diamonds show solution-based positive control. Transcription reactions were incubated for time periods as shown above at 37 °C. RW/6147/16

Whilst Figure 3.21 shows that lyophilized ~2 mg DOPE lipid buttons loaded with 1 µg linear *ds*DNA were transcriptionally active, Figure 3.22 shows that rehydrated DOPE buttons that had not been rehydrated with isotonic saline solution prior to loading with *ds*DNA *via* extended incubation were not significantly transcriptionally active, after any period of incubation, with very little mRNA synthesized over the course of the investigation (<2500 ng of mRNA from any given time point). The lack of transcriptional activity from these DNA-DOPE buttons was speculated to be due to the omission of the rehydration of each lipid button with isotonic saline solution prior to partitioning of linear *ds*DNA within the H_{II} phases; the same experiment was thus performed using DNA-DOPE lipid buttons that had been treated to rehydration with isotonic saline solution during their preparation (Figure 3.23).

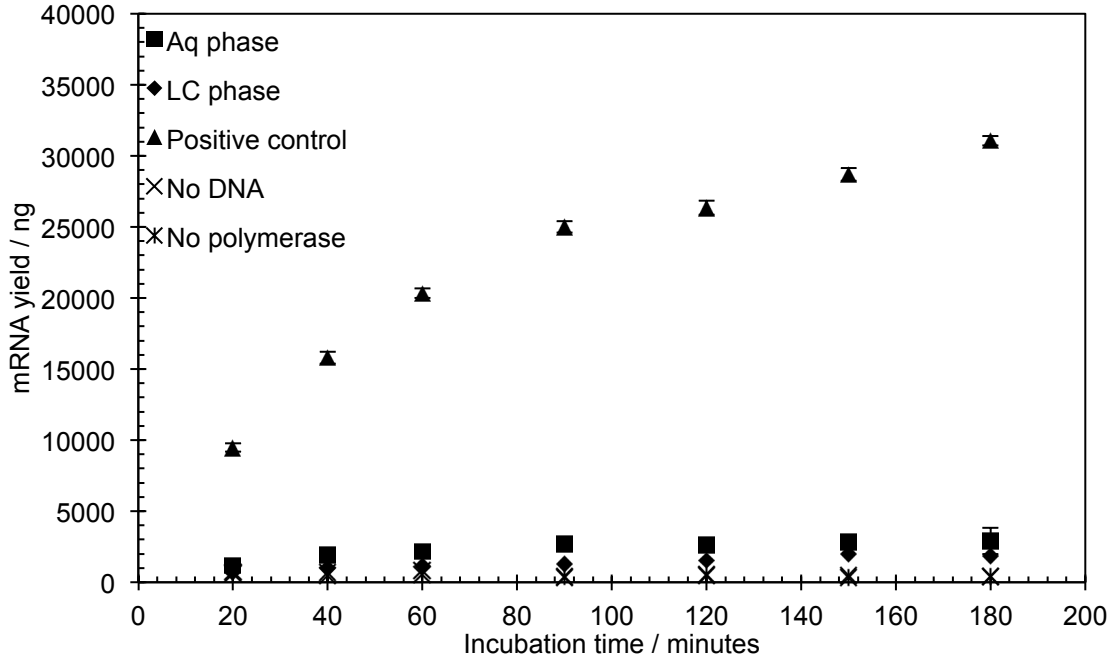

Figure 3.23 Time-course investigation: Amount of mRNA produced by transcription reactions from rehydrated ~2 mg DOPE-DNA H_{II} phases (130 h incubation, 37 ˚C) compared to an equal amount of template *ds*DNA in solution. Black squares show aqueous supernatant mRNA from DOPE-DNA H_{II} phases that **had** been rehydrated with isotonic saline prior to *ds*DNA incubation; black diamonds show liquid crystalline phase mRNA from DOPE-DNA H_{II} phases that **had** been rehydrated with isotonic saline prior to *ds*DNA incubation; black triangles show negative controls (no T7RNAP); hollow diamonds show solution-based positive control. Transcription reactions were incubated for time periods as shown above at 37 ˚C. RW/6147/17

Rehydration of the lipid buttons with isotonic saline solution prior to partitioning of linear *ds*DNA within the DOPE lipid buttons had no beneficial effect upon transcriptional activity from the buttons (Figure 3.23), with again very little mRNA produced over the course of the time course investigation (<3000 ng of mRNA for any given time point). This set of results confirmed that the rehydration of DOPE buttons with isotonic saline solution was of no perceivable benefit to either partitioning of the *ds*DNA within the phase, or to the transcriptional activity of DNA-DOPE lipid buttons, when the buttons had been prepared *via* extended incubation over 100 h (37 ˚C) with linearized *ds*DNA and complete transcription buffer solution containing 25 mM $MgCl_2$.

The results presented in Figures 3.22 and 3.23 were most unexpected; firstly, the enlarged ~6.5 mg DOPE buttons loaded with 4 µg *ds*DNA (data shown in Figure 3.20) were transcriptionally active; secondly, partition coefficient analysis by DNA gel electrophoresis had shown that all of the DOPE lipid buttons used for these investigations were pre-loaded with ~1 µg linear *ds*DNA, with only trace amounts of linear *ds*DNA present within the supernatant incubation solutions after 130 h

incubation. With the lipid buttons known to contain ~1 µg linear *ds*DNA, it is thought that either the assay conditions were unsuitable for transcription by T7 RNA polymerase; that the *ds*DNA contained within the liquid crystalline phase structure was inaccessible for transcription; or that, like the partitioning of linear *ds*DNA within DOPE H_{II} phases, the transcription process proceeds slowly and thus higher levels of transcriptional activity may be observed after a further period of incubation.

3.7 Establishment of a reliable transcription assay using DOPE H_{II} phases

3.7.1 Optimized transcription assay parameters for using DOPE H_{II} phases

Following the experiments described within this chapter, a recommended protocol for the partitioning of linear *ds*DNA within the liquid crystalline phase of DOPE lipid buttons was established, the details of which are as follows:

- ~2 mg DOPE lipid buttons;
- Optional rehydration of the lipid buttons with isotonic saline solution (2 µL per lipid button);
- Incubation of the lipid buttons, for a minimum of 100 h at 37 °C, with a supernatant solution layered above the buttons comprising of
    - 1 µg linearized *ds*DNA
    - 25 mM $MgCl_2$
    - trizma (40 mM)
    - spermidine (2.5 mM)
    - triton X-100 (0.01% v/v)
    - dithiothreitol (DTT, 10 mM)
    - RNAsin (10 mM);
- Analysis of the partition coefficient using quantitative DNA gel electrophoresis.

Investigations into the transcriptional activity of DNA-DOPE lipid buttons prepared *via* either lyophilization or 100+ h incubation have shown that further investigation is required to better understand the nature of transcription in the presence of *ds*DNA-containing DOPE H_{II} phases. Lipid buttons prepared *via* the lyophilization method had higher transcriptional activity compared to buttons prepared *via* 100+ h incubation, yet were shown to contain similar quantities of template *ds*DNA within the phase, so theoretically both preparations should be able to sustain similar levels of transcription under identical assay conditions.

Although higher transcriptional yields could likely be achieved when transcription is later performed on the DNA-DOPE buttons by using an incubating solution of transcription buffer solution containing 40 mM $MgCl_2$, a concentration of 25 mM is suggested in case any $MgCl_2$ is retained within the DOPE lipid buttons post incubation with linearized template *ds*DNA; at $MgCl_2$ concentrations above ~45 mM, transcriptional activity has been shown to be significantly inhibited.

3.8 Discussion

Comparison of the previously reported lyophilization method of DNA-DOPE lipid button preparation[15] and the newly-developed extended incubation method of preparation has shown that either method is suitable for the partitioning of linearized *ds*DNA within the H_{II} liquid crystalline phase of DOPE lipid buttons. After 100 hours, $K_p < 0.008$ for DOPE-DNA lipid buttons prepared *via* either method. Quantitative DNA gel electrophoresis was shown to produce reproducible values of the partition coefficient (K_p) when compared to the previously established technique using PCR, which allowed for more rapid preparation and analysis of lipid button samples.

Assessment of the individual effect of transcription buffer components upon linear *ds*DNA partitioning was made, with the observation made that those components which contribute significantly to the overall ionic strength of the solution cause *ds*DNA to partition within the phase. This supports the argument presented by Corsi *et al.* (2008)[15] that the interaction of *ds*DNA with the H_{II} phase of DOPE is directed by ionic interactions between the *ds*DNA and the lipid phase. These interactions are likely due to a bridging effect between the negative charges upon the phosphate backbone of the *ds*DNA molecules and the negative charges upon the phosphate headgroups of the DOPE molecules by cationic molecules present within the transcription buffer solution. $MgCl_2$ (25 mM), spermidine (2.5 mM) and DTT (10 mM) were all shown to have a significant effect upon the partitioning of linear *ds*DNA molecules within H_{II} phase DOPE, with the highest levels of *ds*DNA partitioning observed when these components were combined in full transcription buffer solution. Interestingly, when *ds*DNA partitioning is performed using complete transcription buffer solution over an extended period of incubation, the rehydration of the lipid buttons with isotonic saline prior to incubation had no significant effect upon levels of *ds*DNA partitioning observed.

Comparisons were then made between the transcriptional activity of DNA-DOPE lipid buttons prepared *via* both the lyophilization and 100+ h incubation method. Lipid buttons prepared *via* lyophilization were shown to possess a significantly higher level of transcriptional activity, although this was still lower than could be achieved from a traditional solution-phase transcription assay. The discrepancies between the transcriptional activity of DNA-DOPE lipid buttons prepared *via* either lyophilization or 100+ h incubation must arise from the conditions under which they are prepared. Lyophilization requires the freeze-drying of DOPE lipid buttons, which have had a solution of template *ds*DNA layered upon them, followed by rehydration of the buttons with isotonic saline solution prior to their use in a transcription assay. The extended

incubation method of DNA-DOPE lipid button preparation involves the incubation of a DOPE H_{II} phase button with template *ds*DNA solution supplemented with complete transcription buffer for 100+ h (37 ˚C), followed by extraction of the supernatant solution and refrigerated storage prior to their use in a transcription assay. Partition coefficient (K_p) analysis data presented within this chapter has shown that the partitioning of linear *ds*DNA within DOPE H_{II} phases is a slow process; it is therefore possible that the lyophilization method, due to the vacuum environment required, is forcing molecules of linear *ds*DNA to become absorbed into the phase pores towards the upper surface of the phase, or even to become adsorbed upon the surface of the phase, thus making the template *ds*DNA more accessible for transcription by T7 RNA polymerase. By allowing linear *ds*DNA to become partitioned within the H_{II} phase of DOPE buttons *via* extended incubation in transcription buffer solution, the molecules of linear *ds*DNA are allowed to naturally assume the most favourable position within the phase; if molecules of *ds*DNA partition deep within the pores of the phase, or indeed if a phase pore is occupied by multiple molecules of linear *ds*DNA arranged end-to-end, then less template *ds*DNA is going to be accessible for transcription by T7 RNA polymerase.

As discussed in this chapter, the transcription of template *ds*DNA contained within the inverse hexagonal phase of DOPE lipid buttons requires further investigation to better understand the nature of the system; this will be revisited in Chapter 4 as part of the studies into the feasibility of batch transcription from *ds*DNA-containing H_{II} phase DOPE lipid buttons.

3.9 Annex

3.9.1 Annex 1: DOPE lipid button calculations

For a 2.0 mg DOPE lipid button:

$$m = 2.0\ mg \equiv 2\times10^{-3}\ g$$

$$\rho = 0.9\ g\ cm^{-3} \equiv 0.9\times10^{6}\ g\ m^{-3}$$

$$v = \frac{m}{\rho} = \frac{2\times10^{-3}\ g}{0.9\times10^{6}\ g\ m^{-3}} = 2.22\times10^{-9}\ m^{3}$$

$$v_{sphere} = \frac{4}{3}\pi r^{3}$$

$$\therefore\ v_{hemisphere} = \frac{1}{2}\left(\frac{4}{3}\pi r^{3}\right) \qquad (v_h)$$

$$v_h = \frac{2}{3}\pi r^{3}$$

$$r^{3} = \frac{3v_h}{2\pi}$$

$$r = \sqrt[3]{\frac{3v_h}{2\pi}} = 1.02\times10^{-3}\ m$$

1 hole per area (A)

$$A = (4)^2 \sin 60^{\circ}$$

$$A = 1.386\times10^{-17}\ m^{2}$$

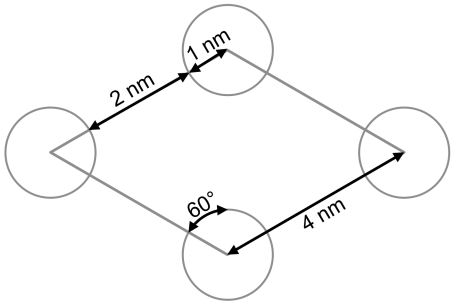

$$A_{hole} = \pi(1\times10^{-9})^{2}$$

$$A_{hole} = 3.142\times10^{-18}\ m^{2}$$

$$A_{exc.\ hole} = 1.072\times10^{-17}\ m^{2}$$

Figure 3.24 Diagram illustrating the dimensions of the inverse hexagonal phase structure. The circular regions represent the pores in the inverse hexagonal phase.

DNA dimensions (*lin*T7-Luc *ds*DNA, as used by Corsi *et al.*, 2008):
4331 base pairs; 3.4 Å per base unit

$$\therefore\ l_{T7-Luc} = 1.47\times10^{-6}\ m$$

$$d_{T7-Luc} \sim 2\times10^{-9}\ m$$

Longitudinal x sectional area of *ds*DNA = 2.94 x 10^{-15} m^2

1 µg of 4331 bp T7-Luc DNA ~ 3.5×10^{-13} moles ~ 2.11×10^{11} molecules *ds*DNA
10 µg of 4331 bp T7-Luc DNA ~ 3.5×10^{-12} moles ~ 2.11×10^{12} molecules *ds*DNA

$$A_{convex} = \frac{1}{2}(4\pi r^2)$$
$$A_{convex} = 2\pi r^2$$
$$A_{convex} = 6.54\times10^{-6}\ m^2$$
$$\therefore 4.72\times10^{11}\ pores\ in\ phase\ surface$$
$$\therefore 4.72\times10^{11}\ DNA\ molecules\ in\ pores$$
$$= 7.8\times10^{-13}\ moles\ of\ DNA\ in\ pores$$

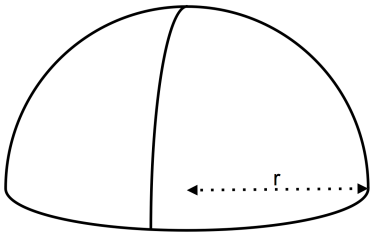

Figure 3.25 Diagram showing the estimated convex surface area available on a 2 mg DOPE lipid button.

Based upon the estimated area of the convex surface, 2.22×10^{9} DNA molecules could adsorb on surface (equivalent to loading lipid button with 0.01 µg DNA).

$$A_{planar} = \pi r^2$$
$$A_{planar} = 3.27\times10^{-6}\ m^2$$
$$\therefore 2.36\times10^{11}\ pores\ in\ phase\ surface$$
$$\therefore 2.36\times10^{11}\ DNA\ molecules\ in\ pores$$
$$= 3.9\times10^{-13}\ moles\ of\ DNA\ in\ pores$$

$$A_{holes\ total} = 7.41\times10^{-7}\ m^2$$
$$A_{planar-holes} = 2.53\times10^{-6}\ m^2$$

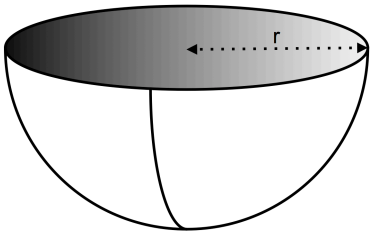

Figure 3.26 Diagram showing the estimated planar surface area available on a 2 mg DOPE lipid button. The total planar surface area of the lipid button is comprised of 7.41×10^{-7} m^2 pore openings and 2.53×10^{-6} m^2 lipid surface between the pore openings.

Based upon the estimated area of the planar surface, 1.11×10^{9} DNA molecules could adsorb on surface (equivalent to loading lipid button with 0.005 µg DNA)

Assuming the DNA partitions within the holes of the DOPE inverse hexagonal liquid crystalline phase, the phase would have a total capacity for 1.17×10^{-12} moles of T7-Luc DNA, equal to 7.1×10^{11} molecules, based on the assumption that each pore houses one molecule of 4331 bp T7-Luc DNA.

3.9.2 Annex 2: Partition coefficient (K_p) quantification

3.9.2.1 K_p quantification by PCR

The polymerase chain reaction (PCR) had been previously used to investigate the partitioning of linear *ds*DNA into the inverse hexagonal phase of DOPE,[18] thanks to its ability to detect and amplify small quantities of template *ds*DNA, and because of the specificity offered by designing primers and PCR cycles to amplify only a specific sequence within the *ds*DNA. PCR primers were designed for amplification of the green fluorescent protein (GFP) gene sequence present in pT7GFP, producing a PCR product of known length (717 bp), allowing for clear identification and quantification of the PCR product by gel electrophoresis and NanoDrop UV-visible spectrophotometry.

Table 3.2 PCR primer specification for amplification of green fluorescent protein sequence from pT7GFP.

Primer	Length	MW	Tm°	Dimer	Secondary	GC%	Sequence (5'-3')
T7GFP-FWD	33	10283	71.1	No	Weak	39.3%	GTTGTTGGATCCATGAGTAAAGGAGAAGAACTT
T7GFP-REV	36	11000	73.9	No	Weak	41.6%	GTTGTTGAGCTCCTATTTGTATAGTTCATCCATGCC

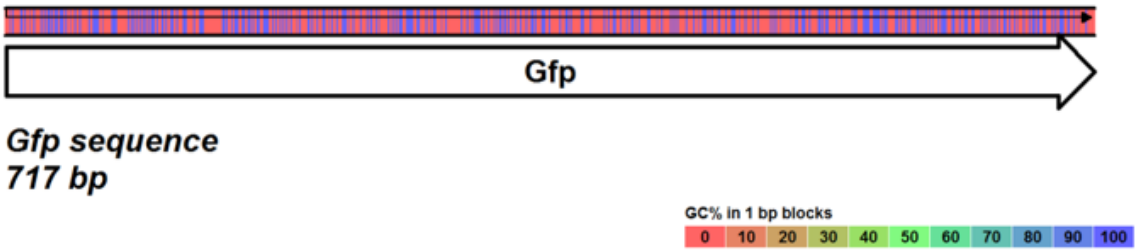

Figure 3.27 Sequence map of amplified green fluorescent protein (GFP) gene. Colour coding denotes GC% in 1 bp blocks.

To quantify the amount of *ds*DNA left in the aqueous supernatant solution above the DOPE lipid buttons post-incubation (typically ~100 h, 37 °C), an aliquot of the supernatant (4 out of a total of 20 µL) was extracted and diluted with nuclease-free water (36 µL). An aliquot (2 µL) of this diluted solution was then amplified using Promega GoTaq DNA polymerase, to the specifications detailed below, prior to purification using a QIAGEN QIAquick® PCR purification kit. A calibration curve (utilizing a logarithmic DNA dilution series of 5x triplicate *ds*DNA template concentrations) to compare the PCR product concentration to the template *ds*DNA concentration was produced for each set of PCR reactions, allowing for accurate

quantification of the amount of template *ds*DNA left in the solution above the lipid button post-incubation, which was normalised to account for any fluctuations in polymerase activity. The partition coefficient (K_p) was then calculated for each DOPE-DNA H_{II} phase.

Table 3.3 PCR reaction mixture component specification for amplification of GFP sequence in pT7GFP.

Component	Volume (µL)	Final concentration
Nuclease-free water	29.75	-
dNTPs (2 mM each)	5	0.2 mM each
5x GoTaq® green buffer (Promega, M7911)	10	1.5 mM $MgCl_2$
T7GFP-FWD primer (10 mM)	1.5	0.3 mM
T7GFP-REV primer (10 mM)	1.5	0.3 mM
GoTaq® polymerase (Promega, M3171)	0.25	1.25 u*
DNA template aliquot	2	-

** One unit of GoTaq® polymerase is defined as the amount of enzyme required to catalyze the incorporation of 10 nanomoles of dNTPs into acid-soluble material in 30 minutes at 74 ˚C, using Promega's Standard DNA Polymerase Assay Condition.*

Table 3.4 PCR thermal cycler programme specification for amplification of GFP sequence in pT7GFP.

Step	Temperature (˚C)	Duration (s)	Cycles
1	94	120	1
2	94	60	30
	50	30	
	72	60	
3	72	300	1
4	4	Hold	1

3.9.2.2 K_p quantification by DNA gel electrophoresis

A method was developed to quantify the amount of linear *ds*DNA remaining in the aqueous supernatant solution above DOPE lipid buttons post-100 h incubation, and thus calculate a value for the partition coefficient (K_p), which gave good agreement to the partition coefficients calculated using the PCR method for DOPE-DNA lipid buttons produced under homologous incubation conditions (section 3.9.2.1).

Post-100h incubation, all of the aqueous supernatant solution was loaded from a DOPE lipid button onto a 1% agarose gel, prepared using tris-acetate-EDTA (TAE) buffer. Gels contained ethidium bromide to a final concentration of 0.5 µg/mL to allow visualization of the DNA bands using a UV transilluminator. Samples were run against NEB 2-log ladder and against a gradient of known amounts of linearized plasmid DNA (e.g. 5, 10, 50 and 100 ng). Gels were then electrophoresed at 3.5 V/cm, before being visualized using a Syngene UV transilluminator, with images captured and recorded using Syngene GeneSnap software (Figure 3.28).

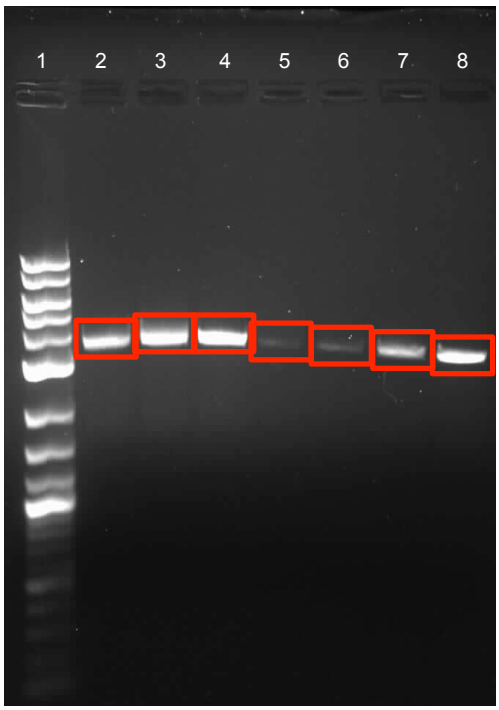

Figure 3.28 DNA gel electrophoresis for analysis of DOPE lipid buttons A16-18. A grayscale (0-255) 80x50 pixel sample for each of the highlighted DNA bands was analysed. Image processed using ImageJ64 freeware. **Lanes:** NEB 2-log ladder N3200 (lane 1); post-100h incubation supernatant solution (lanes 2-4); 5, 10, 50 and 100 ng *lin*pRSET-EmGFP reference *ds*DNA (lanes 5-8). RW/6511/04

Images captured using the GeneSnap software were imported into ImageJ64, a freeware program for scientific image processing. For each DNA band, an area encompassing the band, typically around 80x50 pixels, was analysed using grayscale

histogram analysis. This assigned an intensity value to each pixel within each band's analysis area, from 0 to 255 (where white = 0, and true black = 255), from which the sum of the intensities per pixel was calculated. A band containing an increased amount of DNA would lead to a higher sum of the intensity per pixel, as there would be a higher concentration of ethidium bromide present, increasing the level of fluorescence and thus intensity observed. Conversely, an area of the agarose gel with little to no DNA present, would give rise to a very low sum of the intensities per pixel in the area selected for grayscale histogram analysis.

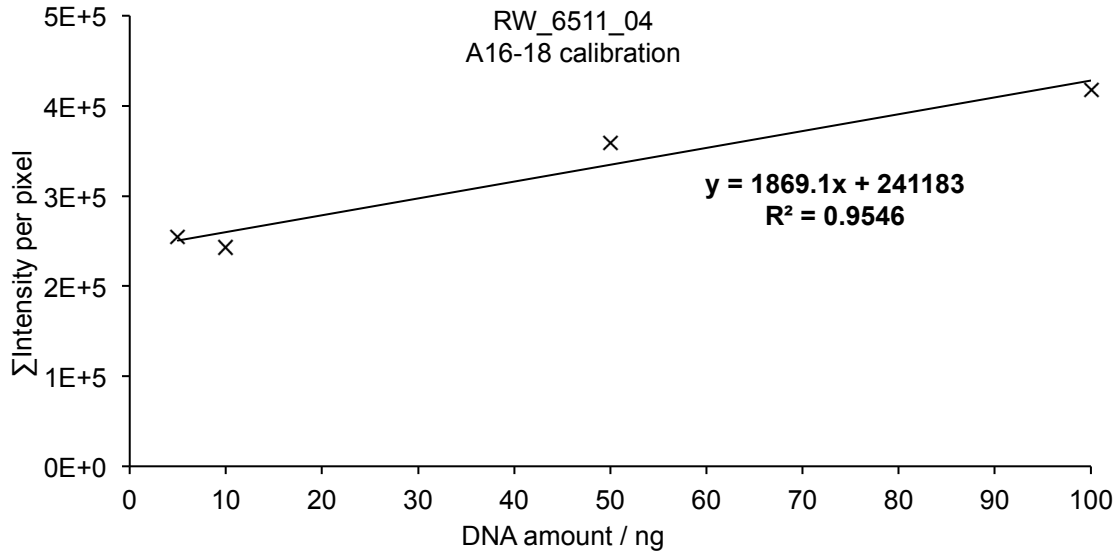

Figure 3.29 DNA gel electrophoresis template DNA amount calibration plot for partition coefficient (K_p) analysis of lipid buttons A16-17. RW/6511/04

Using the sum intensity per pixel calibration plot for each DNA gel, an example of which is shown in Figure 3.29, the sum intensity per pixel observed for each DNA band arising from post-incubation supernatant solution was used to estimate the amount of DNA present in the band. The estimate for the amount of DNA present within the band seen on the gel then allowed for the partition coefficient to be calculated. The error associated with the calculated quantity of DNA in a particular band is taken as ± (0.5 x quantity of DNA in the faintest visible reference DNA band).

Whilst this method has shown good reproducibility to the K_p analysis values attained using the PCR method, care must be taken to ensure that the gel image does not becomes overexposed; the in-built histogram feature within the Syngene GeneSnap software can be used to monitor the pixel intensity distribution across the image being captured. Overexposure of the gel images would lead to an underestimation of the amount of DNA present within a band, and thus give rise to an inaccurate calculation of the partition coefficient for each lipid button analysed using that particular gel.

3.10 References

1. Porter, D. L., Levine, B. L., Kalos, M., Bagg, A. & June, C. H. Chimeric antigen receptor-modified T cells in chronic lymphoid leukemia. *N. Engl. J. Med.* **365,** 725–733 (2011).

2. Biffi, A. *et al.* Lentiviral hematopoietic stem cell gene therapy benefits metachromatic leukodystrophy. *Science (80-.).* **341,** 1233158 (2013).

3. LeWitt, P. A. *et al.* AAV2-GAD gene therapy for advanced Parkinson's disease: a double-blind, sham-surgery controlled, randomised trial. *Lancet Neurol.* **10,** 309–319 (2011).

4. Berg, J. M., Tymoczko, J. L. & Stryer, L. in *Biochem. Textb.* 1120 (2006).

5. Safinya, C. R. Structures of lipid-DNA complexes: supramolecular assembly and gene delivery. *Curr. Opin. Struct. Biol.* **11,** 440–448 (2001).

6. Chesnoy, S. & Huang, L. Structure and function of lipid-DNA complexes for gene delivery. *Annu. Rev. Biophys. Biomol. Struct.* **29,** 27–47 (2000).

7. Koltover, I., Salditt, T., Rädler, J. O. & Safinya, C. R. An inverted hexagonal phase of cationic liposome-DNA complexes related to DNA release and delivery. *Science (80-.).* **281,** 78–81 (1998).

8. Safinya, C. R. *et al.* Cationic liposome-DNA complexes: from liquid crystal science to gene delivery applications. *Philos. Trans. A. Math. Phys. Eng. Sci.* **364,** 2573–96 (2006).

9. Patil, S. D., Rhodes, D. G. & Burgess, D. J. Anionic liposomal delivery system for DNA transfection. *AAPS J.* **6,** e29 (2004).

10. Li, S. & Huang, L. Nonviral gene therapy: promises and challenges. *Gene Ther.* **7,** 31–34 (2000).

11. Felgner, P. L. *et al.* Lipofection: a highly efficient, lipid-mediated DNA-transfection procedure. *Proc. Natl. Acad. Sci. U. S. A.* **84,** 7413–7417 (1987).

12. Caplen, N. J. *et al.* Liposome-mediated CFTR gene transfer to the nasal epithelium of patients with cystic fibrosis. *Nat. Med.* **1,** 39–46 (1995).

13. Hafez, I. M. & Cullis, P. R. Roles of lipid polymorphism in intracellular delivery. *Adv. Drug Deliv. Rev.* **47,** 139–148 (2001).

14. Zabner, J., Fasbender, A. J., Moninger, T., Poellinger, K. A. & Welsh, M. J. Cellular and molecular barriers to gene transfer by a cationic lipid. *J. Biol. Chem.* **270,** 18997–19007 (1995).

15. Corsi, J. *et al.* DNA that is dispersed in the liquid crystalline phases of phospholipids is actively transcribed. *Chem. Commun.* 2307–2309 (2008). doi:10.1039/b801199k

16. Francescangeli, O., Pisani, M., Stanic, V., Bruni, P. & Weiss, T. M. Evidence of an inverted hexagonal phase in self-assembled phospholipid-DNA-metal complexes. *Europhys. Lett.* **67,** 669–675 (2004).

17. Wagner, K., Harries, D., May, S., Kahl, V. & Rädler…, J. Direct evidence for counterion release upon cationic lipid-DNA condensation. *Langmuir* **16,** 303–306 (2000).

18. Black, C. F., Wilson, R. J., Nylander, T., Dymond, M. K. & Attard, G. S. Linear dsDNA partitions spontaneously into the inverse hexagonal lyotropic liquid crystalline phases of phospholipids. *J. Am. Chem. Soc.* **132,** 9728–9732 (2010).

19. Tate, M. W. & Gruner, S. M. Temperature dependence of the structural dimensions of the inverted hexagonal (HII) phase of phosphatidylethanolamine-containing membranes. *Biochemistry* **28,** 4245–4253 (1989).

20. Lin, A. J. *et al.* Three-dimensional imaging of lipid gene-carriers: membrane charge density controls universal transfection behavior in lamellar cationic liposome-DNA complexes. *Biophys. J.* **84,** 3307–3316 (2003).

21. Wynveen, A., Lee, D. J., Kornyshev, A. A. & Leikin, S. Helical coherence of DNA in crystals and solution. *Nucleic Acids Res.* **36,** 5540–5551 (2008).

22. Budker, V. G., Godovikov, A. A., Naumova, L. P. & Slepneva, I. A. Interaction of polynucleotides with natural and model membranes. *Nucleic Acids Res.* **8,** 2499–2515 (1980).

23. Khvorova, A., Kwak, Y. G., Tamkun, M., Majerfeld, I. & Yarus, M. RNAs that bind and change the permeability of phospholipid membranes. *Proc. Natl. Acad. Sci. U. S. A.* **96,** 10649–10654 (1999).

24. Vlassov, A., Khvorova, A. & Yarus, M. Binding and disruption of phospholipid bilayers by supramolecular RNA complexes. *Proc. Natl. Acad. Sci. U. S. A.* **98,** 7706–7711 (2001).

25. Vlassov, A. & Yarus, M. Interaction of RNA with phospholipid membranes. *Mol. Biol.* **36,** 389–393 (2002).

26. Janas, T. & Yarus, M. Specific RNA binding to ordered phospholipid bilayers. *Nucleic Acids Res.* **34,** 2128–2136 (2006).

27. Wilson, R. J., Tyas, S. R., Black, C. F., Dymond, M. K. & Attard, G. S. Partitioning of ssRNA Molecules between Preformed Monolithic H(II) Liquid Crystalline Phases of Lipids and Supernatant Isotropic Phases. *Biomacromolecules* **11,** 3022–3027 (2010).

28. Smith, S. B., Cui, Y. & Bustamante, C. Overstretching B-DNA: The Elastic Response of Individual Double-Stranded and Single-Stranded DNA Molecules. *Science (80-.).* **271,** 795–799 (1996).

29. Vlassov, A. Assay of random RNA oligomerisation in buffers with high concentrations of divalent metal ions. *Nucleosides Nucleotides & Nucleic Acids* **23,** 999–1001 (2004).

Chapter 4:

Batch Transcription in the Presence of DNA-containing H_{II} Phases

4. Batch Transcription in the Presence of DNA-containing H_{II} Phases

4.1 Rationale

Having established the optimal conditions for single-shot solution phase transcription assays and partitioning of linear *ds*DNA into DOPE H_{II} phases, as detailed in Chapters 2 and 3, investigations were made into the viability of multiple cycle batch-wise transcription from these phases, with a view of obtaining data that would guide the development of a continuous-flow semi-biotic system.

In terms of potential biotechnology applications, the benefits of performing multiple cycle batch-wise transcription reactions are tangible; through using an immobilized *ds*DNA template for multiple transcription assays, template *ds*DNA is no longer discarded during the transcription assay purification process, leading to reduced template *ds*DNA requirements, which in turn reduces the amount of laboratory time spent preparing cultures, harvesting and then purifying plasmid *ds*DNA. For example, if the template *ds*DNA required for one solution-based transcription could be contained within a DOPE H_{II} phase and used instead for 10 batch-wise transcription reactions, this would provide a ten-fold reduction in the template *ds*DNA requirement of the transcription process, directly reducing laboratory time and cost requirements. However, this benefit is negated unless multiple cycle batch-wise transcription from DNA-containing H_{II} phases can offer an acceptable output yield of mRNA across the multiple cycles. It was expected that mRNA yields should be acceptable from multiple-cycle batch-wise transcription across the lifetime of a DNA-containing H_{II} phase, as previous research has shown that mRNA preferentially partitions into an isotropic solution above a pre-formed monolithic H_{II} phase, especially once a small accretion layer of mRNA molecules had formed upon the phase surface during the first batch transcription.[1]

In order for *ds*DNA-containing H_{II} phases to offer a viable method of template *ds*DNA provision for batch, or indeed continuous-flow, transcription, it was necessary to investigate the expected yields per batch transcription, the accessibility of the contained template *ds*DNA, and the stability of the H_{II} phase over successive batch transcriptions. Through assessment of these three key issues, it was intended that we could characterize the initial batch transcription system, before making modifications to the system parameters in an effort to maximise mRNA yields and phase lifespan.

Reports within the literature offer support for the theoretical use of *ds*DNA-containing H_{II} phases for transcription. *ds*DNA has been shown to remain transcriptionally active once partitioned within the inverse hexagonal phase of DOPE, whilst mRNA has been shown to preferentially reside in an isotropic solution layered above DNA-DOPE lipid

buttons.[1-3] The preference of mRNA to remain in solution should thus enable its efficient extraction and purification, whilst leaving the *ds*DNA molecules partitioned within the liquid crystalline phase in situ. Alternative techniques involving the immobilization of *ds*DNA for the purposes of molecular biology syntheses have also been reported; *ds*DNA immobilized upon protein-gels ('P-gels'),[4] within synthetic gene brushes,[5] and upon microsphere beads,[6] have all been shown to be transcription or translation active.

With the long-term goal of having a *ds*DNA-containing H_{II} phase as a core component within a continuous-flow semi-biotic device, it was crucial that investigations into the batch transcription system would allow for the behaviour of these *ds*DNA-containing liquid crystalline phases to be fully characterized. As with any electronic system, core system components would need quantified and reproducible performance specifications upon that device engineers can rely on. As a potential core biological component in a semi-biotic system, end users would want to know the optimum operating conditions for the component (i.e. the buffer composition and transcription assay components), the expected mRNA yields and the maximum operational time of the component before possible refurbishment or replacement.

4.2 Methodology

4.2.1 Phase preparation

Lipid phases were prepared as per the method detailed in section 3.2.

Lipid buttons were prepared by dispensing aliquots of DOPE dissolved in chloroform solution (6 µL, 0.5 mg µL-1) into PCR tubes via Eppendorf pipette with suitable filtered tip, minimizing smearing of the solution when dispensing. Solutions were then allowed to stand (15 minutes, RT) in capped tubes, before centrifugation (17,000 g, 30 seconds, RT) to ensure all lipid/chloroform solution was located at the bottom of the PCR tubes. The PCR tubes were then uncapped and warmed (2 hours, 50 ˚C) to aid the removal of chloroform, before drying the samples overnight using freeze-drying apparatus. Note that the vacuum was applied slowly, to minimize the bubbling of chloroform solution. Upon complete chloroform removal, the DOPE liquid crystalline phases appeared as a white to translucent 'button' at the bottom of the PCR tubes.

Composite lipid phases (consisting of two or more lipid components) were prepared by weighing out the dry lipid components, in the required mole fractions for the composition to be produced, before being dissolved in chloroform and formed into lipid buttons, as per the method described above.

After rehydration of the lipid buttons with isotonic saline (2 µL), the phases were preloaded with linear *ds*DNA *via* incubation with linear *ds*DNA, $MgCl_2$ and transcription buffer, typically for 100 h (unless specified otherwise) at 37 ˚C, using an incubator. The aqueous supernatant solution was then removed post-incubation, with the *ds*DNA-containing lipid buttons stored (capped) in a refrigerator (4 ˚C) until required.

4.2.2 Batch transcription

Batch transcription cycles were performed on lipid buttons, preloaded with linear *ds*DNA, prepared as described in section 4.2.1. Lipid buttons were loaded with 1 µg of linear *ds*DNA (unless stated otherwise) to achieve a total *ds*DNA concentration of 0.05 µg/µL per 20 µL transcription assay, analogous to positive control transcription assays in solution. Transcription assay solution (20 uL) was layered upon each *ds*DNA containing lipid buttons, forming an aqueous supernatant phase above each button. The specification of the transcription assay solution for multiple-cycle batch transcription (unless stated otherwise) is presented in Table 4.1.

Table 4.1 Composition of transcription assay in the presence of *ds*DNA-containing lipid buttons

Component	**Volume of stock component per assay (20 µL)**	**Component concentration per assay (20 µL)**
Nuclease-free water	14.95 µL	-
rNTPs (80 mM each)	1.25 µL	20 mM (5 mM each)
10x transcription buffer	2 µL	1x
$MgCl_2$ (0.5 M)	1 µL	25 mM
T7 RNA polymerase	0.8 µL	40 u

For each cycle of batch transcription, lipid buttons overlaid with transcription assay solution were incubated for 2 h (37 °C), prior to supernatant removal by Eppendorf pipette and purification of the mRNA product. Lipid buttons were then either subjected to successive cycles of batch transcription, or refrigerated (4 °C) until required for the further transcription cycles.

4.2.3 Electrospray ionization mass spectrometry (ESI-MS)

Electrospray ionization mass spectrometry (ESI-MS) was performed on a DOPE lipid button sample prior to and after multiple-cycle batch transcription. This allowed for the analysis of how successive cycles of batch transcription affected the stability and integrity of the lipid phase, as any degradation of the DOPE would be evident through the presence of additional fragments on the post-batch transcription mass spectra of the lipid sample.

Details of the ESI-MS facility and preparation of samples for ESI-MS can be found in Annex 1 (section 4.7.1).

4.2.4 Small-angle X-ray scattering (SAXS)

Small-angle X-ray scattering (SAXS) analysis was performed for a variety of lipid samples under a number of controlled incubation conditions relevant to the multiple-cycle batch transcription system. This allowed for confirmation of the phase structure and lattice parameters of these lipid samples, which could then be applied to the analysis of the data from multiple-cycle batch transcription experiments.

Details of the SAXS facility and preparation of samples for SAXS can be found in Annex 2 (section 4.7.2).

4.2.5 Methods of analysis

4.2.5.1 Partitioning of DNA

The partition coefficient for all *ds*DNA partitioning investigations presented in this chapter were calculated using the method detailed in section 3.2.

The partition coefficients presented throughout this chapter were obtained by using quantitative analysis of DNA gel electrophoresis on the post-incubation supernatant solution, as detailed in section 3.9, Annex 2. Reference samples of known concentration linear *ds*DNA were run at the same time as the post-incubation supernatant samples, allowing for a calibration curve of DNA amount versus gel band intensity to be produced. An estimate of the amount of linear *ds*DNA present in the post-incubation supernatant was then made, using the observed intensity of the gel band compared to the specific calibration curve for that DNA gel.

4.2.5.2 Transcriptional yield

UV-visible spectrophotometry was performed using a NanoDrop ND-1000 instrument to quantify the concentration of all mRNA samples purified. For analytical purposes, measurements were recorded in triplicate, with the mean concentration and standard deviation calculated. Using the NanoDrop nucleic acid software, measurements were processed using type ratio RNA-40 for purified mRNA samples. Concentration values were recorded in units of ng μL^{-1}, along with associated 260/280 and 260/230 sample absorbance ratios as a measure of sample purity and integrity.

A 260/280 ratio of ~2.0 is generally accepted as pure for RNA, whilst a 260/230 ratio appreciably lower than 1.8 may indicate the presence of co-purified contaminants.

4.2.5.3 Agarose gel electrophoresis

DNA and RNA samples were routinely tested for purity and integrity using agarose gel electrophoresis throughout the work presented in this chapter. Protocols for both DNA and RNA gel electrophoresis can be found in Appendix A.

4.2.5.4 Electrospray ionization mass spectrometry (ESI-MS)

Electrospray ionization mass spectrometry was performed using a Micromass Quattro Ultima triple quadrupole mass spectrometer equipped with an electrospray ionization interface. The purpose of ESI-MS sample analysis within this research was establish whether the degradation of *ds*DNA-containing DOPE H_{II} phase lipid buttons was occurring over successive cycles of batch transcription.

Within the triple quadrupole ESI mass spectrometer, a collision gas injected into the second quadrupole causes fragmentation of the precursor ions. A comparison of the mass lost between the first quadrupole, which scans for precursor ions, and the third quadrupole, which scans for daughter ions caused by the fragmentation at quadrupole 2, can be used to detect phospholipids that undergo a constant loss between the first and second quadrupoles; DOPE undergoes loss of a fragment with mass 141 between quadrupole one and two, hence neutral loss (NL) of 141 scans are used to select for DOPE. For the purposes of this research, NL 141 spectra were compared prior to and after successive cycles of batch transcription on *ds*DNA-containing H_{II} phase DOPE lipid buttons.

4.2.5.5 Polarizing light microscopy

Polarizing light microscopy was used to quantitatively analyse the phase structure of lipid buttons under a variety of incubation conditions relevant to the multiple-cycle batch transcription system. Optical texture images captured using this technique (Figure 4.1) could then be compared over time to allow for identification of any potential phase changes over the course of successive cycles of batch transcription; a phase change away from inverse hexagonal, where we have shown that *ds*DNA will partition into the phase pores, could restrict the availability of the contained *ds*DNA for transcription.

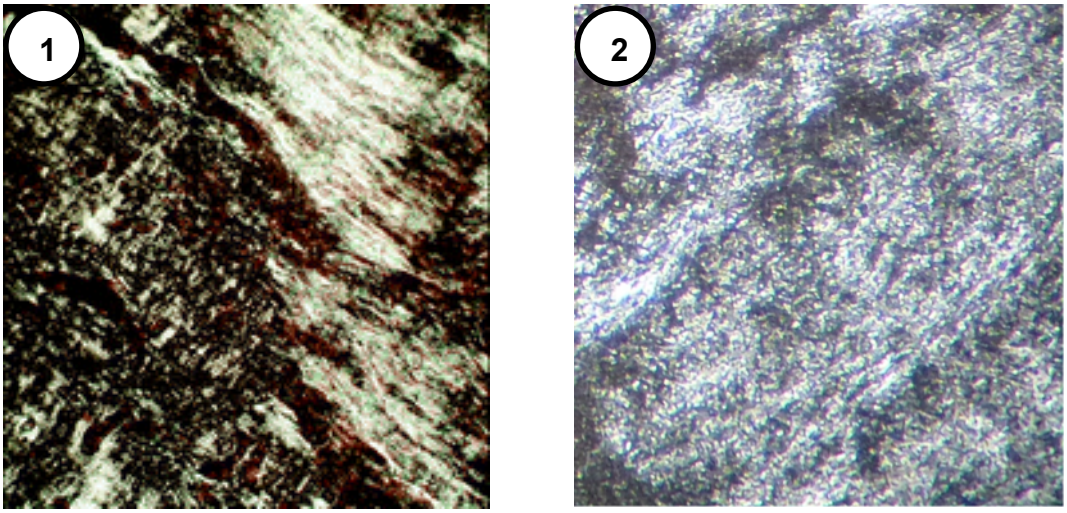

Figure 4.1 H_{II} phase DOPE optical texture captured using polarizing microscopy. **(1)** H_{II} phase DOPE preloaded with *lin*T7luc *ds*DNA *via* lyophilization. Image published by Corsi *et al*. (2008) [2]. **(2)** H_{II} phase DOPE preloaded with *lin*pRSET-EmGFP *ds*DNA *via* 100 h incubation in the presence of transcription buffer and $MgCl_2$ (25 mM).

Small-angle X-ray scattering was used to verify the phase structures identified by polarizing light microscopy, whilst also allowing for qualitative analysis of phase parameters, such as the lattice parameter, under a range of controlled temperature and incubation conditions.

4.2.5.6 Small-angle X-ray scattering (SAXS)

SAXS patterns were captured using a MAX-lab, in-house developed, software package for the I911-4 beamline. These SAXS patterns were integrated radially from the centre of the diffraction pattern, giving a plot of X-ray intensity as a function of distance from the centre of the scattering pattern, q (Equation 4.1).

$$q = \frac{4\pi \sin\theta}{\lambda} \qquad \textbf{4.1}$$

An example plot of X-ray intensity as a function of q is presented in Figure 4.2; the plot shown is for a H_{II} phase DOPE sample (premixed with salmon sperm *ds*DNA).

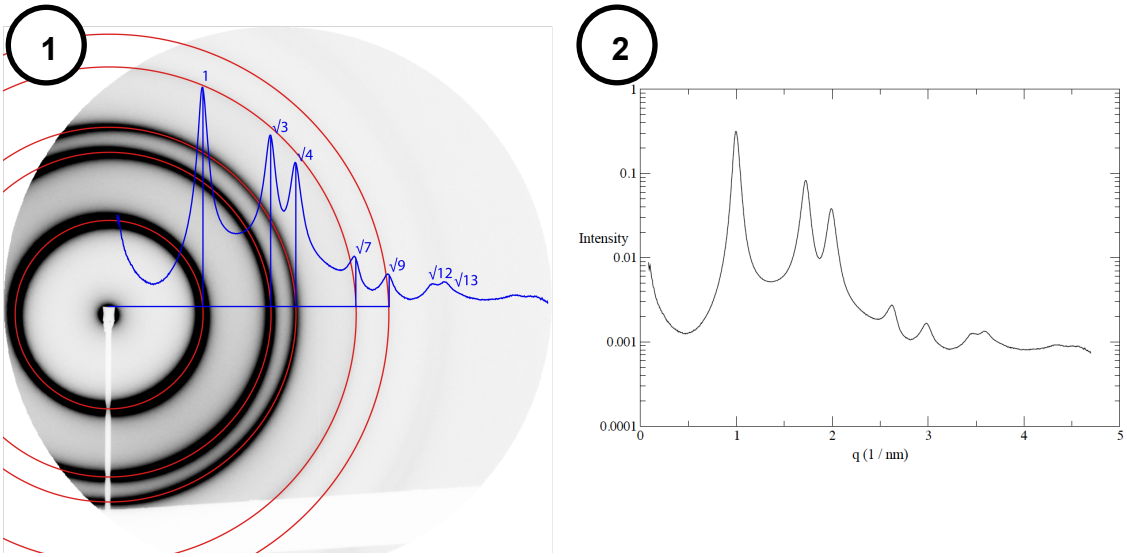

Figure 4.2 Analysis of a H_{II} phase DOPE sample run on the I911-4 SAXS beamline at MAX-lab, SE. **(1)** SAXS pattern (greyscale circles, where black indicates high X-ray intensity and light grey indicates low X-ray intensity) for a H_{II} phase DOPE sample (premixed with salmon sperm *ds*DNA, 37 °C). The squared ratios of the reciprocal spacings (blue text) of the observed peaks are indicated on the integrated one-dimensional patterns (blue line). **(2)** Plot of X-ray intensity as a function of *q* for a H_{II} phase DOPE sample (premixed with salmon sperm *ds*DNA, 37 °C).

The peaks observed on the intensity versus *q* plot for each lipid sample were compared to the expected characteristic peaks for a phase structure, which are readily available in the literature,[7] allowing for confirmation of the sample phase structure. Miller indices, their associated ratios, and the lattice spacing (*d*) for lamellar, hexagonal and cubic ($Ia\bar{3}d$, $Pn\bar{3}m$) are shown in Table 4.2.

Quantitative analysis of the phase structure was performed by comparison of the lattice parameters for individual lipid samples. The lattice parameter was calculated from the Miller index factors for the planes of a given phase structure and the distance of the characteristic peaks from the centre of the scattering pattern, using Equation 4.2:

$$a = \text{Miller index factor} \times \frac{2\pi}{q} \qquad \textbf{4.2}$$

where *a* is the lattice parameter, *q* is the distance from the centre of the scattering pattern, and the Miller index factor is a combination of the Miller indices for a specific plane of an identified phase structure. For example, for the H_{II} phase plane with Miller indices (110), the Miller index factor is equal to $2/\sqrt{3}$.

Table 4.2 Miller indices, ratios and lattice spacing (*d*) for inverse hexagonal (H_{II}) and cubic ($Ia\bar{3}d$, $Pn\bar{3}m$) liquid crystalline phases.

Phase	Lattice spacing (*d*)	Space group	Miller indices	Ratios
Lamellar	$d = \frac{2\pi}{q} = \frac{a}{\sqrt{h^2}}$		100	1
			200	2
			300	3
			400	4
Hexagonal	$d = \frac{2\pi}{q} = \frac{1}{\sqrt{\frac{4}{3a^2}(h^2 + k^2 + hk)}}$		100	1
			110	√3
			200	2
			210	√7
			220	√12
			300	3
Cubic	$d = \frac{2\pi}{q} = \frac{a}{\sqrt{h^2 + k^2 + l^2}}$	$Ia\bar{3}d$	211	√6
			220	√8
			321	√14
			400	4
			420	√20
			332	√22
		$Pn\bar{3}m$	110	√2
			111	√3
			200	2
			211	√6
			220	√8
			221	3

4.3 Batch transcription from DOPE H_{II} phases

4.3.1 Viability of batch transcription

To assess the viability of multiple-cycle batch transcription, DOPE H_{II} phases were preloaded with 1 µg or 10 µg of linear *ds*DNA *via* incubation in transcription buffer solution above the H_{II} phase for 100 h (37 ˚C). Partitioning of *ds*DNA into the phase was confirmed by DNA gel electrophoresis of the incubation solution prior to performing transcription cycle 1. Successive transcription cycles were performed, each for 2 h incubation periods (37 ˚C), and compared to a solution-based positive control transcription assay that was incubated simultaneously. Transcription cycles were performed until the mRNA yields obtained became consistently low, indicating the approximate end of the phases' transcriptionally active lifespan.

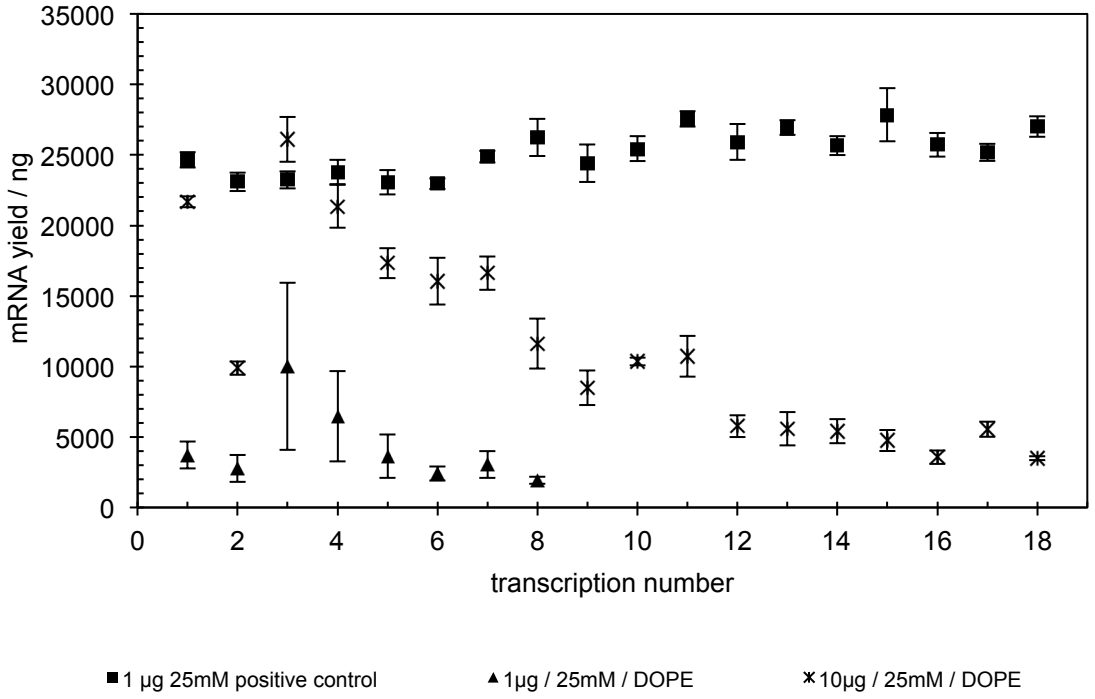

Figure 4.3 mRNA yields from multiple-cycle batch transcription using DOPE H_{II} phases preloaded with 1 µg (black triangles) or 10 µg (black asterisks) of linear *ds*DNA *via* incubation for 100 h (37 ˚C) in transcription buffer solution containing 25 mM $MgCl_2$. H_{II} phases were incubated for 2 hours (37 ˚C) per transcription. One-off 1 µg *ds*DNA positive control (black squares) transcription assays, containing 25 mM $MgCl_2$, are shown for comparison. RW/6605/02

The data presented in Figure 4.3 clearly shows that multiple-cycle batch transcription from DOPE H_{II} phases preloaded with *ds*DNA in this manner has a limited lifespan; after a number of successive transcriptions, the mRNA yields produced from each transcription start to significantly reduce, from a peak level observed at the third batch

transcription (on average 10.0 µg mRNA for phases containing 1 µg *ds*DNA, or 26.1 µg mRNA for phases containing 10 µg *ds*DNA). This observation was consistent for both 1 µg and 10 µg *ds*DNA preloaded H_{II} phases, although H_{II} phases loaded with the higher amount of *ds*DNA sustained transcription for roughly twice the time achieved from the lesser-loaded phases.

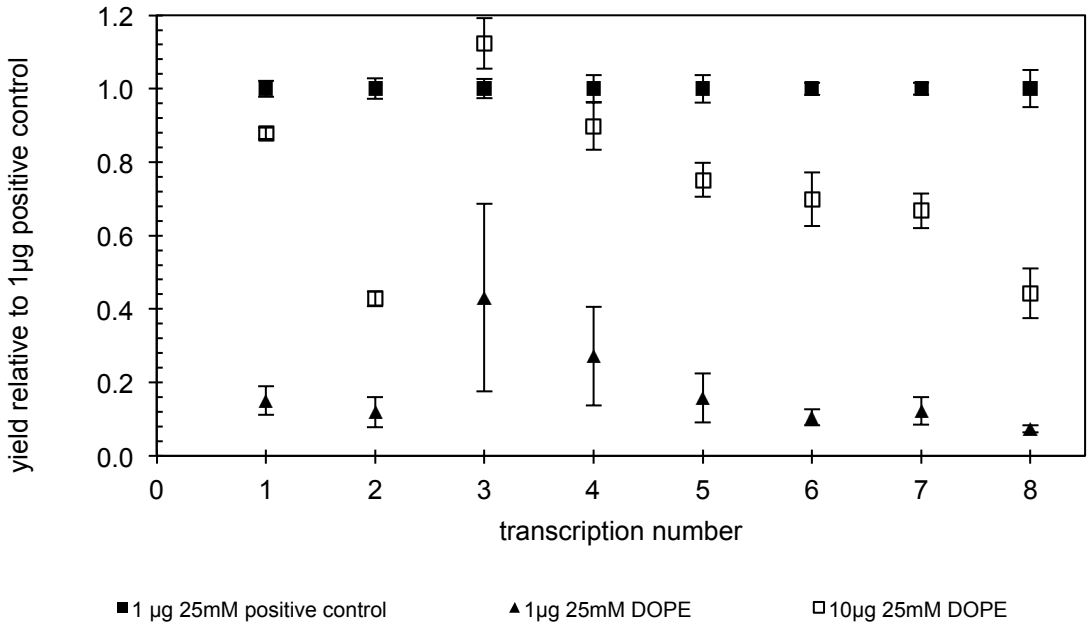

Figure 4.4 Transcriptional yields, relative to 1 µg *ds*DNA positive control transcription assays (black squares), from multiple-cycle batch transcription from DOPE lipid buttons preloaded with 1 µg (black triangles) or 10 µg (hollow squares) linear *ds*DNA, prepared by 100 h incubation (37˚C) with transcription buffer containing 25 mM $MgCl_2$. Individual transcription assay incubations were for 2 h (37 ˚C). RW/6605/02

With DOPE H_{II} phases preloaded with 1 µg linear *ds*DNA, mRNA yields from successive batch transcriptions never surpass the yield obtained from a solution-based positive control assay (Figure 4.4). The peak mRNA yield from 1 µg H_{II} phases during the third batch transcription is, on average, 40% of the positive control yield; it is only when the H_{II} phase is preloaded with 10 µg of DNA that mRNA yields exceed that of the 1 µg positive control, and that occurs only once, again for the peak in transcriptional activity observed during the third batch transcription.

To best compare the level of transcriptional activity from *ds*DNA-containing DOPE H_{II} phases across multiple-cycle batch transcription, the cumulative mRNA yield for 1 and 10 µg *ds*DNA containing H_{II} phases was compared to the cumulative yield from successive solution-based 1 µg *ds*DNA positive control transcription assays (Figure 4.5). This comparison highlights the reduction in transcriptional activity of the DNA-containing H_{II} phases over time; by the tenth successive transcription, a solution-based transcription assay using ten aliquots of 1 µg template *ds*DNA can produce

242 µg mRNA, while a DOPE H_{II} phase preloaded with one aliquot of 10 µg template *ds*DNA can produce only 159 µg mRNA (65.7% of the solution-based transcription assay yield).

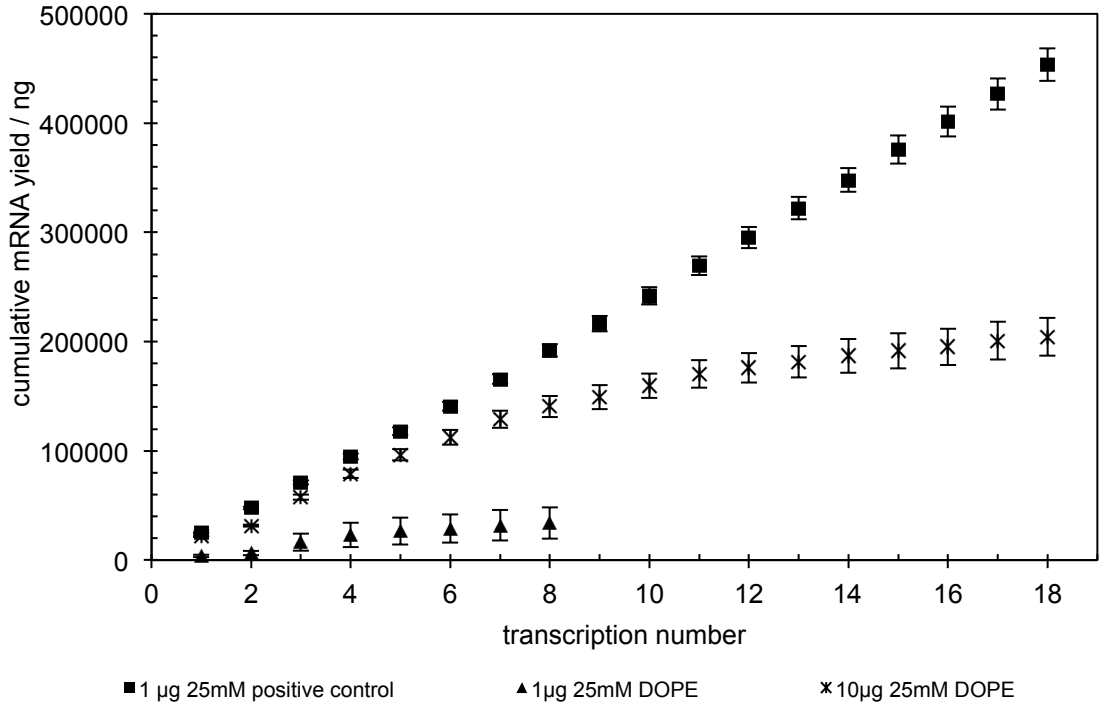

Figure 4.5 Cumulative mRNA yield from multiple-cycle batch transcription from 1 µg and 10 µg *ds*DNA-containing DOPE H_{II} phases. Phases were incubated for 2 hours (37 ˚C) per transcription. Results are shown for batch transcription assays from DOPE H_{II} phases containing either 1 µg *ds*DNA with 25 mM $MgCl_2$ (black triangles) or 10 µg *ds*DNA with 25 mM $MgCl_2$ (black asterisks). One-off 1 µg *ds*DNA positive control transcription assays containing 25 mM $MgCl_2$ (black squares) are shown for comparison. RW/6605/02

The loss of transcriptional activity observed from these initial investigations into the viability of multiple-cycle batch transcriptions was not wholly unsurprising; with such a complex system, it might be expected that a limitation upon system lifetime would be encountered. Limits upon system lifetime could potentially be caused by the prolonged incubation of the lipid phases in transcription solutions of high ionic strength (above $MgCl_2$ concentrations of ~45 mM, transcriptional activity is severely reduced for solution phase transcriptions) or by the accumulation of degraded materials, such as DTT or T7 RNA polymerase, from previous cycles of transcription. There are many parameters to optimize and several components liable to experience degradation over time, for example, the contained *ds*DNA and the DOPE H_{II} phase. Through investigation into why transcriptional activity was decreasing over successive batch transcriptions from a single H_{II} phase, it was envisaged that the system parameters could be optimized, resulting in an extended transcriptionally active lifetime, and yielding higher cumulative mRNA yields than had been initially achieved. Even with a finite lifetime, *ds*DNA-containing H_{II} phases could offer potential as a provider of template

*ds*DNA for transcription within a continuous-flow transcription device, providing the liquid crystalline phase could be regenerated or replaced when it had come to the end of its lifetime.

4.3.2 Accessibility of template DNA

With the loss in transcriptional activity of DNA-containing DOPE H_{II} phases over successive batch transcriptions, it was pertinent to calculate the amount of template *ds*DNA that was required to produce the mRNA yields observed for each batch transcription. Through a calibration plot of mRNA yield versus template DNA concentration for solution-based transcription assays performed above DOPE H_{II} phases, it became possible to estimate the amount of template *ds*DNA required to produce a given mRNA yield. Should the cumulative amount of template *ds*DNA required to produce the obtained mRNA yields across successive batch transcriptions exceed the amount of *ds*DNA initially preloaded into the DOPE H_{II} phase, it could be assumed that at least a proportion of the *ds*DNA was remaining associated with the H_{II} phase throughout the multiple-cycle batch transcription process.

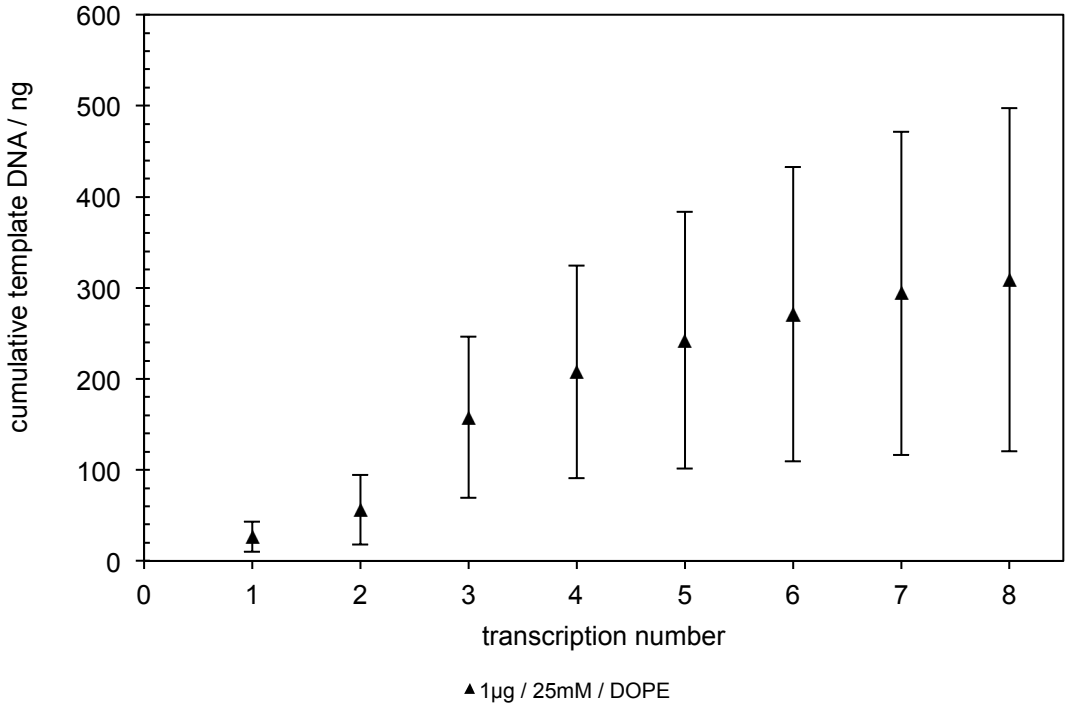

Figure 4.6 Cumulative calculated template DNA required to produce the obtained mRNA yields from multiple-cycle batch transcription using 1 µg *ds*DNA-containing DOPE H_{II} phases (black triangles). Phases were initially preloaded with 1,000 ng template *ds*DNA (y-axis maxima). RW/6605/02

When calculating the cumulative template DNA required to produce the obtained mRNA yields from DOPE H_{II} phases preloaded with 1 µg (Figure 4.6) or 10 µg (Figure 4.7) linear *ds*DNA, the level of error associated with the calculated amount of template *ds*DNA required for phases containing 1 µg *ds*DNA is substantial due to the variation in mRNA yields from individual lipid buttons. It is likely that these variations are due to imperfections in the individual lipid button physical properties, for example the available surface area and the overall number of *ds*DNA-containing pores accessible from the surface of the phase.

For both 1 µg and 10 µg *ds*DNA preloaded DOPE H_{II} buttons, it was clear that the level of transcriptional activity observed, across 8 and 18 successive batch transcriptions, respectively, required less than half of the template *ds*DNA contained within the phase. Within experimental error, both the H_{II} phases preloaded with 1 and 10 µg *ds*DNA resulted in transcriptional yields that were consistent with having been produced by template *ds*DNA amounts equating to approximately 40% of the total amount of initially compartmentalized *ds*DNA, over the transcriptionally-active lifetime of the phase.

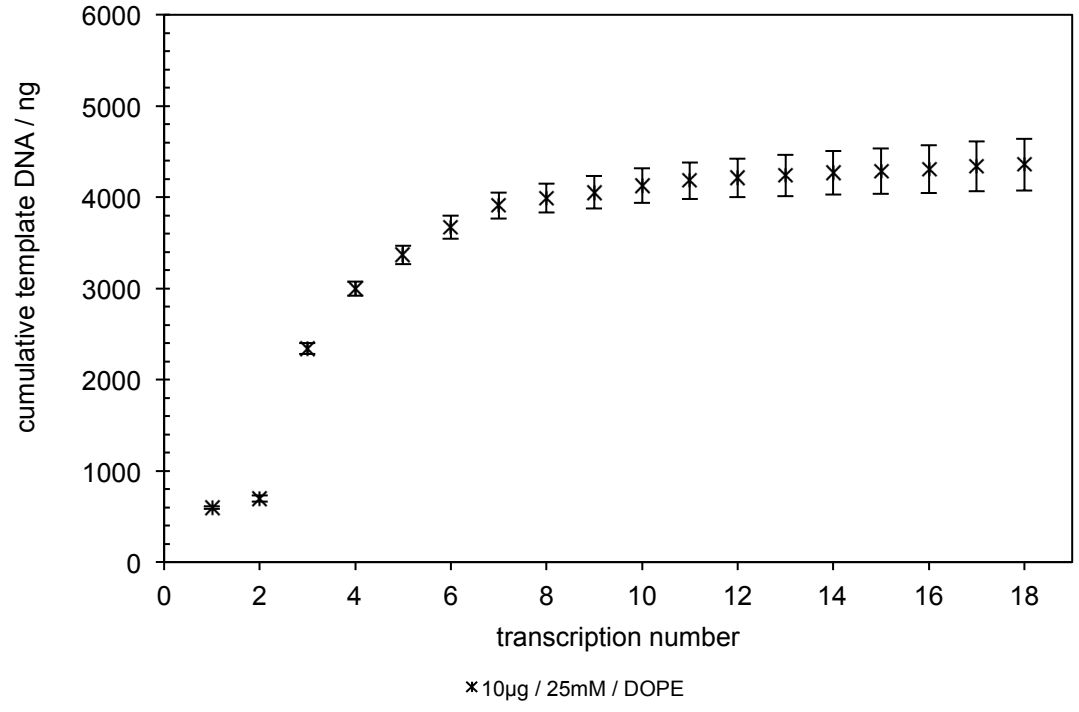

Figure 4.7 Cumulative calculated template DNA required to produce the obtained mRNA yields from multiple-cycle batch transcription using 10 µg *ds*DNA-containing DOPE H_{II} phases (black asterisks). Phases were initially preloaded with 10,000 ng template *ds*DNA (y-axis maxima). RW/6605/02

As previously discussed, it would be expected that the lifetime of any biological component in a system would have a finite lifetime; however, based upon the calculations for the amount of template *ds*DNA required to produce the mRNA yields obtained for successive batch transcriptions, it was apparent that the accessibility of the template *ds*DNA compartmentalized within the DOPE H_{II} phases was reducing over time. It would be expected, assuming *ds*DNA accessibility remained constant and that all *ds*DNA molecules were equally accessible, that the calculated amount of *ds*DNA template would tend towards the amount of *ds*DNA initially preloaded into the phase (i.e. 1 µg or 10 µg for the data sets presented in Figures 4.6 and 4.7).

The observation that both DOPE H_{II} phases preloaded with 1 or 10 µg of *ds*DNA lost transcriptional activity when T7 RNA polymerase had transcribed template *ds*DNA from the phase equivalent to approximately 40% of the *ds*DNA loaded within the phase provided three possible issues for the system; firstly, less than half of the *ds*DNA compartmentalized within the phase was accessible over the duration of successive batch transcriptions; secondly, that the multiple-cycle batch transcription process was having a degrading effect upon the DOPE H_{II} phase, causing *ds*DNA to become less accessible over time; thirdly, that accessible *ds*DNA compartmentalized within the phase was becoming degraded or lost over the duration of successive batch transcriptions. As a consequence, investigations were designed and conducted to establish the most probable cause of the loss of transcriptional activity and apparent inaccessibility of approximately 60% of the total template *ds*DNA compartmentalized within DOPE H_{II} phases under multiple-cycle batch transcription conditions.

4.3.3 Mass spectrometry

With the possibility that multiple-cycle batch transcription was causing degradation to the integrity of the DOPE H_{II} phase, electrospray-ionization mass spectrometry of a DOPE lipid button preloaded with 1 µg linear *ds*DNA was performed prior to and after multiple-cycle batch transcription, under the conditions described in section 4.3.1. For the liquid crystalline phase to remain transcriptionally active, the *ds*DNA within it has to remain accessible for transcription by RNA polymerases. Degradation of the DOPE molecules forming the liquid crystalline phase could cause a shift away from the observed inverse hexagonal phase, potentially leading to either the inaccessibility of the template *ds*DNA partitioned within it or the leaching of *ds*DNA from inside the liquid crystalline structure.

Comparison of the NL 141 mass spectra, used for the identification of PE and lysoPE during mass spectrometry lipid profiling, allowed for qualitative analysis of whether

the multiple-cycle batch transcription process was causing the degradation of DOPE molecules within the liquid crystalline phases (Figure 4.8).

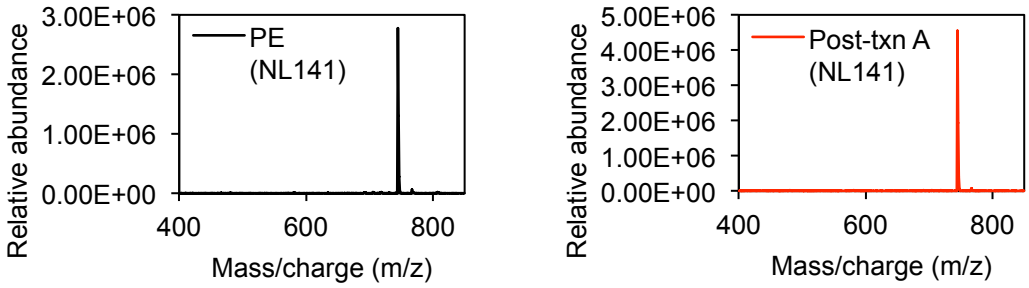

Figure 4.8 A comparison of the neutral loss of fragment 141 (NL 141) mass spectra for DOPE H_{II} phases before (left, black trace) and after (right, red trace) multiple-cycle batch transcription. RW/6295/10

The comparison between the NL 141 mass spectra before and after multiple-cycle batch transcription (Figure 4.8) clearly shows that structural degradation of DOPE molecules within the lipid button has not occurred, as there were no additional fragments identified on the mass spectra post-batch transcription. It was therefore concluded that if multiple-cycle batch transcriptions were potentially having any effect on the phase integrity, it was through factors other than lipid degradation.

4.3.4 Polarizing microscopy

Polarizing microscopy of DOPE lipid buttons under a variety of experimental conditions was performed in an attempt to observe whether multiple-cycle batch transcription affected the integrity of the H_{II} phase structure. Imaging of the lipid buttons allowed for qualitative comparison of the phase structures, which could offer an explanation as to why transcriptional activity was lost after successive batch transcription cycles.

Figure 4.9 shows the polarizing microscopy images of DOPE lipid buttons under a variety of experimental conditions relevant to the multiple-cycle batch transcription process; inset 1 shows the expected inverse hexagonal (H_{II}) phase of DOPE at 37 ˚C.[7] It is clear that the incubation of the DOPE H_{II} phase with linear *ds*DNA, transcription buffer, and 25 mM $MgCl_2$, to compartmentalize the *ds*DNA within the phase prior to batch transcription, has a minimal degrading effect upon the phase structure, with a clear H_{II} phase observed in Figure 4.9 insets 2-5, although slightly less birefringence is observed after the full 100 h incubation (Figure 4.9, inset 5). After 10 cycles of batch transcription, there is a greater loss of birefringence in the DOPE lipid sample (Figure 4.9, inset 6), indicating some degradation of the initial inverse hexagonal phase structure of the lipid button, although some H_{II} structure is apparent.

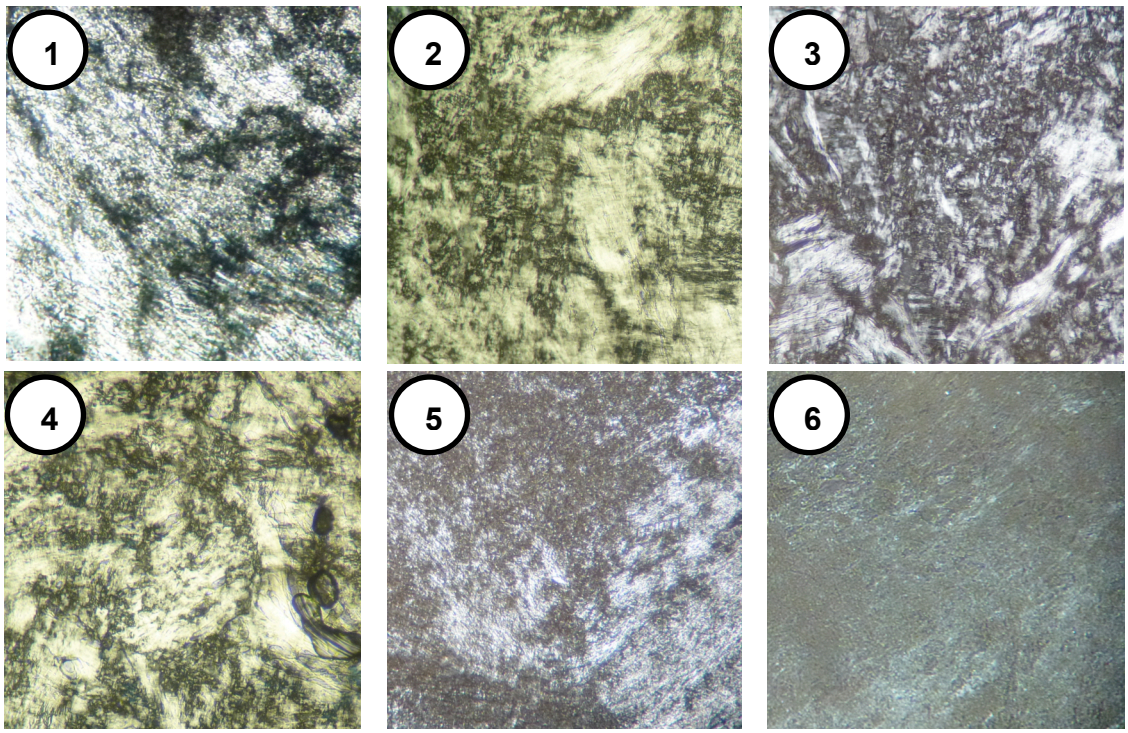

Figure 4.9 Polarizing microscopy images of DOPE lipid buttons at various stages before, during and after the batch transcription process. **(1)** DOPE H_{II} phase, 37 °C. **(2)** DOPE after 24 hours incubation at 37 °C with transcription buffer. **(3).** DOPE after 24 hours incubation at 37 °C with transcription buffer and 1µg linearised pRSET-EmGFP *ds*DNA. **(4)** DOPE after 100 hours incubation at 37 °C with transcription buffer. **(5)** DOPE after 100 hours incubation at 37 °C with transcription buffer and 1µg linearised pRSET-EmGFP *ds*DNA. **(6)** DOPE after 10x 2 hour batch transcriptions at 37 °C.

The observed reduction in sample birefringence of DOPE lipid buttons after multiple cycles of batch transcription is likely due to the deposition of salts within the lipid sample, caused by the repetitive layering of transcription assay solution above the DOPE lipid button over successive batch transcriptions. Increasing salt concentration within the phase due to build-up of $MgCl_2$ would reduce the ability of the lipid button to remain as a lyotropic liquid crystalline H_{II} phase. This was not unexpected; literature already describes how the structure of lipid membranes can be affected by the presence of biological buffers in assay solutions.[8] Indeed, our own SAXS analysis of DOPE H_{II} phases in the presence of a concentration gradient of $MgCl_2$ show how the lattice parameter of the inverse hexagonal phase structure increase with increasing salt concentration (Figure 4.10). This is likely due to increasing levels of electrostatic repulsion as the concentration of divalent magnesium cations within the liquid crystalline phase is increased.

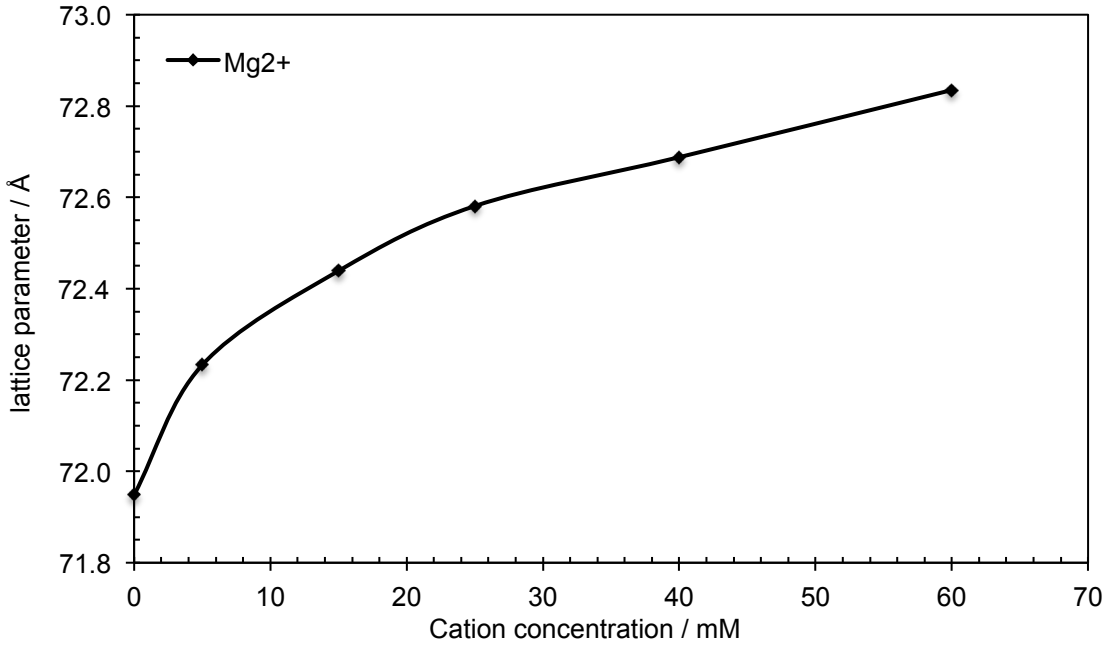

Figure 4.10 A comparison of the lattice parameter for DOPE H_{II} phases (black diamonds) across a concentration gradient of $MgCl_2$, 37 °C. MAX-lab data, September 2012.

Whilst it is clear that an increase in salt concentration enlarges the lattice parameter of DOPE H_{II} phases, and there is degradation in the integrity of the H_{II} phase structure over multiple cycles of batch transcription from it, it is unclear whether this degradation is the primal cause of the prevention of transcriptional activity after successive batch transcriptions. It is possible that partitioned *ds*DNA initially contained within the pores of the H_{II} phase could become inaccessible for transcription after successive transcription cycles, due to degradation of the phase structure (Figure 4.9).

4.4 Identifying the location of template DNA

Fluorescence microscopy time-lapse imaging has shown that linear *ds*DNA partitions into the H_{II} phase of DOPE in the presence of transcription buffer (Figure 4.11), rather than purely associating with the H_{II} phase surface.[3] This is in agreement with the proposition discussed in Chapter 3 that it is entropically favourable, under these conditions, for the linear *ds*DNA to reside within the pores of the H_{II} phase in a DOPE button, rather than remain within an aqueous supernatant solution layered above the lipid button. The observation that *ds*DNA partitioning requiring approximately 100h for $K_p < 0.005$ also supports the phenomenon of *ds*DNA partitioning to within the phase pores, rather than the occurrence of phase surface association; were the *ds*DNA merely associating with the phase surface, partitioning of 1 µg linear *ds*DNA out of the aqueous supernatant solution would be expected to occur in a far quicker timescale than 100 h.

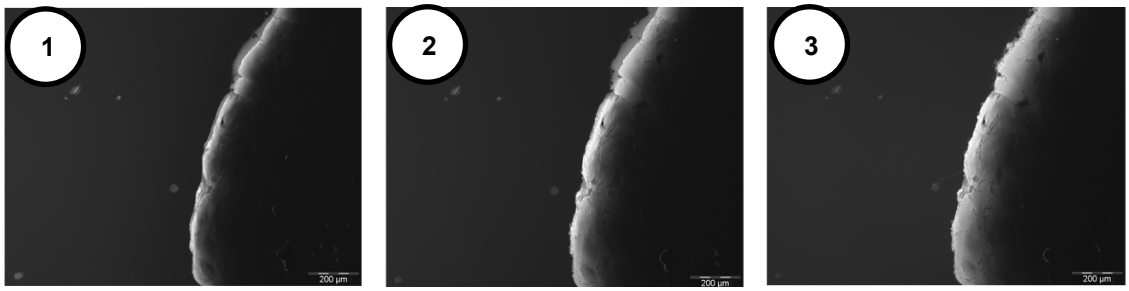

Figure 4.11 Time-lapse fluorescence microscopy images showing the penetration of linear *dsDNA* into a thin layer (~100 µm thick) of H_{II} phase of DOPE sandwiched between a microscope slide and coverslip. **(1)** The DOPE H_{II} phase in excess buffer containing propidium iodide without DNA. **(2)** The same system 5 minutes and **(3)** 15 minutes after the addition of *lin-pT7luc* DNA. Published by Black *et al.* (2010) [3].

4.4.1 Further investigation into incubation conditions

With DNA partitioning studies and time-lapse fluorescence-microscopy imaging both supporting the phenomenon of *ds*DNA partitioning into the pores of the H_{II} phase of DOPE lipid buttons in the presence of transcription buffer, it was intriguing that transcription activity reduced over multiple cycles of batch transcription, with the cumulative mRNA yield from multiple cycles of batch transcription tending towards a plateau. This was of particular interest as the calculations into the amount of template *ds*DNA required to produce the mRNA yields achieved was less than half of the amount of template *ds*DNA preloaded into the lipid buttons (section 4.3.2); the reduction in the transcriptional activity observed was therefore not attributable to a lack of *ds*DNA partitioned within the H_{II} phase, as over 50% of the *ds*DNA initially preloaded into the H_{II} phase remained so after a substantial number of batch transcription cycles.

When pre-loading DOPE H_{II} phase lipid buttons with linear *ds*DNA, an aqueous supernatant solution (20 µL) containing the linear *ds*DNA, transcription buffer and 25 mM $MgCl_2$ is layered above the lipid button into which the *ds*DNA will partition. These conditions are ideal for this purpose, as they are homologous to the conditions under which transcription occurs, except for the omission of ribonucleotide triphosphates (rNTPs) and T7 RNA polymerase during the 100 h incubation to partition the linear *ds*DNA. With transcriptional activity reducing over subsequent batch transcription cycles, and transcription assay conditions only varying from the initial 100 h incubation conditions through the presence of rNTPS and T7 RNA polymerase, investigations into the effect of these transcription assay components upon *ds*DNA partitioning into DOPE H_{II} phases were undertaken.

4.4.1.1 Effect of ribonucleotide triphosphates upon DNA partitioning

Comparing the similarity between rNTPs and T7 RNA polymerase to the linear *ds*DNA that had been partitioned into the pores of H_{II} phase DOPE during this research, it was clear that rNTPs were more likely to present a hindrance to *ds*DNA partitioning than T7 RNA polymerase. Firstly, T7 RNA polymerase is a considerably larger molecule than linear *ds*DNA; as a consequence, the ability of T7 RNA polymerase to partition within the H_{II} phase pores, which have a diameter of 4 nm [9], would be significantly reduced compared to linear *ds*DNA. Secondly, ribonucleotide triphosphates are in considerable excess throughout the duration of a standard transcription assay solution; ~2.4×10^{17} bases are present in a 20 µL solution at an rNTPs concentration of 20 mM, yet only ~2.9×10^{16} of these rNTPS are used to produce the product mRNA of a typical positive control reaction (assuming a mRNA yield of 23.8 µg). Lastly, the physical structure of rNTPS (Figure 4.12) is more closely matched to that of linear *ds*DNA, which has already been shown to successfully partition into the pores within H_{II} phase DOPE lipid buttons.[3]

As discussed in Chapter 3, the likely reasoning for the partitioning of linear *ds*DNA within DOPE H_{II} phases is the entropic increase in the system, caused by the release of monovalent countercations (such as Na^+) and counteranions into the supernatant transcription assay solution above a lipid button. The monovalent countercations were initially associated with the negatively charged phosphate backbones of the linear *ds*DNA molecules, whilst the displaced monovalent counteranions (such as Cl^-) were previously associated with divalent cations (such as Mg^{2+}) that bridged the negatively-charged DOPE lipid head groups within the H_{II} phase pores. The resultant increase in configurational entropy of the system, caused by the change in electrostatic

interactions, observed when linear *ds*DNA partitions within DOPE H_{II} phase pores is a sufficient driving force for the process.

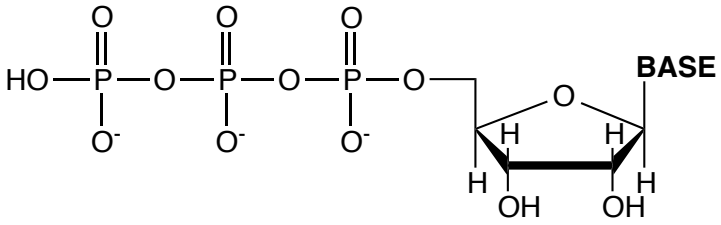

where **BASE** can be:

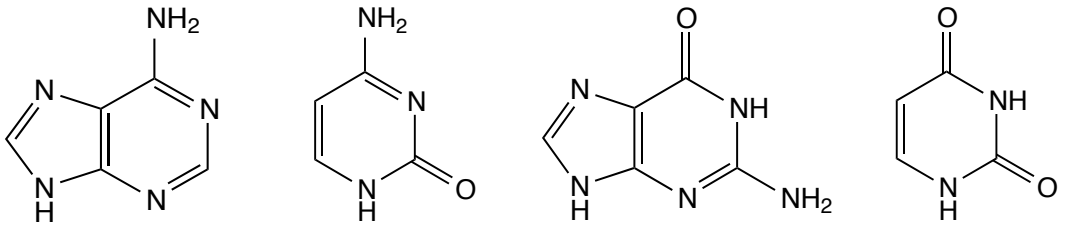

Figure 4.12 Structure of a ribonucleotide triphosphate.

Assuming that rNTPs are likely to interact with the DOPE H_{II} phase in a similar manner to linear *ds*DNA, due to their structural similarities, they are likely to cause similar changes to the electrostatic interactions, thus also causing a change in configurational entropy of the system. Comparing rNTPs and linear *ds*DNA, rNTPs have two additional negatively charged phosphate groups per base; it follows that, per base, rNTPs can potentially associate with thrice as many monovalent countercations as linear *ds*DNA is able to. Within a 20 µL transcription assay solution containing 1 µg *lin*pRSET-EmGFP *ds*DNA, producing a yield of 23.8 µg mRNA, ~2.1 x 10^{17} rNTP bases are unused by the end of the reaction, which would be able to release a maximal total of 6.3 x 10^{17} monovalent countercations, should the full complement of these unused rNTPs partition within the H_{II} phase. 1 µg of *lin*pRSET-EmGFP *ds*DNA, however, will only release a maximal total of 1.8 x 10^{15} monovalent countercations, should all of this *ds*DNA partition within the pores of the H_{II} phase. For both *ds*DNA and rNTPs, a number of counteranions equivalent to the number of countercations released will be displaced upon partitioning into the H_{II} phase pores; it follows, therefore, that partitioning of all excess rNTPs will displace a total of ~1.3 x 10^{18} counterions, whilst partitioning of 1 µg of *lin*pRSET-EmGFP *ds*DNA will displace a total of ~3.6 x 10^{15} counterions. It was therefore expected that the partitioning of rNTPs would be more entropically favourable when compared to the partitioning of linear *ds*DNA into the H_{II} phase pores of DOPE lipid buttons.

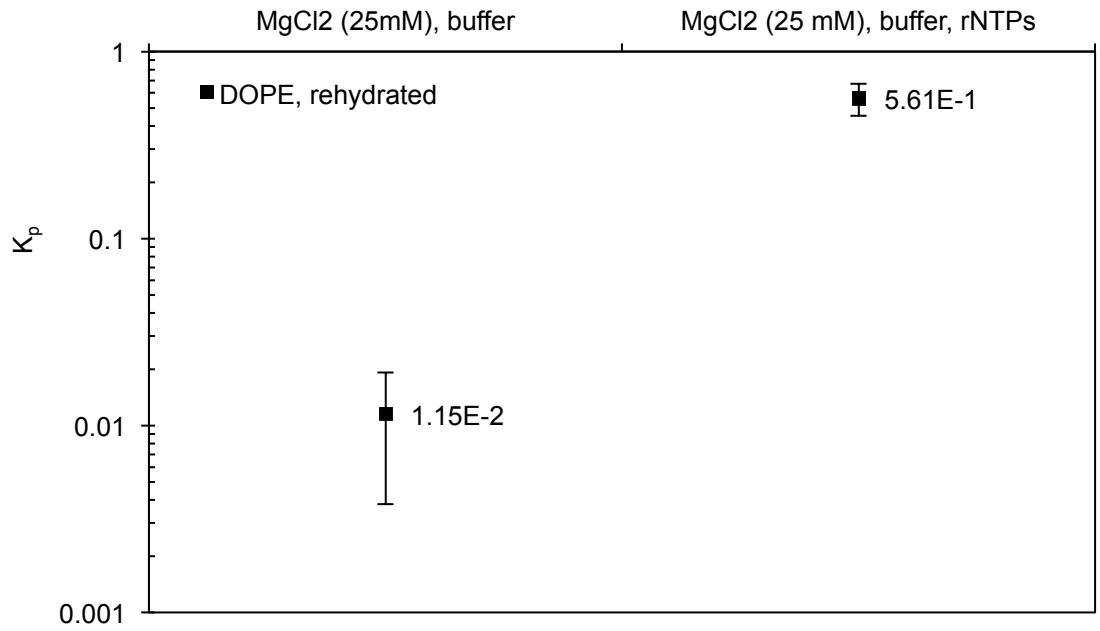

Figure 4.13 The influence of rNTPs on the partitioning of *ds*DNA into the rehydrated H_{II} phases of DOPE lipid buttons. Lipid buttons were prepared by rehydration with isotonic saline prior to incubation of *ds*DNA in the supernatant liquid (transcription buffer, 25 mM $MgCl_2$) above the H_{II} phase. Data are for *lin*pRSET-EmGFP and for a total incubation time of 100 h (37 °C). RW/6511/14

As predicted by the calculations showing greater increase in the entropy of the system, caused by the displacement of up to 360 times more counterions, Figure 4.13 shows how the presence of rNTPs (20 mM) in addition to linear *ds*DNA (1 µg), transcription buffer and $MgCl_2$ (25 mM), the linear *ds*DNA present in solution no longer substantially partitions within the pores of H_{II} phase DOPE lipid buttons.

4.4.1.2 Addition of ribonucleotide triphosphates to DNA-containing DOPE H_{II} phases

With the presence of rNTPs in the lipid button initial incubation solution clearly inhibiting the partitioning of *ds*DNA into the pores of DOPE H_{II} phases, an investigation was then carried out into whether rNTPs would cause the displacement of compartmentalized *ds*DNA from within preloaded DOPE H_{II} phase lipid buttons. As discussed in section 4.3, *ds*DNA-containing DOPE H_{II} phase lipid buttons lose transcriptional activity after multiple cycles of successive batch transcription; this loss in transcriptional activity could potentially have been caused by the removal of linear *ds*DNA from within the H_{II} phase if rNTPs were partitioning into the phase preferentially. It was therefore important to investigate any displacement effect caused by rNTPs upon the linear *ds*DNA contained within these DOPE lipid buttons, which was

naturally of particular concern due to the inhibition of significant *ds*DNA partitioning over the course of the 100 h incubation observed in Figure 4.13.

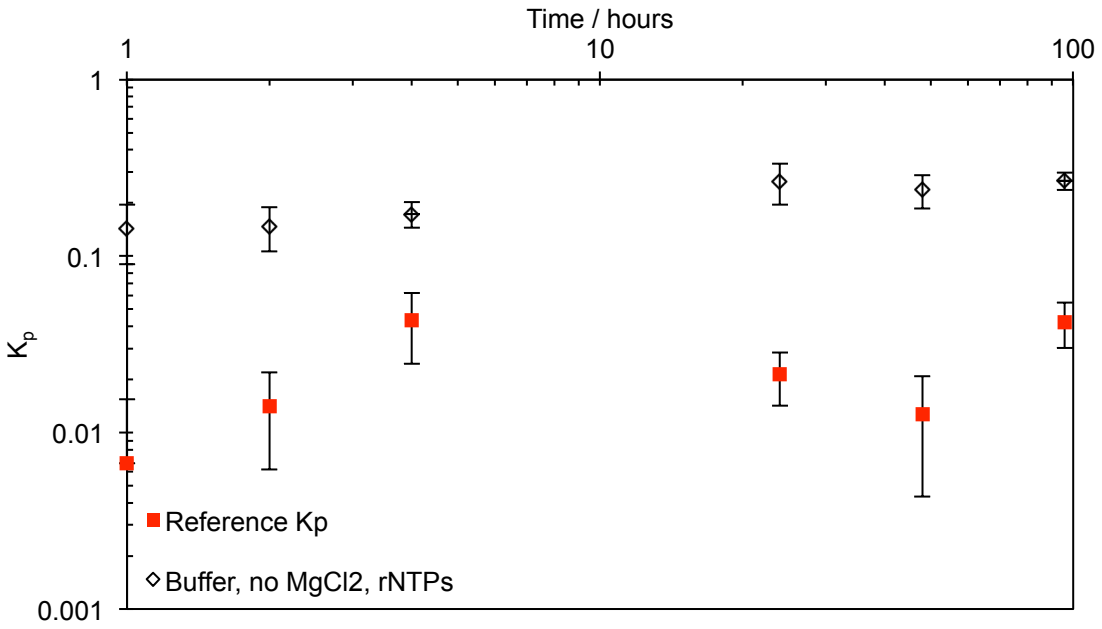

Figure 4.14 The influence of rNTP addition (20 mM) upon DOPE lipid buttons preloaded with 1 µg of linear *ds*DNA. Lipid buttons were prepared by rehydration with isotonic saline prior to incubation (100 h, 37 ˚C) of *ds*DNA in the supernatant liquid (transcription buffer, 25 mM $MgCl_2$) above the H_{II} phase, before discarding the supernatant solution and replacing with 20 µL transcription buffer and rNTPs solution, incubating for a further equivalent time period (37 ˚C). Red squares show the partition coefficient prior to rNTP incubation; hollow diamonds show the partition coefficient post rNTP incubation. RW/6511/17

The addition of rNTPs to DOPE lipid buttons preloaded with 1 µg of linear *ds*DNA caused the leaching of *ds*DNA out of the H_{II} phase pores and into the supernatant solution layered above (Figure 4.14). Incubation of the phases with rNTPs for increasing amounts of time, however, produced only a small increase in the amount of *ds*DNA leached from the phase; after a 1 h incubation period, the phase contained an average of 857 ng *ds*DNA, whilst after a 100 h incubation period, the phase contained an average of 733 ng *ds*DNA. Of relevance to the multiple-cycle batch transcription system, however, is that after a 2 h incubation period, an average of 853 ng *ds*DNA is left within the phase; assuming that 1 µg of *ds*DNA is preloaded into a phase, it could be expected that up to ~147 ng of linear *ds*DNA might be caused to be displaced from within the H_{II} phase pores, due to the presence of rNTPs in the transcription assay solution layered above the lipid button, for each cycle of batch transcription. If this amount of linear *ds*DNA was caused to leach from within the phase for each batch transcription cycle, it would be expected that transcriptional activity would be lost within approximately 7 cycles of successive batch transcription, whilst the mRNA yields observed would be broadly similar for each batch transcription cycle, due to the presence of ~147 ng of leached *ds*DNA in solution for batch transcription cycles 1-7.

As seen in Figure 4.3, this was clearly not the case, with a defined peak in transcriptional activity during the third cycle of batch transcription followed by a decrease in transcriptional activity over time. It is clear, therefore, that the presence of rNTPs do not cause a constant amount of linear *ds*DNA to become displaced from within the phase for successive cycles of batch transcription, and that the dynamics of the DOPE lipid button batch transcription system are complex, due to the evolution of the counterion and rNTP concentrations within the system over time.

4.5 Leaching of *ds*DNA from DOPE H_{II} phases

The results presented so far in this chapter have shown that the transcriptional activity of *ds*DNA-containing DOPE H_{II} phases decreases over successive cycles of batch transcription, yet the integrity of the H_{II} phase appeared to remain, and the presence of rNTPs in solution when preloading H_{II} phases with linear *ds*DNA significantly inhibited the partitioning of that *ds*DNA into the phase. When added to phases already preloaded with *ds*DNA *via* the incubation method, the presence of rNTPs appeared to cause compartmentalized *ds*DNA to leach out from within the phase. It was therefore assumed likely that the rNTPs present within transcription assay solutions were in fact the cause for a proportion of the observed loss in transcriptional activity over successive batch transcriptions. The partitioning of *ds*DNA into DOPE H_{II} phases is a slow process; with rNTPs apparently likely causing the leaching of compartmentalized *ds*DNA from within the phase during each transcription cycle, the assay incubation time would be too short for a significant amount of any leached *ds*DNA to repartition back into the H_{II} phase. As a consequence, leached *ds*DNA would remain within the transcription assay supernatant above the phase, becoming lost during the removal of the supernatant as part of the RNA purification process after each batch transcription cycle.

4.5.1 Quantification of leached *ds*DNA

With it suspected that rNTPs present in transcription assay solutions were causing the leaching of *ds*DNA from within DOPE H_{II} phases, efforts were made into quantifying the amount of *ds*DNA that was leaching during individual transcription cycles. This was done by taking a aliquot of the post-transcription assay solution (25%) and loading it onto an agarose gel for DNA gel electrophoresis, alongside known reference amounts of linear *ds*DNA. The intensities of the leached *ds*DNA bands were then compared to the intensities of the reference *ds*DNA bands, allowing for the estimation of the amount of leached *ds*DNA loaded onto the gel; applying a scaling factor to correct for the loading of only a portion of the post-transcription assay solution onto the gel allowed for approximation of the total amount of *ds*DNA leached per batch transcription. The advantage of loading only a proportion of the post-transcription assay solution was that this allowed for the remainder of the assay solution to be purified and the resultant mRNA yield quantified.

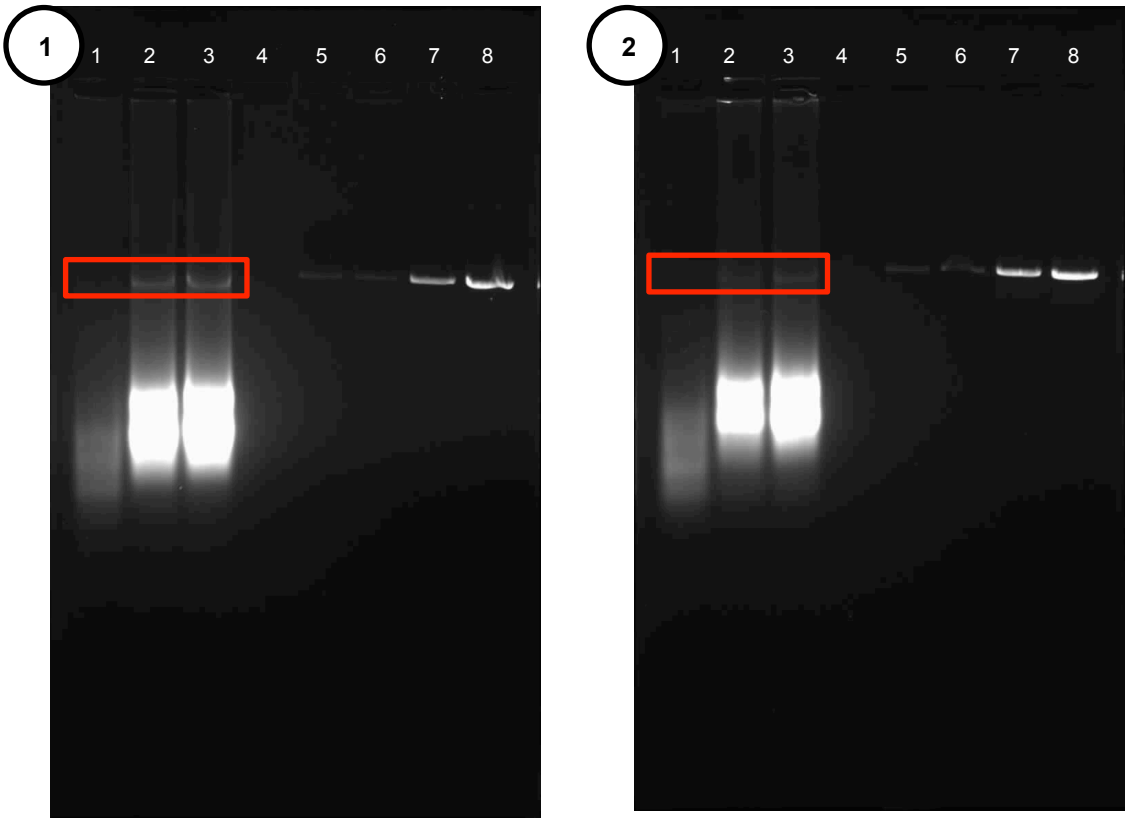

Figure 4.15 DNA gel of post-batch transcription DOPE lipid buttons after successive transcription cycles. DOPE H_{II} phases were preloaded with 1 µg *lin*pRSET-EmGFP *via* 100 h incubation (37 ˚C) 25 mM $MgCl_2$ and transcription buffer (RW/6605/02). **1).** DNA gel of ¼ of the post-transcription supernatant after the third batch transcription (lanes 1-3) against 5, 10, 500 and 100 ng *lin*pRSET-EmGFP reference *ds*DNA (lanes 5-8). **2).** DNA gel of ¼ of the post-transcription supernatant after the fourth batch transcription (lanes 1-3) against 5, 10, 50 and 100 ng *lin*pRSET-EmGFP reference *ds*DNA (lanes 5-8).

DNA gel electrophoresis of post-batch transcription transcription assay solution confirmed the presence of template *ds*DNA (Figure 4.15); the red box in gel lanes 1-3 of gels one and two highlights the template dsDNA bands. As the only source of *ds*DNA within the system is that which was initially compartmentalized within the DOPE H_{II} phase, this observation supports the suspicion that *ds*DNA was being leached from the H_{II} phase and then lost during RNA purification processes.

Once the amounts of leached *ds*DNA had been quantified *via* DNA gel electrophoresis, a comparison was then made between the amounts of *ds*DNA observed to be leaching from within the H_{II} phase for each batch transcription, and the amount of template *ds*DNA that was required, per batch transcription, to produce the mRNA yields observed. This comparison would then remove doubt as to whether the mRNA yields achieved from DNA-containing H_{II} phases was caused by *ds*DNA associated within the phase or rather by *ds*DNA that had leached from the phase into the transcription assay supernatant.

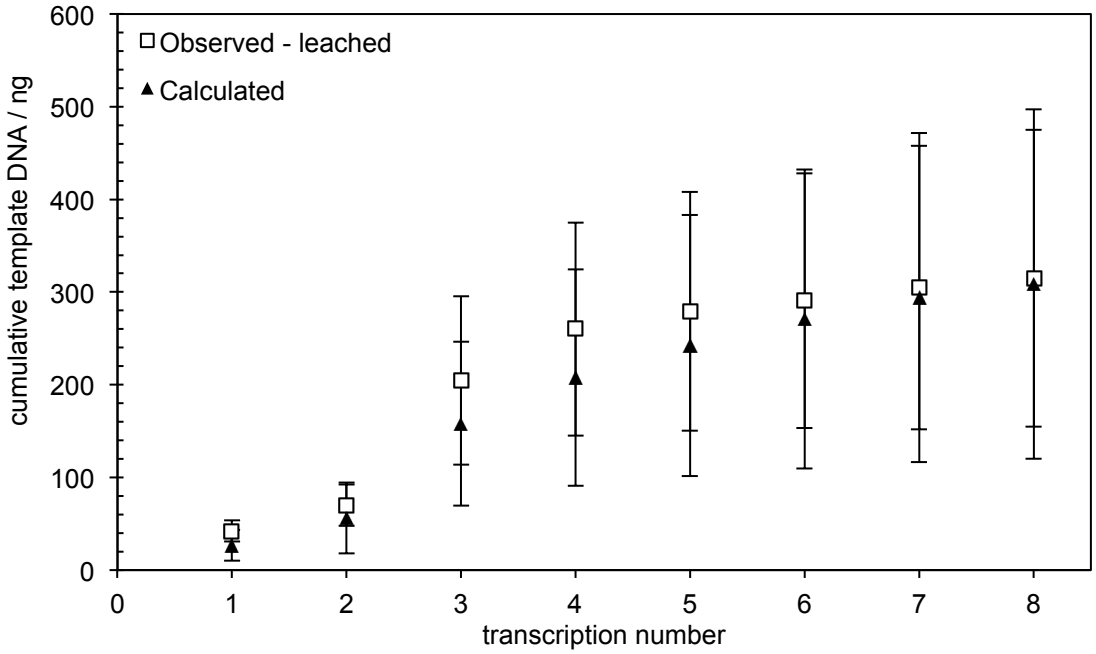

Figure 4.16 A comparison of the cumulative calculated template DNA required to produce the obtained mRNA yields (black triangles) to the observed *ds*DNA leached from within the phase (hollow squares) during multiple-cycle batch transcription using 1 µg *ds*DNA-containing DOPE H_{II} phases. Phases were initially preloaded with 1,000 ng template *ds*DNA (y-axis maxima). RW/6605/02

Figures 4.16 and 4.17 compare the amount of cumulative template *ds*DNA observed to have leached, by quantification using DNA gel electrophoresis, from within DOPE H_{II} phases, preloaded with 1 or 10 µg linear *ds*DNA, across the duration of multiple-cycle batch transcription, to the amount of cumulative template *ds*DNA calculated to have been required to produce the mRNA yields achieved. Within experimental error, it is clear that the amount of *ds*DNA observed to leach from within the DOPE H_{II} phases preloaded with 1 µg of *ds*DNA (Figure 4.16) is consistent with the amount of template *ds*DNA required to produce the mRNA yields obtained from batch transcription. It was deduced, therefore, that all transcriptional activity observed when using DOPE H_{II} phases preloaded with 1 µg of *ds*DNA is attributed to the *ds*DNA that had leached from within the phase during each cycle of batch transcription. This contrasts to the results observed from DOPE H_{II} phases preloaded with 10 µg of *ds*DNA (Figure 4.17); under homogeneous batch transcription assay conditions, the amount of *ds*DNA estimated by DNA gel electrophoresis to have leached from within the DOPE H_{II} phase was lower than the total amount of template *ds*DNA required, for the third batch transcription cycle onwards, to produce the mRNA yields obtained. There are two possible explanations for this observation; firstly, the ability of the gel-based technique for detecting larger amounts of leached *ds*DNA is not as sensitive as would be desired, leading to conservative estimation of the amount of *ds*DNA present on the gel; or

secondly, that a small proportion of the mRNA yields obtained was produced by template *ds*DNA being transcribed whilst it was still associated with the H_{II} phase.

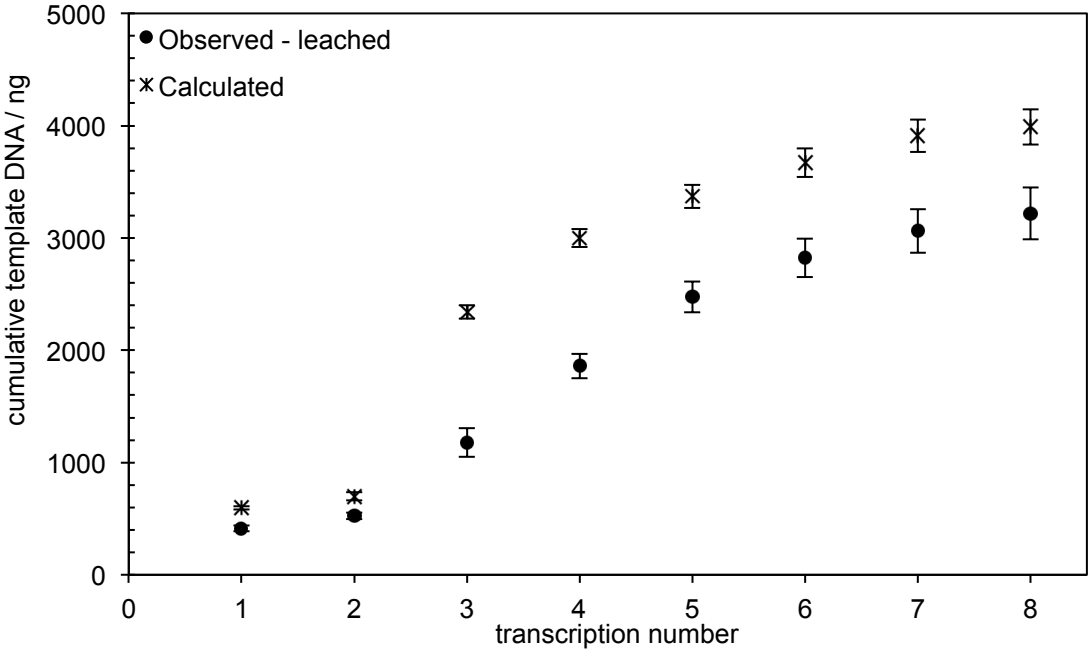

Figure 4.17 A comparison of the cumulative calculated template DNA required to produce the obtained mRNA yields (black asterisks) to the observed *ds*DNA leached from within the phase (black circles) during multiple-cycle batch transcription using 10 μg *ds*DNA-containing DOPE H_{II} phases (black asterisks). Phases were initially preloaded with 10,000 ng template *ds*DNA (y-axis maxima). RW/6605/02

By the eighth batch transcription cycle from DOPE H_{II} phases preloaded with 10 μg of *ds*DNA, the observed amount of *ds*DNA leached from within the phase was equal, on average, to 80.6% of the cumulative calculated amount of template *ds*DNA required to produce the observed mRNA yields. This had steadily increased from 51.0% at the third batch transcription. This suggested that a likely conservative estimate of the amount of *ds*DNA leaching during the third batch transcription had caused the drop in observed leached *ds*DNA, relative to the calculated amount of template *ds*DNA required, or that the proportion of template *ds*DNA that was transcribed whilst being associated with the H_{II} phase was gradually lost over successive batch transcription cycles, causing the proportion of leached *ds*DNA responsible for the obtained mRNA yields to increase over multiple cycles.

4.5.2 Minimizing leaching through modification of the batch transcription system

With a number of sets of experimental data supporting the observation that *ds*DNA was being leached from within the phase during batch transcription, consideration was given to the reason for the loss of template *ds*DNA from within the phase structure.

Firstly, it was possible that, over the course of multiple-cycles of batch transcription, increasing amounts of rNTPs were preferentially partitioning within the pores of the phase, causing the ejection of the *ds*DNA. Secondly, whilst mass spectrometry had shown that there was no degradation in the DOPE molecules of the phase, polarizing microscopy had shown the loss of birefringence over time during repeated batch transcription from lipid buttons; this suggested that the lipid phase may have started to shift away from the H_{II} phase, a change which could potentially release previously partitioned *ds*DNA molecules back into solution. Thirdly, the RNA polymerases may pull the linearized *ds*DNA molecules out of the H_{II} phase pores during the process of transcription, but due to the slow nature of *ds*DNA partitioning (as observed during the *ds*DNA partition coefficient experiments described in Chapter 3) the ejected molecules of *ds*DNA are unable to partition back within the phase prior to the end of the transcription reaction (typically 2 hours).

In an attempt to minimize the observed leaching of template *ds*DNA from within the H_{II} phase of DOPE lipid buttons under batch transcription conditions, it was decided to trial modifications to the following three sets of system parameters:

- initial *ds*DNA incubation conditions;
- liquid crystalline phase conditions;
- transcription assay components composition.

Through modification of these parameters and assessment of the impact upon the leaching of *ds*DNA during transcription they had it was hoped that an improved method of *ds*DNA partitioning and multiple-cycle batch transcription could be established.

4.5.3 Increasing the assay concentration of $MgCl_2$

As observed and discussed in Chapter 3, the presence and concentration of divalent magnesium cations in supernatant *ds*DNA incubation solutions have a considerable effect upon the partitioning of linear *ds*DNA into H_{II} phases; if the magnesium ion concentration were too low, *ds*DNA partitioning would be slowed or severely impeded. It therefore seemed prudent that the first investigations into the batch transcription system modifications were those into the supplementation of supernatant *ds*DNA incubation solutions and subsequent batch transcription assays with additional magnesium chloride. Results discussed in Chapter 2 detail how the transcriptional yields achieved from solution-based positive controls are optimal when the transcription assays contain approximately 40 mM $MgCl_2$; however, above 40 mM $MgCl_2$, transcriptional activity reduces dramatically, which would become a significant problem for the multiple-cycle batch transcription should levels of $MgCl_2$ build up in the H_{II} phase across subsequent batch transcription cycles.

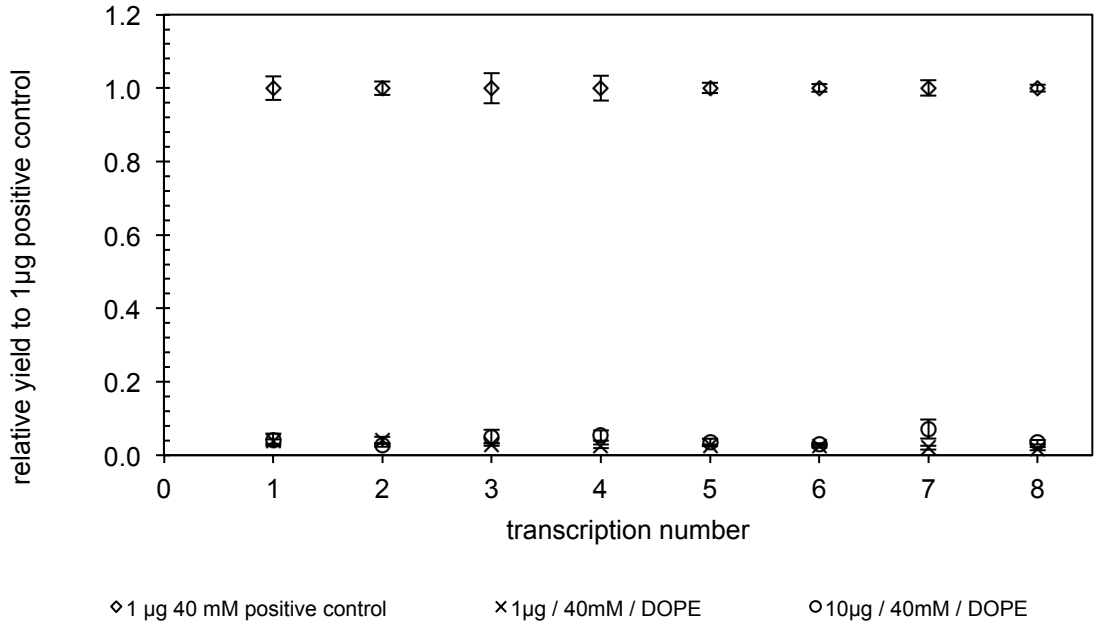

Figure 4.18 Transcriptional yields, relative to positive control transcription assays (hollow diamonds), from multiple-cycle batch transcription from DOPE lipid buttons preloaded with 1 µg (black crosses) or 10 µg (hollow circles) linear *ds*DNA, prepared by 100 h incubation (37˚C) with transcription buffer and 40 mM $MgCl_2$. Individual transcription assay incubations were for 2 h (37 ˚C). RW/6605/02

DOPE buttons were preloaded with either 1 or 10 µg or linear *ds*DNA under 40 mM $MgCl_2$ conditions did not show any transcriptional activity, across a run of 8 subsequent batch transcription cycles (Figure 4.18). During each transcription cycle, the DOPE buttons had a fresh 20 µL of transcription assay solution layered on top of

them; it is likely that the combination of $MgCl_2$ from initial *ds*DNA incubation in addition to the supplementary $MgCl_2$ in the transcription assay solution rendered these DOPE phases transcriptionally inactive, due to the high levels of $MgCl_2$ present. The loss of transcriptional activity when increasing the incubation and transcription assay conditions from 25 mM to 40 mM highlights the inherent sensitivity of the system to the ionic conditions present.

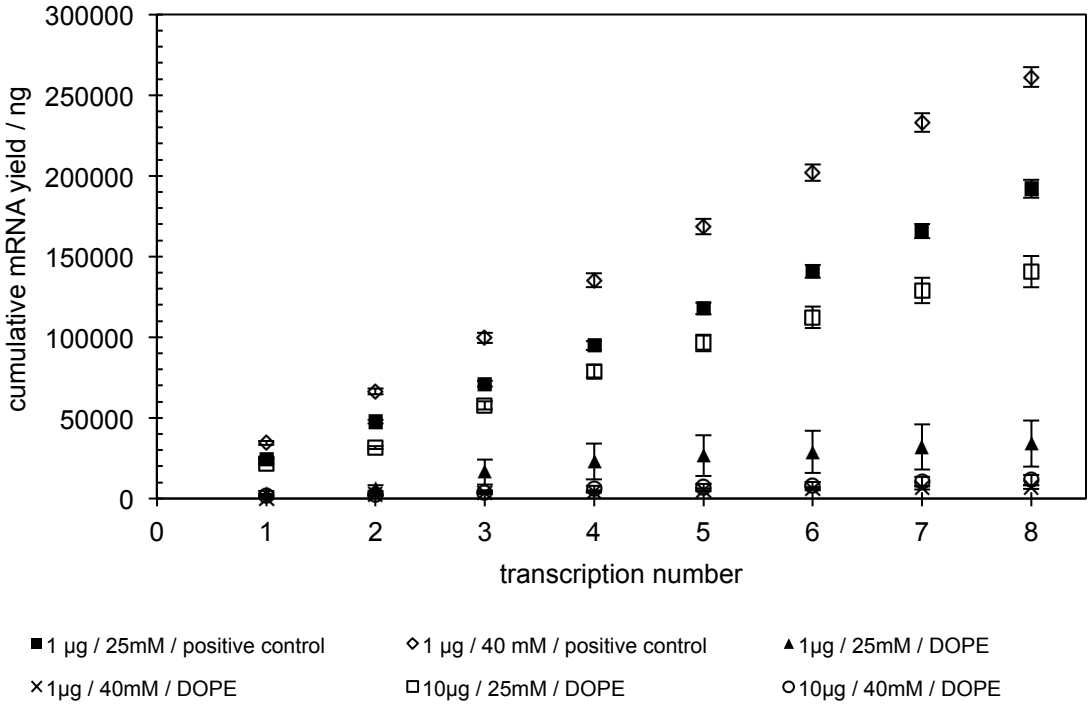

Figure 4.19 The effect of $MgCl_2$ concentration upon the cumulative mRNA yield from multiple-cycle batch transcription from 1 µg and 10 µg *ds*DNA-containing DOPE H_{II} phases. Phases were incubated for 2 hours (37 °C) per transcription. Results are shown for batch transcription assays from DOPE H_{II} phases containing either 1 µg *ds*DNA with 25 mM $MgCl_2$ (black triangles) or 40 mM $MgCl_2$ (black crosses), or 10 µg *ds*DNA with 25 mM $MgCl_2$ (hollow squares) or 40 mM $MgCl_2$ (hollow circles). One-off 1 µg *ds*DNA positive control transcription assays for 25 mM $MgCl_2$ (black squares) and 40 mM $MgCl_2$ (hollow diamonds) are shown for comparison. RW/6605/02

Comparison between the cumulative mRNA yields from DOPE phases preloaded with 1 or 10 µg *ds*DNA under 25 mM or 40 mM $MgCl_2$ conditions highlights the disparity in transcriptional activity (Figure 4.19). The lack of transcriptional activity observed from DOPE phases incubated under 40 mM $MgCl_2$ conditions meant that improvements in transcriptional yield or longevity from multiple-cycle batch transcription were unlikely to be found through variation of cation concentrations during incubation and transcription, and so investigation into modifications to the H_{II} phase were undertaken.

4.5.4 Viability of DOPE lipid buttons doped with cationic lipid: DOTAP

In work previously published, we described the effect of charged lipids upon the partitioning of *ds*DNA into the H_{II} phase of the zwitterionic lipid DOPE [3]. This was done through doping DOPE phases with either the cationic lipid DOTAP (Figure 4.20) and the anionic lipid DOPA, in 90:10 ratios. It was evident, both for lyophilization and 14 hour aqueous incubation methods, that the presence of charged lipids had a profound effect upon the partitioning of *ds*DNA into the H_{II} phase; Figure 4.21 clearly shows that the presence of the cationic lipid DOTAP increased *ds*DNA partitioning (lowering K_p), whilst the presence of the anionic lipid DOPA decreased *ds*DNA partitioning (increasing K_p).

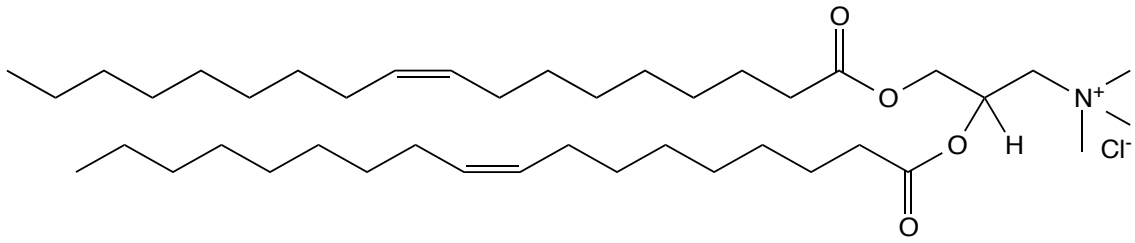

Figure 4.20 Structure of the cationic lipid 1,2-dioleoyl-3-trimethylammonium-propane (DOTAP), in its purchased form as a chloride salt.

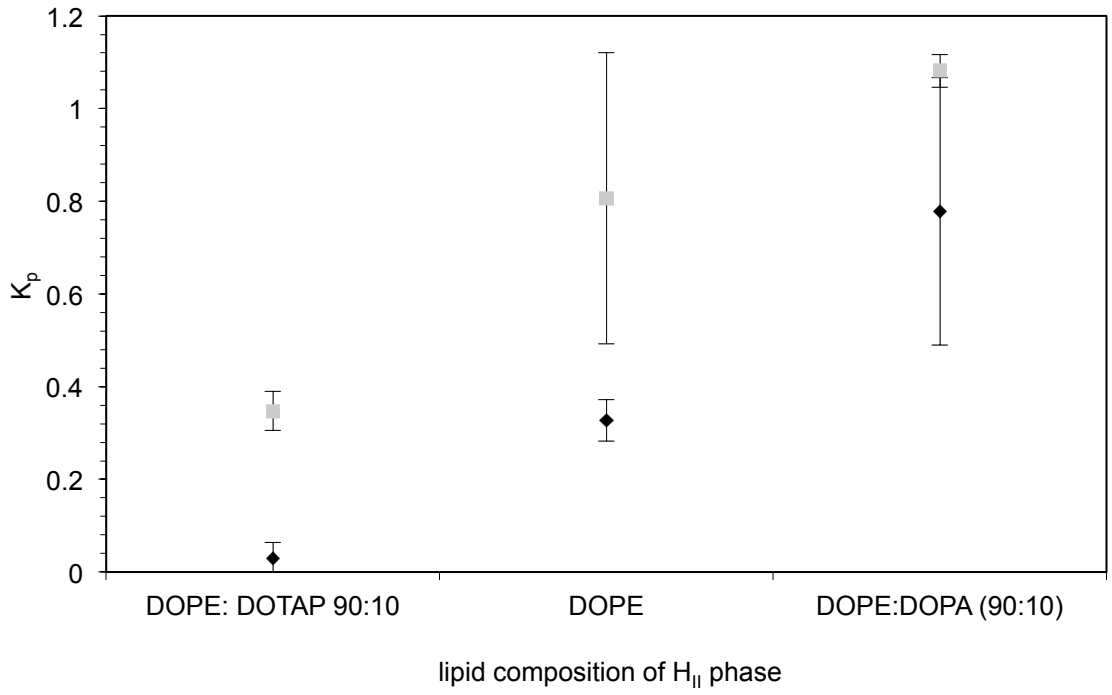

Figure 4.21 The influence of charged lipids on the partitioning of *ds*DNA into the H_{II} phases of lipids. Black diamonds represent lipid buttons prepared by lyophilization; grey squares represent lipid buttons prepared by incubation of *ds*DNA in the supernatant liquid above the H_{II} phase. Data are for *lin*pT7GFP and for a total incubation time of 14 h (37 °C). Published by Black *et al.* (2010) [3].

With the doping of DOPE H_{II} phases with cationic lipid significantly increasing the partitioning of *ds*DNA into the phase, lowering the partition coefficient, it was hoped that the addition of DOTAP in small quantities to DOPE H_{II} phases used for batch transcription would subjugate the issue of *ds*DNA leaching from the phase with subsequent batch transcription cycles. Previous experiments looking at the rate at which *ds*DNA partitioning occurs over time have shown that partitioning into the phase from the incubating supernatant liquid above is a relatively slow process (approximately 100 h for $K_p < 0.005$) and so by doping the phase with the cationic lipid, *ds*DNA should be increasingly attracted towards the phase which would both reduce the likelihood of leaching and encourage the re-partitioning of *ds*DNA back into the phase, should any have been able to leach out. However, should the proportion of DOTAP in the H_{II} phase be too high, the more increased the likelihood of the contained *ds*DNA becoming immobilized within the phase, thus being inaccessible for transcription.

4.5.4.1 DNA partitioning into DOPE:DOTAP lipid buttons

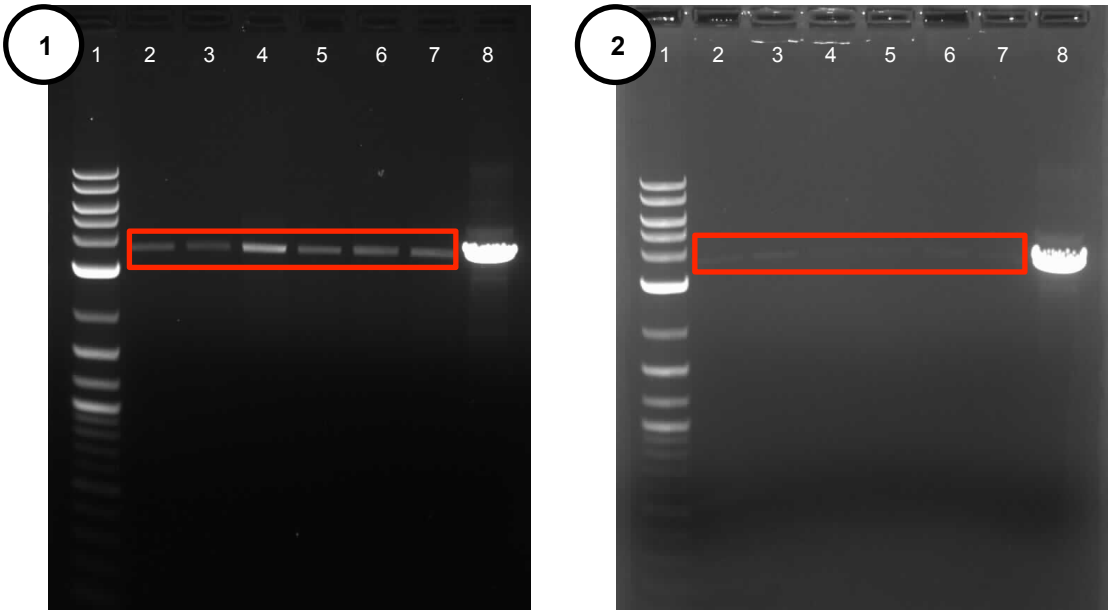

Figure 4.22 DNA gel comparison of DOPE vs. DOPE95:DOTAP5 lipid buttons after 100 h incubations with 1 µg *lin*pRSET-EmGFP, 25 mM $MgCl_2$ and transcription buffer (RW/6456/02). **1).** DNA gel showing DOPE lipid button post-incubation (100 h, 37 ˚C, 25 mM $MgCl_2$, buffer) solutions (lanes 2-7) against NEB 2-log DNA ladder (lane 1) and 1 µg *lin*pRSET-EmGFP reference *ds*DNA (lane 8). **2).** DNA gel showing DOPE95:DOTAP5 lipid button post-incubation (100 h, 37 ˚C, 25 mM $MgCl_2$, buffer) solutions (lanes 2-7) against NEB 2-log DNA ladder (lane 1) and 1 µg *lin*pRSET-EmGFP reference *ds*DNA (lane 8).

In agreement with expectations, 1µg of linearized *ds*DNA, initially located in the supernatant liquid above the lipid button, partitioned into the H_{II} phase to a greater

degree in DOPE doped with DOTAP (DOPE95:DOTAP5) than into DOPE alone (Figure 4.22). This is caused by the increased electrostatic interaction between the additional positive charges within the H_{II} phase and the negatively charged phosphate backbone of the linear *ds*DNA present within the system.

Following the success of the partitioning study into compartmentalization of linear *ds*DNA within DOPE95:DOTAP5 lipid buttons, investigations progressed into firstly assessing the effect of cationic lipid presence upon solution-based transcription, and secondarily the viability of multiple-cycle batch transcription from these cationic lipid composite phases.

4.5.4.2 Batch transcription from DOPE:DOTAP lipid buttons

Prior to conducting multiple-cycle batch transcription from DOPE95:DOTAP5 lipid buttons preloaded with 1 µg of linear *ds*DNA, solution-based control transcription assays were performed above DOPE95:DOTAP5 lipid buttons that contained no *ds*DNA. This offered insight into the effect of cationic lipid upon transcriptional yields under controlled conditions excluding effects due to *ds*DNA partitioning, accessibility or leaching.

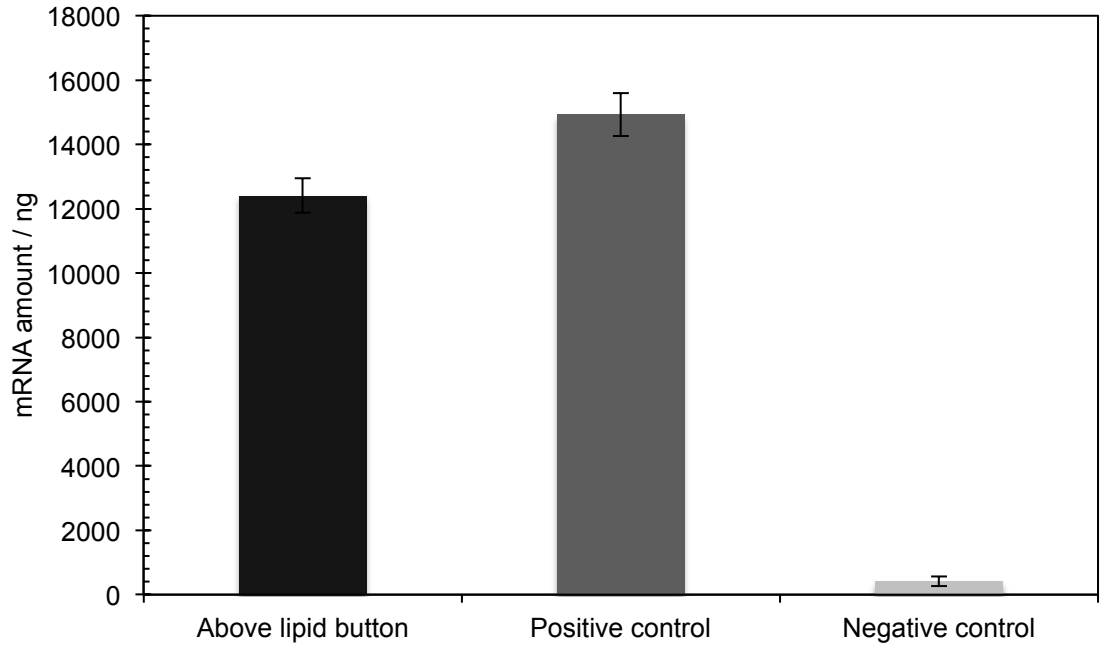

Figure 4.23 The effect of cationic lipid addition to a DOPE H_{II} phase (DOPE95:DOTAP5) upon transcriptional yields from transcription in supernatant solution above the phase, compared to a positive and negative control. RW/6456/01

Figure 4.23 shows that cationic lipid addition to H_{II} phase lipid buttons, of primarily DOPE composition (DOPE95:DOTAP5), caused an average reduction in the transcriptional yield of 16.9% compared to a positive control transcription assay performed in the absence of a H_{II} phase lipid. The presence of cationic lipid within the H_{II}-phase lipid buttons, although causing a slight reduction in transcriptional activity, did not significantly inhibit transcription. Transcription assay incubations were performed for 2 h at 37 ˚C; it is expected that within this timeframe, a small amount of linear *ds*DNA contained initially within the supernatant solution started to partition within the H_{II} phase, reducing the availability of template *ds*DNA for transcription in solution, hence reducing the transcriptional yield observed from above the DOPE95:DOTAP5 lipid buttons.

The observed transcriptional activity in solution above DOPE95:DOTAP5 H_{II} phases indicated the suitability of these composite lipid buttons for multiple-cycle batch transcription, the results of which are shown in Figure 4.24.

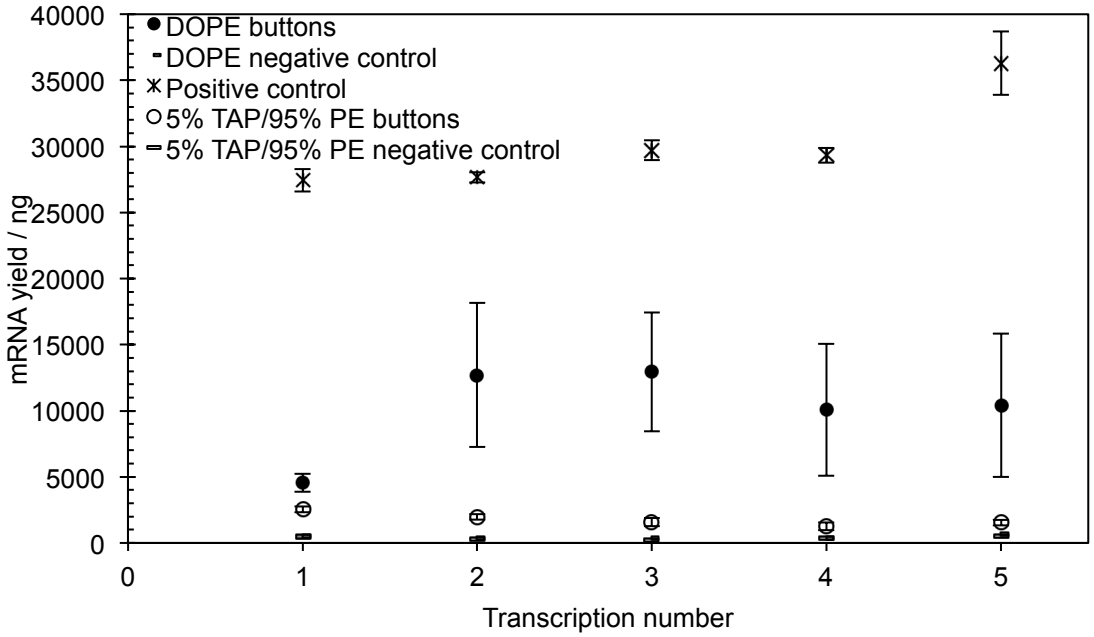

Figure 4.24 Transcriptional yields from multiple-cycle batch transcription from DOPE95:DOTAP5 (hollow circles) and DOPE (black circles) lipid buttons preloaded with 1 µg linear *ds*DNA, prepared by 100 h incubation (37˚C) with transcription buffer and 25 mM $MgCl_2$. Data are compared to transcriptional yields from positive control solution-based transcription assays for each batch transcription. Individual transcription assay incubations were for 2 h (37 ˚C). RW/6456/02

Multiple-cycle batch transcription was performed for 5 subsequent batch transcriptions using DOPE95:DOTAP5 and DOPE H_{II} phases containing 1 µg linear *ds*DNA (Figure 4.24); during none of the batch transcription cycles did the DOTAP-supplemented H_{II}

phases show significant transcriptional activity, whilst transcriptional activity was observed from the DOPE only H_{II} phases. It seems likely that the very reason for doping DOPE H_{II} phases with cationic DOTAP, the provision of additional positive charges within the phase to minimize leaching of *ds*DNA, was also the reason for inhibition of transcription activity. With an abundance of positive charges within the H_{II} phase of DOPE95/DOTAP5 lipid buttons, the linear *ds*DNA contained within would be more strongly associated with the phase pores than for DOPE lipid buttons. With previous results in this chapter describing how observed transcription yields appear to be resultant from *ds*DNA leached from within the phase alone, it suggests that T7RNA polymerase is unable to transcribe *ds*DNA whilst it is contained within the pores of H_{II} phases.

The lack of transcriptional activity observed from DOPE95:DOTAP5 lipid buttons preloaded with 1µg linear *ds*DNA under multiple-cycle batch transcription conditions meant that further alternative modifications to the system's lipid phase or incubation conditions were required.

4.5.5 Viability of monoolein-based lipid buttons

With multiple-cycle batch transcription from DNA-containing DOPE H_{II} phases doped with the cationic lipid DOTAP not offering a viable alternative to pure DOPE H_{II} phases, investigations were undertaken into the possibility of using the unsaturated monoglyceride monoolein (Figure 4.25) to produce phases capable of both containing linear *ds*DNA (to a comparable level of partitioning as was previously achieved with pure DOPE) and allowing multiple-cycle batch transcription under the same assay conditions.

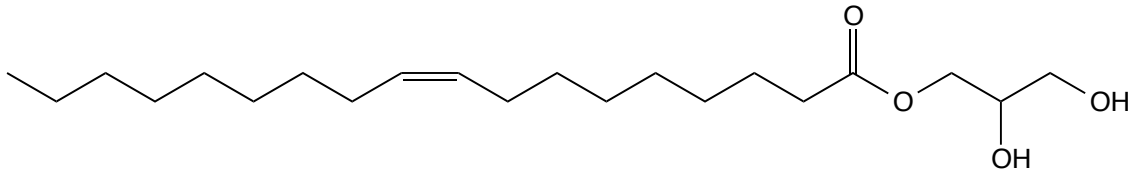

Figure 4.25 Structure of the unsaturated monoglyceride monoolein (MO).

The reported use of monoolein within biological applications, such as for drug delivery and protein crystallization, has seen a large increase during the last few decades[10]. Of particular relevance to this research, are the publications detailing how bicontinuous cubic phases of monoolein can be used for the controlled release of nuclear DNA [11] or have biological molecules, such as cytochrome-c [12], α-chymotripsin [13], or insulin [14], incorporated into them. It therefore seemed logical that investigations into the use of

monoolein for DNA compartmentalization for the purpose of multiple-cycle batch transcription seemed a logical next-step in the attempt to improve the aforementioned batch transcription system.

4.5.5.1 DNA partitioning into monoolein-based buttons

With the intended use of monoolein bicontinuous cubic phases for multiple-cycle batch transcription, SAXS analysis was performed to compare the lattice parameters and phase structures of monoolein under incubation conditions relevant to this research (Figure 4.26).

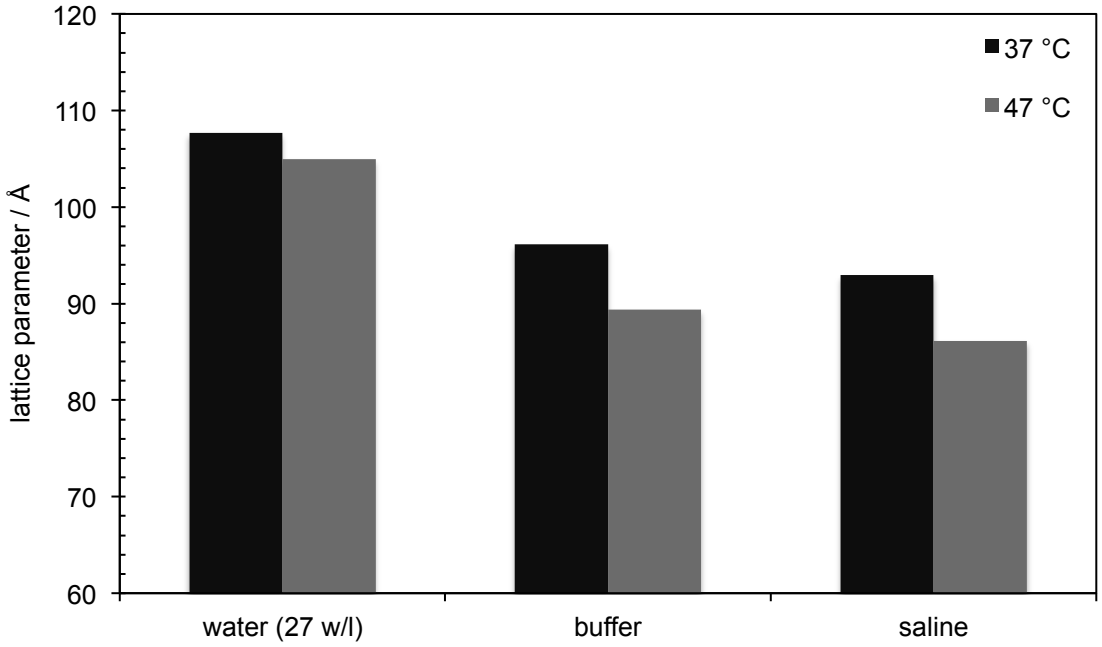

Figure 4.26 A comparison of the lattice parameter for monoolein under differing ionic conditions (27 waters per lipid, transcription buffer, isotonic saline) at 37 ˚C (black bars) and 47 ˚C (grey bars). Monoolein exhibits Ia$\bar{3}$d phase structure under 27 waters per lipid conditions and Pn$\bar{3}$m phase structure under transcription buffer or isotonic saline conditions. MAX-lab data, February 2012.

SAXS analysis of monoolein confirmed that under conditions of 27 waters per lipid, it exhibited Ia$\bar{3}$d phase structure, whilst under conditions of transcription buffer or isotonic saline, it exhibited a Pn$\bar{3}$m phase structure; a reduction in the lattice parameters for all incubation conditions was observed when increasing the incubation from 37 ˚C to 47 ˚C. When comparing the lattice parameters observed for monoolein under all incubation conditions investigated (Figure 4.26) to the smaller lattice parameter of 71.79 Å for DOPE under isotonic saline conditions at 37 ˚C, it was expected that the Pn$\bar{3}$m cubic structure of monoolein (observed under increased ionic

conditions) should be capable of containing linear *ds*DNA as had been observed with H_{II}-phase DOPE.

However, during attempts to incubate preformed monoolein phases with 1 µg of linear *ds*DNA, under homogeneous incubation conditions to that of the DOPE H_{II} phase preparations, it became clear that pure monoolein was unsuitable for numerous reasons. When preparing the preformed phases, it was particularly difficult to produce consistently sized and shaped phases, which would have created significant disparities in the *ds*DNA compartmentalization abilities of individual monoolein phases, and it was often troublesome to successfully remove the chloroform solvent without significant loss of monoolein.

In an attempt to produce more stable and comparable monoolein-based phases, monoolein was doped with either the zwitterionic lipid DOPE or cationic lipid DOTAP. Again, SAXS analysis was performed and a comparison made between the phase structures and lattice parameters of DOPE, monoolein and composite MO:DOTAP and MO:DOPE phases, under transcription buffer and salmon sperm *ds*DNA conditions at 37 ˚C (Figure 4.27). Compositions of MO:DOTAP (60:40) and MO:DOPE (70:30) were identified as potential candidates for *ds*DNA partitioning investigations, as they produced the most distinct $Pn\bar{3}m$ and H_{II} phases, respectively. With some compositions producing suspected biphasic structures, they would have been unsuitable for *ds*DNA partitioning investigations as the level of *ds*DNA partitioning observed would have likely been affected by the proportion and physical location of each phase within an individual preformed lipid button. X-ray diffraction data for these observations can be found in section 4.7.2, Annex 2.

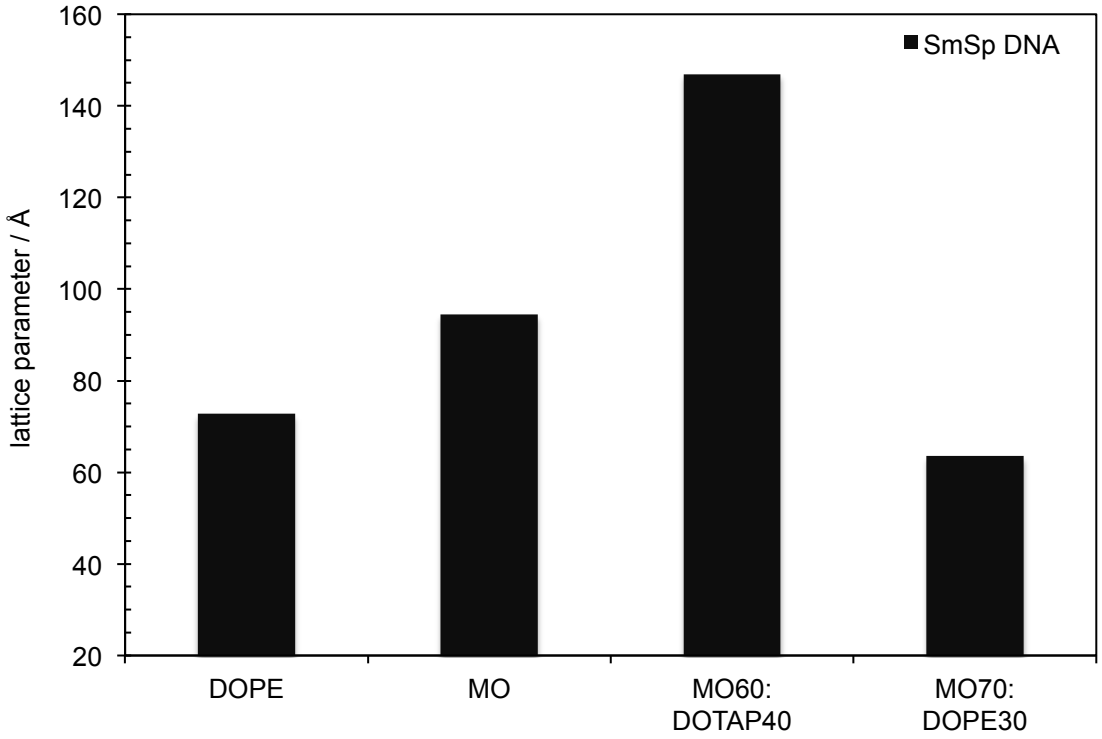

Figure 4.27 A comparison of the lattice parameters of DOPE, monoolein, monoolein:DOTAP (60:40) and monoolein:DOPE (70:30) when containing salmon sperm *ds*DNA at 37 °C. MAX-lab data, February 2012.

Composite lipid buttons of monoolein:DOTAP (60:40) and monoolein:DOPE (70:30) were successfully produced using the same fabrication method as per DOPE H_{II}-phase lipid buttons. Incubations with 1 µg of linearized *ds*DNA, transcription buffer, across a concentration gradient of $MgCl_2$, were performed for 100 hours (as per previous investigations for DOPE H_{II} phases). The amount of *ds*DNA left in the aqueous incubation supernatant, post-incubation, was analyzed using DNA gel electrophoresis and the partitioning coefficient, K_p, calculated (Figure 4.28).

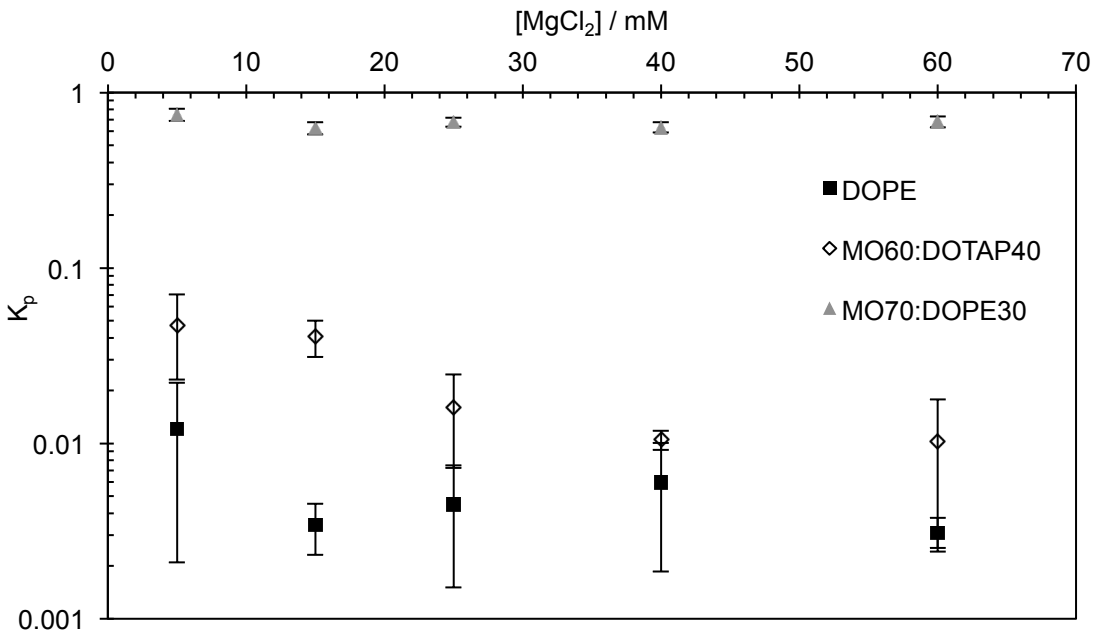

Figure 4.28 The effect of $MgCl_2$ concentration upon the partitioning of 1 µg linear *ds*DNA into DOPE (black squares), MO60:DOTAP40 (hollow diamonds), and MO70:DOPE30 (grey triangles), when incubating with full transcription buffer for 100 hours (37 °C). The benchmark for comparison is the K_p data for DOPE H_{II} (black squares). RW/6511/04

The levels of *ds*DNA partitioning observed for the composite monoolein:DOTAP (60:40) and monoolein:DOPE (70:30) 'lipid buttons' differed significantly to those that had been achieved using DOPE H_{II} phases, for both monoolein compositions. Whilst MO60:DOTAP40 phases enabled partitioning of *ds*DNA into the phase, this was lower, at all concentrations of $MgCl_2$, than the comparable DOPE H_{II} phases. At the standard incubation conditions, with 25 mM $MgCl_2$, MO60:DOTAP40 had an average K_p value of 0.016, compared to DOPE which had an average K_p value of 0.005. Whilst it was encouraging that the observed $Pn\bar{3}m$ phase of MO60:DOTAP40 was capable of *ds*DNA containment, it was most disappointing that it wasn't able to match, or indeed exceed, the level of partitioning previously achieved with DOPE alone. *ds*DNA partitioning results for MO70:DOPE30 were surprising; whilst SAXS analysis had shown the phase structure was inverse hexagonal (H_{II}), the phase did not allow significant levels of *ds*DNA partitioning into it – at the standard incubation conditions, with 25 mM $MgCl_2$, MO70:DOPE30 has an average K_p value of 0.679, compared to the average K_p for DOPE of 0.005. A K_p value of 0.679 for MO70:DOPE30 equates to 32.1% of the linear *ds*DNA partitioning into the phase; this is broadly equivalent to the 30% DOPE composition of the MO70:DOPE30 lipid buttons, suggesting that potentially *ds*DNA has partitioned only into the available DOPE, and not into the monoolein present. With the observed disappointing *ds*DNA partitioning for monoolein-based composites, investigations were not continued into monoolein-based multiple-cycle batch transcription.

4.5.6 Substitution of Mg^{2+} for alternative cations

The results presented in section 4.5.3, from the investigation into the effect upon multiple-cycle batch transcription of increasing $MgCl_2$ incubation and transcription assay concentrations highlighted the sensitivity of the system towards ionic concentrations. When $MgCl_2$ concentrations were increased from 25 to 40 mM, *ds*DNA-containing DOPE H_{II} phases become transcriptionally inactive, yet partitioning of *ds*DNA into the H_{II} phase increased (thus K_p was reduced). Further modifications of the incubation and transcription assay ionic conditions were investigated through the substitution of Mg^{2+} for alternative di, tri- and tetra-valent cations. This investigation had two primary objectives; the impact of alternative cations upon *ds*DNA partitioning into DOPE H_{II} phases, and the effect of alternative cation presence upon transcription yields.

Although *ds*DNA partitioning into H_{II} phases has not been attempted previously using divalent cations other than Mg^{2+}, there are examples in the literature describing the successful use of alternative divalent cations in transcription systems [15] and the beneficial supplementation of transcription systems with monovalent cations, such as K^+, Cs^+ and Na^+ [16].

4.5.6.1 DNA partitioning using alternative di-, tri- and tetra-valent cations

Partitioning of *ds*DNA using alternative cations was investigated in the first instance using the group 2 metal cations Ca^{2+} and Ba^{2+}, and the transition metal cation Mn^{2+}. Group 2 metal cations were selected due to the expectation that they were most likely to have a similar effect upon *ds*DNA partitioning as had been observed with Mg^{2+}, whilst Mn^{2+} was also trialed on the basis that it had been reportedly used to support transcription instead of Mg^{2+} in *in vitro* transcription assays.[17]

The effect of alternative divalent cations, at 25 mM concentration, upon the partitioning of 1 µg linear *ds*DNA into pre-formed DOPE H_{II} phases was negligible (Figure 4.29). Any of Mg^{2+}, Ca^{2+}, Mn^{2+} or Ba^{2+} ensured sufficient partitioning of *ds*DNA into the H_{II} phase, such that the partition coefficient, K_p, was lower than 0.005 after incubation for 100 h (37 °C) in the presence of transcription buffer, which was the benchmark value for K_p achieved during previous *ds*DNA partitioning experiments. Within experimental error, all of the divalent cations trialed offered comparable partition coefficients, allowing the decision about the divalent cation of choice to use

for the partitioning of *ds*DNA into H_{II} phases to be made upon the basis of which cation was most compatible with the transcription system.

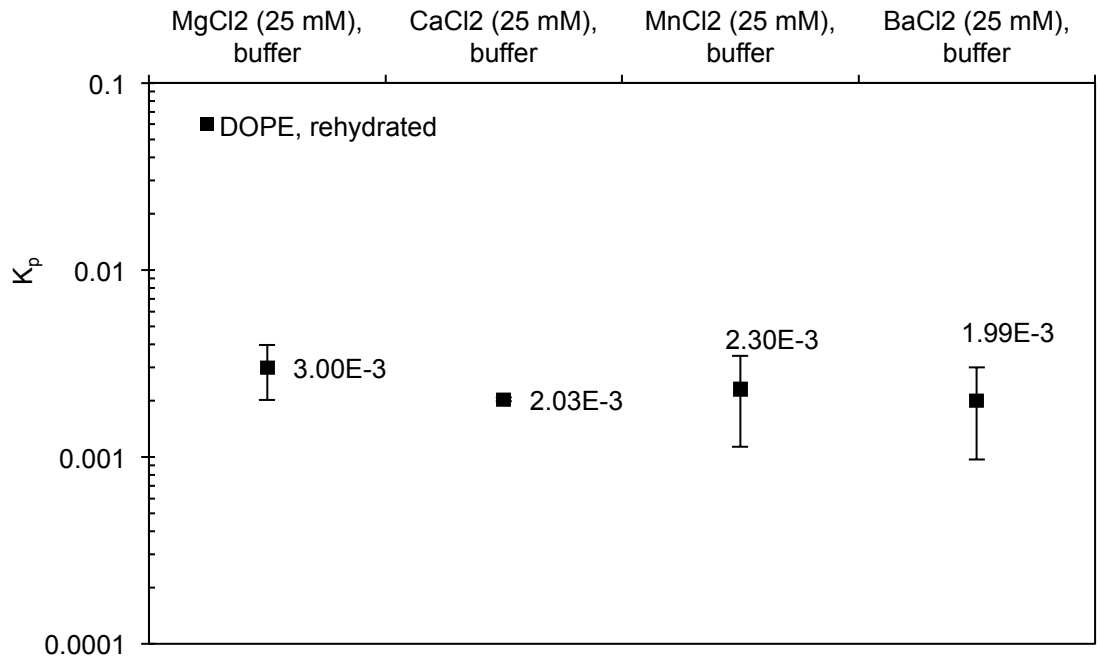

Figure 4.29 The effect of alternative divalent cations (25 mM) upon the partitioning of 1 µg linear *ds*DNA into DOPE H_{II} phases (black squares), when incubating with transcription buffer for 100 hours (37 °C). The benchmark for comparison is the K_p data for DOPE incubated with 25 mM $MgCl_2$ and transcription buffer ($K_p = 3.00 \times 10^{-3}$). RW/6511/07

To supplement the results observed in Figure 4.29, for alternative divalent cations, a comparison was made into the effect that increasing cationic charge had upon *ds*DNA partitioning, by substituting 25 mM $MgCl_2$ for either 25 mM hexamminecobalt (III) chloride or 2.5 mM spermine (IV) tetrachloride (Figure 4.30). Concentrations of 25 mM for Co^{3+} and 2.5 mM for $spermine^{4+}$ were chosen so that results would be comparable for the existing partition coefficient data, presented in Chapter 3, for 25 mM Mg^{2+} and 2.5 mM $spermidine^{3+}$, both of which are standard components within the transcription assay compositions used in this research.

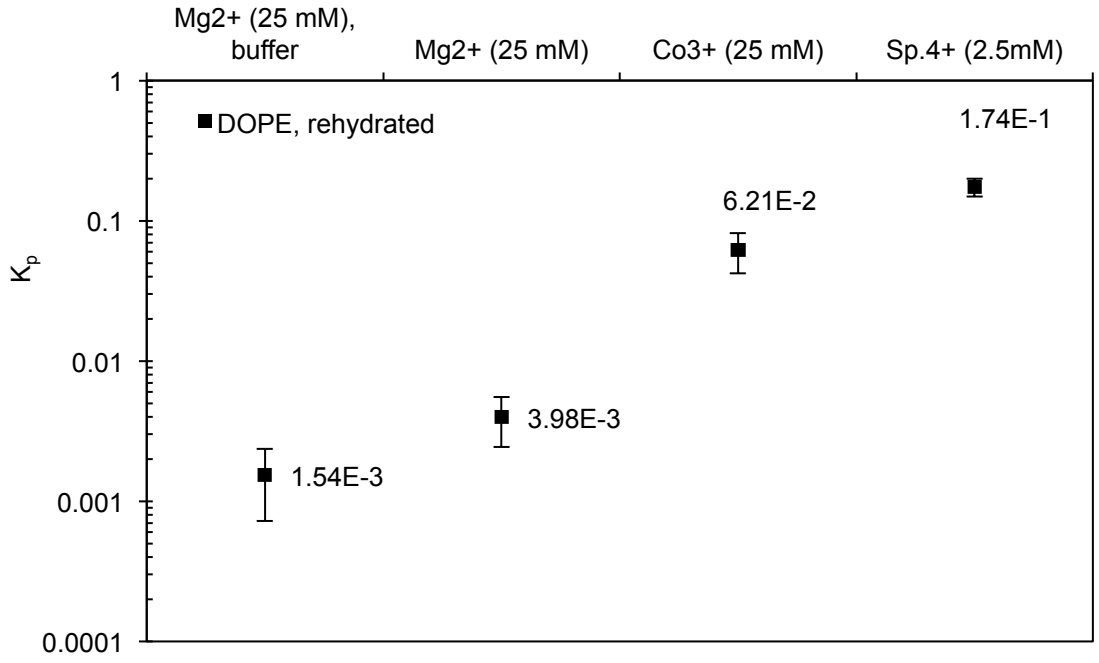

Figure 4.30 The effect of a tri-valent (Co^{3+}, 25 mM) and tetra-valent (spermine^{4+}, 2.5 mM) cations upon the partitioning of 1 µg linear *ds*DNA into DOPE H_{II} phases (black squares), when incubating for 100 hours (37 ˚C). The benchmark for comparison is the K_p data for DOPE incubated with 25 mM $MgCl_2$ and transcription buffer (K_p = 1.54 x 10^{-3}). RW/6511/27

Increasing the positive charge on cationic species present during the 100 h incubation of linear *ds*DNA in the presence of DOPE H_{II} phases had a negative effect upon the amount of *ds*DNA that partitioned into the H_{II} phase (K_p increased). The partition coefficient for 25 mM Mg^{2+} was 3.98 x 10^{-3}, with K_p reduced to 6.21 x 10^{-2} for 25 mM Co^{3+}. This compares to the partition coefficient for 2.5 mM spermidine^{3+} of 2.07 x 10^{-2}, with K_p reduced to 1.74 x 10^{-1} for spermine^{4+}. In both cases, a significant reduction in the level of partitioning of linear *ds*DNA into the H_{II} phase is observed when divalent cations are replaced by trivalent cations, and trivalent cations are replaced by tetravalent cations.

It was therefore clear that the use of divalent cations was optimal for the partitioning of *ds*DNA into DOPE H_{II} phases, in the presence of transcription buffer over 100 h incubation periods (37 ˚C).

4.5.6.2 Transcription using alternative divalent cations

Of crucial importance to this research was the ability of DOPE H_{II} phases to be transcriptionally active for multiple-cycle batch transcription; with partitioning of *ds*DNA using alternative divalent cations occurring to a comparable extent to that achieved when using $MgCl_2$, assessment of the transcriptional viability of *ds*DNA-

containing H_{II} phases prepared using these alternative divalent cations was important. Solution-based transcription assays were, therefore, set up that either omitted 25 mM $MgCl_2$ in favour of 25 mM of an alternative divalent cation (Figure 4.31), or were supplemented with 25 mM of alternative divalent cation in addition to the 25 mM $MgCl_2$ typically present in a transcription assay (Figure 4.32).

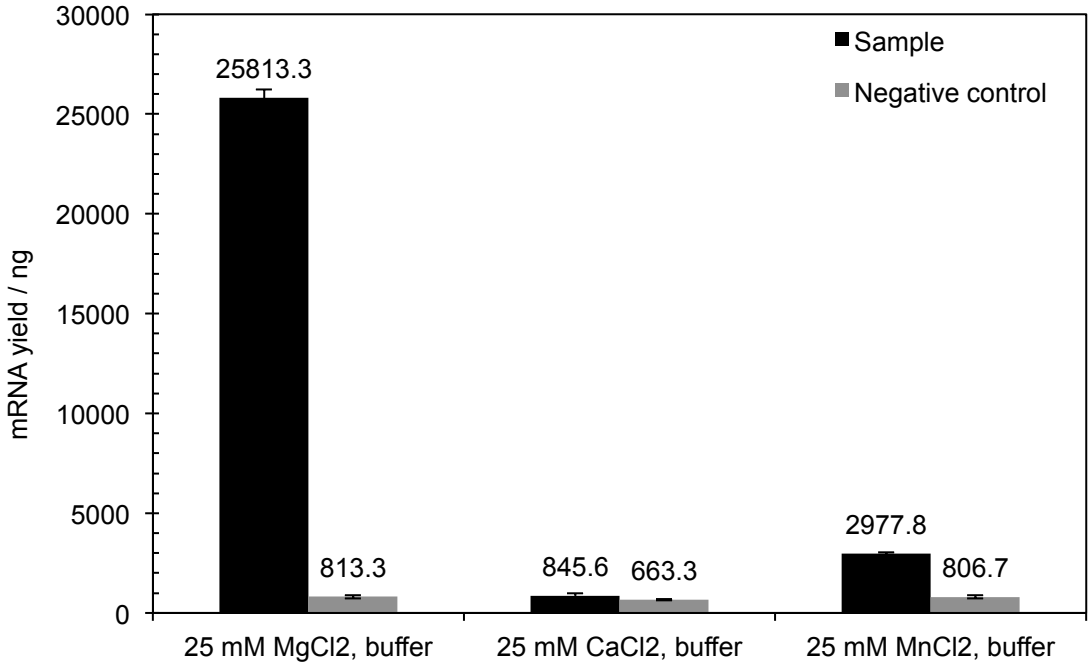

Figure 4.31 The effect of substitution of Mg^{2+} for alternative upon transcriptional yields from transcription in solution, compared to their respective negative controls. Results are not shown for 25 mM $BaCl_2$ due to precipitation within the transcription assay solution. Transcription assays were incubated for 2 h (37 ˚C). RW/6511/07

Solution-based transcription assays were performed where 25 mM $MgCl_2$ was substituted for the same concentration of $CaCl_2$, $MnCl_2$ or $BaCl_2$ (Figure 4.31). Transcriptional yields from 25 mM $BaCl_2$ assays were not quantified due to precipitation occurring within the transcription assay solution prior to RNA purification. It is apparent that the presence of alternative divalent cations within the transcription assay had a profound negative effect upon the transcriptional yield; Ca^{2+} inhibited transcription, with mRNA yields comparable to the negative controls assays run, whilst Mn^{2+} significantly reduced the yield of mRNA to 11.5% of the yield achieved when Mg^{2+} is present in solution. To further understand the cause of the negative impact upon transcriptional activity, transcription assays were run where 25 mM of either Ca^{2+} or Mn^{2+} was supplementary to 25 mM Mg^{2+}. This offered an insight into which divalent cation was likely preferentially interacting in the transcription process; if Mg^{2+} were preferentially interacting, then transcriptional activity should be retained; if either Ca^{2+}

or Mn^{2+} were preferentially interacting, then transcriptional activity should be reduced to levels comparable to those presented in Figure 4.31.

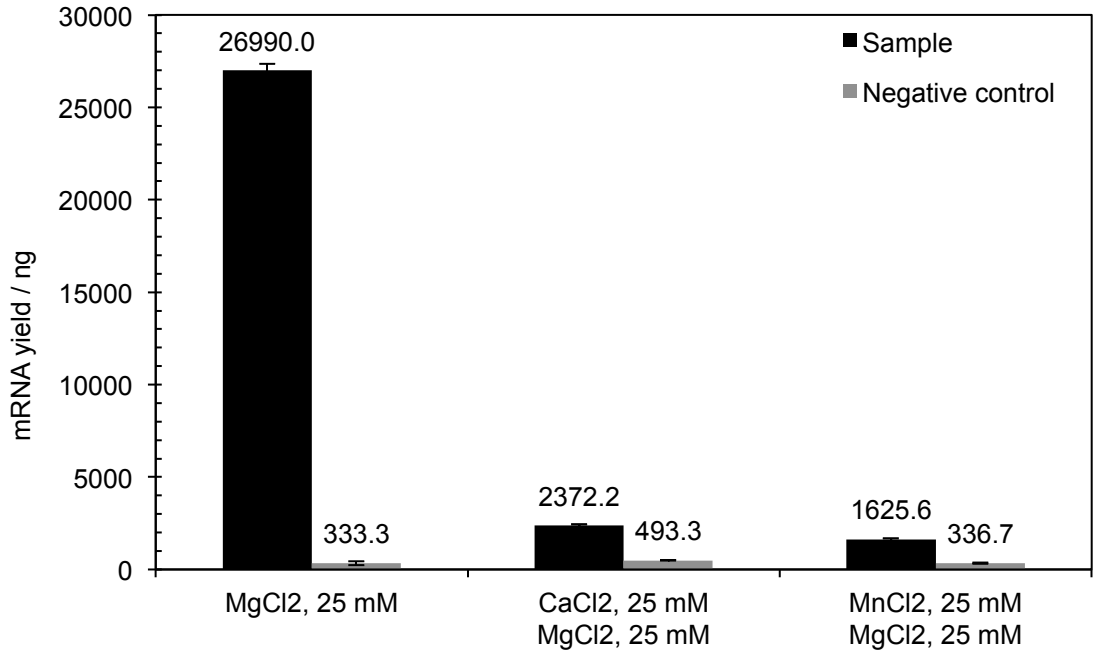

Figure 4.32 The effect of supplementation of 25 mM Mg^{2+} with 25 mM Ca^{2+} or Mn^{2+} upon transcriptional yields from transcription in solution, compared to their respective negative controls. Transcription assays were incubated for 2 h (37 °C). RW/6511/19

Figure 4.32 shows the mRNA yields achieved when 25 mM $MgCl_2$ was supplemented with an additional 25 mM of either $CaCl_2$ or $MnCl_2$ during solution-based transcription assays. These supplemented transcription assays could be described in two distinct ways; firstly, that they contain two distinct sets of 25 mM divalent cations, and secondly, that they contain an overall concentration of 50 mM divalent cations. Results presented in Chapter 3 discuss the effect of Mg^{2+} concentration upon transcriptional yields; for 25 mM Mg^{2+} an average yield of 26.7 µg RNA is obtained, whilst for 50 mM Mg^{2+} an average yield of 31.5 µg is achieved. It is evident that a concentration of 50 mM of divalent cations in itself isn't inhibitory in its effect upon transcriptional yields, thus the reduction in transcriptional yields from supplementation of transcription assays with addition of 25 mM alternative divalent cations is due to the presence of the secondary divalent cations alone. Transcriptional yields for both 25 mM Ca^{2+} and 25 mM Mn^{2+} supplementation were 8.8% and 6.0%, respectively, of the yield achieved for a standard 25 mM Mg^{2+} transcription. These results imply that the transcription system utilized in this research preferentially associates with the alternative divalent cations present in solution over Mg^{2+} cations, with a reduction in transcriptional activity greater than 90%.

Whilst the successful partitioning of *ds*DNA into DOPE H_{II} phases using alternative divalent cations, and to a lesser extent tri- and tetra-valent cations, was an interesting discovery, the stark reduction observed in transcriptional activity in the presence of alternative divalent cations meant that DOPE H_{II} phases prepared using these modified incubation solutions would have been unsuitable for multiple-cycle batch transcription.

4.5.7 Addition of trehalose to the transcription assay

With neither the modifications to the DNA-containing phase composition or the incubation and transcription assay cation concentrations offering a viable method for batch transcription that subjugated the previously observed leaching of *ds*DNA from the phase used for containment, addition of the molecular crowding agent trehalose to the batch transcription assay was investigated. Trehalose has been commonly used as a crowding agent in biological systems in an attempt to maximize desired product yields from solution-based assays, due to the effect of crowding agents in concentrating the remaining assay components, or to stabilize protein structures.[18,19] The presence of molecular crowding agents within the transcription assay supernatant solution should also reduce any entropic gains *ds*DNA molecules previously experienced when leaching from within the liquid crystalline phase.

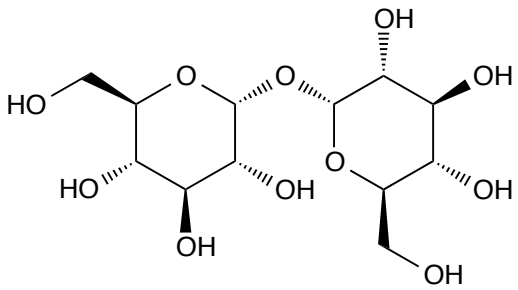

Figure 4.33 Structure of the disaccharide trehalose, a common molecular crowding agent in biological systems.

Macromolecules, and thus molecules acting as molecular crowding agents, are present in the interior of all cells, estimated to be typically between 20-30% of the total cell volume.[19,20] Whilst Ellis (2001) describes how molecular crowding had oft been neglected during *in vitro* studies of biological systems, there are now increasing numbers of publications reporting the use of molecular crowding agents with positive effect for *in vitro* transcription-translation applications.[21–23]

There were three primary incentives to introducing trehalose into the batch transcription assay: the presence of large transcription assay molecules (e.g. T7 RNA polymerase); a potential increase in the observed RNA yields per batch transcription

due to concentration of assay components; prevention or slowing of *ds*DNA leaching from within the DOPE H_{II} phase due to the reduced diffusion of molecules caused by increased molecular crowding in solution.[24]

Firstly, the introduction of trehalose, or indeed any molecular crowding agent, will reduce the volume of a solution that is physically available for other molecules to reside in; in this case, the transcription assay components and any *ds*DNA that could potentially leach from the DOPE H_{II} phase. Through reducing this available volume, large molecules such as T7 RNA polymerase will become concentrated and so potentially increasing the rate of transcription.

Secondly, Ge *et al.* (2011)[25] report that the addition of molecular crowding agents to a transcription assay with template *ds*DNA containing the T7 promoter enhanced the mRNA yield achieved when compared to a control dilute solution (with composition similar to the control transcription assays used within this research). It was reported that mRNA yields were increased 4-fold when using 20% w/v Ficoll-70 and 'dramatically' when using 0-5.4% w/v PEG-8000, offering hope that the addition of molecular crowding agents, in the form of 10% wt and 20% wt trehalose, to batch transcription reactions may also increase mRNA yields.

Finally, batch transcription from DNA-containing DOPE H_{II} phases was impeded by the leaching of *ds*DNA from the H_{II} phase; the introduction of trehalose to increase the level of molecular crowding would thus reduce the ability of molecules to diffuse within the transcription assay solution, including the ability of compartmentalized *ds*DNA to diffuse from within the phase and into the transcription assay solution layered above. If observed to be true experimentally, this phenomenon would have prolonged the transcriptionally active lifespan of a DNA-containing DOPE H_{II} phase.

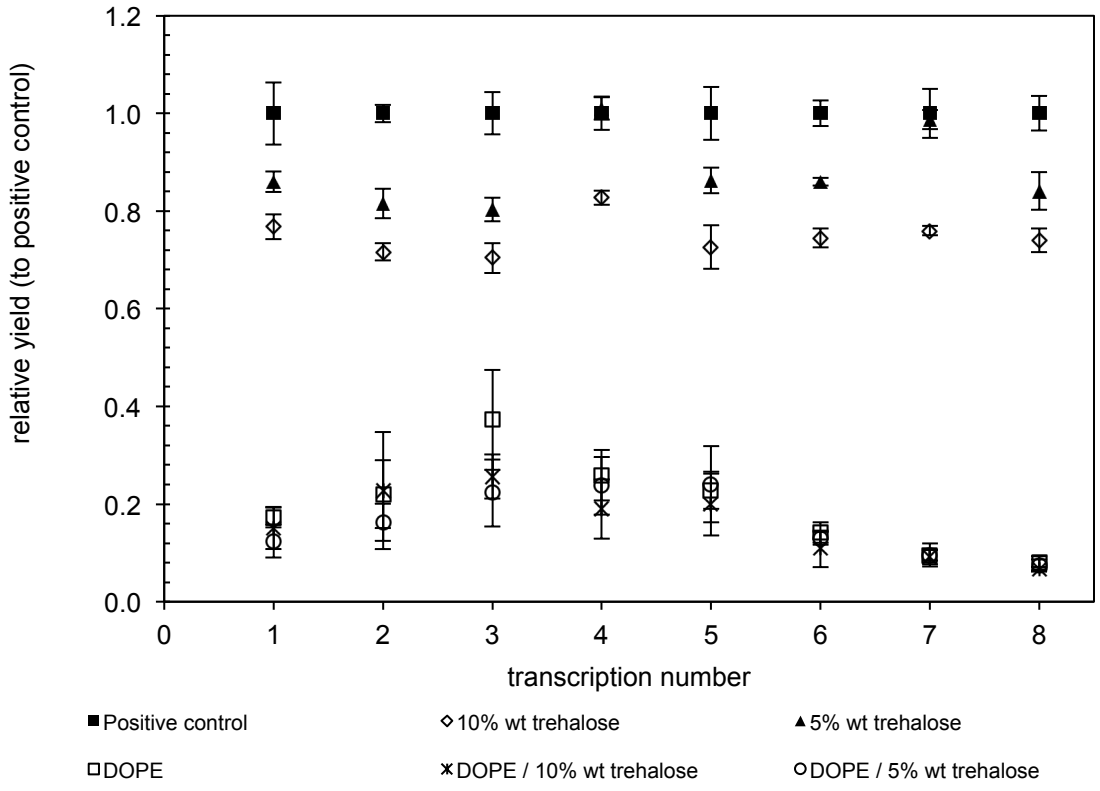

Figure 4.34 The effect of the addition of trehalose, acting as a molecular crowding agent, to multiple-cycle batch transcription from 1 µg *ds*DNA-containing DOPE H_{II} phases. Phases were incubated for 2 hours (37 °C) per transcription. Results are shown for non-crowded (hollow squares), 10% wt trehalose (black asterisks) and 5% wt trehalose (hollow circles) lipid-based batch transcription assays. mRNA yields were compared to non-crowded one-off positive control transcription assays (black squares) to calculate the relative mRNA yields. One-off positive control transcription assays for both 10% wt trehalose (hollow diamonds) and 5% wt trehalose (black triangles) were also performed. RW/6511/23

Figure 4.34 shows the results obtained from the batch transcription investigation into the addition of 10% wt and 5% wt trehalose as a molecular crowding agent. It is surprising to observe that, converse to the observations reported by Ge *et al.* (2011)[25] when using Ficoll-70, transcription yields were actually reduced for both 10% wt and 5% wt trehalose when compared to an uncrowded transcription assay. Comparison of the molecularly-crowded control transcription yields to the trehalose-free positive control yield identifies that 10% wt and 5% wt trehalose additions see reductions in the amount of mRNA produced per assay of typically 72-80% and 80-88% respectively. Whilst this would not be described as a 'dramatic' drop in transcriptional yields, it is reasonable to assume that the trehalose is inhibitory towards transcription in a similar way to the observations reported by Ge *et al.* (2011) when using 0-5.4% w/v PEG-8000.[25] The presence of 5% wt and 10% wt trehalose is likely to have significantly reduced the ability of the transcription assay components to diffuse throughout the solution. This is coherent with the observation that increasing from 5% wt to 10% wt

trehalose addition sees a further reduction in transcriptional activity from the one-off controls.

When observing the effect of trehalose addition upon the transcriptional yields obtained from multiple-cycle batch transcription, it is clear to see that neither 10% nor 5% wt trehalose have any significant benefit. Within experimental error, the transcriptional yields observed in Figure 4.34 for 0%, 5% and 10% wt trehalose are comparable. The presence of trehalose in batch transcription assays has, however, had a small effect in the reduction of the peak *ds*DNA leaching, and thus transcriptional activity, during the third batch transcription when compared to a trehalose-free assay. The slight reduction in peak *ds*DNA leaching, seen during batch transcription 3, supports the theory that the presence of trehalose is reducing the rate of diffusion of molecules in solution, causing *ds*DNA to be leached more slowly during the third batch transcription. It is possible that only a small reduction is observed as the presence of molecular crowding agents causing a reduction in the rate of diffusion had a more significant impact upon large structure macromolecules, such as T7RNA polymerase, rather than the comparatively linear *ds*DNA initially contained within the DOPE H_{II} phases.

Unsurprisingly, the cumulative mRNA yields, shown in Figure 4.35, confirm that the addition of trehalose to multiple-cycle batch transcription assays from DNA-containing DOPE H_{II} phases have no beneficial effect upon the system. By the eighth batch transcription, 0%, 5% and 10% lipid-based assays have all produced a comparable yield of mRNA, with the same trend followed. This observation contrasts with the one-off solution-based controls, which were 88% and 75% of the yield observed from the non-crowded control, for 5% and 10% wt trehalose, respectively. Therefore, the addition of trehalose as a molecular crowding agent at 5 and 10% wt concentrations was unsuccessful in both prolonging the active lifespan of the DNA-containing H_{II} phases and in achieving higher cumulative mRNA yields.

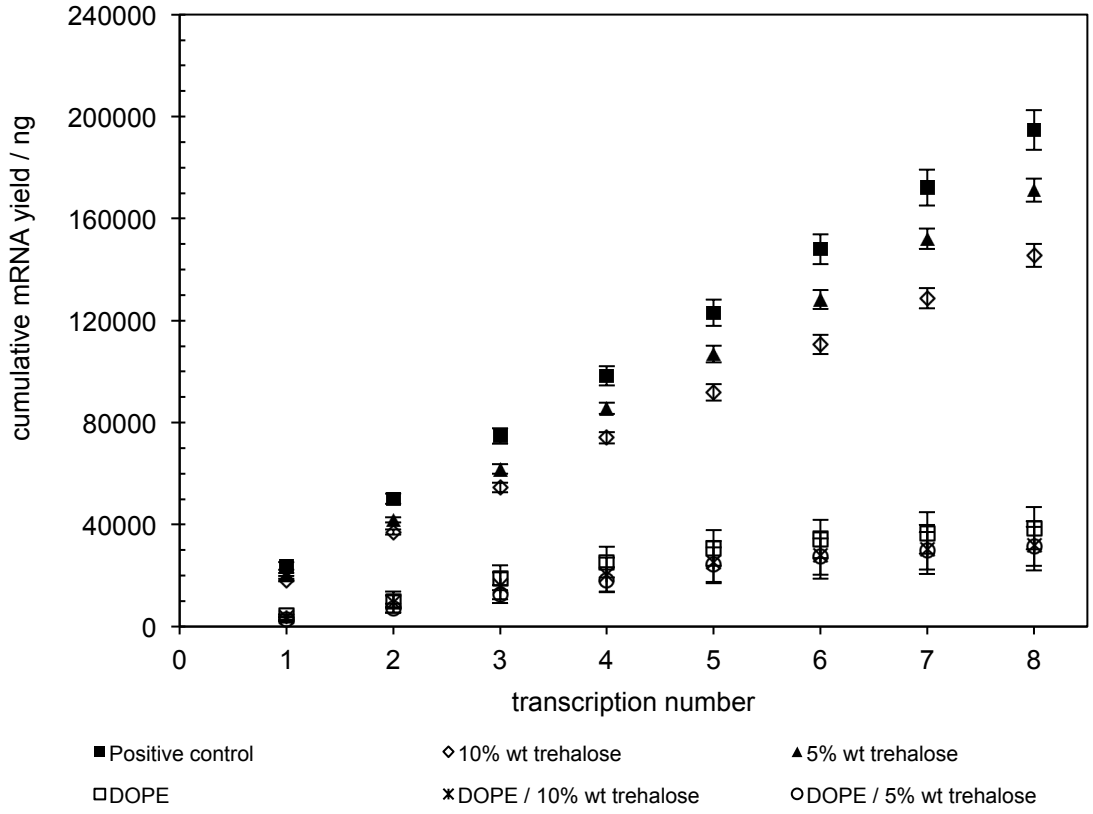

Figure 4.35 The effect of the addition of trehalose, acting as a molecular crowding agent, to the cumulative mRNA yield from multiple-cycle batch transcription from 1 µg *ds*DNA-containing DOPE H_{II} phases. Phases were incubated for 2 hours (37 °C) per transcription. Results are shown for non-crowded (hollow squares), 10% wt trehalose (black asterisks) and 5% wt trehalose (hollow circles) lipid-based batch transcription assays. One-off positive control transcription assays for non-crowded (black squares), 10% wt trehalose (hollow diamonds) and 5% wt trehalose (black triangles) were also performed. RW/6511/23

4.6 Discussion

It is evident from the literature, and experimental results detailed herein, that DOPE H_{II} phases are suitable vessels for linear *ds*DNA containment, due to the spontaneous partitioning of linear *ds*DNA into the phase.[2,3] Conversely, *ss*RNA molecules preferentially reside in isotropic solution above the phase, for example in a transcription assay reaction solution, with only a small proportion of *ss*RNA associating with the surface of the H_{II} phase, forming an accretion layer tens of molecules thick.[1] The *ds*DNA and *ss*RNA partitioning properties of DOPE H_{II} phases supported their use as ideal candidates for template *ds*DNA vessels for sustained batch or continuous-flow transcription by RNA polymerase. It was expected that linear *ds*DNA would remain associated with the DOPE H_{II} phase, remaining transcriptionally active for sustained or subsequent transcriptions, whilst transcribed *ss*RNA would preferentially reside in solution, making it easily extracted from the system for purification.

When investigating the suitability of these DNA-containing H_{II} phases for the sustained provision of template *ds*DNA required for batch transcription, the results detailed in this chapter have shown that these phases are unsuitable for sustaining batch transcription over prolonged time periods due to the leaching of linear *ds*DNA from the phases with subsequent transcriptions. Whilst it was possible to transcribe from the phases' contained *ds*DNA using T7 RNA polymerase, the mRNA yields peaked and soon began to subside, with linear *ds*DNA visible upon the DNA gel analysis performed for each batch transcription. Upon analysis of the DNA gels, the levels of transcription observed from DNA-containing DOPE H_{II} phases are likely due to the amount of linear *ds*DNA that has leached from the phase into the transcription assay solution residing above the phase surface during transcription. A comparison between the calculated amounts of template *ds*DNA required to produce the observed yields of mRNA per transcription reaction to the quantified amount of leached *ds*DNA (visible by DNA gel electrophoresis) was made. This identified that, for DOPE H_{II} phases containing 1 µg of linear *ds*DNA, the observed amounts of leached *ds*DNA from DNA gel electrophoresis were equal, within experimental error, to the calculated amounts of template *ds*DNA required to produce the observed mRNA yields. When increasing the amount of contained linear *ds*DNA to 10 µg, the observed amount of leached *ds*DNA are between 25% and 38% lower than the calculated amounts of template *ds*DNA required. However, it is clear from the experimental observations that, although a minority of batch transcription activity may be from *ds*DNA associated with the DOPE H_{II} phase, the majority of batch transcription can be attributed to the presence of leached *ds*DNA in solution.

Efforts to subjugate the issue of template *ds*DNA leaching from DOPE H_{II} phases during batch transcription through modification of the lipid phase or incubation conditions highlighted the sensitivity of the system to these parameters.

Magnesium chloride concentrations were increased, from 25 mM to 40 mM, for both the partitioning of linear *ds*DNA into DOPE H_{II} phases and for the subsequent batch transcriptions; experimental results detailed in Chapters 2 and 3 show that a concentration of 40 mM $MgCl_2$ improves mRNA yields from solution-based transcription assays and also does not significantly reduce the rate of *ds*DNA partitioning when compared to the previous incubation conditions (25 mM $MgCl_2$). However, when subjected to batch transcription testing, DNA-containing DOPE H_{II} phases prepared using 40 mM $MgCl_2$ incubation and transcription assay conditions produced negligible mRNA yields, both for phases containing 1 µg and 10 µg linear *ds*DNA. It was therefore evident that increased levels of magnesium chloride in the system have a debilitating effect upon batch transcriptional activity.

Modifications to the H_{II} phase were then trialled in a secondary attempt to conquer the dilemma of *ds*DNA leaching; these phase modifications included the doping of DOPE with a small quantity of the cationic lipid DOTAP, and the production of monoolein-based buttons that were doped with either DOPE or DOTAP. DOPE95:DOTAP5, MO60/DOTAP40 and MO70/DOPE30 were produced and confirmed by SAXS analysis to be H_{II} inverse hexagonal, $Pn\bar{3}m$ cubic and H_{II} inverse hexagonal phases, respectively. All three composite phases were subjected to linear *ds*DNA partitioning studies, with only DOPE95:DOTAP5 and MO60:DOTAP40 phases susceptible to significant *ds*DNA partitioning. Only DOPE95:DOTAP5 phases showed comparable levels of partitioning to pure DOPE H_{II} phases, thus they were the only composite phases to progress onto prolonged batch transcription analysis. With positive transcription controls performed above composite DOPE95/DOTAP5 H_{II} phases producing mRNA yields only 17% lower than an aqueous positive control, it was unexpected to observe that this composite phase almost completely inhibited batch transcription, failing to provide a viable alternative to DNA-containing DOPE H_{II} phases.

Substitution of 25 mM Mg^{2+} in the *ds*DNA incubation solution for alternative divalent cations (Ca^{2+}, Mn^{2+} and Ba^{2+}) showed that it was possible to achieve the same level of linear *ds*DNA partitioning into DOPE H_{II} phases as occurs with 25 mM Mg^{2+}. However, transcriptional activity was severely impaired when these alternative divalent cations were present in transcription assays, even when assays were additionally supplemented with 25 mM Mg^{2+} cations, thus making DNA-containing DOPE H_{II} phases prepared using alternative divalent cations unsuitable for batch transcription.

In a final attempt to subjugate the leaching of *ds*DNA from DOPE-containing H_{II} phases, trehalose addition in 5% wt and 10% wt was added to batch transcription assays to act as a crowding agent, in an attempt to reduce the amount of aforementioned *ds*DNA leaching. Whilst 5%wt and 10%wt trehalose addition had a negative effect upon positive control transcriptional yields, at typically 80-88% and 72-80% of the mRNA yield of a trehalose-free transcription assay, this would have been an acceptable trade-off had the presence of trehalose significantly prolonged the batch transcriptional activity of DNA-containing DOPE H_{II} phases. The presence of trehalose in batch transcription assays reduced the peak in *ds*DNA leaching, and thus transcriptional activity, during the third batch transcription when compared to a trehalose-free assay, however it has no appreciable effect in prolonging the lifetime of the phase, with 0% wt, 5% wt and 10% wt trehalose batch transcription assays all producing comparable cumulative mRNA yields, within experimental error, by the eighth batch transcription.

Despite modifications being made to both the phase composition and *ds*DNA/phase incubation conditions, they bore no fruit in offering an alternative batch transcription system from which transcriptional activity was prolonged through reduction in the levels of *ds*DNA leached. By incubating linear *ds*DNA with transcription buffer containing 25 mM $MgCl_2$ for 100 hours at 37 ˚C in the presence of DOPE H_{II} phases, limited lifespan batch transcription can be performed allowing a cumulative yield of 33.9 ± 14.3 μg mRNA produced after eight batch transcriptions (16 hours total incubation at 37 ˚C) from a single DOPE H_{II} phase initially containing 1 μg template linear *ds*DNA. This compares to 24.7 ± 0.5 μg mRNA yield from a single transcription assay in solution, containing 1 μg of linear *ds*DNA (2 hour incubation at 37 ˚C).

Although the use of DNA-containing DOPE H_{II} phases have clear limitations with regard to their use for prolonged batch transcription, they do offer a method of template *ds*DNA delivery within a limited timeframe. Chapter 5 presents the research conducted into the possibility of a continuous-flow semi-biotic device based upon the concept of DNA-containing DOPE H_{II} phases.

4.7 Annex

4.7.1 Annex 1: Electrospray ionization mass spectrometry

4.7.1.1 University of Southampton facility: ESI-MS

Electrospray ionization mass spectrometry (ESI-MS) was performed in the School of Chemistry, at the University of Southampton, using a Micromass UK Quattro Ultima triple quadrupole mass spectrometer equipped with an electrospray ionization interface.

4.7.1.2 ESI-MS Sample preparation

DOPE lipid samples were dissolved in butanol:methanol:water:ammonia (conc.) (2:6:1.6:0.4) and introduced in to the mass spectrometer by syringe pump at a flow rate of 5 µL/min. Nitrogen was used as the cone and desolvation gas and argon as the collision gas (3.5×10^{-3} mbar). Data was acquired and processed using MassLynx NT software before being exported to Microsoft Excel for analysis.

The DOPE internal standard used for the ESI-MS reported in this chapter was prepared by Stephanie M. Tweed, at the University of Southampton.

4.7.1.3 Materials

DOPE (850725P) was supplied by Avanti Polar Lipids Inc., USA. HPLC grade butanol, methanol, ammonia (conc.) and water were provided by Fisher Scientific UK Ltd. Nitrogen and argon gases were provided by BOC Industrial Gases, UK.

4.7.2 Annex 2: Small-angle X-ray spectroscopy

4.7.2.1 MAX-lab facility: Beamline I911-4 (SAXS)

Small-angle X-ray spectroscopy was performed at the MAX-lab facility at Lund University, SE, using the I911-4 SAXS beamline. It is one of five stations using the I911 Cassiopeia beamline on the 1.5 GeV ring MAX II. The I911-4 beamline offers a predicted photon flux of $5x10^{10}$ photons / s across a sample spot size of 0.3 x 0.3 mm^2. Diffraction patterns were initially detected using a 165 mm marCCD X-ray detector but this was upgraded mid-2012 to a Dectris PILATUS 1M fast readout, low noise pixel detector.[26]

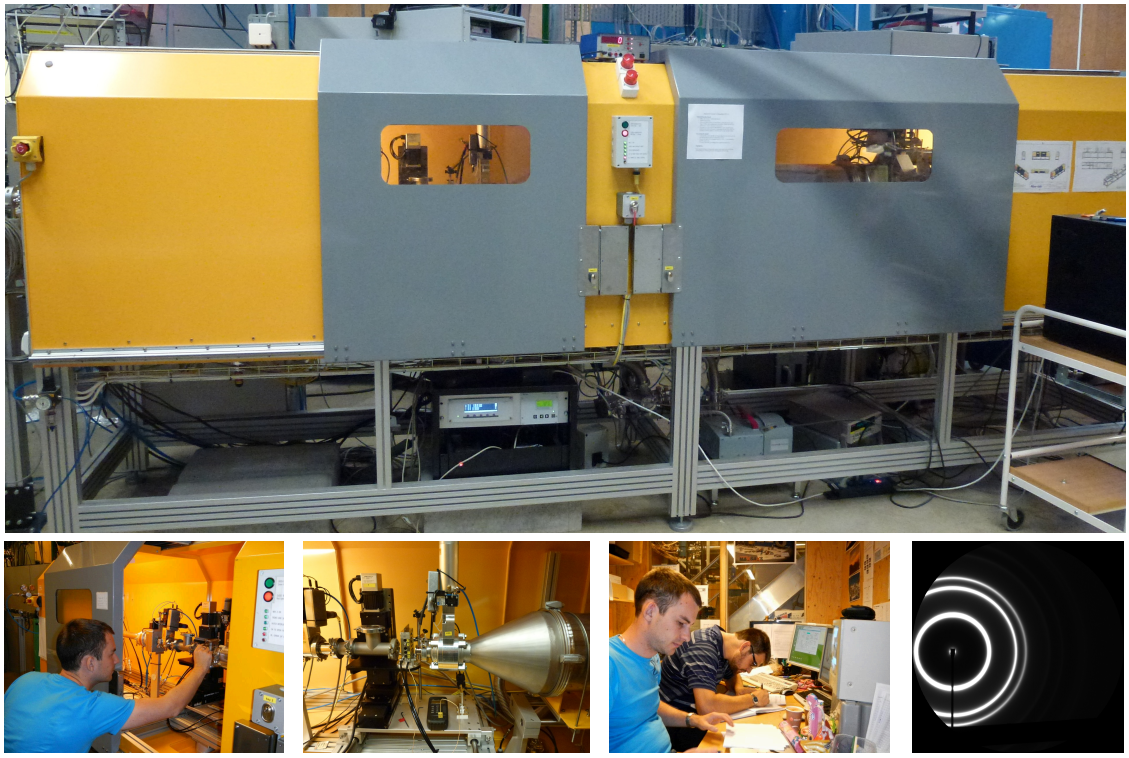

Figure 4.36 Top: The experimental hutch of beamline I911-4 at MAX-lab, SE. **Bottom left-right:** Samples carriers were loaded into the temperature-controlled sample holder; up to five samples could be loaded into the experimental hutch; diffraction patterns were recorded and analysed to identify the phase structure and lattice parameter; a diffraction pattern for H_{II} phase DOPE obtained using the I911-4 beamline at MAX-lab.

4.7.2.2 SAXS sample preparation

Lipid samples were sandwiched between 4 μm transparent X-ray film (Ultralene 3525, SPEX SamplePrep LLC, USA) and loaded into a sample carrier. Sample carriers were then mounted into a multiple-sample holding block that was temperature-controlled via an external waterbath. The temperature of the sample holder was additionally monitored by thermocouple, with block temperatures recorded alongside the SAXS diffraction

patterns. Samples were exposed to the X-ray beam for a specified exposure time, typically 60 s to minimize sample damage, with the diffraction pattern captured by either a bidimensional 165mm marCCD (February 2012) or a Dectris PILATUS 1M (September 2012) X-ray detector and recorded to a computer, before being integrated radially from the centre of the diffraction pattern to produce the characteristic peaks of a particular phase structure.

4.7.2.3 Materials

DOPE (850725P) and DOTAP (890890P) were supplied by Avanti Polar Lipids Inc., USA. Monoolein (31-1810) was supplied by Larodan Fine Chemicals AB, SE. rNTPs and T7RNA polymerase were provided by New England Biolabs Inc., USA. Biological-grade metal chloride salts, spermidine, spermine, DTT and salmon testes DNA (sodium salt) were provided by Sigma Aldrich Company LLC, USA. Whilst Sigma does not determine the molecular weight of their DNA from salmon testes (product D1626), there is a report of a salmon testes DNA (sodium salt) purchased from Sigma having an average molecular weight of 1.3 x 10^6 (ca. 2000 bp),[27] making it 1,600 bp shorter than the linearized pRSET-EmGFP *ds*DNA used in the transcription studies presented herein. Type 1 ultrapure, nuclease-free water was provided using a Barnstead Nanopure Life Science UV/UF water purification system.

4.7.2.4 Phase analysis

Lipid phases under incubation conditions of particular relevance to this research had their phase structure identified through comparison of their radial integration peaks to the expected Miller indices peak ratios for various phase structures, for example H_{II}, $Pn\bar{3}m$ and $Ia\bar{3}d$. Sample assignment diagrams are shown in Figures 4.37-4.39 (see Figure 4.40 for schematics for each of the identified phase structures).

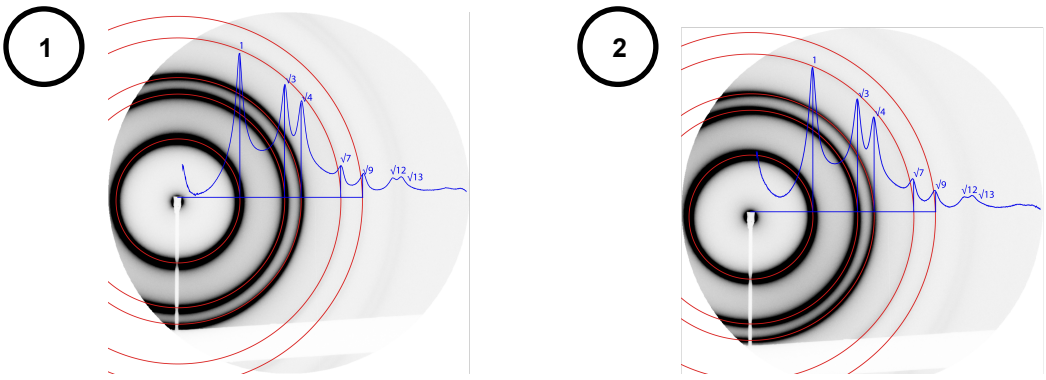

Figure 4.37 1) DOPE sample (H_{II} phase, a = 71.79 Å) under isotonic saline conditions, 37 ˚C; **2)** DOPE sample (H_{II} phase, a = 72.77 Å) premixed with salmon sperm *ds*DNA, 37 ˚C. MAX-lab data, February 2012.

Consistent with previously published data from Black *et al.*, Figure 4.37 shows that DOPE samples prepared containing isotonic saline solution or salmon sperm *ds*DNA form inverse hexagonal (H_{II}) phases at 37 ˚C.[3]

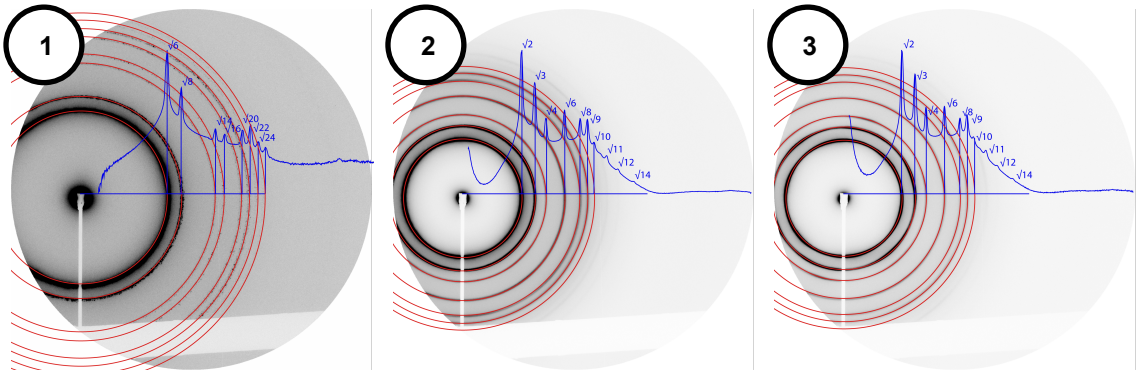

Figure 4.38 1) Monoolein sample (Ia$\bar{3}$d phase, a = 107.70 Å) with 27 waters per lipid, 37 ˚C; **2)** Monoolein sample (Pn$\bar{3}$m phase, a = 92.96 Å) under isotonic saline conditions, 37 ˚C; **3)** Monoolein sample (Pn$\bar{3}$m phase, a = 94.46 Å) premixed with salmon sperm *ds*DNA, 37 ˚C. MAX-lab data, February 2012.

Figure 4.38, inset 1, shows the cubic Ia$\bar{3}$d phase of monoolein, in agreement with phase observations published within the literature.[10] Addition of isotonic saline solution or salmon sperm *ds*DNA has driven the phase from Ia$\bar{3}$d cubic to Pn$\bar{3}$m cubic, with an associated reduction in the lattice parameter of the phases (Figure 4.38, insets 2 and 3).

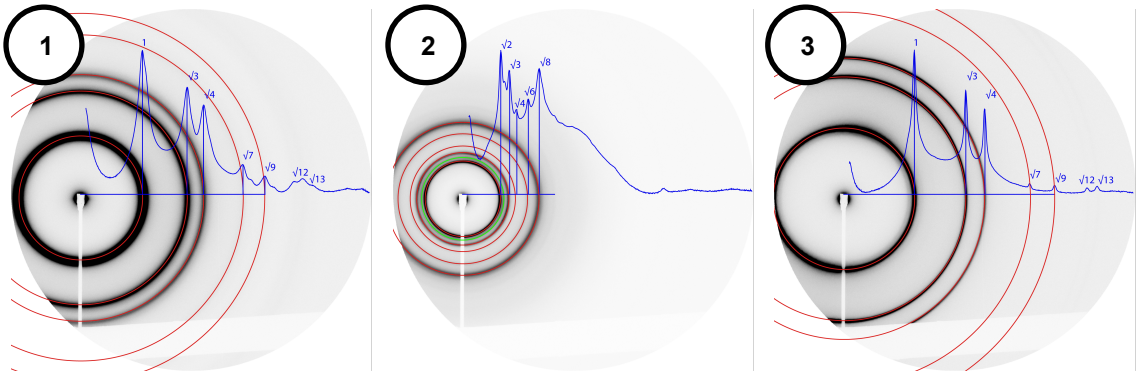

Figure 4.39 1) DOPE95:DOTAP5 composite sample (H_{II} phase, a = 72.04 Å) premixed with salmon sperm *ds*DNA, 37 ˚C; **2)** MO60:DOTAP40 composite sample (mostly Pn$\bar{3}$m phase, although a broad peak masks the identification of a potential secondary phase, a = 92.96 Å) premixed with salmon sperm *ds*DNA, 37 ˚C; **3)** MO70:PE30 composite sample (H_{II} phase, a = 63.54 Å) premixed with salmon sperm *ds*DNA, 37 ˚C. MAX-lab data, February 2012.

Addition of the cationic lipid DOTAP to DOPE, such that DOTAP made up a mole percentage of 5% of the lipid sample, produced an inverse hexagonal phase when premixed with salmon sperm *ds*DNA at 37˚C (Figure 4.39, inset 1). The presence of 5%

DOTAP within the DOPE produced only a small reduction in the lattice parameter to 72.04 Å, suggesting the lipid sample should possess a similar ability to contain linearized *ds*DNA within the pores of the H_{II} phase as samples prepared from DOPE alone. Insets 2 and 3 of Figure 4.39 show the diffraction rings caused by the $Pn\bar{3}m$ and H_{II} phases of the composite samples MO60:DOTAP40 and MO70:PE30, respectively.

Figure 4.40 presents schematics of the inverse hexagonal (H_{II}) and cubic $Ia\bar{3}d$ and $Pn\bar{3}m$ liquid crystalline phase structures. Rules for identifying each of the phases discussed herein are presented within the methodology section of this chapter (Table 4.2, Section 4.2.5.6).

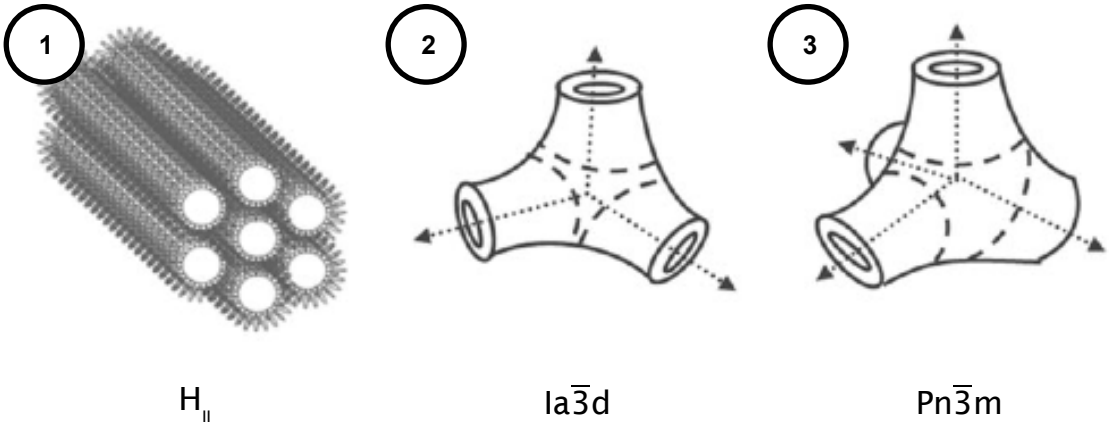

Figure 4.40 1) Inverse hexagonal (H_{II}) phase structure; 2) $Ia\bar{3}d$ cubic phase structure; 3) $Pn\bar{3}m$ cubic phase structure. Reproduced from Kulkarni *et al. Phys. Chem. Chem. Phys.*, 2011, **13**, 3004, with permission from the PCCP Owner Societies.[10]

4.8 References

1. Wilson, R. J., Tyas, S. R., Black, C. F., Dymond, M. K. & Attard, G. S. Partitioning of ssRNA Molecules between Preformed Monolithic H(II) Liquid Crystalline Phases of Lipids and Supernatant Isotropic Phases. *Biomacromolecules* **11,** 3022–3027 (2010).

2. Corsi, J. *et al.* DNA that is dispersed in the liquid crystalline phases of phospholipids is actively transcribed. *Chem. Commun.* 2307–2309 (2008). doi:10.1039/b801199k

3. Black, C. F., Wilson, R. J., Nylander, T., Dymond, M. K. & Attard, G. S. Linear dsDNA partitions spontaneously into the inverse hexagonal lyotropic liquid crystalline phases of phospholipids. *J. Am. Chem. Soc.* **132,** 9728–9732 (2010).

4. Park, N., Um, S. H., Funabashi, H., Xu, J. & Luo, D. A cell-free protein-producing gel. *Nat. Mater.* **8,** 432–437 (2009).

5. Buxboim, A., Daube, S. S. & Bar-Ziv, R. Synthetic gene brushes: a structure-function relationship. *Mol. Syst. Biol.* **4,** 181 (2008).

6. Kwon, Y.-C. C., Hahn, G.-H. H., Huh, K. M. & Kim, D.-M. M. Synthesis of functional proteins using Escherichia coli extract entrapped in calcium alginate microbeads. *Anal. Biochem.* **373,** 192–196 (2008).

7. Seddon, J. M. Structure of the inverted hexagonal (HII) phase, and non-lamellar phase-transitions of lipids. *Biochim. Biophys. Acta* **1031,** 1–69 (1990).

8. Peiró-Salvador, T., Ces, O., Templer, R. H. & Seddon, A. M. Buffers may adversely affect model lipid membranes: a cautionary tale. *Biochemistry* **48,** 11149–11151 (2009).

9. Tate, M. W. & Gruner, S. M. Temperature dependence of the structural dimensions of the inverted hexagonal (HII) phase of phosphatidylethanolamine-containing membranes. *Biochemistry* **28,** 4245–4253 (1989).

10. Kulkarni, C. V, Wachter, W., Iglesias-Salto, G., Engelskirchen, S. & Ahualli, S. Monoolein: a magic lipid? *Phys. Chem. Chem. Phys.* **13,** 3004 (2011).

11. Clogston, J. & Caffrey, M. Controlling release from the lipidic cubic phase. Amino acids, peptides, proteins and nucleic acids. *J. Control. Release* **107,** 97–111 (2005).

12. Kraineva, J., Narayanan, R. A., Kondrashkina, E., Thiyagarajan, P. & Winter, R. Kinetics of lamellar-to-cubic and intercubic phase transitions of pure and cytochrome c containing monoolein dispersions monitored by time-resolved small-angle X-ray diffraction. *Langmuir* **21,** 3559–3571 (2005).

13. Kraineva, J., Nicolini, C., Thiyagarajan, P., Kondrashkina, E. & Winter, R. Incorporation of alpha-chymotrypsin into the 3D channels of bicontinuous cubic lipid mesophases. *Biochim. Biophys. Acta* **1764,** 424–433 (2006).

14. Kraineva, J., Smirnovas, V. & Winter, R. Effects of lipid confinement on insulin stability and amyloid formation. *Langmuir* **23,** 7118–7126 (2007).

15. Zhang-Keck, Z. Y., Eckstein, F., Washington, L. D. & Stallcup, M. R. A role for divalent cations in specifying the start site for transcription from chromatin templates in vitro. *J. Biol. Chem.* **263,** 9550–9556 (1988).

16. So, A. G., Davie, E. W., Epstein, R. & Tissières, A. Effects of cations on DNA-dependent RNA polymerase. *Proc. Natl. Acad. Sci. U. S. A.* **58,** 1739–1746 (1967).

17. Chebotareva, N. A., Kurganov, B. I. & Livanova, N. B. Biochemical effects of molecular crowding. *Biochem. Biokhimiia* **69,** 1239–1251 (2004).

18. Davis-Searles, P. R., Saunders, A. J., Erie, D. A., Winzor, D. J. & Pielak, G. J. Interpreting the effects of small uncharged solutes on protein-folding equilibria. *Annu. Rev. Biophys. Biomol. Struct.* **30,** 271–306 (2001).

19. Ellis, R. J. Macromolecular crowding: obvious but underappreciated. *Trends Biochem. Sci.* **26,** 597–604 (2001).

20. Ellis, R. J. Macromolecular crowding: an important but neglected aspect of the intracellular environment. *Curr. Opin. Struct. Biol.* **11,** 114–119 (2001).

21. Bakke, C. K., Jungbauer, L. M. & Cavagnero, S. In vitro expression and characterization of native apomyoglobin under low molecular crowding conditions. *Protein Expr. Purif.* **45,** 381–392 (2006).

22. Batra, J., Xu, K., Qin, S. & Zhou, H.-X. X. Effect of macromolecular crowding on protein binding stability: modest stabilization and significant biological consequences. *Biophys. J.* **97,** 906–911 (2009).

23. Nakano, S., Karimata, H. T., Kitagawa, Y. & Sugimoto, N. Facilitation of RNA enzyme activity in the molecular crowding media of cosolutes. *J. Am. Chem. Soc.* **131,** 16881–16888 (2009).

24. Zimmerman, S. B. & Minton, A. P. Macromolecular crowding: biochemical, biophysical, and physiological consequences. *Annu. Rev. Biophys. Biomol. Struct.* **22,** 27–65 (1993).

25. Ge, X., Luo, D. & Xu, J. Cell-free protein expression under macromolecular crowding conditions. *PLoS One* **6,** e28707 (2011).

26. Labrador, A., Cerenius, Y. & Svensson…, C. The yellow mini-hutch for SAXS experiments at MAX IV Laboratory. in *J. Phys. Conf. Ser.* 072019 (2013). at <http://iopscience.iop.org/1742-6596/425/7/072019>

27. Tanaka, K. & Okahata, Y. A DNA-Lipid Complex in Organic Media and Formation of an Aligned Cast Film. *J. Am. Chem. Soc.* (1996). at <http://pubs.acs.org/doi/abs/10.1021/ja9617855>

Chapter 5:

Towards the Development of a Semi-biotic Device

5. Towards the Development of a Semi-biotic Device

5.1 Rationale

Semi-biotic systems are systems that incorporate biologically derived components and integrates them with synthetic components to produce a hybrid 'semi-biotic' device.[1] As part of the research from NEONUCLEI, project no. 12967 funded under the European Union FP6 framework, a basic semi-biotic system was designed to enable continuous-flow transcription of linearized T7 dsDNA, from within the inverse hexagonal phase of 1,2-dioleoyl-sn-glycero-3-phosphoethanolamine, utilizing a polydimethylsiloxane (PDMS) microfluidic chassis.[2] Through utilizing a microfluidic chassis, it was envisaged that such a hybrid device could offer continuous-flow transcription, using a re-usable DNA template, requiring only the provision of transcription reaction consumables. This offered a distinct advantage over the commercially available transcription kits, by allowing continuous production of mRNA from a re-usable DNA template, rather than being constrained to the batch reaction methods required by traditional solution phase commercial transcription systems, which require the reaction to be halted, processed and then another reaction set-up to produce mRNA over an extended period of time.

The *in vitro* expression of proteins, *via* coupled cell-free transcription-translation is an exciting biological application of microfluidic devices, of which existing examples can be found in the literature.[3-5] Whilst the production of a coupled transcription-translation microfluidic device is not novel, our proposal to use a DNA-containing monolithic H_{II} phase of DOPE as a vessel for the provision of template DNA within the microfluidic device for transcription is novel, and should present a device that is unique within its field for it's application of lyotropic liquid crystalline phases in the process of protein expression using a microfluidic device.

In 2005, Dittrich *et al.* developed a microfluidic device capable of coupled transcription-translation and detection of the expressed protein (red-shifted mutant green fluorescent protein - rsGFP) *via* fluorescence spectroscopy. As proposed herein, Dittrich *et al.* used polydimethylsiloxane to manufacture their device, with their device bonded to a glass substrate. The method of coupled transcription-translation utilized by Dittrich involves the formation of a water-in-oil emulsion, where templates from a gene library are continually mixed with the transcription/translation mix upon pumping into the microfluidic device *via* syringe pump. *In vitro* protein expression then occurs during the transport of the emulsion through the microfluidic device channel, under continuous flow supplied by syringe pump, with the microfluidic device subjected to heating (37 °C).

Building upon the work of Dittrich *et al.* (2005), Courtois *et al.* (2008) developed an integrated device, again using a PDMS and glass construction, for measuring protein expression in microdroplets.[5] The device utilized the components of a commercially available protein expression system, with the *E. coli* lysate and amino acids supplied from one input flow, and the ribosomes, tRNA, translation factors, ribonucleotides and DNA template supplied by a second input flow. Both input flows were added to the device at an equal constant rate, with droplet formation occurring. Unlike the coupled transcription/translation device produced by Dittrich *et al.* 2005), incubation was performed at room temperature for 6.5 hours, during which the expression of proteins occurred *in vitro*. Integrated measurement of protein expression is then performed *via* laser-induced fluorescence detection at the reservoir outlet where the droplets formed flow out of the device channel. Importantly, the method utilized by Courtois *et al*. ensured that the microdroplets formed contained only one molecule of DNA template (per droplet), which led to an increased level of protein expression when compared to the expression observed during previous experiments where droplets contained multiple DNA templates. This observation validated cell-free expression using microdroplet formation as a viable high-throughput method of protein expression using microfluidics.

Unlike the microfluidic devices reported by Dittrich *et al.* and Courtois *et al.*, the proposed semi-biotic device offers the advantage that the template *ds*DNA required for mRNA or protein synthesis is immobilized on a surface contained within the device, meaning that the template *ds*DNA could be used for extended periods of transcription or translation. Within systems where the template *ds*DNA is not immobilized, the *ds*DNA is typically discarded during the purification of the desired reaction products, with fresh template *ds*DNA required to be produced and added alongside the assay reagents for subsequent synthesis reactions. This inevitably leads to an increase in experimental costs and processing time, due to the need to produce a far greater amount of suitable template *ds*DNA than if the template could be reused for multiple reactions or an extended period of continuous-flow synthesis.

In contrast to previously reported microfluidic devices for coupled transcription-translation, a semi-biotic device incorporating biological and synthetic components could be designed to be modular; splitting each of the device functions into separate but connectable ‘plug and play’ modules would allow the device to be tailored for a particular use. For example, in a situation where synthesis of mRNA alone was required, only the transcription module would be necessary, with transcription being performed under optimal conditions within a custom-designed transcription module. For protein synthesis, the transcription module could be connected to a downstream

translation module; mRNA would be produced in the first module before being fed into the translation module, where protein synthesis could be performed under the optimal conditions for translation. A modular 'plug and play' system would be advantageous as the end user is able to customize the device depending upon the product they wish to produce, with the knowledge that each individual module is optimized for a specific biological process to give the best yield. This modular approach would enable semi-biotic devices to have far greater appeal in terms of the range biological products they could generate; potential uses of a semi-biotic device utilizing immobilized template dsDNA include the production of RNAs, peptide and protein synthesis. Further development could allow for the integration of combined detection, decision and response systems within a device, allowing for efficient, fully autonomous and regulated production of specific complex biomolecules on demand.

5.2 Methodology

5.2.1 Phase preparation

Lipid phases were prepared as per the method detailed in sections 3.2 and 4.2.

Lipid buttons were prepared by dispensing aliquots of DOPE dissolved in chloroform solution (6 µL, 0.5 mg µL-1) into PCR tubes via Eppendorf pipette with suitable filtered tip, minimizing smearing of the solution when dispensing. Solutions were then allowed to stand (15 minutes, RT) in capped tubes, before centrifugation (17,000 g, 30 seconds, RT) to ensure all lipid/chloroform solution was located at the bottom of the PCR tubes. The PCR tubes were then uncapped and warmed (2 hours, 50 °C) to aid the removal of chloroform, before drying the samples overnight using freeze-drying apparatus. Note that the vacuum was applied slowly, to minimise the bubbling of chloroform solution. Upon complete chloroform removal, the DOPE liquid crystalline phases appeared as a white to translucent 'button' at the bottom of the PCR tubes.

After rehydration of the lipid buttons with isotonic saline (2 µL), the phases were preloaded with linear *ds*DNA *via* incubation with linear *ds*DNA, $MgCl_2$ and transcription buffer, for 100 h at 37 °C, using an incubator. The aqueous supernatant solution was then removed post-incubation, with the *ds*DNA-containing lipid buttons then smeared into the microfluidic device lipid well, sealed and then refrigerated (4 °C) until required for use.

5.2.2 PDMS microfluidic device

Polydimethylsiloxane (PDMS, Figure 5.1) is an ideal material for the rapid prototyping and production of microfluidic devices.[6] Due to the flexible nature of the polymer, and the relatively simple construction methods, devices can be fashioned in a relatively short timescale and without the need for expensive or complicated micro-machined connections, to allow for a watertight connection between the device and any input/output tubing.[7] As per the transcription device produced by Foley (2008),[2] the prototype microfluidic transcription devices described herein were constructed using PDMS, due to its biocompatibility, rapid prototyping and low cost.[8–10] The method of prototype production using PDMS was based upon the procedure used by Foley, utilizing an Ordyl SY355 laminate to produce a template stamp for the upper and lower device layers, from which the PDMS could be cast and then assembled together to form a complete device.[11]

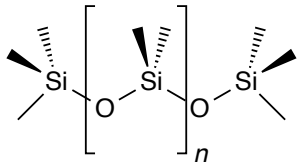

Figure 5.1 Structure of the silicone polydimethylsiloxane (PDMS).

Another advantage of using PDMS to fabricate a microfluidic device is the ability to produce the device in constituent parts, which can then be easily bonded together, using surface oxidation, to ensure a leak-free bond between parts. Through exposing pre-molded PDMS layers to oxygen plasma, surface oxidation exposes silanol groups (OH) that form covalent siloxane bonds (Si-O-Si), through a condensation reaction, when brought into contact with another surface oxidized layer of PDMS.[6,12] The formation of these covalent siloxane bonds between PDMS layers ensures an irreversible, leak-free PDMS-PDMS bond, making surface oxidation *via* oxygen plasma treatment an ideal method for simple fabrication of a microfluidic device from several PDMS parts.

Details of the PDMS microfluidic device fabrication can be found in section 5.7.1, Annex 1.

5.2.3 Continuous-flow transcription

Continuous-flow transcription was performed in two ways using the PDMS microfluidic device; firstly, using H_{II} phase DOPE preloaded with linear *ds*DNA to provide the template for transcription; secondly, running positive control transcription assays, containing the *ds*DNA template in solution, in the absence of H_{II} phase DOPE. Both of these methods ensured a theoretical provision of linear *ds*DNA template equivalent to 0.05 µg / µL, regardless of whether the template *ds*DNA was in solution or instead compartmentalized within lipid smeared into the lipid well of the device. The specification of the transcription assay conditions for continuous-flow transcription is presented in Table 5.1.

Table 5.1 Composition of transcription assay for continuous-flow transcription experiments. For positive control transcription assays, template *ds*DNA was in solution with no lipid present within the microfluidic device.

Component	Component concentration
rNTPs (80 mM each)	20 mM (5 mM each)
10x transcription buffer	1x
$MgCl_2$ (0.5 mM)	25 mM
T7 RNA polymerase	40 u
*lin*pRSET-EmGFP *ds*DNA	Equivalent to 0.05 µg / µL

The microfluidic device was heated from underneath using a thermostatically controlled hotplate, with the inner PDMS temperature monitored by thermocouple. A transcription assay component solution was injected into the device, at a constant specified rate, from a glass Hamilton syringe using a Harvard NanoMite syringe pump and controller.

5.2.4 Methods of analysis

5.2.4.1 Transcriptional yield

UV-visible spectrophotometry was performed using a NanoDrop ND-1000 instrument to quantify the concentration of all mRNA samples purified. For analytical purposes, measurements were recorded in triplicate, with the mean concentration and standard deviation calculated. Using the NanoDrop nucleic acid software, measurements were processed using type ratio RNA-40 for purified mRNA samples. Concentration values were recorded in units of ng μL^{-1}, along with associated 260/280 and 260/230 sample absorbance ratios as a measure of sample purity and integrity.

A 260/280 ratio of ~2.0 is generally accepted as pure for RNA, whilst a 260/230 ratio appreciably lower than 1.8 may indicate the presence of co-purified contaminants.

5.2.4.2 PDMS microfluidic device temperature monitoring

The temperature of the microfluidic device was monitored using a Pico TC-08 thermocouple with a type K surface probe, operating at a frequency 1 Hz. Injection of transcription assay components into the device was only performed once the PDMS temperature was at 37 °C and the thermocouple data showed that the temperature had been stable for a minimum of 30 minutes.

5.3 Designing a continuous-flow transcription device

5.3.1 Previous device design

The initial microfluidic device for transcription from a DNA-containing DOPE H_{II} phase produced by Foley in 2008 under the NEONUCLEI research programme was a basic PDMS structure, consisting of an upper and lower layer, bonded by plasma treating the surfaces of the upper and lower PDMS layers. There was a simple input and output tube system, with transcription components pumped through the device *via* a BASi Bee syringe pump and controller unit, at a flow-rate of 0.5 µL/min. The DNA-containing DOPE H_{II} phase was contained within a 1 mm^3 well, sufficient to house approximately 1 mg of DNA-containing lipid. Figure 5.2 shows an image of the device, where the input and output tubes can be seen, alongside the circular pools either end of the channel running above the lipid well.

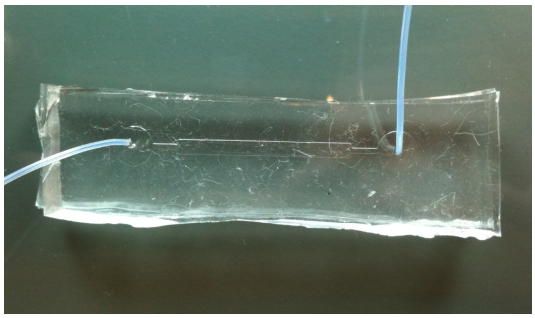

Figure 5.2 The microfluidic device for transcription produced under the NEONUCLEI research programme. The dimensions of the well for containment of the DNA-containing DOPE were 20 mm (length) x 1 mm (width) x 0.05 mm deep. This produced a containment well of volume 1 mm^3, sufficient to contain approximately 1 mg of lipid, itself containing 1 µg linear *ds*DNA to act as a template for transcription.

The device designed by Foley was capable of housing approximately 1 mg of DNA-containing DOPE; this amount was chosen rather than the more usual 2 mg of lipid used for DOPE-containing lipid buttons for several reasons. Firstly, in order to house 2 mg of lipid, the dimensions of the microfluidic device would have needed to have been increased, either through doubling the length, width, or depth of the lipid well, leading to a doubling in the volume of lipid it was possible to accommodate. Whilst theoretically not a problem, one of the primary aims was to develop a small microfluidic device, and as such, it would have been undesirable to have any larger dimensions than those specified by Foley (see Figure 5.2 caption). Secondly, 2 mg of H_{II} phase DOPE is a huge excess of lipid for 1 µg of *lin*T7GFP to partition into. By reducing the mass of lipid to 1 mg, not only can the device dimensions be halved, but also there is still an excess of lipid available to ensure complete partitioning of *ds*DNA within the H_{II} phase. Thirdly, by increasing the volume of lipid accommodated within the

microfluidic device, and knowing that 2 mg of lipid is a huge excess of lipid for the complete partitioning of 1 µg of DNA into the aqueous pores of the H_{II} phase, transcription would be spread out across a much greater surface area compared to a device that had a smaller surface area but far higher number of available *ds*DNA molecules for transcription per unit area. It would be far more efficient having a microfluidic device with a compact lipid containing well but a high density of *ds*DNA-containing pores over the well.

We have reported previously that, based upon the unit cell dimension (*d*) of H_{II} phase DOPE at 37 °C in water ($7.0 \pm 0.4 \times 10^{-9}$ m), there is estimated to be approximately 1.5-3.0×10^{11} aqueous pores in contact with the supernatant, for a 2 mg DOPE lipid button. Assuming *lin*pRSET-EmGFP is in the B-DNA form, and that it is fully extended (3600bp, length ~1.2×10^{-6} m), it is possible for all ~2.7×10^{11} molecules of DNA in the 1 µg incubated in the presence of the H_{II} phase to be accommodated within the pores of the phase. Importantly, this estimate assumes the minimal partitioning of only one molecule of *ds*DNA per pore. With a lipid button radius of ~1.5×10^{-3} m, the pores of the phase can theoretically have a depth of in the region of 10^{-3} m, sufficient to house in the region of 10^{3} molecules of *lin*T7GFP *ds*DNA, assuming the DNA is fully extended and were to line the pore in a head-to-tail arrangement, as to completely fill the pore. Therefore, by reducing the lipid mass by half, there should still be a large excess of available phase pores for DNA partitioning, with multiple *ds*DNA molecules able to occupy pores within the H_{II} phase.

Whilst a flow rate of 0.5 µL/min was used during the microfluidic experiments performed by Foley, his research determined that a flow rate of 6.67 µL/min or less would provide sufficient flow to enable transcription activity equivalent to a 60 minute batch transcription incubated at 37 °C. A slower flow-rate reduces the pressure upon the microfluidic device, including inlet and outlet tube connections that are prone to leakages under the high pressures caused by high flow rates, and increases the amount of the time that the transcription components are in contact with the DNA-containing DOPE. Theoretically, a slower flow rate for a continuous-flow transcription reaction would be the equivalent of an increased incubation time for a comparative batch method transcription reaction, and as such, higher yields of RNA isolation should be achieved. However, through decreasing flow rate, the transcription components will spend a greater amount of time at room temperature within the syringe pump, prior to reaching the DNA-containing lipid, which could have a detrimental effect upon the transcriptional activity over time.

A basic continuous-flow transcription reaction, using the prototype microfluidic device designed by Foley, containing a DNA-DOPE phase produced *via* the lyophilization method of preparation, achieved RNA isolation concentrations of between 20-40 ng/μL for an incubation period of between 40-120 minutes (Foley, 2008).[2]

5.3.2 Fabrication using PDMS

Fabrication of a new device was essential, due to the previous prototype transcription device produced by Foley being unsuitable for further use. As Foley's device was produced in 2008, the DOPE-DNA liquid crystalline phase within the device would have degraded and due to the plasma treatment of the upper and lower PDMS layers, it would not be possible to regenerate the device by replacing the expired DOPE with a new batch of DNA-containing DOPE. With it necessary to produce a new microfluidic device for transcription from a DNA-containing DOPE liquid crystalline phase, the opportunity was taken to assess the previous design, proposed by Foley, and redesign a new microfluidic device based upon Foley's findings and the experimental findings from the data presented in chapters 3 and 4.

The basic requirements of the new device were simple, shared with those of Foley's device; an input and output tube for transcription components, a well for housing the DNA-containing liquid crystalline phase, and a channel running above the well to carry the transcription components across the liquid crystalline phase (see Figure 5.3).

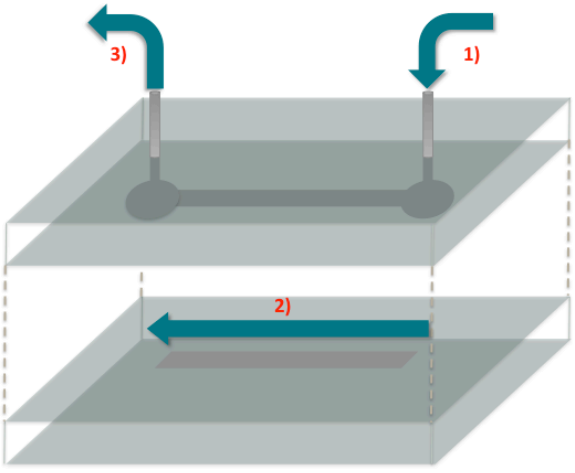

Figure 5.3 Schematic of the microfluidic device designed for transcription from DNA-containing H_{II} phase DOPE. **1)** Transcription components are fed into the microfluidic device from a syringe pump at a constant-flow rate. **2)** Transcription components flow from inlet across the DNA-containing H_{II} phase, between both PDMS layers. **3)** mRNA remains in solution and exits the device *via* the outlet tubing, ready for collection and purification.

A new microfluidic device for transcription was designed, based upon the prototype design by Foley, although with reduced lipid well dimensions, accommodating 75% of the total lipid accommodated in the device fabricated by Foley. Whilst this reduced the overall device size, it was expected that no considerable reduction in amount of mRNA isolated from the device would be observed, as the same amount of linear template *ds*DNA could still be theoretically contained within the reduced lipid amount. As discussed in section 5.3.1, the 1 mg of lipid accommodated by Foley's device was still an excess of lipid for the complete partitioning of 1 µg *lin*pRSET-EmGFP *ds*DNA into the phase pores, assuming that multiple molecules of linear *ds*DNA would occupy each pore within the phase. By producing a smaller device, the overall channel length through which the transcription components had to run through was reduced also – thus reducing the span of the device over which it would have been possible for a leak to occur, offering an additional benefit. The new prototype device parameters are compared to those of Foley's prototype in Table 5.2.

Table 5.2 A comparison of the initial and new prototype device parameters.

Parameter	Initial prototype	New prototype
Lipid well length	20 mm	15 mm
Lipid well width	1 mm	1 mm
Lipid well depth	0.05 mm	0.05 mm
Volume of lipid accommodated	1 mm^2	0.75 mm^2
Available lipid surface area	20 mm^2	15 mm^2

The method of construction was rapid prototyping using Ordyl SY355 laminate to produce an upper and lower layer stamp template, from which the upper and lower layers were cast using PDMS (10 parts PDMS base to 1 part curing agent). Bonding between the two PDMS layers of the initial prototype device was performed using oxygen plasma treatment. A full fabrication procedure can be found in the Supporting Information. Transcription components were pumped through the device using a Harvard NanoMite syringe pump, supplying a constant flow of 0.5 µL/min, as per Foley's device, and the device heated to support transcription *via* thermostatically controlled hot plate. Lipid buttons were produced *via* the 100-hour incubation method, with supplementation of the DNA solution with full transcription buffer prior to incubation in the presence of the DOPE liquid crystalline phase.

Whilst plasma treatment of PDMS offers a method of irreversibly bonding the PDMS layers of the device together,[13] it is not possible to plasma treat the lower PDMS layer

once the DNA-containing liquid crystalline phase has been deposited into the containment well. The upper and lower PDMS layers of the device therefore have to be plasma treated prior to deposition of the DNA-containing liquid crystalline phase into the containment well. Post-plasma treatment, the PDMS layers to be bonded would ideally make contact with each other as soon as possible, with heat treatment to ensure an irreversible bond. However, with the deposition of lipid into the containment well, the period of time between plasma treatment and bonding is increased significantly (to approximately 5 minutes) whilst deposition of the lipid occurs. The temperature at which heat treatment is performed at also has to be reduced, to in the region of 50 ˚C, down from 80 ˚C, to ensure that the likelihood of decomposition or degradation of the DNA-containing liquid crystalline phase was minimised. Both of these factors have a negative impact upon the effectiveness of plasma treatment in bonding the upper and lower PDMS device layers, and it was found that leaks would often occur between the two layers of the device, due to insufficient bonding.

With the method of lipid deposition improved and the time required for deposition reduced (ca. 2 minutes), a sufficient bond between the upper and lower PDMS layers was achieved using plasma treatment such that flow-rate testing of the device could be performed. Flow-rates of between 0.5 to 5 µL/min were trialed, and were found to be suitable for the new device design, with no apparent leaking at the PDMS to tubing connections. However, after extended periods of continuous-flow (30-120 minutes) at all flow-rates, the bond between the upper and lower PDMS layers was broken, with leaks forming through the sides of the microfluidic device. It was concluded, therefore, that plasma treatment did not offer a viable method of bonding the upper and lower PDMS device layers in conjunction with the use of DNA-containing lipid phases unless an improved protocol could be developed. Figure 5.4 shows the new prototype PDMS device (plasma bonded) during flow-rate testing.

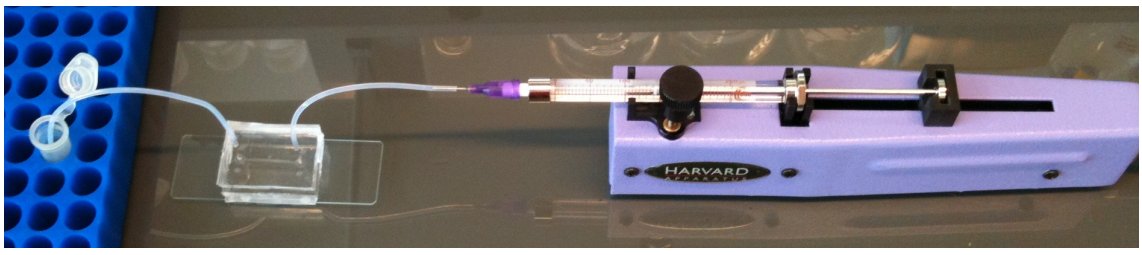

Figure 5.4 Microfluidic device designed for transcription from a DNA-containing H_{II} phase. Transcription assay components are fed into the device from a Harvard NanoMite syringe pump at a rate of 0.5 µL/min, with the transcription product and any waste consumables collected in a microcentrifuge tube, ready for purification.

Continuous-flow transcription was unsuccessful using the new prototype design, heating *via* thermostatically controlled hotplate and pumping transcription components through the device at a constant flow rate of 0.5 µL/min (data not shown).

5.3.3 Optimization of device design

Due to the failure in securing a prolonged watertight bond between the two PDMS layers of the new design prototype microfluidic device, investigation into the development of an improved method of bonding was conducted. Literature sources report that, as well as *via* low temperature plasma treatment, watertight covalent seals can be formed between smooth, clean PDMS surfaces when they are pressed against each other, for example by the use of mechanical force.[7,14] After discussion with Xavier Casadevall i Solvas (Department of Chemistry, Imperial College London), during the Sensor Workshop "Microfluidics and Sensor Technology for Oceanographic and Environmental Science Applications", it was mused that the most practical method of achieving a watertight seal for a microfluidic device containing a temperature and plasma sensitive DNA lipoplex, would be through the use of mechanically-applied pressure. Through utilizing metal clamps to press the upper and lower PDMS layers of the device together, a temporary watertight bond could be formed. The microfluidic device could be constructed with greater ease using clamps than was possible through the plasma bonding method, allowing more time for deposition of the DNA-containing liquid crystalline phase into the containment well. An additional advantage was that the device could now be easily deconstructed, cleaned, and the DNA-containing lipid phase renewed as desired, without the necessity of producing an entirely new microfluidic device.

However, whilst the utilization of clamps provided a watertight seal between the two PDMS layers, the previous method of incubation (thermostatically controlled hotplate) was no longer viable, due to the arms of the clamps protruding. The protrusion of the clamp arms prevented the device from sitting flush on top of the hotplate, which meant that a new method of incubating the device had to be established. Several trials were conducted using the clamp-based device (Figure 5.5) with incubation using a waterbath, warmed to 37 °C. The clamps provided a good watertight seal, preventing penetration of the device by the temperature-controlled water, and release of the transcription reaction solution from within the device.

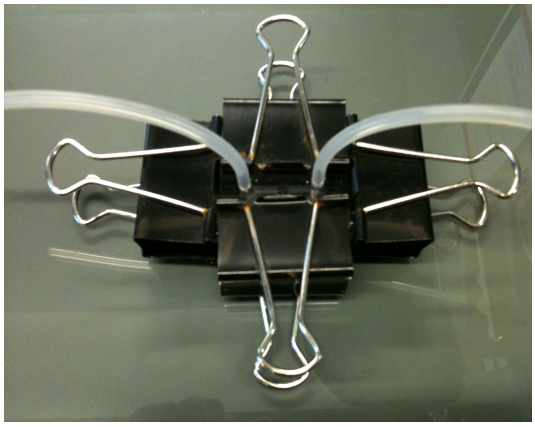

Figure 5.5 Second generation microfluidic device. The PDMS device can be deconstructed, cleaned, refilled with lipid and then sealed using the clamps to provide a watertight seal, unlike the plasma-treated PDMS device, which had upper and lower layers that were irreversibly bonded together.

Continuous-flow transcription experiments using the clamp-based microfluidic device have to date not successfully produced mRNA from DNA-containing DOPE H_{II} phases. This could be for a number of reasons; *ds*DNA contained within the lipid pores could have become inaccessible when the lipid button is smeared into the PDMS well; continuous-flow conditions do not allow rNTPs sufficient time to displace the compartmentalized *ds*DNA from within the lipid phase; transcription assay components became degraded during their injection from the syringe pump reservoir to within the microfluidic device channel; the incubation environment within the device could be suboptimal for transcriptional activity to be observed.

5.4 Viability of a continuous-flow transcription device

With continuous-flow transcription experiments using the PDMS microfluidic device loaded with *ds*DNA-containing DOPE not yielding transcription product, contrary to the observation of transcription product under the batch transcription conditions described in Chapter 4, investigations had to be made into the viability of a continuous-flow microfluidic transcription device fabricated from PDMS. The intended outcome of the experiments presented within section 5.4 was to identify any device parameters that were likely having an inhibitory effect upon transcriptional activity. Three relevant device parameters were investigated in the absence of *ds*DNA-containing DOPE, allowing for elimination of any effects upon transcriptional activity caused by the leaching of *ds*DNA from within the H_{II} phase DOPE; the effect of atmospheric conditions upon mRNA yield, the effect of transcription components delivery time prior to incubation within the microfluidic device transcription channel, and the effect of PDMS and in-device incubation upon transcriptional yields from a positive control transcription assay.

5.4.1 Effect of atmospheric conditions upon mRNA yield

Unlike the transcription experiments described in chapters 3 and 4, where transcription assays are performed in sealed microcentifuge tubes, incubation of the transcription assay solution in a PDMS microfluidic device is not entirely sealed from the atmosphere. Whilst injection of transcription assay components occurs from a sealed Hamilton syringe into the transcription channel between the upper and lower PDMS layers of the microfluidic device, the output tubing deposits the post-transcription solution into an open microcentrifuge tube; upon collection of a specified volume of post-transcription assay solution (typically 20 µL), the crude mRNA product was then purified using a Qiagen mRNA purification kit, as per one-off and batch transcription assays. Naturally, during the initial injection of transcription assay components into the microfluidic device, the transcription channel is also previously empty and so the first portion of transcription assay solution will be substantially more exposed to the atmosphere than subsequent portions of transcription assay. It was important, therefore, to make assessment of the effect of transcription assay incubation atmosphere upon the transcriptional yield obtained (Figure 5.6).

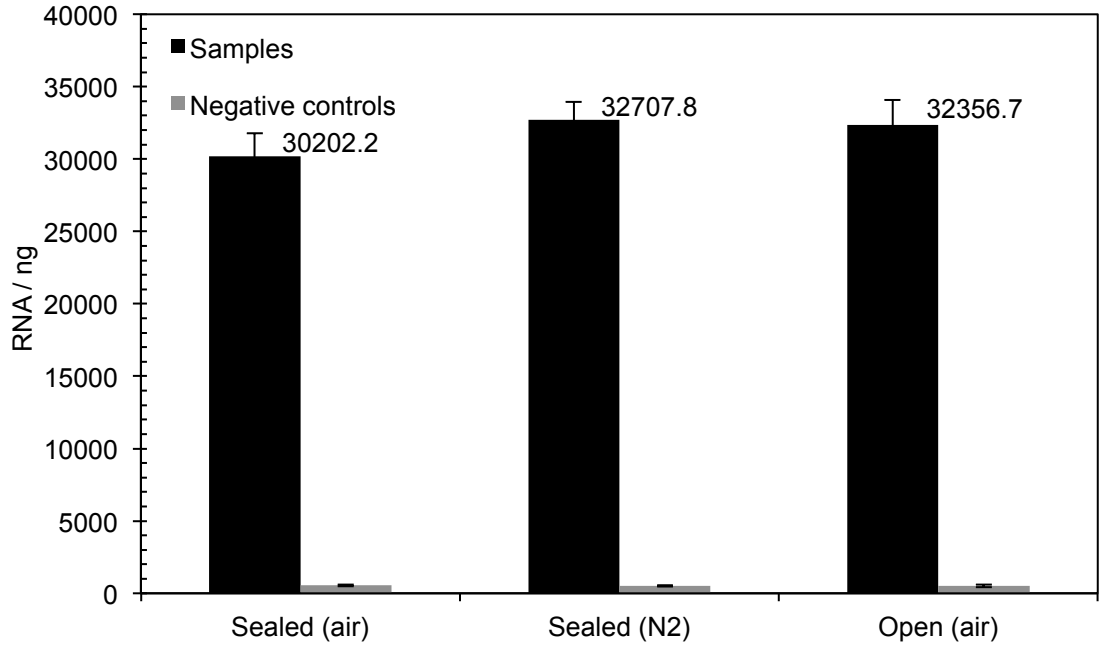

Figure 5.6 A comparison of the effect of incubation atmosphere upon transcription yield (2 h, 37 ˚C). Transcription assays were performed under nitrogen, in a sealed microcentrifuge tube, or open to the air. The positive control transcription assay for comparison was the sealed (air) sample. Transcription assays were prepared using a mastermix solution made from fresh transcription component stocks to ensure there had been minimal previous exposure to air prior to this experiment. RW/6511/03

Figure 5.6 clearly shows that changing the incubation atmosphere had, within experimental error, no appreciable effect upon the transcriptional activity observed from transcription assays in solution. Regardless of whether transcription assays (2 h, 37 ˚C) were performed in microcentrifuge tubes sealed under air (positive control) or nitrogen, or in microcentrifuge tubes left open to air, the transcriptional yields observed were comparable. As a result, it can be assumed that the fact that the microfluidic device is open to the atmosphere at the outlet tubing end will have no degradative effect upon the transcriptional yield that could be expected under continuous-flow conditions.

5.4.2 Effect of transcription components delivery time upon mRNA yield

Another potential cause of reduction of the transcriptional yield obtained from the PDMS microfluidic device prototype was the extended amount of time the transcription assay solution had to spend at room temperature prior to incubation at the temperatures required for transcription (~ 37 ˚C). When a one-off positive control transcription assay in solution was prepared, transcription assay components were quickly assembled on ice, with the complete transcription assay then incubated in a pre-equilibrated waterbath (typically 2 h, 37 ˚C), so the transcription assay components

spent a minimal amount of time at temperatures where they could become degraded prior to being used for transcription. In contrast to this, the microfluidic device is fed by transcription assay components under continuous-flow conditions from a glass Hamilton syringe, loaded upon a combined syringe pump and controller, which is not under temperature control. The transcription assay components, therefore, remain at room temperature until their injection into the microfluidic device, where the transcription assay solution will be incubated at ~ 37 ˚C within the transcription channel. This could potentially present a significant problem for the later portions of transcription assay solution injected into the device; components will have remained unused, at room temperature, for a significant number of hours prior to being incubated within the transcription channel of the device, thus these components will be far more likely to have degraded prior to incubation under optimal transcription conditions.

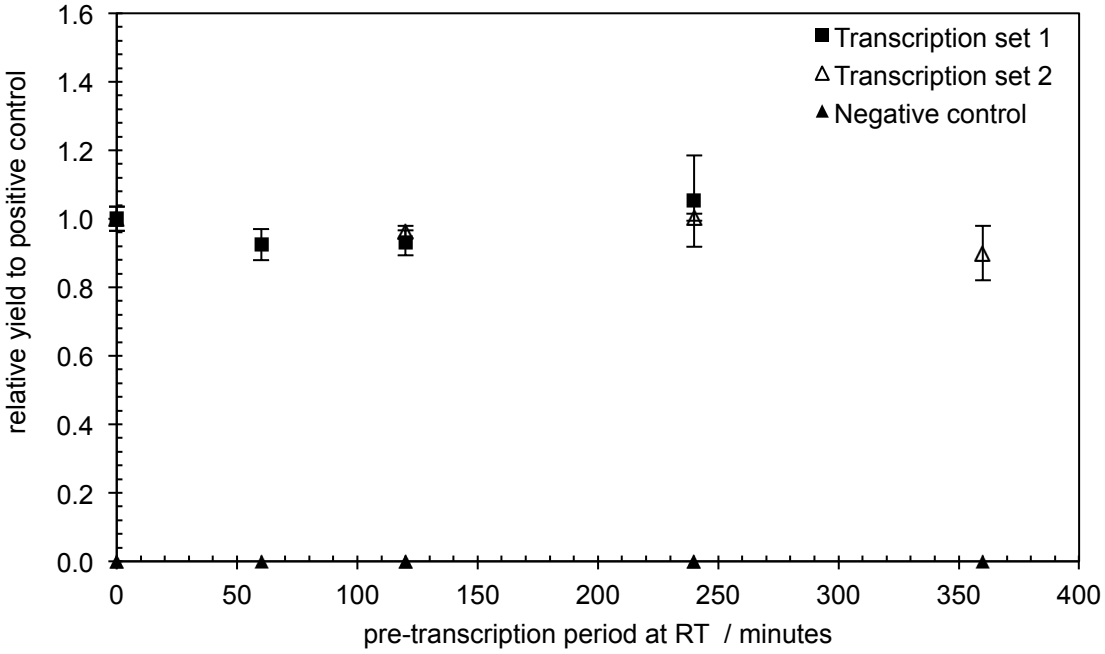

Figure 5.7 Effect of pre-transcription period at room temperature, prior to incubation under standard transcription assay conditions (2 h, 37 ˚C), upon transcription yield. Transcription set 1 (black squares) and transcription set 2 (hollow triangles) were prepared in an identical manner but at different times on the same date. RW/6511/16

The effect of the pre-transcription period transcription assay components spent at room temperature prior to incubation was investigated through by setting up parallel solution-based transcription assays which were stored at room temperature for increasing periods of time, prior to incubation under standard transcription assay conditions (2 h, 37 ˚C). For time periods of up to 6 hours at room temperature, transcription assay solution remained as transcriptionally-active as a homogeneous

assay solution that had spent no time at room temperature prior to incubation, within experimental error (Figure 5.7). Beneficially, this observation therefore meant that, for transcription assay solution within the syringe pump feeding the microfluidic device, no degradative effect upon transcriptional activity was observed for up to 6 hours spent at room temperature prior to incubation within the transcription channel of the device (~ 37 ˚C).

5.4.3 Device trial using positive control transcription assay

With investigations into the effect of pre-transcription incubation at room temperature identifying that transcription assay components could spent up to 6 hours at room temperature without any significant degradation in the transcriptional yield observed (Figure 5.7), an experiment was designed to assess the viability of transcription within the prototype PDMS continuous-flow device when the device was heated from below using a thermostatically-controlled hotplate. Complete transcription assay solution, including linearized template *ds*DNA, were loaded into a glass SGE syringe, controlled using a Hamilton NanoMite syringe pump, and injected into the prototype PDMS continuous-flow device, at a continuous rate of 167 nL/min, once the upper PDMS layer of the device had reached a stable temperature of ~37 ˚C (as determined by thermocouple, measuring at a frequency of 1 Hz).

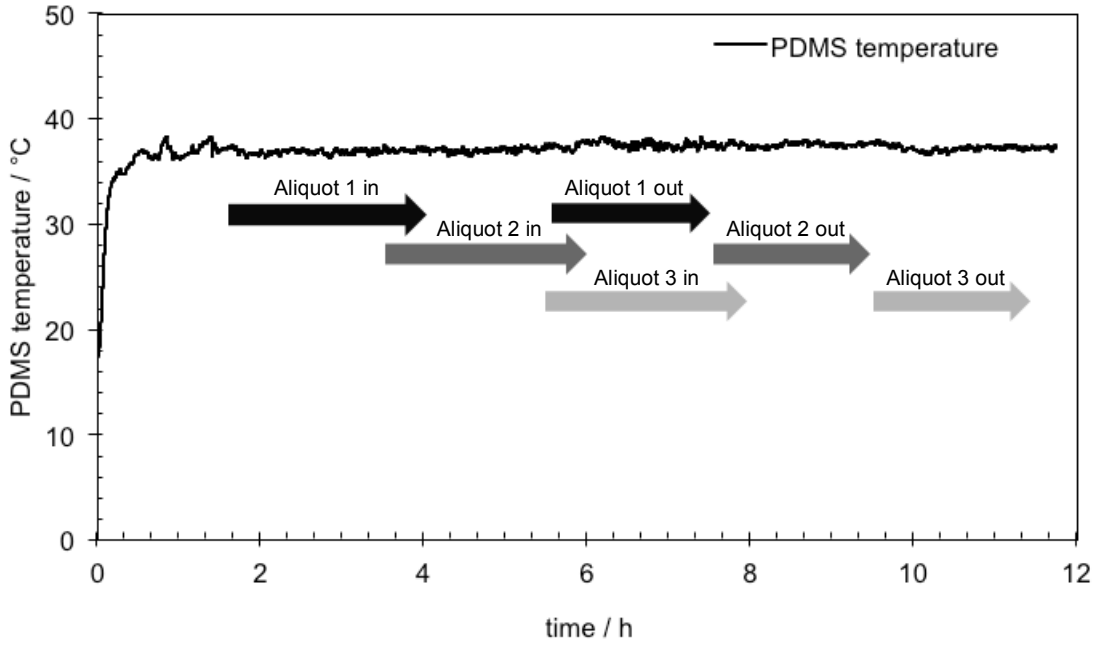

Figure 5.8 Thermocouple monitoring of the PDMS temperature (1 Hz) within the core of the microfluidic device upper layer. Arrows indicate the period transcription assay solution spent travelling within the inlet and outlet tubing, forming aliquots 1, 2 and 3 (2 h collection period each) which were later analyzed for quantity and quality of transcription product. RW/6511/22

Figure 5.8 presents the thermocouple trace of the device upper PDMS layer, with the location of the transcription assay solution for analysis aliquots 1-3 within the input and output tubing highlighted. For the duration of the investigation, the core of the device upper PDMS layer remained within a temperature range of 36.2-38.5 ˚C. Transcription aliquots 1-3 were formed by collecting the outlet solution for set periods of two hours each, from the commencement of solution discharge at ~5h40. Each aliquot was purified, using the same method as per all other transcription investigations reported herein, and then analyzed for their mRNA concentration (Figure 5.9).

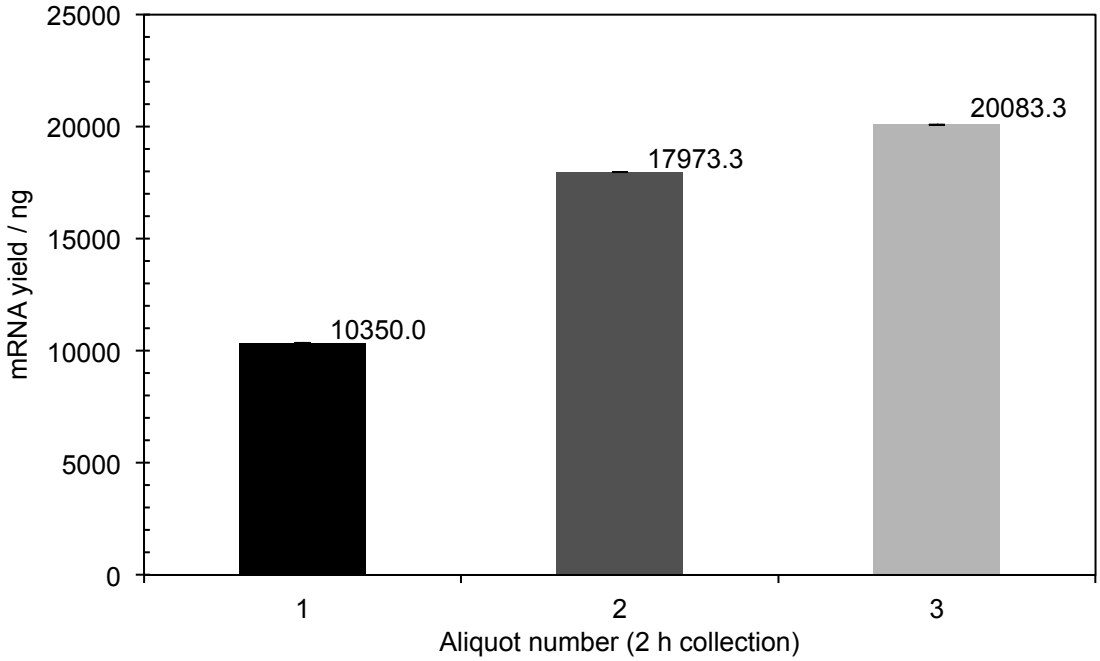

Figure 5.9 Transcription product concentrations from incubation of positive control transcription assay solution within the microfluidic device. Aliquots are comprised of the transcription product from three successive 2 h collection periods. RW/6511/22

Transcription aliquots 1-3, produced *via* hotplate incubation of the prototype PDMS continuous-flow device, all contained substantial quantities of *lin*pRSET-EmGFP mRNA, as determined by NanoDrop UV-visible spectrophotometry (Figure 5.9). As the investigation progressed, the amount of product mRNA within the device outlet solution increased from 10350.0 ng (aliquot 1) to 20083.3 ng (aliquot 3). This observation indicates that the use of PDMS for the prototype continuous-flow device did not prevent the transcription of template *ds*DNA; however, the mRNA yield achieved for aliquot 3 (20083.3 ng), the aliquot with the highest transcriptional yield, was only two-thirds of that achieved in a standard transcription reaction (30202.2 ng,

Figure 5.6) performed in a microcentrifuge tube and incubated in a thermostatically-controlled waterbath (37 ˚C, 2 h).

The reduced yields observed for transcription aliquots 1-3 from the continuous-flow prototype device were intriguing; a previous investigation had shown that room temperature incubations of the transcription assay solution prior to incubation at 37 ˚C caused no significant reduction in transcription yield (Figure 5.7), indicating that the thermally unregulated storage of the transcription assay solution, loaded upon the syringe pump prior to incubation within the heated layers of the PDMS device (~ 37 ˚C), was unlikely to have caused the drop in transcription yield. Additionally, a temperature gradient investigation into solution-based transcription had shown that good transcriptional yields could be achieved could be achieved, using a homologous transcription assay solution, across a broad temperature range from 30-38 ˚C (Figure 2.10), suggesting that the reduced yields observed for aliquots 1-3 in Figure 5.9 were unlikely to have been principally caused by inefficiencies in thermal regulation of the PDMS prototype device. Thermocouple monitoring of the device throughout the investigation had shown that the temperature of the PDMS device upper layer remained within an appropriate temperature range; even when considering the poor thermal conductivity of PDMS (~ 0.2 Wm/K),[15] it is unlikely that the temperature of the device channel would have been significantly below that recorded by the thermocouple, as it monitored the temperature in the PDMS layer above the device channel, whilst the prototype device was heated by thermostatically-controlled hotplate underneath the lower PDMS layer of the device.

5.5 Discussion

A new prototype microfluidic device, fabricated using a PDMS rapid prototyping technique, was produced for use under continuous-flow transcription conditions with *ds*DNA-containing DOPE liquid crystalline phases. Testing of the prototype device identified that when oxygen plasma treatment was used to seal the upper and lower PDMS layers together, leaks between the two layers formed over the course of pumping transcription assay solution through the device. The most suitable method for sealing the device was found to be the use of mechanical clamps, which also enabled ease of dismantling the device, cleaning it and replacing the liquid crystalline phase, whilst the most effective method of incubation was to heat the device from underneath using a thermostatically-controlled hotplate. Despite some optimization of the device design, mRNA was not produced within the device when the template *ds*DNA was supplied *via* DOPE liquid crystalline phase located within the device channel. This is perhaps not surprising, as the smearing of the liquid crystalline phase within the device channel could have trapped template *ds*DNA, making it inaccessible for transcription when compared to the preformed 'lipid buttons' from which transcription had been observed from previously.

To test the proof of concept for the PDMS device design, complete transcription assay solution (including linearized template *ds*DNA) was fed through the microfluidic device with the PDMS temperature monitored for stability over the course of the investigation. Purification of aliquots of post-reaction solution from the device showed that it was indeed capable of producing mRNA, albeit with mRNA yields significantly lower than were expected. This observation was particularly surprising, as one of the key reasons for the choice of PDMS for fabrication of the continuous-flow device prototype was its reported compatibility with a host of biological reagents and processes, and that it is known to be non-toxic to proteins.[8,16] Despite these properties, however, complete transcription assay solution run through the PDMS device failed to produce mRNA yields that were comparable to the yields that could be achieved by *in vitro* solution phase transcription in a microcentrifuge tube. The third and final output aliquot pumped from the device (collected over a two hour period) contained the highest mRNA yield from the device, which was only two-thirds (20083.3 ng) of a standard solution-based transcription reaction yield (30202.2 ng). Thermocouple monitoring of the uppermost PDMS layer confirmed that the device temperature remained within a suitable range for the duration of the investigation (Figure 5.8), indicating that a different factor must have been limiting the rate of transcription within the prototype device and thus the overall mRNA yields purified from each aliquot collected. The increase in mRNA yields purified from successive aliquots, each collected over a two

hour period, from 10350.0 ng (aliquot 1) to 17973.3 ng (aliquot 2) and then to 20083.3 ng (aliquot 3), show that the transcriptional activity within the device increased over time, as the unidentified factor limiting transcriptional activity decreased over the course of the investigation.

Based upon the investigations described within this chapter, there are two potential justifications for this phenomenon. Firstly, it could be that the transcription solution to first enter the device, and thus be first collected from the device as aliquot 1, spends a greater amount of time in contact with the air that initially fills the empty channel within the device. This may lead to the increased oxidation of transcription assay components, such as the reducing agent dithiothreitol and T7 RNA polymerase, that were first injected into the device, resulting the initially low level of transcriptional activity observed. Whilst a control experiment investigating the effect of atmosphere on transcriptional activity found no significant difference between air or nitrogen gas (Figure 5.6), the experiment was performed for an incubation period of 2 hours; by the time the first aliquot had passed through the PDMS device and been collected, a period of ~6 h had elapsed since transcription assay solution was first injected into the device (Figure 5.8), during which time it is expected that some oxidation would have occurred.

The second theory accounting for the initially low transcriptional activity observed within the device is that there could be undesirable interactions between the transcription assay components and the inner PDMS surfaces of the main channel through the device. A review of published literature on the use of PDMS microfluidic devices for molecular biology indeed contains some reports of the absorption of small hydrophobic molecules by PDMS, of adsorption of proteins by PDMS surfaces, and of biological assays that have had their solution osmolarity significantly altered due to the evaporation of water through PDMS.[17–19] It is therefore quite possible that some of the components of the transcription assay were absorbed by the fabric of the device, or that the transcription assay solution composition was altered due to evaporation of water from the device, and that a proportion of the T7 RNA polymerase may have become adsorbed to the PDMS surface, all of which would have contributed towards the lower than expected levels of transcriptional activity.

While PDMS is still generally accepted as a suitable material for the fabrication of microfluidic devices for molecular biology purposes, it is becoming more widely acknowledged that particular attention has to be paid to the interactions of PDMS with biological assay components, as untreated PDMS is not as biocompatible as it was once considered.[18] A variety of techniques to help address the issues of absorption,

adsorption, and the evaporation of water from microfluidic devices fabricated from PDMS have been reported in the literature. Eddington *et al.* (2006)[20] and Lee *et al.* (2003)[21] present methods of removing low molecular weight silicone molecules from the bulk PDMS *via* ageing and extraction using high-solubility solvents, respectively, which was shown to reduce hydrophobic recovery (after oxygen plasma treatment) and increase the resistance of the PDMS towards solvents; excess cross-linking agent can be added during the preparation of PDMS in order to reduce the evaporation of water, reportedly by up to 2.5 times when compared to the level observed when Sylgard 184® PDMS (Dow-Corning, USA) is prepared using the standard base to curing agent mixing ratio of 10:1;[22] undesirable surface adsorption of biological molecules can be minimized by first adsorbing bovine serum albumin (BSA) to the PDMS surfaces before injection of assay components within the device,[23] or through modification of the PDMS surface with a silane, which reportedly reduced non-specific protein adsorption by up to 98%.[24]

Evaluating the techniques detailed above for increasing the biocompatibility of PDMS microfluidic devices, the use of excess cross-linking reagent, as reported by Chang *et al.* (2003), to minimize water evaporation, and the prior adsorption of BSA to the PDMS surfaces, as reported by Ostuni *et al.* (2001), would be strongly recommended in an attempt to increase the transcriptional activity from the prototype PDMS device described herein. Neither of these recommended improvements relies upon oxygen plasma treatment or permanent surface modification of the PDMS through addition of silane/PEG structures of considerable steric bulk. This should, therefore, increase the flexibility of the revised PDMS device in terms of the future method of template *ds*DNA immobilization within, and in terms of the variety of biological processes future device modules may be able to sustain.

The experiments presented within this chapter have established proof of concept for a continuous-flow device fabricated from PDMS using rapid prototyping techniques; however, further modifications to the device design and optimization of the assay parameters are required to develop the concept from a rudimentary continuous-flow transcription device, albeit one requiring input of solution phase template *ds*DNA, into a continuous-flow semi-biotic device. A number of potential future device design developments to enable further progress towards the goal of a working transcription and translation-capable semi-biotic device are mooted in section 5.6 – 'Future device design'.

5.6 Future device design

5.6.1 Utilization of a cassette-based system

An option for the future evolution of the transcription module of a semi-biotic device would be the utilization of a 'cassette'-based design, which would allow for the easy replenishment of the internal *ds*DNA-containing DOPE H_{II} phase. Obviously, this would require further investigation into the optimal phase composition for enabling template *ds*DNA accessibility under continuous-flow conditions, but it would ensure that the format of the lipid was as close as possible to the previous investigations into batch transcription from lipid buttons, unlike the previous microfluidic device design where the *ds*DNA-containing lipid button was smeared into a 0.75 mm^3 well, resulting in substantial variation away from the conditions present within the batch transcription investigations presented in Chapter 4.

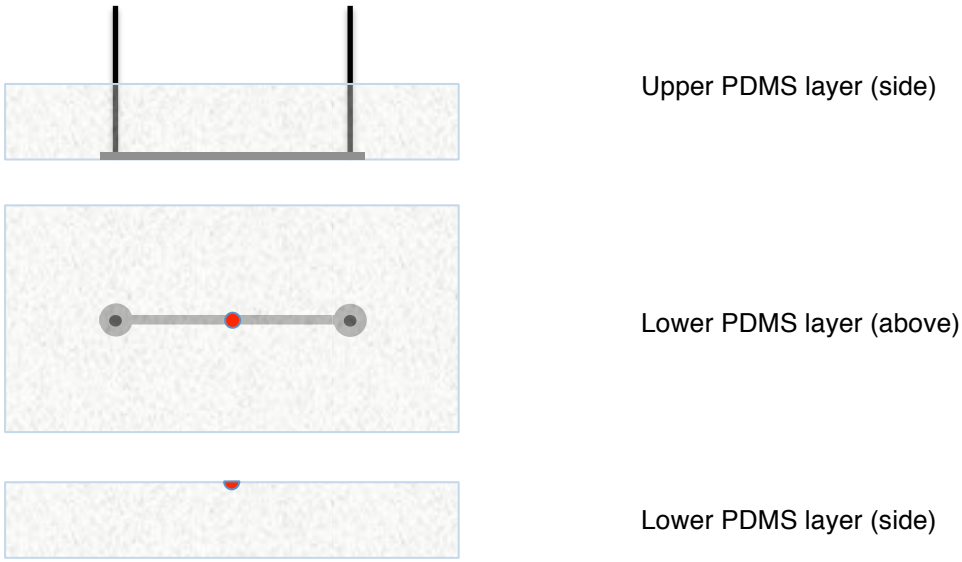

Figure 5.10 Schematic of a cassette-based system – red marker in lower PDMS layer highlights location of a removable lipid button cassette. The cassette would be preloaded with DNA-containing H_{II} phase DOPE and could be replaced at will. This device design would require mechanical clamping of the upper and lower PDMS layers together, as the PDMS layers could not be permanently bonded together using plasma treatment.

The 'cassette' would consist of a small section of PCR tube, containing a standard DNA-containing lipid button, which could be deposited into a small well of equal dimensions in the lower PDMS layer (see Figure 5.10). Advantageously, this method would remove the need for scraping the H_{II} phase into a shallow rectangular containment well, and would offer better opportunity for comparison with the previous transcription experiments using the lipid button system. Whilst only a concept design

at present, prototype mouldings for the upper and lower PDMS layers have been produced, enabling a better analysis of the potential benefits and disadvantages of the cassette-based system. It is expected, however, that the manipulation of the flow above a lipid button 'cassette' could raise a significant challenge, due to the considerably reduced available surface area of the lipid compared to the microfluidic device design incorporating a shallow rectangular *ds*DNA-containing lipid well.

5.6.2 Magnetic beads: an alternative method for DNA immobilization

Whilst the use of lyotropic liquid crystalline phases for template *ds*DNA containment within a continuous-flow device for transcription and translation was a novel application, the immobilization of *ds*DNA for transcription and translation has been previously reported in the literature; papers discussing biological syntheses utilizing immobilized *ds*DNA have been published by a number of scientists, using a variety of techniques, such as protein-producing gels (or 'P-gels'),[25] gene brushes upon planar surfaces,[26] and gene brushes attached to microsphere structures.[27-29] The use of any one of these techniques for template *ds*DNA immobilization would negate the need for use of lyotropic liquid crystalline phases for *ds*DNA containment, removing the issue of *ds*DNA leaching from within the phase, and thus the loss of template *ds*DNA, over successive cycles of transcription.

*ds*DNA immobilized within a hydrogel has been shown, by Park *et al.* (2009), to remain transcription and translation active, with the protein-producing hydrogel structure termed a 'P-gel' or protein-gel.[25] The P-gel was created through the cross-linking of linear plasmids, containing the desired gene, with X-shaped DNA (X-DNA); the optimal X-DNA:gene ratio was identified to be 2000:1 for *Renilla luciferase* expression. Park *et al.* demonstrated that P-gel micropads, when placed in a feeding solution of transcription-translation components, could undergo *in vitro* translation for more than 36 hours, producing functional proteins at a rate of up to 5 $mgmL^{-1}$; the P-gel assay was up to 300x more efficient than a traditional cell-free solution phase system (SPS), whilst the SPS assay suffered from a plateau in the yield of functional protein produced after around 12 hours of incubation. The expression of *Renilla luciferase via* P-gel reached a plateau when 400 ng plasmid was distributed across 400 micropads, with further increases in plasmid quantities within the micropads giving no significant additional yield of *Renilla luciferase* protein.

With the ability to easily form P-gel micropads, modification of a transcription-translation continuous-flow device to incorporate a P-gel structure would be possible; particular consideration would need to be given to the longevity of the P-gel within a

continuous-flow environment, however, and the ability with which the P-gel structure could be removed and replaced, or regenerated, to allow the device to continue to function for extended periods of time.

Another method of protein expression using immobilized *ds*DNA is synthetic gene brushes. Synthetic gene brushes consist of linearized *ds*DNA, which is end immobilized upon a surface, such as Buxboim's biocompatible monolayer 'daisy' surface.[30] Buxboim's 'daisy' monolayer contains regularly spaced amine groups which are able to chemically bind with biotin, which is then able to bind with streptavidin-conjugated linear *ds*DNA. As per P-gels, an optimal loading of *ds*DNA within the structure is required to generate the highest yields of protein – for example, optimal gene spacing of approximately 60 nm upon the surface could yield up to 1000 fmol of mRNA from only 7.5 fmol of genes in a period of 3 hours.[26] However, unlike the P-gel system for protein synthesis, the direction of the gene promoter in relation to the immobilization surface also significantly affects the yield of mRNA or protein achieved; transcription from genes with surface orientated promoters gave rise to mRNA yields up to five-times higher than achieved from solution orientated promoters (when transcribing from 1.8 kb units), which may be due to steric issues between RNA polymerase and streptavidin at the surface end of the linear *ds*DNA units.[31] The additional complexities of gene brushes, such as the specificity of the promoter direction, gene density and composition, and steric issues arising from RNA polymerase confined within the layers of the brush during transcription,[32] when compared to transcription and translation from P-gels, make them less attractive as a method of template *ds*DNA immobilization for incorporation within a continuous-flow transcription and translation device.

An improvement upon immobilization of *ds*DNA upon planar surfaces is the immobilization of *ds*DNA utilizing microspheres of calcium alginate or polystyrene, for example. A considerable benefit in using a 3D structure is the ability to increase transcription and translation yields thanks to the increase in the surface area available for assay components to diffuse to and for reaction products to diffuse away from. Whilst calcium alginate beads have been shown to sustain protein expression, as they are able to capture the cell extracts required for protein synthesis, such as *Escherichia coli* extract,[33] they would likely not withstand the sustained pressure and flow conditions within a continuous-flow transcription translation device and would suffer from degradation in their structural integrity over time. Solid microspheres, such as those fabricated from streptavidin-coated polystyrene, have been reported to be able to withstand relatively high pressure, for example within a flow cytometer, and are synthesized in a similar way to the synthetic gene brushes described above, utilizing

streptavidin-biotin chemistry.[27] Protein synthesis is then initiated through incubation of the microspheres in a commercially available cell-free extract. Successive transcription reactions have been supported by *ds*DNA immobilized on streptavidin-coated agarose microspheres (Marble *et al.*, 1995), although the system did require supplementation with additional fresh template *ds*DNA to maintain the initially observed levels of transcription.[28] The study by Marble *et al.* (1995) reported that the solid phase system returned similar initial reaction rates and yields to commercially available solution phase systems; this is particularly exciting as, subject to longevity analysis of the spheres and optimization of the assay conditions, the microspheres could support sustained transcription and translation without the requirement for provision of new template *ds*DNA every time, unlike cell-free solution phase systems, where template *ds*DNA is typically lost during the purification process.

With solid microspheres, such as those fabricated from polystyrene, shown to withstand relatively high-pressure environments, they have the potential for successful incorporation within a continuous-flow environment. However, an issue with the use of polystyrene microspheres would be the ability to fix the microspheres in the desired location, for example the temperature-controlled incubation chamber, within the device. This problem could be alleviated through the use of paramagnetic streptavidin microsphere beads, as reported by Fujita *et al.* (1993), which still utilize streptavidin-biotin chemistry for immobilization of the template *ds*DNA, but offer the advantage of being able to be held in a particular location within a magnetic field.[29] Similarly to Marble *et al.* (1995), Fujita *et al.* (1993) reported similar amounts of mRNA was produced to solution phase systems and that the paramagnetic beads remained transcriptionally-active across multiple transcription reactions.

Out of the solid phase techniques describe above, the use of paramagnetic microsphere beads for *ds*DNA immobilization, as reported by Fujita *et al.* in 1993,[29] appears the most suitable technique for use within a continuous-flow device for transcription and translation; template *ds*DNA can be readily attached to the beads, which are easily held in place using magnetism (and thus could also be easily replenished when required), and the use of a microsphere for *ds*DNA immobilization increases the surface area available for diffusion of assay reagents to the template *ds*DNA when compared to a planar immobilization surface.

5.6.3 Coupled transcription/translation

The development of a translation module to be located downstream from the transcription module of a continuous-flow transcription translation device would form part of the secondary stage of development of the proposed transcription-translation device prototype. Whilst there are numerous reports in the literature of coupled transcription and translation from immobilized template *ds*DNA, these rely upon combined transcription and translation using commercially available cell-free extract solutions. It is envisaged that, through separating the transcription and translation components of the device, a plug and play device could be fabricated that could be tailored to suit a particular use. For example, a synthetic RNA foundry would only require the transcription module, which could later be connected to a translation module if full protein synthesis were desired. Additionally, the separation of transcription and translation into two distinct modules would allow for each module to utilize the optimal conditions for each reaction, leading to improved yields of mRNA and protein, rather than performing coupled transcription-translation under compromised conditions, achieving lower individual yields of mRNA and protein than may otherwise be achieved.

5.6.4 On-demand detection, decision and response (d^2r)

Once a working, transcription and translation capable, continuous-flow semi-biotic device prototype had been developed, the final envisaged stage of development would be the design, fabrication and commissioning of an integrated, on-demand detection, decision and response (d^2r) system, which would assume full operational control of the semi-biotic device. The purpose of this on-demand system would be to detect a stimulus concentration, trigger injection of assay components into the device and maintain thermostatic control when the stimulus concentration falls below a specified minimum level, produce a known amount of protein *via* coupled transcription and translation modules, and then initiate the shut down of the semi-biotic device upon the stimulus concentration being raised to a specified threshold level. For example, a semi-biotic device with integrated d^2r system, could act as a synthetic pancreas, able to detect, decide and respond to glucose levels in a blood sample, autonomously producing insulin to meet demand. Such a device would be of potential benefit in assisting the control of insulin levels in the increasing number of people suffering from diabetes internationally.[34]

5.7 Annex

5.7.1 Annex 1: PDMS microfluidic device fabrication

5.7.1.1 Production of device template using SY355 photoresist

The protocol for production of the microfluidic device is based upon the protocol reported by Taberham *et al* (2008), using Ordyl SY355 photoresist laminate and PDMS.[11]

Mask designs for the device were produced in-house using CleWin computer-aided design (CAD) software and were printed onto film by the University of Southampton Print Centre. A negative resist film was produced for use with Ordyl SY355 laminate – channels were clear on the film, allowing UV to pass through the film, onto the SY355 laminate. Once developed, the UV-treated features act as protruding templates for the upper and lower PDMS layer channels.

Upper PDMS layer template
Channel: (l) 20,000 µm (w) 1,000 µm (d) 50 µm

Lower PDMS layer template
Lipid well: (l) 15,000 µm (w) 1,000 µm (d) 50 µm

Figure 5.11 Mask design and dimensions. Ordyl SY355 laminate should produce a difference between surface and channel depth of 50 µm. The lower PDMS layer lipid well has a volume of 0.75 mm^3, which is sufficient to house 0.75 mg of DNA-containing H_{II} phase DOPE. By using multiple layers of SY355 laminate, the depth can be doubled (2 layers) and even tripled (3 layers), thus doubling or tripling the volume available for accommodation of DNA-containing lipid.

Glass microscope slides form the substrate upon which Ordyl SY355 laminate was adhered to. The glass substrates were cleaned extensively prior to adhesion, to ensure a good bond between the laminate and the substrate. Substrates were initiallty cleaned in acetone (10 minutes), to remove organic impurities from the substrate surface, before washing with isopropyl alcohol (10 minutes), removing grease or oily contaminates from the substrate. When cleaning, a cotton bud was used to wipe the slide from one side to the other, ensuring a continuous action from substrate edge to edge, to prevent deposition of contaminates in the centre of the substrate surface. The washing process can be repeated, until the substrate is thoroughly clean, ensuring that

the final wash is always with isopropyl alcohol. Post-washing, the substrate was dried using a high-pressure nitrogen gun, and subjected to a dehydration bake (200 ˚C, overnight) to ensure complete removal of moisture from the substrate surface.

Ti primer (2 mL) was applied to each dried substrate, and spin coated (3,000 rpm, 20 seconds), using an Electronic Systems spin coater, to ensure an even coating. Once coated, The Ti-primed substrates were then heated (120 ˚C, 2 minutes) using a hotplate. Ordyl SY355 laminate was applied to the substrates and laminated (Mega Electronics Photo Pro 33 laminator, 95 ˚C, speed 1), using thin cardboard as a carrier sheet. The laminated substrates were then allowed to relax (1 hour, RT) in dark conditions (laminate sensitive to UV). After allowing the laminate to relax, the plastic film protecting the laminate was removed, and the printed film mask applied print-down onto the laminate, before exposure to high-intensity UV radiation using a vacuum UV exposure unit (Mega Electronics AY315 - 25 seconds). The mask is then peeled off post-exposure, and the SY355 laminate subjected to a post-exposure bake (80 ˚C, 4 minutes) using a hotplate. The baked laminate is then developed using BMR developer solution (3 minutes, with agitation and washing using Pasteur pipette), before rinsing with BMR rinse (90 seconds) and finally deionized water. The rinsed substrates were dried using a high-pressure nitrogen gun. UV exposure and development removes the laminate that was not exposed to UV, leaving protruding features where the laminate was exposed to UV. Post-development, the substrates were hard-baked (200 ˚C, 2 hours) using a programmable oven (Heraeus UT6), with the temperature increased from room temperature to the hard-baking temperature at 60 ˚C per hour, and again decreased from the hard-baking temperature to room temperature at the same rate after 2 hours hard-baking.

Treatment of the hard-baked stamps with 2% trichloro-perfluorooctyl-silane in ethanol solution (45 minutes), rinsing with deionized water and oven baking (120 ˚C, 20 minutes), rendered the stamp surface less adhesive and ready for fabrication of the PDMS device layers.

5.7.1.2 Production of device PDMS layers

The PDMS layers used to construct the microfluidic device were constructed by pouring degassed PDMS (10:1 ratio of PDMS to curing agent) on top of the upper and lower layer stamps, which were encased in a temporary foil tray. The PDMS covered stamps were degassed for a second time, removing any air trapped in the PDMS, before curing the samples in an oven (80 ˚C, 1 hour). Once cured, the PDMS was cut and peeled away

from the stamps, with inlet and outlet holes made in the upper PDMS layer using a fine hole-punch tool.

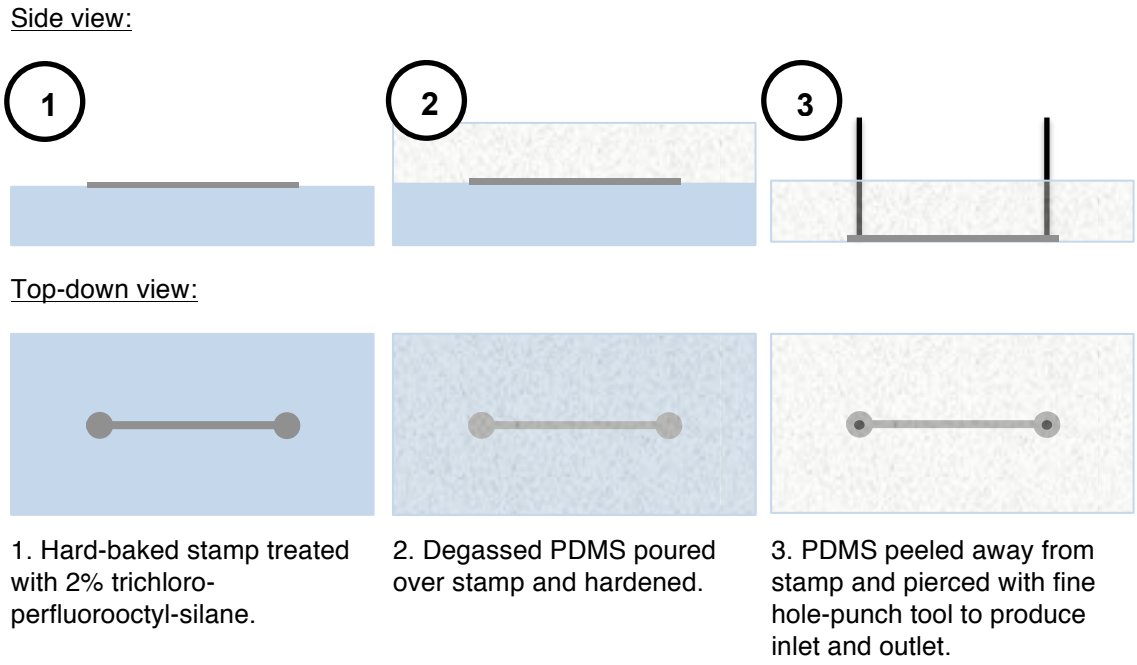

Figure 5.12 Schematic of PDMS layer fabrication using an Ordyl SY355 laminate stamp.

5.7.1.3 Assembling microfluidic device *via* plasma ashing

The first method of bonding the upper and lower PDMS layers was done by plasma ashing. The upper and lower layers were inserted into the plasma asher (Diener Electronic Femto Plasma Asher), feature-side up, and exposed to oxygen plasma (70-80% of 90 sccm/min O_2, 100 W, 30 seconds). Post-plasma ashing, the lipid sample was scraped into the lower layer well as quickly as possible, and the upper and lower PDMS layers aligned by eye and pressed together. The combined layers were then heated at 50 °C using a hotplate, increasing the strength of the bond between the upper and lower PDMS layers.

5.7.1.4 Assembling microfluidic device *via* mechanical clamping

The second method of bonding the upper and lower PDMS layers was a reversible method, using clamps to press the layers together. Once the lipid sample had been scraped into the lower layer well, the layers were aligned by eye and clamped together using four metal paper clamps. The clamps sealed the layers together sufficiently well to ensure that no fluid leaked from the channels, and prevented fluid from leaking into the channel when the device was placed into a waterbath. Unlike the plasma ashing

method, the two layers can be taken apart, cleaned and re-bonded using the clamp method.

5.7.1.5 Injection of transcription assay components

Transcription assay components were pumped through the microfluidic device using a Harvard NanoMite syringe pump and controlled, supplying the components at a specified continuous-flow rate.

5.8 References

1. Attard, G. S. Semibiotics.org. (2008). at <http://www.semibiotics.org/cms/>

2. Foley, T. MChem Project Report, University of Southampton. (2008).

3. Dittrich, P. S., Jahnz, M. & Schwille, P. A new embedded process for compartmentalized cell-free protein expression and on-line detection in microfluidic devices. *Chembiochem* **6,** 811–814 (2005).

4. Gulati, S. *et al.* Opportunities for microfluidic technologies in synthetic biology. *J. R. Soc. Interface* **6 Suppl 4,** S493–506 (2009).

5. Courtois, F. *et al.* An integrated device for monitoring time-dependent in vitro expression from single genes in picolitre droplets. *Chembiochem* **9,** 439–446 (2008).

6. Duffy, D. C., McDonald, J. C., Schueller, O. J. A. & Whitesides, G. M. Rapid prototyping of microfluidic systems in poly(dimethylsiloxane). *Anal. Chem.* **70,** 4974–4984 (1998).

7. Whitesides, G. M. & Stroock, A. D. Flexible methods for microfluidics. *Phys. Today* **54,** 42–48 (2001).

8. Whitesides, G. M. The origins and the future of microfluidics. *Nature* **442,** 368–373 (2006).

9. Regehr, K. J. *et al.* Biological implications of polydimethylsiloxane-based microfluidic cell culture. *Lab Chip* **9,** 2132–2139 (2009).

10. El-Ali, J., Sorger, P. K. & Jensen, K. F. Cells on chips. *Nature* **442,** 403–411 (2006).

11. Taberham, A., Kraft, M., Mowlem, M. & Morgan, H. The fabrication of lab-on-chip devices from fluoropolymers. *J. Micromechanics Microengineering* **18,** 64011 (2008).

12. Duffy, D. C., Schueller, O. J. A., Brittain, S. T. & Whitesides, G. M. Rapid prototyping of microfluidic switches in poly(dimethyl siloxane) and their actuation by electro-osmotic flow. *J. Micromechanics Microengineering* **9,** 211–217 (1999).

13. Ng, J. M. K., Gitlin, I., Stroock, A. D. & Whitesides, G. M. Components for integrated poly(dimethylsiloxane) microfluidic systems. *Electrophoresis* **23,** 3461–3473 (2002).

14. McDonald, J. C. *et al.* Fabrication of microfluidic systems in poly(dimethylsiloxane). *Electrophoresis* **21,** 27–40 (2000).

15. Dow Corning Corporation. Sylgard(R) 184 material properties. (2013).

16. Delamarche, E., Bernard, A., Schmid, H., Michel, B. & Biebuyck, H. Patterned delivery of immunoglobulins to surfaces using microfluidic networks. *Science (80-.).* **276,** 779–781 (1997).

17. Paguirigan, A. & Beebe, D. From the cellular perspective: exploring differences in the cellular baseline in macroscale and microfluidic cultures. *Integr. Biol.* **1,** 182–195 (2009).

18. Toepke, M. & Beebe, D. PDMS absorption of small molecules and consequences in microfluidic applications. *Lab Chip* **6,** 1484–1486 (2006).

19. Chumbimuni-Torres, K., Coronado, R. & Mfuh…, A. Adsorption of proteins to thin-films of PDMS and its effect on the adhesion of human endothelial cells. *RSC Adv.* **1,** 706–714 (2011).

20. Eddington, D., Puccinelli, J. & Beebe, D. Thermal aging and reduced hydrophobic recovery of polydimethylsiloxane. *Sensors Actuators B …* **114,** 170–172 (2006).

21. Lee, J., Park, C. & Whitesides, G. Solvent compatibility of poly (dimethylsiloxane)-based microfluidic devices. *Anal. Chem.* **75,** 6544–6554 (2003).

22. Chang, W., Akin, D., Sedlak, M. & Ladisch…, M. Poly (dimethylsiloxane)(PDMS) and silicon hybrid biochip for bacterial culture. *Biomed. …* **5,** 281–290 (2003).

23. Ostuni, E., Chen, C., Ingber, D. & Whitesides, G. Selective deposition of proteins and cells in arrays of microwells. *Langmuir* **17,** 2828–2834 (2001).

24. Jon, S., Seong, J., Khademhosseini, A. & Tran…, T. Construction of nonbiofouling surfaces by polymeric self-assembled monolayers. *Langmuir* **19,** 9989–9993 (2003).

25. Park, N., Um, S. H., Funabashi, H., Xu, J. & Luo, D. A cell-free protein-producing gel. *Nat. Mater.* **8,** 432–437 (2009).

26. Buxboim, A., Daube, S. S. & Bar-Ziv, R. Synthetic gene brushes: a structure-function relationship. *Mol. Syst. Biol.* **4,** 181 (2008).

27. Nord, O., Uhlén, M. & Nygren, P.-A. Microbead display of proteins by cell-free expression of anchored DNA. *J. Biotechnol.* **106,** 1–13 (2003).

28. Marble, H. A. & Davis, R. H. RNA transcription from immobilized DNA templates. *Biotechnol. Prog.* **11,** 393–396 (1995).

29. Fujita, K. & Silver, J. Surprising lability of biotin-streptavidin bond during transcription of biotinylated DNA bound to paramagnetic streptavidin beads. *Biotechniques* **14,** 608–617 (1993).

30. Buxboim, A., Bar-Dagan, M., Frydman, V. & Zbaida…, D. A single-step photolithographic interface for cell-free gene expression and active biochips. *Small* **3,** 500–510 (2007).

31. Daube, S. S., Bracha, D., Buxboim, A. & Bar-Ziv, R. H. Compartmentalization by directional gene expression. *Proc. Natl. Acad. Sci. U. S. A.* **107,** 2836–2841 (2010).

32. Buxboim, A., Daube, S. S. & Bar-Ziv, R. Ultradense synthetic gene brushes on a chip. *Nano Lett.* **9,** 909–913 (2009).

33. Kwon, Y.-C. C., Hahn, G.-H. H., Huh, K. M. & Kim, D.-M. M. Synthesis of functional proteins using Escherichia coli extract entrapped in calcium alginate microbeads. *Anal. Biochem.* **373,** 192–196 (2008).

34. Scully, T. Outlook Diabetes: Diabetes in Numbers. *Nature* **485,** S2 (2012).

Chapter 6:

Conclusions

6. Conclusions

6.1 Approach

The transcriptional activity of linearized *ds*DNA partitioned within the inverse hexagonal (H_{II}) phase of the phospholipid 1,2-dioleoyl-*sn*-glycero-3-phosphoethanolamine (DOPE), as reported previously by Corsi *et al*. (2008), was used as a basis for the development of a prototype continuous-flow semi-biotic device.

Solution phase *in vitro* transcription, using a commercially available transcription kit, was characterized to find the optimal transcription assay parameters. An optimized protocol for solution phase transcription assays was developed, including the recommended specifications of components for a home-made transcription assay buffer. Once an optimal solution phase transcription assay was developed, the partitioning of linearized *ds*DNA into DOPE H_{II} phase lipid buttons was investigated.

Analysis of nucleic acid partitioning within the system confirmed the high level of *ds*DNA partitioning into the H_{II} phase of DOPE lipid buttons over extended time periods, both when lipid buttons were prepared *via* the previously reported lyophilization method, and *via* 100 h incubation (37 ˚C) in the presence of complete transcription buffer. A new experimental method to quantify the *ds*DNA partition coefficient was developed utilizing quantitative DNA gel electrophoresis, which was shown to give comparable results and levels of experimental error to the previous PCR-based technique. Analysis of *ds*DNA and mRNA partitioning in the presence of DOPE H_{II} phase lipid buttons confirmed the suitability of the lipid buttons for transcription, with linearized *ds*DNA partitioning within the phase structure and mRNA preferentially residing within the aqueous supernatant above the phase. The transcriptional activity of these phases was investigated, with experimental data showing that lipid buttons prepared *via* lyophilization had a greater transcriptional activity than buttons prepared *via* 100 h incubation, despite sharing similar partition coefficients (after 2 hours of assay incubation, lyophilized buttons produced a mean mRNA yield of ~40 % of that achieved from a solution-phase positive control, whilst buttons produced *via* 100 h incubation produced a mean mRNA yield of approximately 10 % of that achieved from the positive control). An optimal protocol for the partitioning of linearized *ds*DNA within DOPE H_{II} phase lipid buttons was empirically determined.

Further investigations into the transcriptional activity of *ds*DNA-containing lipid buttons were carried out during experiments to develop the system from one-off transcription to multiple-cycle batch transcription (i.e. successive transcription assays performed from the same *ds*DNA-containing lipid button without replenishment of the template *ds*DNA). The batch transcription system was characterized using UV-visible

NanoDrop spectrophotometry, polarizing microscopy, mass spectrometry and small-angle X-ray scattering (SAXS), allowing for the development of an optimal batch transcription protocol. During the investigations, however, *ds*DNA was found to leach from within the DNA-DOPE lipid buttons over successive transcriptions. Further experimentation was performed to investigate the cause of the *ds*DNA leaching from within the H_{II} phase and to find potential methods to minimize or prevent leaching, whilst maintaining transcriptional activity. These included the assessment of the effect of transcription assay components on *ds*DNA partitioning, the use of molecular crowding agents during transcription from DNA-DOPE lipid buttons, and trialing alternative lipid compositions for the containment of the linearized *ds*DNA. Despite significant modifications to the lipid button preparation and batch transcription assay, a system where *ds*DNA leaching was minimized and transcriptional activity retained could not be found.

The aim of the research presented within this thesis was to develop a prototype continuous-flow semi-biotic device, utilizing linearized *ds*DNA partitioned within the H_{II} phase of DOPE for transcription. With experimental data showing the leaching of *ds*DNA from the phases and the failure to maintain transcriptional activity over sustained periods of batch transcription, it was decided to test the proof of concept for a continuous-flow microfluidic transcription device fabricated out of PDMS using rapid prototyping techniques. If the PDMS microfluidic device was shown to be biocompatible with a solution phase transcription reaction, where all of the necessary transcription assay components (including the template *ds*DNA) were pumped into the device by syringe pump, alternative methods for the provision of immobilized template *ds*DNA within the device could then be researched, with a view to their potential integration within a future version of the semi-biotic device prototype.

6.2 Summary of findings

6.2.1 Optimization of the Transcription Assay

The experimental work presented in Chapter 2 was concerned with the optimization of the solution phase transcription assay, using a commercially available transcription kit but with a homemade transcription buffer solution based upon that used in previously published work. It was identified that the transcription buffer composition could be modified to give an improved transcriptional yield through increasing the buffer concentration of $MgCl_2$ from 25 to 40 mM, whilst it was also discovered that there was some flexibility in the transcription assay parameters, which could be of potential benefit for a continuous-flow semi-biotic device. For example, transcription could be performed across a reasonably broad temperature range, from 30-37 ˚C without a significant variation in the yield of mRNA obtained from the assay; within the context of the semi-biotic device, this meant that any fluctuation in the incubation temperature within the device below 37 ˚C but above 30 ˚C should have no appreciable impact upon mRNA yields.

6.2.2 One-off Transcription in the Presence of DNA-containing H_{II} Phases

Analysis of nucleic acid partitioning data confirmed the preference of mRNA to reside within the isotropic supernatant solution above a DOPE lipid button, whilst linearized *ds*DNA partitions within the H_{II} phase when the phase was prepared *via* either lyophilization or 100 h incubation with complete transcription buffer solution; the partition coefficient (K_p) for buttons prepared by either method was below 0.008 after 100 hours, meaning that only 0.2% of the linearized template *ds*DNA remained outside of the phase structure (data for 1 µg linearized pRSET-EmGFP *ds*DNA). Investigations into the driving force for the partitioning of linear *ds*DNA into the H_{II} phase of DOPE during incubation showed that the process was highly driven by the presence of ionic molecules within complete transcription buffer; $MgCl_2$ (25 mM), spermidine (2.5 mM), and DTT (10 mM), all significantly drove the partitioning of linear *ds*DNA into the phase, with optimal *ds*DNA partitioning observed when linearized *ds*DNA was incubated above the phase in the presence of complete transcription buffer solution for 100 hour or more (37 ˚C).

Quantitative DNA gel analysis for determining the partition coefficient of DNA-DOPE lipid buttons was developed and shown to give results in agreement with the previously utilized PCR method; this development offered a significant improvement in the lipid button production process, with partition coefficient analysis able to be

performed in a far more timely manner, whilst retaining similar levels of accuracy and experimental error.

Transcriptional studies into the activity of *ds*DNA-containing DOPE lipid buttons identified that DNA-DOPE lipid buttons prepared either *via* lyophilization or 100 h incubation did not exhibit the same levels of transcriptional activity; phases prepared *via* lyophilization were more transcriptionally active compared to their incubation counterparts, yet had been shown by partition coefficient analysis to contain similar levels of linearized template *ds*DNA. The disparity in transcriptional activity of lipid buttons produced by the two methods is thought to be due to the improved accessibility of the linear *ds*DNA in lipid buttons prepared *via* lyophilization.

6.2.3 Batch Transcription in the Presence of DNA-containing H_{II} Phases

Investigations into batch transcription identified that DNA-containing H_{II} phases were not suitable for supporting sustained transcription. Whilst linearized template *ds*DNA could be easily partitioned within the H_{II} phase of DOPE, it did not remain associated with the phase when subjected to transcription conditions; the leaching of *ds*DNA from within H_{II} phase DOPE lipid buttons may be in some part due to the interactions of significant amount of rNTPs during transcription, which were shown to inhibit the partitioning of *ds*DNA. During a given batch transcription assay, whilst a small minority of transcriptional activity may be due to *ds*DNA associated with the liquid crystalline phase, the majority of activity observed was attributable to the presence of leached *ds*DNA in solution (as identified by quantitative DNA gel electrophoresis of aliquots of post-transcription solution). The leaching of template *ds*DNA out of the lipid buttons dealt a considerable blow to the concept of continuous-flow transcription from DNA-containing liquid crystalline phases.

The sensitivity of the system to ionic conditions was highlighted during the trial of modifications in an attempt to subjugate the issue of template *ds*DNA leaching from within the phase during transcription. Increases in $MgCl_2$ concentration during transcription, from 25 to 40 mM, led to a reduction in transcriptional activity, likely due to the retention of some $MgCl_2$ within the phase structure from the prior partitioning of *ds*DNA process; concentrations of $MgCl_2$ above ~45 mM have been shown to dramatically reduce transcriptional activity for solution phase transcription. Modifications to the lipid button composition, including doping the buttons with the cationic lipid DOPE and the trial of monoolein, were not fruitful in their attempts to produce a transcriptionally active *ds*DNA-containing button. Only DOPE95:DOTAP5 phases showed comparable levels of *ds*DNA partitioning to DOPE, however they

appeared to inhibit transcription with no significant mRNA yields achieved. DNA-DOPE buttons prepared *via* the use of alternative divalent cations, such as Ca^{2+}, Mn^{2+}, and Ba^{2+} showed promising levels of *ds*DNA partitioning, but unfortunately the presence of these cations in the transcription assay severely inhibited transcriptional activity. Supplementation of the transcription assay solution with the crowding agent trehalose reduced the peak amount of *ds*DNA leached from the liquid crystalline phase, but did not significantly increase the overall lifetime of the phase.

6.2.4 Towards the Development of a Semi-biotic Device

With DNA-containing DOPE H_{II} phases shown to leach *ds*DNA within the phase, making them unsuitable for batch or continuous-flow transcription in their current format, attention turned to proving the concept of a continuous-flow semi-biotic device fabricated using PDMS rapid prototyping techniques. An improved PDMS device was fabricated and underwent testing for leaks; the plasma sealing between the upper and lower PDMS layers failed, and so the layers were then held together using mechanical force, offering the ability to dis- and re-assemble the device as required, without having to worry about damaging the fabric of the device. A solution phase transcription assay was run through the device to test for biocompatibility, however reduced transcriptional activity was observed when compared to the positive control assays. This is thought to be due to the absorption and adsorption of biological molecules by the PDMS surfaces; an investigation into the stability of the transcription assay solution at room temperature had shown that no appreciable drop in transcriptional activity was observed for prior room temperature incubation periods of up to 6 hours, so the lack of chilled storage for the transcription solution reservoir prior to injection into the device was unlikely to be responsible for the lower yields observed. Thermocouple monitoring of the device during the transcription assay showed that a suitable temperature can be maintained within the device through heating the PDMS from underneath *via* hotplate, negating the need for the development of an 'on-board' heating device for the prototype.

Despite DNA-containing DOPE H_{II} phases not yet offering a viable method of template *ds*DNA containment for transcription or translation under continuous-flow conditions, the use of P-gels, synthetic gene brushes, or magnetic microsphere beads, could offer alternative methods of *ds*DNA immobilization for this purpose.

6.3 Recommendations for future work

The work presented in this thesis has given a solid basis from which to develop a continuous-flow semi-biotic device. However, there is an appreciable amount of further research that will be necessary to conduct to ensure that a semi-biotic device of efficient performance, intelligent design and successful operation can be developed. From the experiments detailed herein, it is clear that without further development, DNA-DOPE H_{II} phases are unsuitable for the provision of template *ds*DNA for sustained transcription, under either batch-wise or continuous-flow conditions, due to the issues encountered with linearized *ds*DNA leaching from within the H_{II} phase. However, if further investigations into DOPE-DNA H_{II} phases were carried out, it would be prudent to determine if the production of lipid buttons using a DOPE/chloroform solution within polypropylene PCR tubes lead to any significant degradation of the PCR tubes and thus contamination of the DOPE lipid buttons made using this method. Additionally, it would be interesting to investigate whether vesicles are initially produced when transcription assay solution is layered upon *ds*DNA-containing lipid buttons, due to the significant difference in volume of the aqueous and liquid crystalline phases experiences under both batch and continuous-flow conditions.

Alternative methods of *ds*DNA immobilization, for provision of template *ds*DNA within a semi-biotic device environment, could include the use of P-gels, synthetic gene brushes, or magnetic beads. Whilst their reported use in the literature suggests that magnetic beads would be the most suitable, thanks to the ability to be easily located using magnetism and removed for regeneration or replacement, each of the alternatives should be investigated for their ease of integration within a continuous-flow semi-biotic device. Modification of the prototype device described within this thesis would be necessary to ensure magnetic beads could be securely contained under continuous-flow conditions, whilst investigations should also be performed to assess the transcriptional activity of template *ds*DNA tethered to such beads.

The method of supply for transcription assay components into the prototype PDMS device detailed in Chapter 5 involved the components being stored and pumped from within a glass SGE syringe, controlled by a Harvard NanoMite syringe pump. Whilst this offered an incredibly accurate and highly controllable mechanism for transcription component delivery, the physical constraints of the syringe pump controller design prevents the syringe contents from being temperature-controlled before it reaches the transcription device. Whilst this is not an issue for the early stages of transcription, as the first portion of components did not have far to travel through the inlet tubing into the device, over a sustained period of operation, the assay components remaining

within the SGE syringe will spend a considerable amount of time at room temperature prior to injection into the device. Whilst at short time periods, this did not significantly impact upon transcriptional yields, it would be prudent to invest in a method of keeping the assay components chilled whilst in the SGE syringe, as this would undoubtedly extend the operational lifetime of the system.

Although PDMS is a generally convenient material for microfluidic device manufacture, offering rapid prototyping, good biocompatibility and non-toxicity, several publications in the literature have reported that there are a number of performance issues encountered with the use of PDMS devices for molecular biology applications, namely the absorption of biomolecules and the adsorption of proteins. Further investigation, therefore, should be performed into the absorption and adsorption of transcription and translation assay components, and a selection of different proteins and enzymes, to the inner surfaces of a semi-biotic device fabricated from PDMS. The proposed solution to minimize the adsorption of proteins and enzymes would be to run a series of experiments comparing the efficiency of transcription and translation before and after running bovine serum albumin (BSA) through the microfluidic device. BSA is commonly used in biochemical reactions for it's stabilisation properties, and lack of chemical interaction in many biochemical reactions. As stated in Chapter 5, there are reports in the literature that BSA has been used successfully to prevent adhesion of enzymes to reaction tubes and vessels, and so it would be prudent to examine the effect of running transcription and translation assays using the semi-biotic device post-injection of BSA through the device.

Once an optimal fabrication method and design for the semi-biotic device prototype is confirmed, it is proposed that the device should be constructed in 'plug-and-play' modules, to increase the flexibility of the device. For example, transcription and translation should both be performed in standalone modules, such that when the production of mRNA is all that is required, the translation module can simply be disconnected. This 'plug-and-play' compatibility would then allow for role-specific modules, such as analysis or purification units, to be added as and when required, and for individual modules to be regenerated or swapped out and replaced as necessary throughout the lifetime of the semi-biotic device.

Upon fabrication of a working prototype semi-biotic device, full characterisation of the device modules will need to be performed; this work will inevitably entail comparison of the yields obtained from the device to solution phase commercially available transcription-translation kits, and to other transcription-translation systems reported in the literature, such as those utilizing P-gels or synthetic gene brushes. Investigation

into the various controllable parameters, such as the component flow rate, method of incubation, incubation temperature and longevity of the modules under continuous-flow conditions, will also need to be carried out. It is hoped that the device could then be integrated with an optional detection, decision, and response (d^2r) module, to enable fully autonomous and regulated synthesis of a range of biological products, dependent upon the plug-and-play modules connected.

Appendix

Appendix

Appendix A

A1 *ds*DNA preparation

Details on the *ds*DNA preparation protocols can be found in the following sections of the Annex for Chapter 2:

- Cell culture and plasmid preparation (2.6.1.1)
- Linearization of plasmid DNA (2.6.1.2)
- Purification of linearized DNA (2.6.1.3)

A2 mRNA preparation and purification

All transcription experiments described within this thesis were performed using T7 RNA polymerase (NEB, M0251) and ribonucleotides (NEB, N0466) purchased from New England Biolabs, USA, with transcription buffer made in-house to the specifications described in each relevant chapter of this thesis. Assays were incubated at 37 ˚C in a thermostatically controlled waterbath, unless specified otherwise. Samples of mRNA were purified using a QIAGEN RNeasy mini spin kit (QIAGEN, 74106).

A modified version of the QIAGEN RNeasy lipid tissue mini kit purification protocol was used to purify the transcribed mRNA. QIAzol lysis reagent (500 µL) was added to the transcribed mRNA and incubated (RT, 5 minutes). Chloroform (100 µL) was added, before vortexing (RT, briefly) to ensure complete distribution. Centrifugation (13,000 rpm, 10 minutes, RT) separated the aqueous phase, containing the transcribed mRNA. An aliquot of the aqueous top phase was extracted (250 µL), to which ethanol was added (70% v/v, 300 µL). Tubes were vortexed (RT, briefly), before transferring the contents to RNeasy mini kit spin columns (with 2 mL collection tubes). The spin columns were centrifuged (13,000 rpm, 15 seconds, RT), and the washings discarded. The spin column membrane was washed with buffer RW1 (700 µL), before further centrifugation (13,000 rpm, 15 seconds, RT), discarding washings. Buffer RPE (500 µL) was applied to the column membrane, followed by further centrifugation (13,000 rpm, 2 minutes, RT), discarding the organic washings. In a new collection tube (2 mL), the collection column was dried of any residual ethanol from buffer RPE by centrifugation (13,000 rpm, 1 minute, RT). The spin column was then placed in a new collection tube (1.5 mL, microcentrifuge-style) to collect the eluted mRNA. Nuclease-free water was added to the column membrane (50 µL), incubating briefly (1 minute, RT). The column was then centrifuged briefly (13,000 rpm, 15 seconds, RT) before application of the final aliquot of nuclease-free water (50 µL) and a final centrifugation (13,000 rpm, 1 minute, RT). The spin columns were discarded and the eluted mRNA (100 µL in nuclease-free water) concentration determined using NanoDrop spectrophotometry.

A3 DNA gel electrophoresis

DNA gel electrophoresis was performed to quantify the integrity and quality of plasmid DNA prepared using the PureYield plasmid maxi preparation (Promega, A2393) and linearized (XmnI) DNA post-purification using the DNA binding columns supplied in the PureYield plasmid maxi preparation kit. 1.0% agarose pre-cast (Sigma, P5972 or P5472) or home-made gels containing ethidium bromide (~0.5 mg mL^{-1}) were used for all DNA samples analyzed by electrophoresis. For the expected size DNA bands, a 1.0% agarose gel was determined to offer best resolution.

Gels prepared in-house for electrophoresis were prepared using high purity agarose designed for optimal resolution of bands greater than 1 kb (Melford, MB1200). A 1.0% gel was prepared in 1x Bionic buffer (Sigma, B6185) by heat-assisted dissolution (0.5 g in 50 mL). Ethidium bromide (~0.5 mg mL^{-1}) was added to the agarose solution upon cooling, minimizing vaporization of ethidium bromide. The solution was then poured into a casting tray with appropriate size well comb and allowed to set (1 hour). DNA samples for electrophoresis were run against a reference DNA ladder (NEB, N3200) and a circular reference (applicable to linearized DNA samples only). Samples and ladder were prepared as per the specification detailed in Table 7.1.

Table 7.1 DNA gel electrophoresis sample composition

DNA Sample	DNA Ladder (NEB, N3200)	Circular Plasmid Reference
100 ng DNA (*x* µL)	1 µL DNA ladder	100 ng DNA (*z* µL)
5-*x* µL nuclease-free water	4 µL nuclease-free water	5-*z* µL nuclease-free water
1 µL NEB 6x loading buffer	1 µL NEB 6x loading buffer	1 µL NEB 6x loading buffer

Samples prepared as above were then loaded onto the agarose gel and run in either 1x Bionic buffer (150 V) or in 1x TAE buffer (3.5 V / cm) until the dye front neared the end of the gel. Visualization of the gel was performed using a UV transilluminator (Syngene InGenius LXR) and an image recorded using Syngene GeneSnap software.

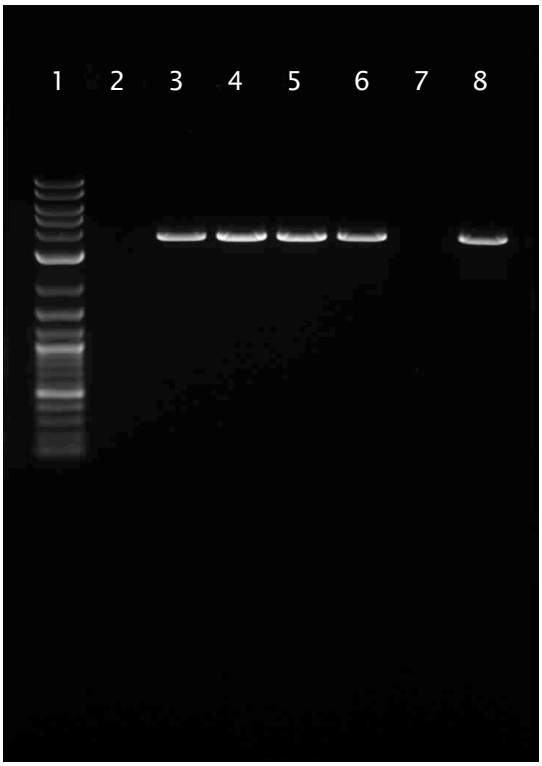

Figure 7.1 1.0% agarose DNA gel for purified *lin*pRSET-EmGFP *ds*DNA. Lane 1: 2-log DNA ladder (NEB, N3200); lanes 3-6: recently linearized pRSET-EmGFP *ds*DNA (3.6 kb), post-purification; lane 7: control *lin*pRSET-EmGFP *ds*DNA (3.6 kb). RW/6511/11

A4 RNA gel electrophoresis

RNA gel electrophoresis was performed to quantify the integrity and quality of samples purified using the QIAGEN RNeasy Lipid Tissue Mini Kit and to confirm that the transcription products were of the size to be expected, based upon the DNA template used in transcription. Gels were run using pre-cast MOPS 1.25% agarose gels (Sigma, P5472) or in-house MOPS 1.0% agarose gels. mRNA samples for electrophoresis were run against a reference RNA ladder (Sigma, R7020) and against a relevant circular and linear plasmid DNA template. Samples, ladder and DNA reference were prepared as per the specification detailed in Table 7.2.

Table 7.2 mRNA gel electrophoresis sample composition

mRNA Sample	RNA Ladder (Sigma, R7020)	DNA template reference
0.5-1 µg RNA (*x* µL)	2 µL RNA ladder	100 ng DNA template (*z* µL)
y µL nuclease-free water	3 µL nuclease-free water	4 µL nuclease-free water
2x loading buffer with EtBr (Sigma, R4268)	10 µL loading buffer with EtBr (Sigma, R4268)	*2z* loading buffer with EtBr (Sigma, R4268)

Post-preparation, as described above, samples were denatured (65 ˚C, 10 minutes) and rapidly cooled (ice bath, 2 minutes) prior to loading into the agarose gel wells. The gel is then run at a constant voltage (3.5 V/cm) in 1x MOPS buffer (Lonza, #50876) until the dye front neared the end of the gel. As per DNA gel electrophoresis, the gel is visualized using a UV transilluminator and an image of the gel recorded.

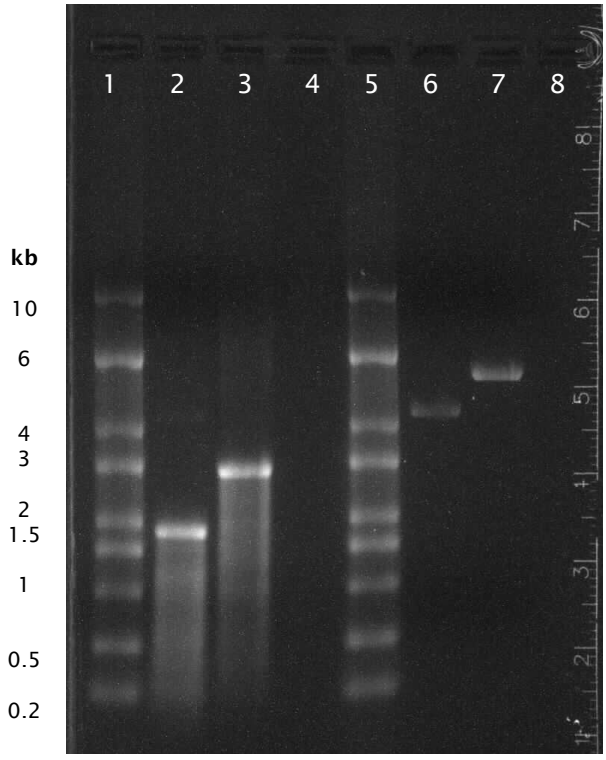

Figure 7.2 1.5% agarose RNA gel showing purified T7luc and T7GFP mRNA, template *lin*T7luc and *lin*T7GFP, and ssRNA ladder (Sigma, R7020). Lanes 1 & 5: 0.2-10 kb RNA marker; lane 2: T7GFP mRNA; lane 3: T7luc mRNA; lane 6: *lin*T7GFP DNA; lane 7: *lin*T7luc DNA. RW/5778/22